UNIVERSITÀ DEGLI STUDI DEL PIEMONTE ORIENTALE
"AMEDEO AVOGADRO"

DEPARTMENT OF PHARMACEUTICAL SCIENCES
Ph.D. in Chemistry & Biology
XXXIII cycle 2017-2020

PHYTOCANNABINOIDS: NOVEL CHEMISTRY OF BIOLOGICAL RELEVANCE

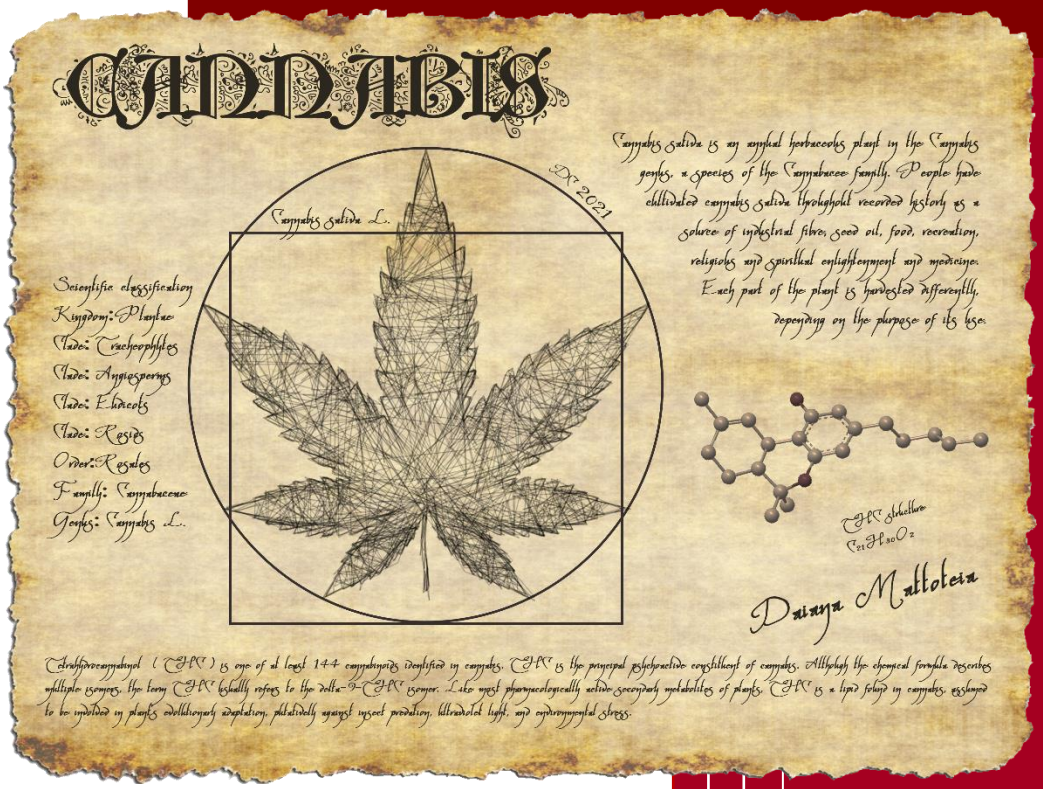

SUPERVISOR

Prof. Giovanni B. APPENDINO

PHD PROGRAM COORDINATOR

Prof. Gian Cesare TRON

PHD STUDENT

Daiana MATTOTEIA

UNIVERSITÀ DEGLI STUDI DEL PIEMONTE ORIENTALE
"AMEDEO AVOGADRO"

DEPARTMENT OF PHARMACEUTICAL SCIENCES
Ph.D. in Chemistry & Biology
XXXIII cycle 2017-2020

PHYTOCANNABINOIDS: NOVEL CHEMISTRY OF BIOLOGICAL RELEVANCE

Drug discovery and development

SSD: CHIM/06

SUPERVISOR

Prof. Giovanni B. Appendino

PHD PROGRAM COORDINATOR

Prof. Gian Cesare Tron

PHD STUDENT

Daiana Mattoteia

UNIVERSITÀ DEL PIEMONTE ORIENTALE
DOTTORATO DI RICERCA
IN CHEMISTRY & BIOLOGY

Via Duomo, 6
13100 – Vercelli (ITALY)

DECLARATION AND AUTHORISATION TO ANTIPLAGIARISM DETECTION

The undersigned DAIANA MATIOTEIA ..... student of the Chemistry & Biology Ph.D course (XXXIII Cycle)

declares:

- to be aware that the University has adopted a web-based service to detect plagiarism through a software system called "Turnit.in",
- his/her Ph.D. thesis was submitted to Turnit.in scan and reasonably it resulted an original document, which correctly cites the literature;

acknowledges:

- his/her Ph.D. thesis can be verified by his/her Ph.D. tutor and/or Ph.D Coordinator in order to confirm its originality.

Date: Novara, 14/01/2021 ..... Signature: .....

XY/tcs
Percorso del file

"Chi non spera l'insperabile, non lo troverà mai

perché l'insperabile è introvabile ed inaccessibile"

Eraclito

TABLE OF CONTENTS

LIST OF ABBREVIATIONS

CBN = cannabinol

CBD = cannabidiol

ECS = Endocannabinoid System

Δ^9-THC = Δ^9-tetrahydrocannabinol

CBG = cannabigerol

CBC = cannabichromene

FM2 = medicinal *Cannabis* variety

OA = olivetolic acid

PKSs = polyketide synthases

LOX = lipoxygenase

HPL = hydroperoxide lyase

AAE = acyl-activating enzyme

CsHCS1 or **CsAAE1** = *Cannabis sativa* **hexanoyl-CoA synthase 1**

CsHCS2 or **CsAAE2** = *Cannabis sativa* **hexanoyl-CoA synthase 2**

OLS/TKS = olivetol synthase/tetraketide synthase

OAC = olivetolic acid cyclase

GPP = geranyl diphosphate

IPP = isoprenoid isopentyl diphosphate

DMAPP = dimethylallyl diphosphate

MEP = methylerythritol phosphate

MEV = mevalonate

FPP = farnesyl diphosphate

NPP = neryl diphosphate

GOT or **CBGAS** = geranyldiphosphate:olivetolate-geranyltransferase

aPT = aromatic prenyltransferases family

CBGA = cannabigerolic acid

CBNRA = cannabinerolic acid

CBGVA = cannabigerovarinic acid

Δ^9-THCA = Δ^9-tetrahydrocannabinolic acid

CBDA = cannabidiolic acid

CBCA = cannabichromenic acid

THCAS = tetrahydrocannabinolic acid synthase

CBDAS = cannabidiolic acid synthase

CBCAS = cannabichromenic acid synthase

ER = endoplasmic reticulum

BSTFA = *N,O*-bis(trimethylsilyl)trifluoroacetamide

TMCS = trimethylchlorosilane

CYP = cytochrome P450

11-hydroxy-Δ^9-THC = 11-hydroxy-Δ9-tetrahydrocannabinol

Δ^9-THC-COOH = 11-nor-9-carboxy-Δ^9-tetrahydrocannabinol

CBs= cannabinoid receptors

CNS = nervous central system

AEA = anandamide or arachidonoyl ethanolamide

2-AG = 2-arachidonoyl glycerol

NAPE = *N*-arachidonoyl phosphatidyl ethanolamine

DAGs = diacylglycerols

FAAH = fatty acid amide hydrolase

MAGL = monoacylglycerol lipase**COX** = cyclooxygenase

TRPV = transient receptor potential vanniloid

GlyRs = glycine receptors

PPAR = peroxisome proliferator-activated receptors

RXR = retinoid X receptor

PPREs = peroxisome proliferator hormone response elements

Bach1 = BTB and CNC homology

MAREs = Maf recognition elements

Nfr2 = nuclear factor erythroid-derived 2-like2

Keap1 = Kelch-like ECH-associated protein 1

CBDQ = cannabidiolquinone

DMP = Dess-Martin periodinane

IBX = 2-iodoxybenzoic acid

SIBX = stabilized 2-iodoxybenzoic acid

BTIB = bis(trifluoroacetoxy)iodobenzene

PIFA = phenyliodine (III)bis(trifluoroacetate)

BBB = blood-brain barrier

DMH = dimethylheptyl

PREFACE

Cannabis sativa L. has been defined a "neglected pharmacological treasure trove" of bioactive compounds (Mechoulam, 2005). As many as 538 secondary metabolites were already mentioned in a review published in 2005 (ElSohly M. A., 2005), and their number has significantly increased over the past decades due a renewed interest in this plant. Table 1 presents a biogenetical classification of the secondary metabolites isolated from *C. sativa* according to the 2005 inventory. Except for cannabinoids, whose inventory has now reached 150 members, updated data on compounds from the other classes are not available. Despite this limitation, the diversity of the constituents is remarkable, and many of them are unique to *C. sativa*. Remarkably, the biological profile of most of them is still unknown. The troubled and controversial history of *C. sativa* and the regulatory complications associated, until recently, even to the study to its non-narcotic constituents are responsible for this discouraging state (Russo, 2007) (Andre C.M., 2016).

The hallmark secondary metabolites of *C. sativa* are the phytocannabinoids, a class of meroterpenoids that, on account of the recent additions to their inventory, now represent its most diverse class of constituents (Hazekamp A, 2010). The aim of this thesis is to contribute to fill the gap between the growing inventory of phytocannabinoids and our meagre knowledge on their chemistry and bioactivity.

COMPOUND CLASS	*COMPOUNDS IDENTIFIED*
Terpenes	> 120
Phytocannabinoids	**> 70**
Hydrocarbons	50
Sugars and related compounds	34
Nitrogenous compounds	27
Non-cannabinoid phenols	25
Flavonoids	23
Fatty acids	22
Simple acids	21
Amino acids	18
Simple ketones	13
Simple esters and lactones	13
Simple aldehydes	12
Proteins, glycoproteins, and enzymes	11
Steroids	11
Elements	9
Simple alcohols	7
Pigments	2
Vitamin	1 (vitamin K)

TABLE 1 **CLASSIFICATION OF ALL CHEMICALS IDENTIFIED IN *C. SATIVA* (AS OF 2005)**

REFERENCES

Andre C.M., H. J. (2016). *Cannabis sativa*: The Plant of the Thousand and One Molecules. Front Plant Sci, 7: p. 19.

ElSohly M. A., S. D. (2005). Chemical constituents of marijuana: The complex mixture of natural cannabinoids. Life Sciences, Volume 78, Issue 5, page 539-548.

Hazekamp A, (2010). J. Chemistry of *Cannabis*. Elsevier

Mechoulam, R. (2005). Plant cannabinoids: a neglected pharmacological treasure trove. British Journal of Pharmacology, 146, 913-915.

Russo, E. (2007). Historu of *cannabis* and its preparations in saga, science, and sobriquet. Che. Biodivers., 4, 1614-1648

CHAPTER 1

INTRODUCTION

1. PHYTOCANNABINOIDS

The first phytocannabinoid isolated was *cannabinol* (CBN, **1**), obtained as a crystalline acetate by Wood, Spivey and Easterfield at Cambridge University in 1898. The gross structure of this compound was elucidated by Cahn in the Thirties of the past century (see Paragraph 4.1), with its complete structure eventually clarified in the following decade by Adams at Illinois University and Todd at Manchester (Appendino, 2020). Cannabinol is an artefact formed from the oxidative degradation of menthyl-type phytocannabinoids, and the first allegedly native phytocannabinoid to be structurally elucidated, except for the location of its endocyclic double bond, was *cannabidiol* (CBD, **2**). In the mid-Fifties of the past century, it was discovered that cannabinoids occur in *C. sativa* in a carboxylated form (*pre-cannabinoids* or *acidic cannabinoids*, **3**) (Santavy & Krejci, 1955). The structure of CBD and the identification of the narcotic constituent of the plant were reported by Mechoulam at Jerusalem University in the early Sixities. (Figure 1)

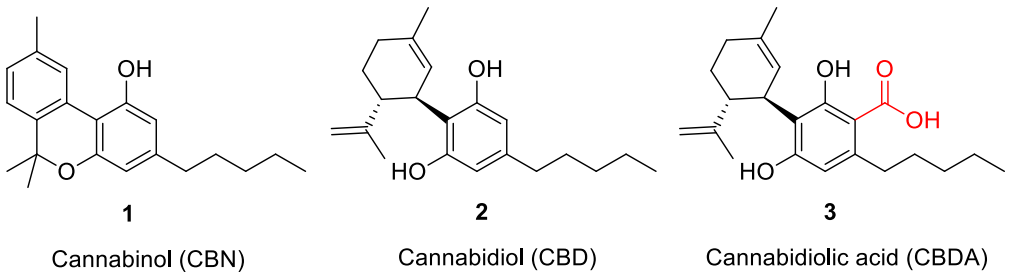

FIGURE 1 **CHEMICAL STRUCTURES OF CBD AND CBDA.**

Many issues regarding *C. sativa* are controversial and ambiguous, even the name cannabinoid, whose use to refer to the hallmark phytochemicals of *C. sativa* can now generate confusion. In the 90s, when specific receptors for these compounds were identified, the word lost its phytochemical and structurally-based meaning, being

used now to refer to structurally diverse compounds sharing the capability to bind the cannabinoid receptors or modulate the Endocannabinoid System (ECS), just like the term opioid is now used for any compounds mimicking the activity of the opium alkaloid morphine. To avoid this confusion, the name *phytocannabinoid* will be used throughout the thesis to refer to the native constituents of *C. sativa*. The name *cannabinoid* will be reserved to the synthetic or semi-synthetic compounds whose structure mimic the one of phytocannabinoids, while the term *endocannabinoid* will be used for the endogenous biological analogues of the *C. sativa* constituents.

1.1 Structural diversity

From a biogenetic standpoint, phytocannabinoids are hybrid compounds, derived from the merging of the mevalonate and polyketides pathways. All phytocannabinoids share a resorcinyl core decorated with *para*-orientated isoprenyl residues and an alkyl side chain. (Figure 2)

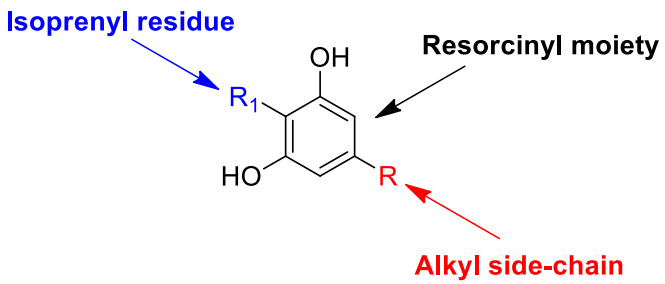

Figure 2 **Structural moieties of a general phytocannabinoid.**

Both the isoprenoid and the polyketide pathways are modular (Hanus & al., 2016), and this modularity represents the major diversification strategy used by the plant to diversify its phytocannabinoid profile, complemented by the oxidative and alkylative modifications of the resorcinyl core.

1.1.1 ISOPRENYL RESIDUE DIVERSITY

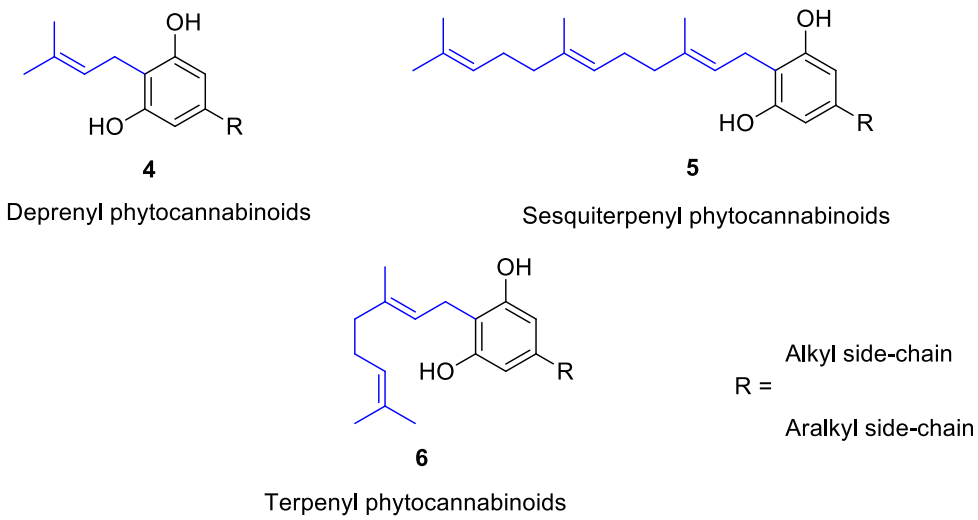

FIGURE 3 **GENERICAL CHEMICAL STRUCTURE OF C-5, C-10 AND C-15 ISOPRENYL PHYTOCANNABINOIDS.**

The isoprenyl residue can show a different oligomerization degree. The ketidic core is usually decorated by a C10 terpenyl moiety (*terpenyl series*, **6**), but analogues belonging to C15 *sesquiterpenyl* (**5**) or C5 *deprenyl series* (**4**) have been characterized both in *C. sativa* and in the taxonomically unrelated species that produce phytocannabinoids (Pollastro & al, 2011). (Figure 3)

Based on the connectivity of the isoprenyl moiety, phytocannabinoids can be classified in nine different type. (Scheme 1)

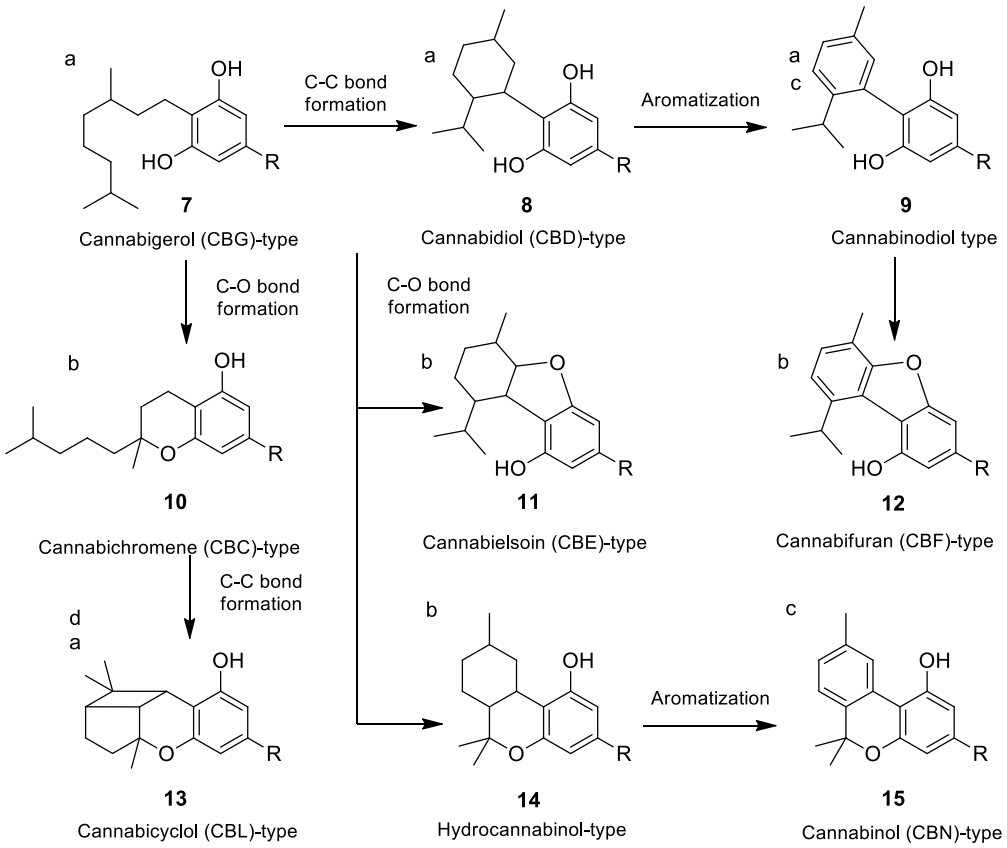

SCHEME 1 **MAJOR SKELETAL TYPES OF PHYTOCANNABINOIDS. A) C-C CONNECTIVITY LINEAR (7), MONOCYCLIC (8 AND 9) OR BICYCLIC (13). B) C-O CONNECTIVITY FROM LINEAR PRECURSORS (10) OR MONOCYCLIC PRECURSORS (14, 11 AND 12). C) AROMATIZATION (9 AND 15). D) CLOSURE OF ADDITIONAL C-BOND (13).** *SOURCE: (HANUS & AL., 2016)*

Despite the remarkable diversity associated to the isoprenyl residue, most phytocannabinoids have been characterized as minor or even trace constituents of *C. sativa*. The most abundant phytocannabinoids have been referred to as the "big four" and are *Δ^9-tetrahydrocannabinol* (Δ^9-THC, **16**), *cannabidiol* (CBD, **2**), *cannabigerol* (CBG, **18**) and *cannabichromene* (CBC, **17**). Another major, albeit not genuine, phytocannabinoid is *cannabinol* (CBN, **1**). (Figure 4)

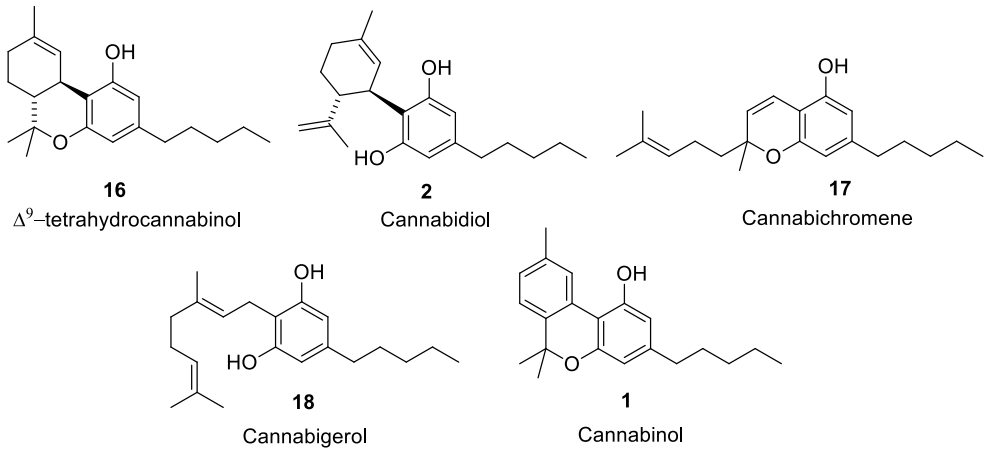

FIGURE 4 **MAJOR PHYTOCANNABINOIDS OF *C. SATIVA*.**

1.1.2 ALKYL SIDE-CHAIN DIVERSITY

The phytocannabinoids in *C. sativa* show an alkyl side-chain with an odd number of carbons, generally a *n*-pentyl side-chain (*olivetoids*, **19**), or less commonly, methyl chain (*orcinoids*, **21**), *n*-propyl chain (*varinoids*, **20**) and *n*-heptyl chain (*phoroloids*, **22**). (Figure 5) While the varinoids are fairly frequent, the orcinoids are much more prevalent in *Rhododendron* species and the phoroloids were isolated only in a specific *Cannabis* variety (Citti & al., 2019). Compounds with an even number of carbons (**23** & **24**), although very rare, have been recently isolated – as trace constituents – from FM2 variety (Citti & al, 2019) (Linciano & al., 2020). (Figure 5)

The odd-numbered alkyl phytocannabinoids are derived from an acetate ketide started, while compounds with an alkyl chain with an even number of carbons are presumably derived from a propionate starter. Modification in the alkyl side chain are not the result of modifications associated to mold contamination (Kajima, 1982) (Robertson & al., 1975). Phytocannabinoids characterized by an aromatic ketide moiety are named *aralkyl phytocannabinoid* (**25**, **26** & **27**) and are also known in the literature as *prenylated bibenzyls* (Hanus & al., 2016) (Pollastro & al., 2017. (Figure 5)

Compounds of this type do not occur in *C. sativa,* but have been isolated from both higher (*Helichrysum, Amorpha, Glycyrrhiza* and other genera) and lower (liverworts from the *Radula* genus) plants (Fuhr & al., 2015) (Pollastro & al., 2017).

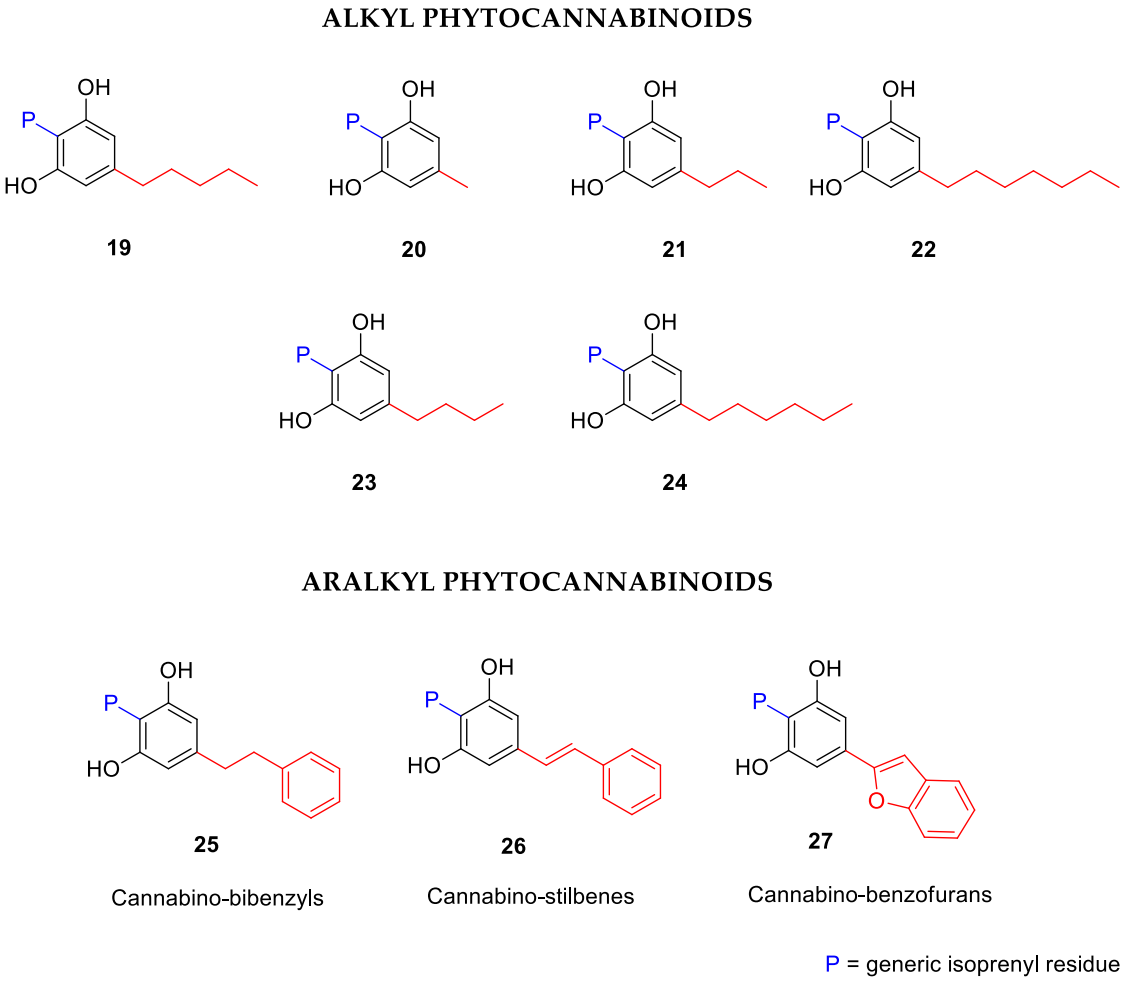

FIGURE 5 **ALKYL AND ARALKYL PHYTOCANNABINOID SERIES.** *SOURCE: (HANUS & AL., 2016)*

1.1.3 RESORCINYL MOIETY DIVERSITY

The most important modification of the resorcinyl moiety is carboxylation since the native form of phytocannabinoids is the carboxylated one. When both phenolic

hydroxyls are free, only one carboxylated form is possible, as exemplified by CBGA (**30**). (Figure 6)

Conversely, two isomeric forms can exist when one of the two oxygen atoms is alkylated, and the resorcinyl core has lost its symmetry plane. The two forms (**31** & **32**) have been isolated for Δ^9-THC and showed very different thermal stability. (Figure 6)

The A-form (**28**), with an intramolecularly H-bonded carboxyl was easily decarboxylated, while the B-form (**29**) was thermally stable (Shani & and Mechoulam, 1974). Remarkably, only one form was isolated for CBC, probably due to its tautomeric equilibrium in which type-1 pre-cannabinoid is favoured by the H-bond between the phenolic hydroxyl and the carboxylic acid. (see Subsection 3.1)

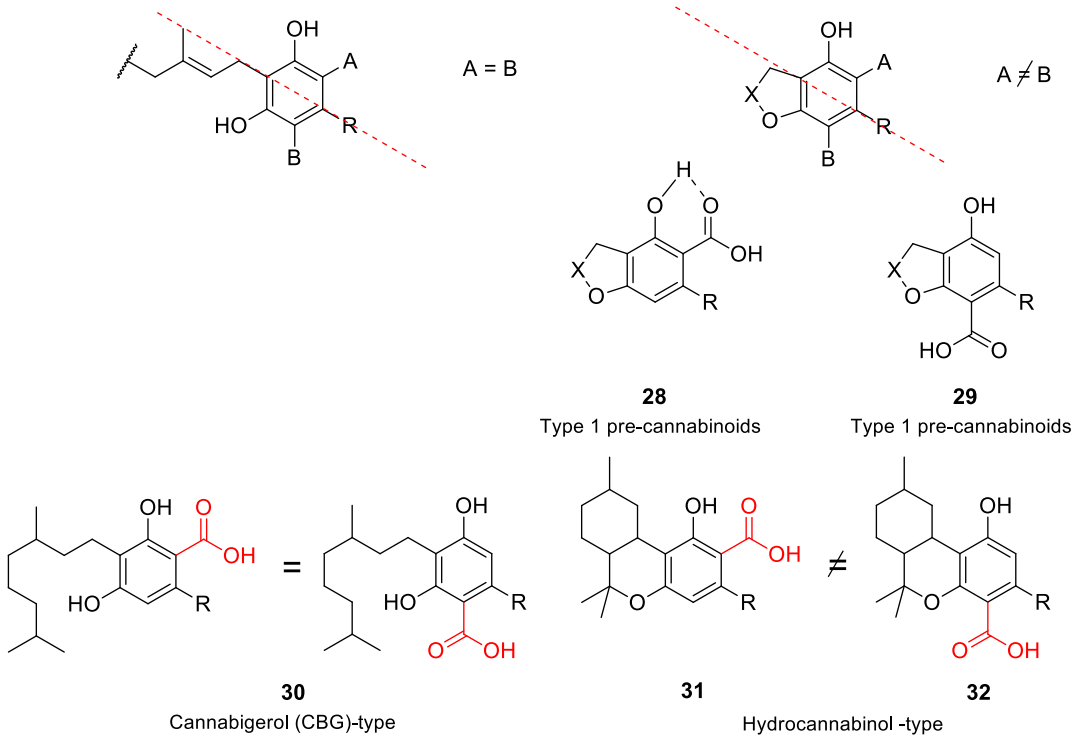

FIGURE 6 **PLANE OF SYMMETRY IN A GENERIC PHYTOCANNABINOID SKELETON WITH A SINGLE BOND BETWEEN THE ISOPRENYL MOIETY AND THE AROMATIC CORE. (SX) ISOMER TYPE 1 (28) AND TYPE 2 (29) OF PRE-CANNABINOIDS. (DX)** *SOURCE: (HANUS & AL., 2016)*

In the living plant decarboxylation is slow, but after harvesting it undergoes acceleration, promoted by light exposure and heat (Wang & al., 2016). The mechanism of the light-promotion is unclear.

Two additional modifications of the resorcinyl core have been reported, namely *O*-methylation and oxidation to quinoid forms.

O-Methylation has been documented on phytocannabinoids having two free hydroxyls. (Figure 7)

These compounds are also easily oxidized to quinoid forms, prone to dimerization. Monomethylated forms have been reported for the *n*-pentyl- and shorter versions of CBD and CBG, while only two cannabinoquinoids have been isolated, also on account of the instability of this type of compounds.

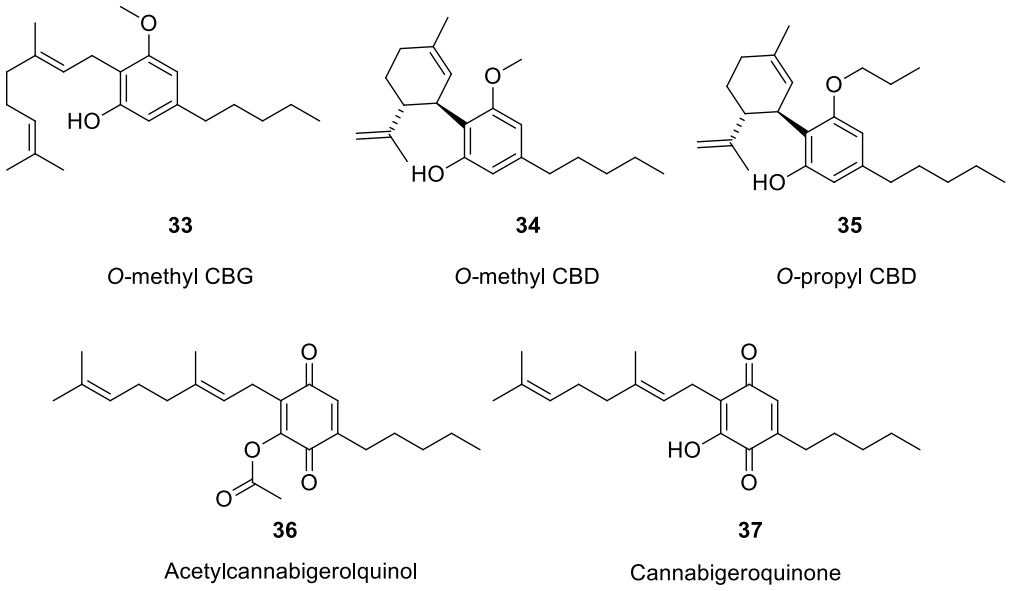

FIGURE 7 **SOME EXAMPLES OF *O*-ALKYL PHYTOCANNABINOIDS AND QUINOIDS ANALOGUES ISOLATED FROM *C. SATIVA*.** *SOURCE: (TATSUO & AL., 1968) (SHOYAMA, 1972) (HENDRIKS & AL., 1978) (RADWAN & AL., 2008) (HUSNI & AL., 2014)*

Based on the topological relationships between the isoprenyl residue and the side-chain, phytocannabinoids cab be sorted out in compounds from the *normal* series **38** (*para*-resorcinyl substitution), and the *abnormal* one **39** (*ortho*-resorcinyl substitution). (Figure 8)

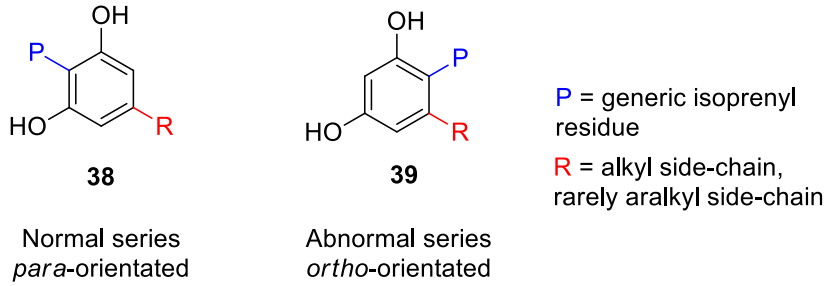

FIGURE 8 **GENERAL STRUCTURE OF NORMAL AND ABNORMAL SERIES OF PHYTOCANNABINOIDS.** *SOURCE: (HANUS & AL., 2016)*

2. THE BIOSYNTHESIS OF PHYTOCANNABINOIDS

2.1 CELLULAR LOCALIZATION

Phytocannabinoids are synthesized in specialized cells, which form the head of secretory structures (*trichomes)* that are common in plants, but whose morphology (Wagner, 1991) and contents (Dayanandan, 1976) are highly differentiated. The role of trichomes is not precisely know. They presumably protect plants from different stress, both physical [*hydric* (reduction of transpiration), *thermal* (freeze resistance), *luminous* (light reflectance)] and *biological* (herbivores and insects deterrence) (Hartsel J.A., 2016) (Clarke R., 1981) (Krings M., 2002). A specialized class of trichomes, the *glandular trichomes*, accumulate sticky resins containing compounds for predators (Hülskamp, 2004) (Taura F. S., 2007). *C. sativa* contains different types of trichomes (Table 1). The *nonglandular* trichomes cover all the surface of the plant and are not involved in cannabinoids and terpenoids accumulation. Both of staminate (male) and pistillate (female) plants present three types of glandular trichomes, namely *bulbous*, *capitate-sessile* and *capitate-stalked* (Happyana, 2013). Their main location are inflorescences, on bracts and new leaves, near each apical tip (Kimura, 1970) (Steinberg, 1975) and a small amount on stems. Roots and seeds have no trichomes and therefore lack cannabinoids, whose only site of storage is represented by glandular trichomes (Figure 9).

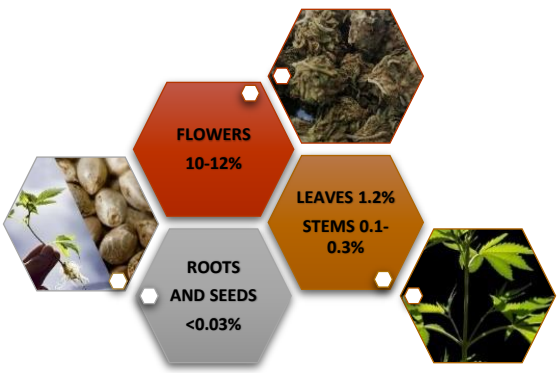

FIGURE 9 **DISTRIBUTION OF PHYTOCANNABINOIDS IN PLANT.**

Trichomes

Classification	Structure	Distribution	Timing of development
Nonglandular trichomes	1) **Noncystolithic trichomes**: long, unicellular, hair-like appendages, highly silicified 2) **Cystolithic trichomes**: short hairs (from 150 µM to 220 µM), more squat, unicellular, claw shape, , containing calcium carbonate	Lower side of vegetative leaves and pistillate bracts	Decrease with age
Glandular trichomes	1) **Bulbous**: with smallest gland 2) **Capitate-sessile**: the structure is simple, and the trichomes head connected directly to the mesophyll cells 3) **Capitate-stalked**: the structure more complex, they developed resin head. They are identifiable by mushroom-like stalk and head appearance	Vegetative leaves and pistillate bracts Bracts and floral leaves	Increase with age
Antherial sessile trichomes	Large size, with a diameter of approximately 70-80 µm	Underside of the anther lobes	

TABLE 1 ***CANNABIS*** **TRICHOMES TYPES.** *SOURCE: ADAPTED FROM (FARAG S., 2017) (DAYANANDAN, 1976)*

Male plants bear fewer glandular trichomes than female ones and, therefore, produce lower amounts of cannabinoids and terpenes (Farag S., 2017). Despite this, a specific male glandular trichome has been found on the anthers (Fairbairn, 1972), referred to as *antherial sessile* trichome. All glandular trichomes synthesize and store cannabinoids, but their capacity to store them varies considerably (Mahlberg P.G., 2004). The small bulbous trichomes lack cannabinoids (Hartsel J.A., 2016), that are primarily stored in the capitate-sessile and capitate-stalked trichomes. The first ones produce cannabinoids during all plant life cycle, but in lower levels compared to the latter, which probably arises from the capitate-sessile form. As matter of fact, the

capitate-stalked form shows an additional stipe that sustains a hemispherical head. Both types have a globose top, like a mushroom head (Dayanandan, 1976), composed of two fundamental portions: 1) *disc cells* and 2) *secretory cavity*.

The *disc cells* are originated by an enlargement and a subsequent division of a single epidermal cell (Mahlberg P.G., 2004) in eight cells (capitate-sessile) or twelve or sixteen cells (capitate-stalked) (Livingston, 2020). The *secretory cavity* is a noncellular dome that raises above the *disc cells*. This is an intrawall space since it is included between the basal cells wall and the outer waxy "sheath", referred as to *cuticle*. The dimensions of the cavity enlarge as secretory vesicles are stored in it (Livingston, 2020) (Mahlberg P.G., 2004). (Figure 10)

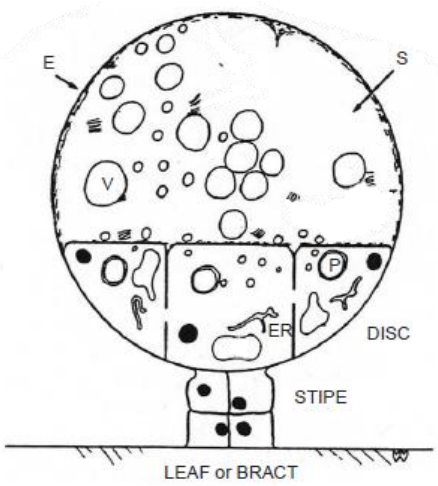

FIGURE 10 **GRAPHIC REPRESENTATION OF A CAPITATE-STALKED GLAND. ER, ENDOPLASMIC RETICULUM; P, PLASTID; V, VESICLE; S, SECRETORY CAVITY; E, CUTICLE.** *SOURCE: ADAPTED FROM (MAHLBERG P.G., 2004)*

The biosynthetic pathway of phytocannabinoids in *Cannabis* is complex, but has been largely clarified (Stout, 2012) (Gagne, 2012) (Luo, 2019). It takes place at different cell types and organelles, since it involves many biosynthetic steps, culminating with the condensation of the polyketide precursor (mostly *olivetolic acid*, OA) with the isoprenyl one (mostly *geranyl diphosphate*) (Fellermeier & Zenk, 1998).

2.2 ENZYMOLOGY

The biosynthesis of cannabinoids is assumed to take place directly in the anatomical structures that store them. *Olivetolic acid* (**40**) is produced in the ketide pathway from the Claisen condensation of the starter hexanoyl-CoA with three malonyl-CoA

molecules, generating a tetraketide-CoA that eventually aromatized via intramolecular crotonization (Fellermeier M. e., 2001) (Rahajo, 2004). This biosynthetic pathway is catalysed by specific polyketide synthases (PKSs) and takes place in cytosol of disc cells (Gülck, 2020). The starter *hexanoic acid* is most likely produced by the degradation of palmitic acid or a C18 unsaturated fatty acid (Stout, 2012). This view is supported by the high *desaturase*, *lipoxygenase* (LOX), and *hydroperoxide lyase* (HPL) activity of glandular trichomes (Livingston, 2020). Hexanoic acid is activated by conversion into hexanoyl-CoA by a specific *acyl-activating enzyme* (AAE) (Stout, 2012). Two types of these enzymes have been identified, *Cannabis sativa hexanoyl-CoA synthase 1* (CsHCS1 or CsAAE1) and *Cannabis sativa hexanoyl-CoA synthase 2* (CsHCS2 or CsAAE2), with CsAAE1 surely involved in this pathway due to its high concentration in trichomes, its high affinity for short-chain fatty acids and its location in cytosol (Hazekamp A, 2010). Malonyl-CoA derive from acetyl-CoA by the action of *acetyl-CoA carboxylase*, which catalyses this specific ATP-dependent carboxylation (Chen, 2011). The PKS *olivetol synthase/tetraketide synthase* (OLS/TKS) and olivetolic acid cyclase (OAC) catalyse the formation of tetraketide-CoA intermediate and then the C2-C7 intramolecular aldol condensation, leading to OA (Taura F. e., 2009) (Gagne, 2012). The existence of additional ketide synthases has been demonstrated (Kajima, 1982): they use different starters, acetyl-CoA or butanoyl-CoA (Valliere, 2019) (Luo, 2019) and are responsible for the production of phytocannabinoids with "shortened" alkyl side chains, having three- (*divarinolic acid*, **41**) or one carbons (*orcinolic acid*, **42**) (Hanus et al. 2016). (Figure 11) The biosynthesis of phytocannabinoids with an even number of carbons is unclear, but they could originate from a starter having an odd number of carbons, like propionic or valeric acid.

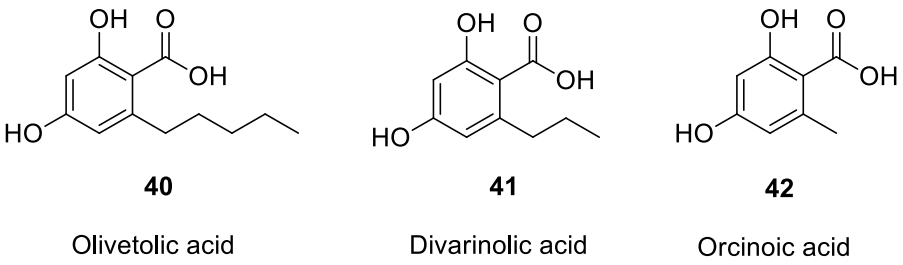

FIGURE 11 **CHEMICAL STRUCTURE OF MAIN AROMATIC PRECURSORS OF PHYTOCANNABINOIDS.**

The isoprenyl moiety is the main differentiation element of phytocannabinoids, and is synthesized from a common precursor, geranyl diphosphate (GPP), from which also the terpenes of the essential oil derive.

Terpenoids are the major group of bioactive natural compounds of plants (Gülck, 2020). In *Cannabis* mono- and sesquiterpenes and their mixtures are responsible of plant's fragrance but could also present some medicinal attributes due to the possible synergy with phytocannabinoids, for which, however, no proof has been presented so far. Monoterpenes are produced in chloroplasts (plastids), while sesquiterpenes are synthesized in cytosol, and are eventually stored in the extracellular cavity as vesicles (Mahlberg P.G., 2004). The biosynthetic pathway of *Cannabis* isoprenoids provides two steps common for both of phytocannabinoids and terpenes:

1. Production of intermediates, as *C5 isoprenoid isopentyl diphosphate* (IPP) and *dimethylallyl diphosphate* (DMAPP), by the plastidial *methylerythritol phosphate* (MEP) pathway or the cytosolic *mevalonate* (MEV) pathway.
2. Condensation between IPP and DMAPP units by different prenyltransferases to provide elongated isoprenoid diphosphate, like GPP or farnesyl diphosphate (FPP).

At this point, two different pathways could be followed:

1. Mono- and sesquiterpenes originate by dephosphorylation and subsequent rearrangement of GPP or FPP, give acyclic or cyclic terpenoids (terpenes and sesquiterpenes); (Scheme 2)
2. Phytocannabinoids originate by Friedel-Craft isoprenylation of resorcinyl aromatics. (Scheme 2)

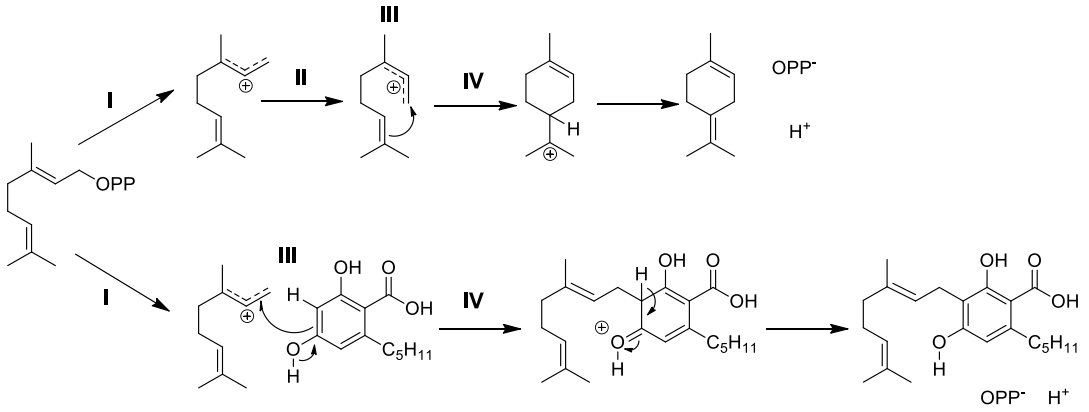

SCHEME 2 **TWO ALTERNATIVES PATHWAYS FOR GPP.** *SOURCE: ADAPTED FROM (BOOTH, 2020)*

From a mechanistic standpoint, the phytocannabinoids pathway can be considered a modification of the classic terpenoid biosynthesis, where the allyl cation generated by ionization of an allyl phosphate is trapped by an activated aromatic, before its rearrangement or intramolecular trapping (Clarke R. a., 2013). (Figure 12)

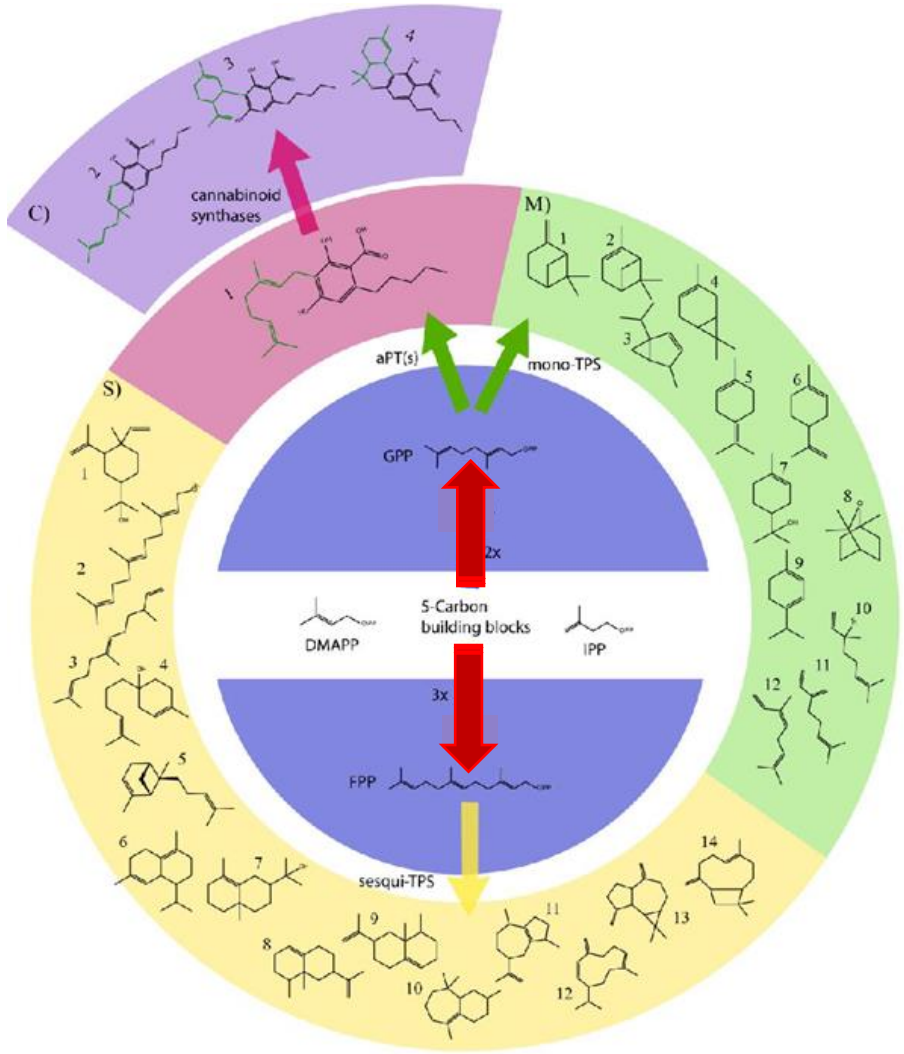

FIGURE 12 **SOME POSSIBLE DESTINIES OF IPP AND DMAPP AFTER CONDENSATION IN *C. SATIVA*.** *SOURCE: ADAPTED FROM (BOOTH, 2020)*

In chloroplasts, IPP and DMAPP are obtained via MEP pathway (98%) from pyruvate and glyceraldehyde-3-phosphate (Fellermeier M. e., 2001), and their head-to-tail condensation is assisted by two forms of the same enzyme, referred to as *geranyl diphosphate synthase* and *neryl diphosphate synthase* (Burke, 1999). However, the major product is *geranyl diphosphate* (**43**) rather than *neryl diphosphate* (NPP, **44**). (Figure 13)

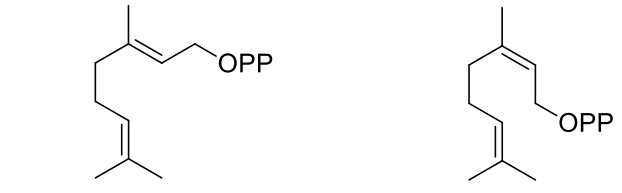

43 Geranyl diphosphate

44 Neryl diphosphate

FIGURE 13 **PRINCIPAL TERPENYL MOIETY PRECURSORS IN PHYTOCANNABINOIDS BIOSYNTHESIS.**

The resorcinyl moiety is prenylated by a specific enzyme, referred to as *geranyldiphosphate:olivetolate-geranyltransferase* (GOT = CBGAS) (Fellermeier & Zenk, 1998). GOT belongs to the transmembrane *aromatic prenyltransferases family* (aPT), shows a Mg^{2+}-dependent enzymatic activity, and is located into the plastidial wall; however, it is not known on which plastidial membrane GOT is present (external, internal, tiliacoidal), and especially if its active site faces the inside or outside of the membrane (Gülck, 2020).

The aromatic binding site of GOT is promiscuous, accepting not only OA, but also divarinic/orcinolic acids as well as *naringenin*, *phlorisovalerophenone*, and *resveratrol* (Page, 2012). On the other hand, the isoprenyl binding site accepts only GPP and NPP as prenyl donors. The CBGA/*cis*-CBGA is usually 2:1, but it changes to 1:1 when CBGAS uses NPP instead of GPP.

Cannabigerolic acid (CBGA, **45**) is the main meroterpenoid synthetised by GOT in trichomes. *Cannabinerolic acid* (CBNRA) and *cannabigerovarinic acid* (CBGVA), are produced in a similar way (Dagenhardt & al., 2017). (Scheme 4)

Despite its promiscuous activity, GOT shows, however, a minor affinity for these resorcinolic acid homologs of OA (Luo, et al., 2019). (Scheme 4)

CBGA is the central precursor of all other acidic phytocannabinoids (Δ^9-THCA **48**, CBDA **47** and CBCA **46**) (Fellermeier & Zenk, 1998). Since CBGA has the lowest

oxidation degree for the isoprenyl moiety, it was suggested being the common precursor by Mechoulam already in 1964 (Gaoni & al., 1964).

The other phytocannabinoids are derived from the oxidative cyclization of CBGA carried out by specific cyclases, also called THCAS, CBDAS and CBCAS. (Scheme 3) These enzymes are cytoplasmatic, and located in the ER (Booth, 2020), making it possible accumulation in secretory cavities. All these enzymes are FAD-dependent, and their products are toxic to plant cells, even from *Cannabis*, highlighting the relevance of accumulation in specific vesicles (Sirikantaramas, 2005). Furthermore, the oxidative cyclases require molecular oxygen for their activity, and generates hydrogen peroxide, a compound toxic to plant cells (Sirikantaramas, 2004). An electrophilic cyclization is responsible for the formation of the cyclohexene ring of CBDA and Δ^9-THCA (Hanus & al., 2016).

The corresponding intermediate shows a C-8 cation (*p*-menthane numbering) whose behaviour depends on the nature of the active site of the cyclase: in CBDAS the enzyme works as a Broensted base, accepting a proton from C-9, with formation of a double bond. Conversely, in THCAS termination takes place by trapping of the C-8 cation by one the *ortho* phenolic hydroxyls, leading, in principle, to a pair of isomers (Δ^9-THCA-A **48** and Δ^9-THCA-B **49**). Despite the actual isolation of Δ^9-THCA-B from *C. sativa*, the enzyme only generates Δ^9-THCA-A (Shoyama & al., 2005). (Scheme 3)

CBCA results instead from an electrocyclic cyclization (Morimoto & al., 1998).

The pivot of this alternative oxygen-independent pathway is the generation of a *quinone methide* from the isomerised benzallyl cation (Scheme 3) (Hanus & al., 2016).

Unlike CBDA and THC which are chiral products with a *trans* absolute configuration (Šantavý, 1964), CBCA is scalemic. It is not known if racemization occurs during decarboxylation, and the optical purity of CBCA is unknown.

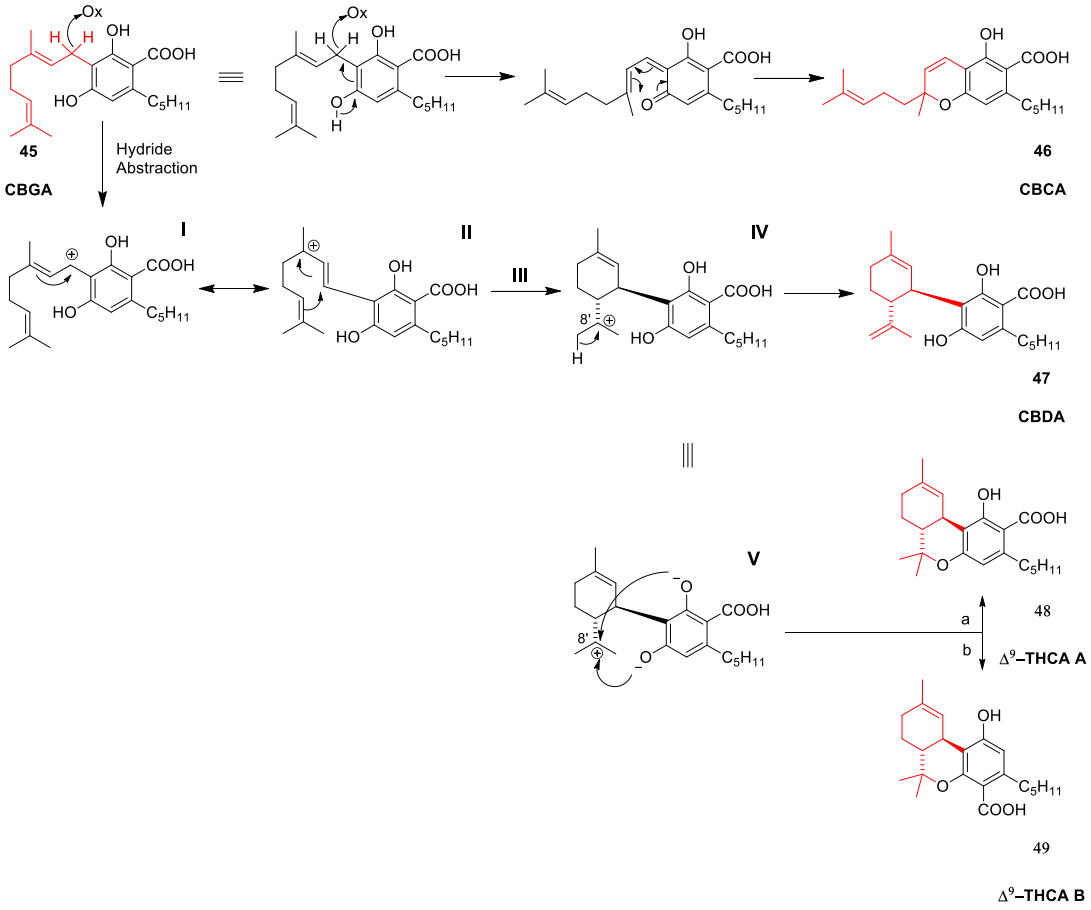

SCHEME 3 **BIOSYNTHETIC PATHWAY OF THE MAJOR PHYTOCANNABINOIDS.** *SOURCE: (HANUS & AL., 2016)*

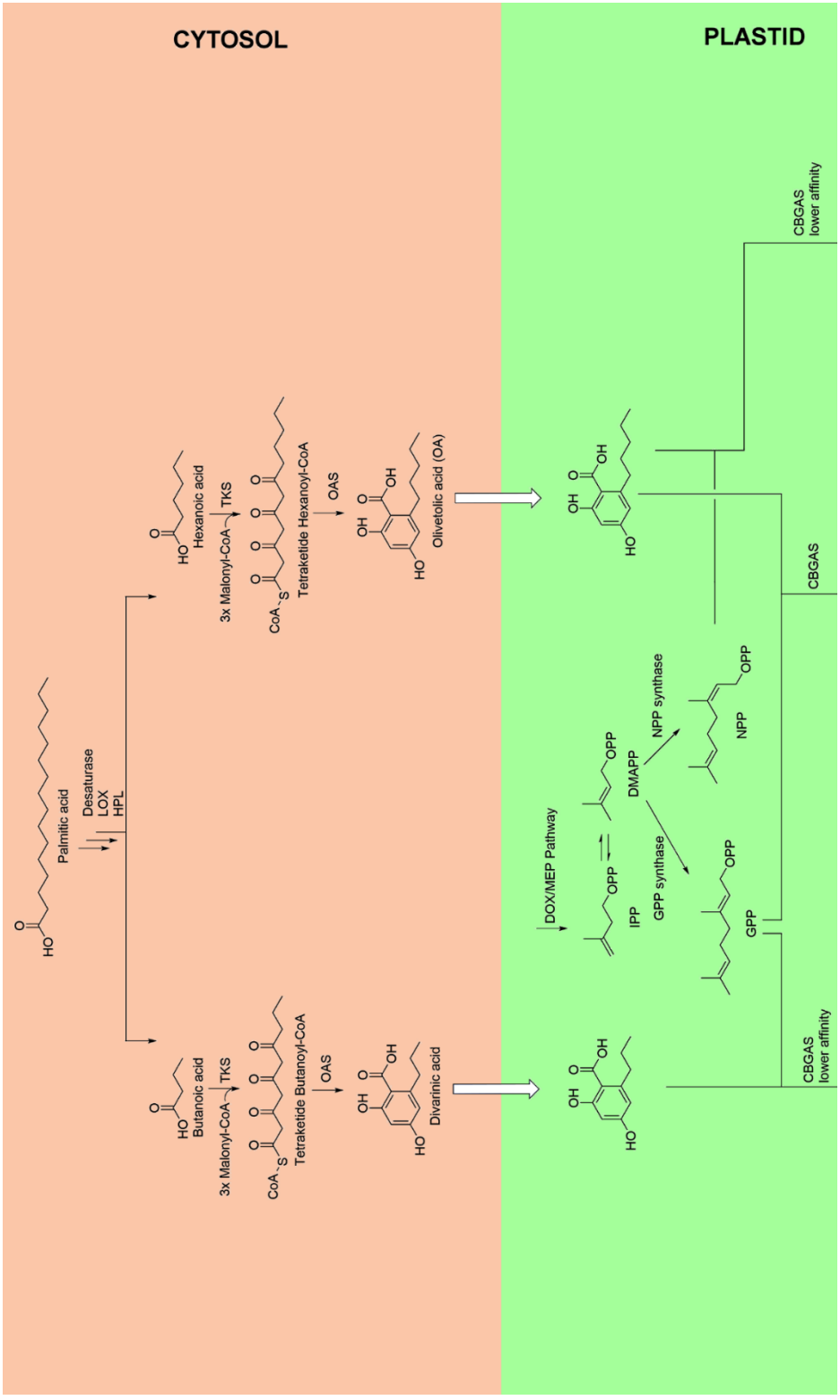
CYTOSOL
PLASTID
Palmitic acid
Desaturase
LOX
HPL
Hexanoic acid
TKS
3x Malonyl-CoA
Tetraketide Hexanoyl-CoA
OAS
Olivetolic acid (OA)
Butanoic acid
TKS
3x Malonyl-CoA
Tetraketide Butanoyl-CoA
OAS
Divarinic acid
DOX/MEP Pathway
IPP
DMAPP
NPP synthase
GPP synthase
NPP
GPP
CBGAS
lower affinity
CBGAS
CBGAS
lower affinity

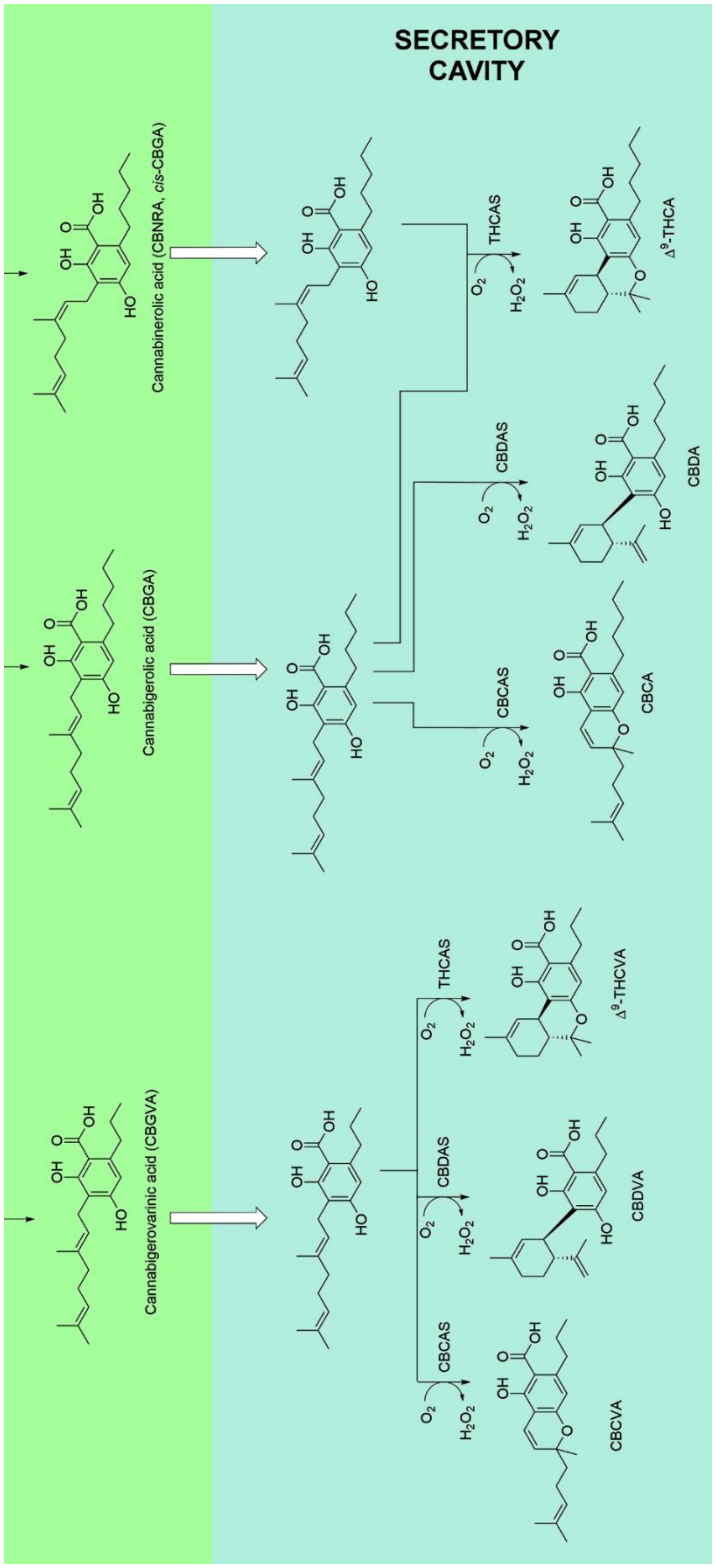

SCHEME 4 **BIOSYNTHETICAL PATHWAY OF MAJOR CANNABINOIDS IN GLANDULAR TRHICOMES FROM PRIMARY TO SECONDARY METABOLITES.** *SOURCE: (DEGENHARDT & AL., 2017) (GÜLCK, 2020)*

3. THE CHEMOTYPE DIVERSITY OF *C. SATIVA*

Phytocannabinoids are the hallmark of *C. sativa*, but their profile of occurrence is highly variable, and this has been proposed as a taxonomic criterium to classify the diversity of the plant. A first system is based on the ratio between the narcotic compound Δ^9-THC and its non-narcotic analogue CBD. The *Δ^9-THC-rich* and *CBD-poor* specimens are classified as "drug-type", while those *Δ^9-THC-poor* and *CBD-rich* are classified as "fiber-type" (Kojoma M. S., 2006) (Lydon J. a., 1987), a classification that goes beyond morphological features (Meijer & Keizer, 1996). Two well-known taxonomic classification use phytocannabinoids as a discriminant criterion:

1. using the Δ^9-THC:CBD ratio, Small and Cronquist (1976) identified a single species (*C. sativa* L.), declined in two subspecies (*sativa* and *indica*), with each subspecies having two varieties (*wild* and *domesticated)*.
2. Hilling and Mahlberg (2004) identified two distinct species (*C. sativa* and *C. indica*), with the terms *sativa* and *indica* having a different meaning from the previous taxonomic systems (Small & Cronquist, 1976) (Anderson, 1980) (Schultes & al., 1974).

Genetically speaking, the alleles B_T- and B_D code for the transcription of the cyclases that generate THC and CBD, respectively, and are characterized by co-dominance. There has also been an intense and artificial human selection through ages, and it is questionable is really spontaneous hemp plant exist nowadays. Genes for the production of phytocannabinoid are inherited independently from those governing plant morphology. For these reasons, a taxonomic classification solely based on phytocannabinoids seems to be improper (de Meijer E., 2014).

To phytocannabinoid profile of *C. sativa* can be assessed using various chromatographic techniques:

- *High-Performance Liquid Chromatography* (HPLC) is the ideal method to quantify the native phytocannabinoids profile of a plant before decarboxylation. This analysis is the only one that can identify pre-cannabinoids without derivatization and avoiding their decarboxylation. The total amount of phytocannabinoids in a sample is the sum of the concentrations of neutral and acidic phytocannabinoids. (Figure 14)

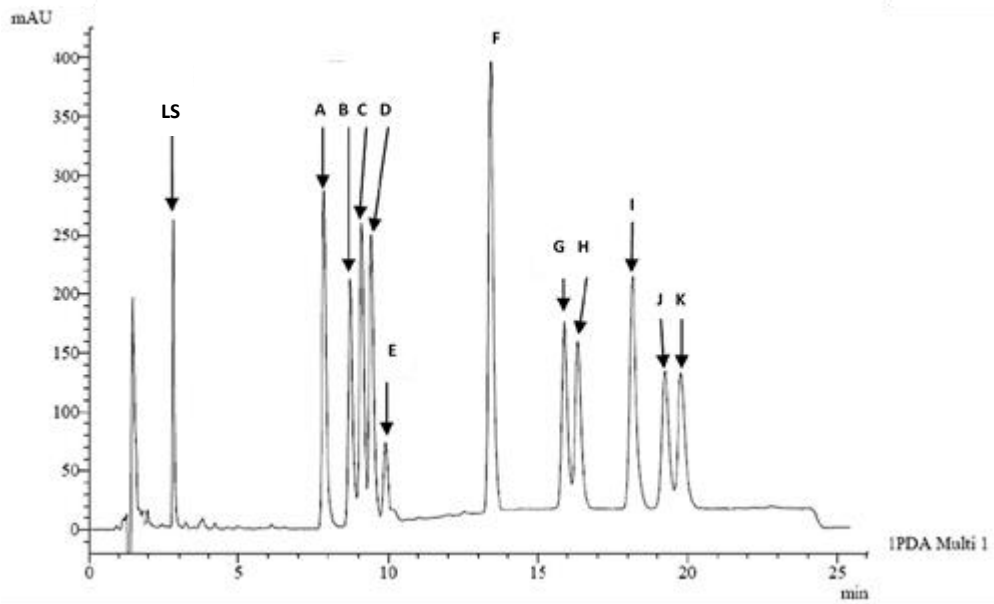

FIGURE 14 **EXEMPLIFICATIVE HPLC CHROMATOGRAM OF A MIXTURE OF PHYTOCANNABINOIDS.** *LEGEND*: **A),** *CBDA*; **B),** *CBGA*; **C)** *CBG*; **D)** *CBD*; **E),** *Δ^9-THCV*; **F)** *CBN*; **G),** *Δ^9-THC*; **H),** *Δ^8-THC*; **I)** *CBL*; **J)** *CBC*; **K)** *THCAA*. *SOURCE: ADAPTED FROM (GUIL & AL., 2015)*

- *Gas Chromatography* (GC) is the more popular method of analysis to quantify phytocannabinoids and the volatile terpenes of the essential oil. (Figure 16) Due to the working temperatures, pre-cannabinoids are decarboxylated, simplifying the phytochemical profile. In this case the total content of phytocannabinoids in the plant sample corresponds to the neutral phytocannabinoids amount measured by the instrument. To perform a GS

analysis of pre-cannabinoids it is necessary protecting through silylation (**51**) the phenolic hydroxyls and carboxylic residues (**50**) (Figure 15)

In this way, the spontaneous decarboxylation is avoided.

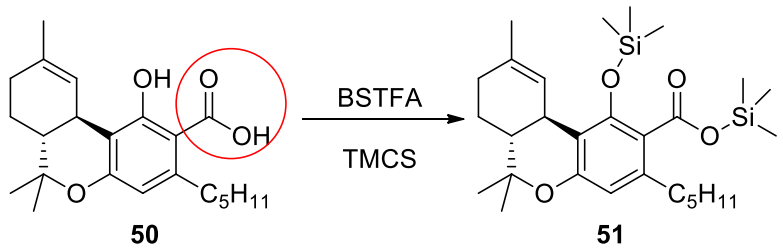

FIGURE 15 **SILYLATION OF CARBOXYLIC MOIETY OF THCA BY N,O-BIS(TRIMETHYLSILYL)TRIFLUOROACETAMIDE.**

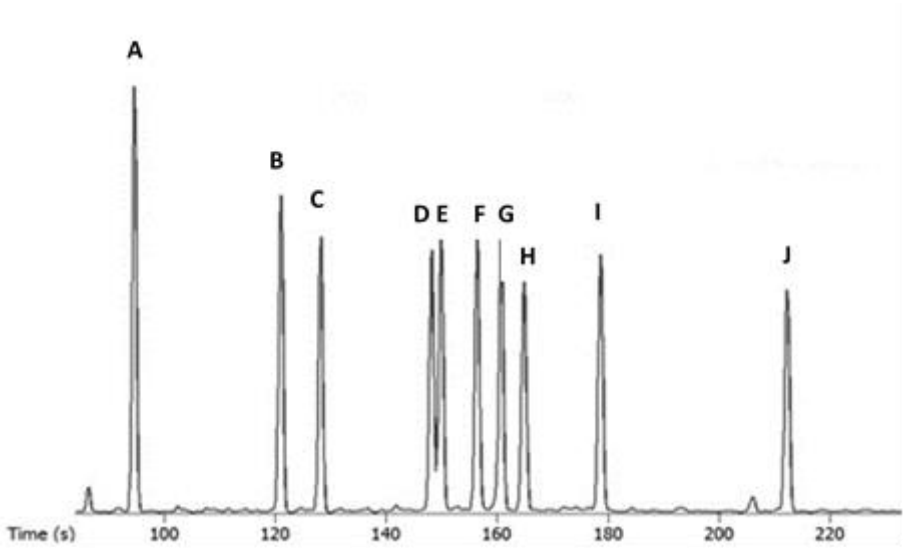

FIGURE 16 **EXEMPLIFICATIVE GC CHROMATOGRAM OF A SILYLATE PHYTOCANNABINOID MIXTURE.** *LEGEND*: **A)** *CBDV*-**2TMS**; **B)** *CBD-2TMS*; **C)** *THCV-1TMS*; **D**) *CBC-1TMS*; **E)** *CBG-2TMS*; **F)** *Δ^8-THC-1TMS*; **G)** *Δ^9-THC-1TMS*; **H**) *CBDA-3TMS*; **I)** *CBN-1TMS*; **J)** *Δ^9-THCA-2TMS*. *SOURCE: ADAPTED FROM (RIGDON, 2015)*

3.1 INHERITANCE

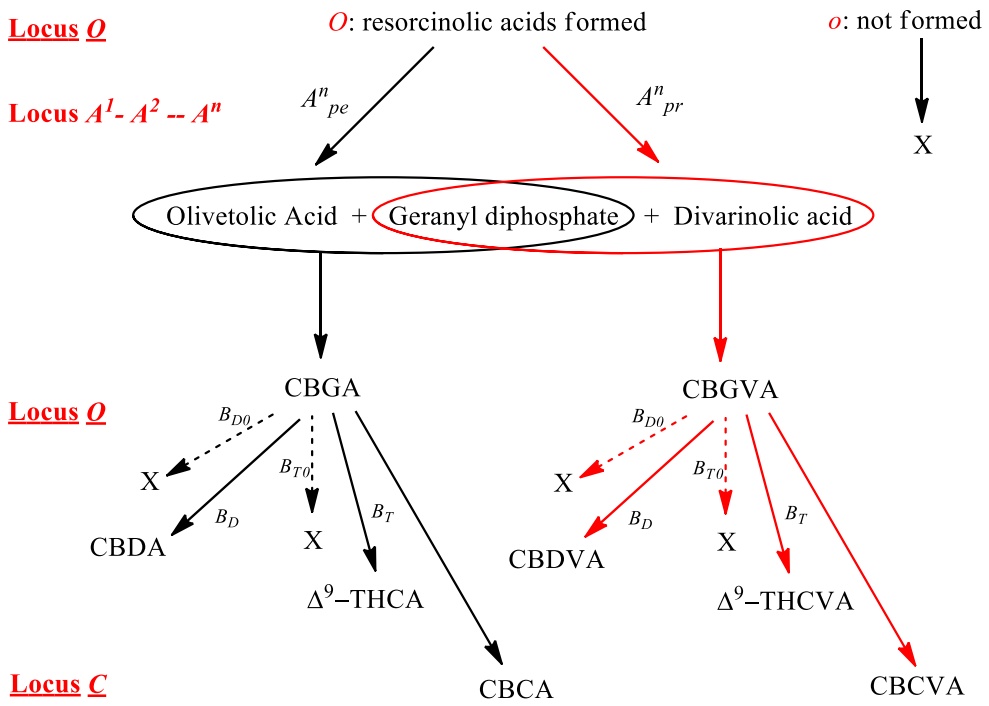

FIGURE 17 **PROPOSAL OF GENETIC MODEL FOR CHEMOTYPE INHERITANCE.** *SOURCE: ADAPTED FROM (DE MEIJER E. , 2014)*

In terms of genetic inheritance (Figure 17), the assumption is done that the various steps of the biosynthesis of phytocannabinoids are associated to single specific alleles combinations and loci:

- *locus O* controls the synthesis of the resorcinyl moiety, with two possible allelic modifications: a) a mutant null allele *o* (leading to a cannabinoid-free chemotype in the homozygous state), and b) a wild type *O* (no interference). The null allele *o* have shown a dominant repressive behaviour since the *O*/*o* genotypes has a 1:10 ratio of the phytocannabinoids amount of the *O*/*O* genotypes;

- *locus A* defines the nature of the alkyl residue, namely if CBGA or CBGVA is formed. The locus carries the alleles $A_{pe}^{1\ to\ n}$ (encoding for OA and subsequently for cannabino-olivetoids) and $A_{pr}^{1\ to\ n}$ (encoding for divarinolic acid and consequently for cannabino-varinoids). Since the propyl:pentyl cannabinoid ratio is not 1:1, the codominant *A* alleles influence the chemotype differently. The synthesis of CBGA or CBGVA by GOT does not present allelism signs: the enzyme seems to be sufficiently promiscuous to catalyse the prenylation of both resorcinyl intermediates;
- *locus B* regulates the oxidative cyclization of CBGA and CBGVA, leading to Δ^9-THCA/Δ^9-THCVA (allele B_T) and CBDA/CBDVA (allele B_D) (de Meijer & al., 2003). Since B_T and B_D are codominant, heterozygous specimens have great amounts both of Δ^9-THCA/Δ^9-THCVA and CBDA/CBDVA; however, the ratios of Δ^9-THCA/CBDA and Δ^9-THCVA/CBDVA are not 1:1. Probably the different catalytic properties of these synthase are related to sequence modulations in B_T and B_D alleles. In locus *B* are also located recessive and minimally or non-functional alleles (called as B_{T0} an B_{D0}) that in a homologous state induce an accumulation of CBGA/CBGVA and a slight Δ^9-THCA/Δ^9-THCVA synthesis (de Meijer & Hammond, 2005) (de Meijer E., 2014);
- *locus C* is responsible for the oxidative electrocyclization of CBGA to CBCA (de Meijer & al., 2009a). Locus *C* shows no allelism, but the CBCA/CBCVA is highly variable within different chemotypes.

  Since the CBCA contents depends on the plant life-cycle, CBCAS might compete with THCAS, and CBDAS for CBGA only in the juvenil stage (Morimoto & al., 1997). This hypothesis has been demonstrated generating morphological mutations (reduction of capitate-stalked trichomes and

increase of capitate-sessile ones) by modulating the *PJG* genes. This "*pjc*" chemotype is not inducible in a "wild type" status specimen.

3.2 TAXONOMY

Depending on the expression of these alleles, chemotypes can be classified in six broad families.

1. THCA-predominant chemotype
2. CBDA-predominant chemotypes (I and II)
3. CBGA-rich chemotype
4. Cannabinoid-free chemotype
5. CBCA-rich chemotype
6. Cannabivarinoids-rich chemotype

3.2.1 THCA-PREDOMINANT CHEMOTYPE

The THCA content is very high, and the CBDA/THCA ratio is obviously low (Pacifico & al., 2006). (Table 2 & Figure 18)

This THCA-predominant chemotype shows a "wild type" condition in alleles at the loci *O, A, B,* and the loci related to *PJG genes*. The generic definition "drug-type" could be improper because also certain fiber strains, coming from the Far-Eastern, belong to this chemotype.

The illegal and recreational market let the circulation of numerous THCA-predominant chemotype clones, whose identity and stability cannot be ensured.

Nowadays, a limited number of THCA clones obtained *Plant Breeders Rights*, as the cultivars used for the *Sativex*® production (de Meijer E., 2014).

	Purity of THCA **in total cannabinoid fraction** (% w/w)	Total **cannabinoid** content/**dry inflorescences (bred clones)** (% w/w)	Total **cannabinoid** content/**dry inflorescences (landrace materials and fiber strains)** (% w/w)
THCA-predominant chemotype	96-98%	25-30%	2-5%

TABLE 2 **QUANTITATIVE ASPECT OF THCA-PREDOMINANT CHEMOTYPE.** *SOURCE: (DE MEIJER E., 2014)*

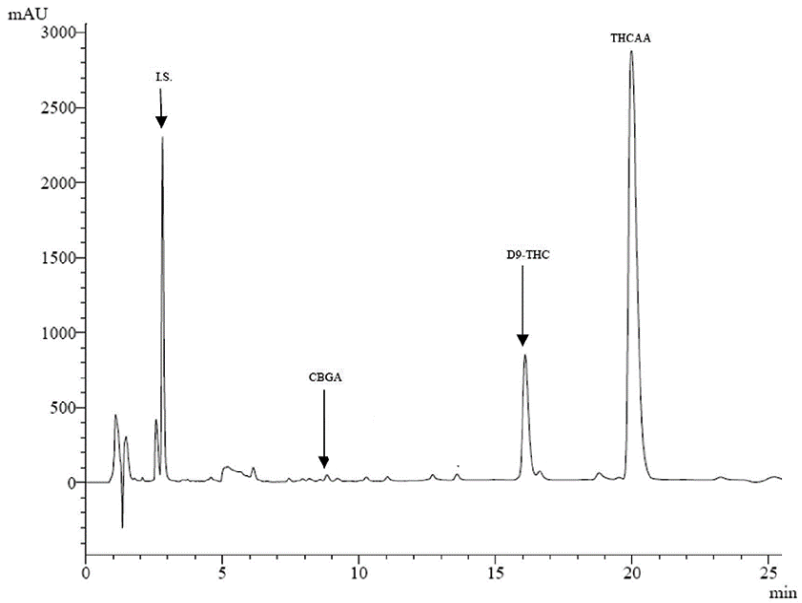

FIGURE 18 **EXEMPLIFICATIVE HPLC CHROMATOGRAM OF AN THCA-PREDOMINANT CHEMOTYPE.** *SOURCE: ADAPTED FROM (GUL & AL., 2015)*

3.2.2 CBDA-PREDOMINANT CHEMOTYPE

In the type I, CBDA is predominant, and shows a "wild type" status fixed in modern fiber and seed hemp cultures, but also present in hashish landraces. Despite the CBDA predominance, this chemotype synthesizes also THCA, and this might be

detrimental for the cultivation of fiber and seed specimens with a fairly high cannabinoid content. Even though the CBDA/THCA ratio is close to 1 (0.5 to 3.0), there is always a weak CBDA prevalence (chemotype II).

The "fiber type" or "no-drug type" strains belong to chemotype CBDA-predominant II, where the THCA content is lower than 0.3% (Pacifico & al., 2006). (Table 3, Figure 19 & Figure 20)

	Purity of CBDA in total cannabinoid fraction **(% w/w)**	**Total** cannabinoid **content**/dry inflorescences (bred clones) **(% w/w)**	**Total** cannabinoid **content**/dry inflorescences (landrace materials and fiber strains) **(% w/w)**	**THCA presence** in total cannabinoid fraction **(% w/w)**
CBDA-predominant chemotype	85-90%	25-30%	1-5%	0.3-5%

TABLE 4 **QUANTITATIVE AND QUALITATIVE ASPECT OF CBDA-PREDOMINANT CHEMOTYPE (I AND II).** *SOURCE: (DE MEIJER E. , 2014)*

The residual presence of THCA could be the result of multiple factors:

- photochemical conversion of CBDA (Lydon & Teramura, 1987);
- second minor cyclisation always carried out by CBDAS, whose gene developed from an ancestral THCAS gene (de Meijer E., 2014);
- THCAS homologous, which shows an aminoacidic difference due to a genetic polymorphism (Kojoma & al., 2006);
- non enzymatic reaction, since in this chemotype are found both of cis and trans THCA isomers (in THCA-predominant chemotype strains only trans isomer occurs) (de Meijer E., 2014).

In Europe around 60 fiber CBDA-predominant chemotype cultivars are now registered.

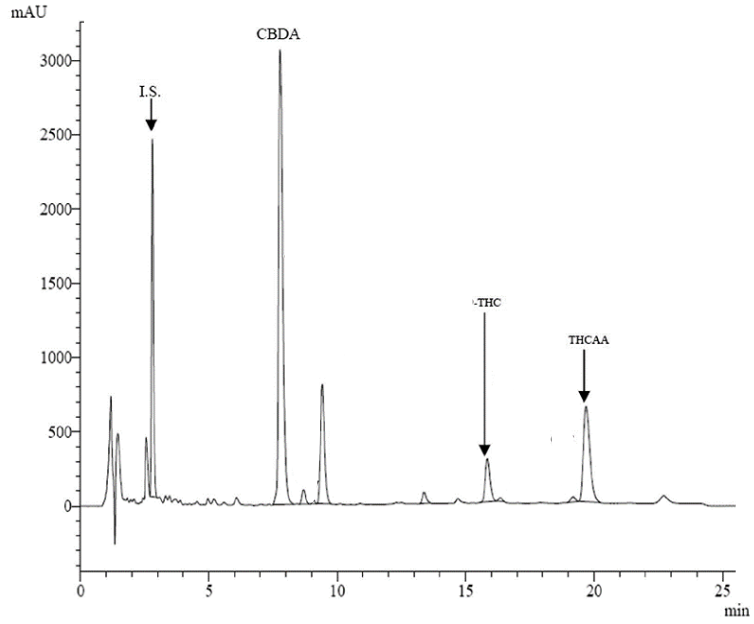

FIGURE 19 **EXEMPLIFICATIVE HPLC CHROMATOGRAM OF AN CBDA-PREDOMINANT CHEMOTYPE (I).** *SOURCE: ADAPTED FROM (GUL & AL., 2015)*

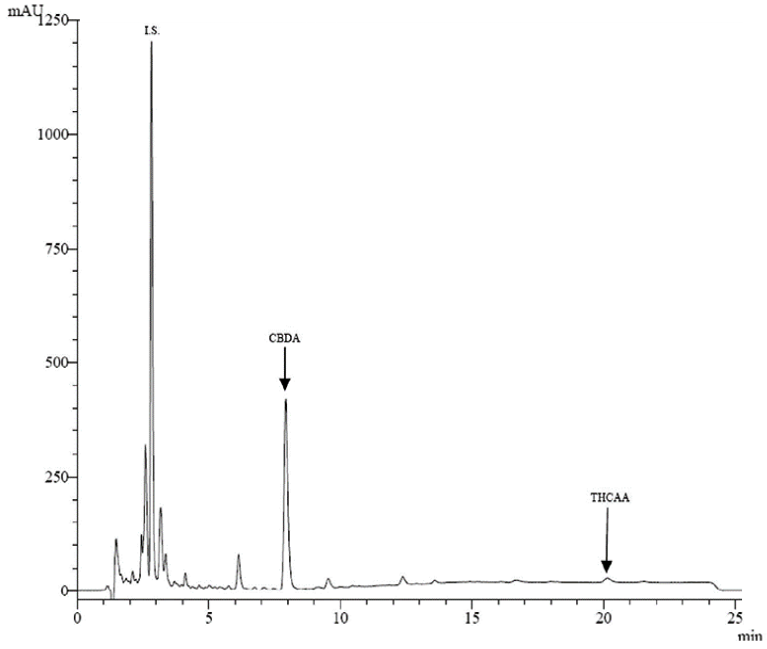

FIGURE 20 **EXEMPLIFICATIVE HPLC CHROMATOGRAM OF AN CBDA-PREDOMINANT CHEMOTYPE (II).** *SOURCE: ADAPTED FROM (GUL & AL., 2015)*

3.2.3 CBGA-RICH CHEMOTYPE

This chemotypes have only recently been described (Fournier & al., 1987).
At the loci *O*, *A* and the ones related to *PJG genes*, this predominance is always related to "wild type" alleles. Neverthless, this chemotype can be obtained inducing a mutation ("null" alleles) at the locus *B*, resulting in an absence of THCAS/CBDAS activity and in the accumulation of CBGA (de Meijer & Hammond, 2005).
Two CBGA-predominant chemotype are possible:

1. the one with a residual presence of CBDA, due to the minimally functional allele B_{D0};
2. the one with a residual presence of Δ^9-THCA, due to the minimally functional allele B_{T0}.

This specific chemotype induces a peculiar phenotypic change: the globose head of glandular trichomes assume a white opaque colour due to the almost total absence of Δ^9-THCA and CBDA. In 2003, the Italian CGBA-rich fiber hemp strain (Carma) obtained Plant Breeders Right (de Meijer E., 2014).

3.2.4 PHYTOCANNABINOID-FREE CHEMOTYPE

A cannabinoid-free chemotype was reported for the first time in 1988 and was characterised by a total lack of glandular trichomes. (Gorshkova & al., 1988). The absence of phytocannabinoids can be obtained by:

- generation of non-functional trichomes;
- modulation of the terpenoid pathway;
- mutation in GOT-expressing gene;
- upstream modification at locus *O*.

However, only the application of the latter mechanism has been reported in literature as an efficient method to induce the generation of a phytocannabinoid-free chemotype (de Meijer & al., 2009b). In the homozygous specimens at locus *O*, the "null" allele cause the total lack of phytocannabinoids, and this factor has been demonstrated to be a dominant repressive regulator, according to backcrossing experiments with high-content plants (de Meijer E., 2014).

These clones are usually characterized by a strong fragrance due to the great amount of terpenes, proving that this knockout modulation influences neither the trichomes functionality nor the terpenoid pathway.

Despite the apparent uselessness, this specific chemotype is a rich source of crude enzymes (for *in vitro* assays) and a material reference for chemical-analytical studies. As a reference plant, the phytocannabinoid-free chemotype has obtained a patent protection and is used in clinical studies as a placebo branch (de Meijer E., 2014).

3.2.5 CBCA-RICH CHEMOTYPE

Natural occurring in Afghan hashish and Korean fiber landraces, the CBCA-rich chemotype is characterised by two related specific morphological aspects:

- the suppression of capitate-stalked trichomes, related to the lack of bracts and bracteoles;
- a great amount of capitate-sessile glands.

The CBCA-rich chemotype is the result of a morphological mutation which mimes a juvenil plant stage when CBCA was more prominent (usually 0-5% in phytocannabinoid fraction of mature specimens of all chemotypes) (de Meijer E., 2014).

3.2.6 CANNABIVARINOIDS-RICH CHEMOTYPE

Cannabivarinoids-rich chemotype naturally occurs, albeit it is pretty rare: a THCVA-rich chemotype, indeed, has been found in China fiber and South Africa marijuana landraces.

Generally, to obtain cannabivarinoids-rich chemotype is necessary inducing some specific allelic modulation at loci *A* and *B*.

It has been demonstrated that THCVA-rich clones can reach a purity equal to 92%: nevertheless, the other main phytocannabinoid synthesized is Δ^9-THCA, an undesirable presence that can only be eliminated by chromatographic purification (de Meijer E., 2014).

4. THE HUMAN RELATIONSHIP WITH *CANNABIS* AND PHYTOCANNABINOIDS

The relationship between human species and *C. sativa* is ancient, with the first contact presumably taking place in central Eurasia 50,000 years ago (Wells & al., 2002) (Forster, 2004). Since then, the relationship has been so advantageous for each species, resulting in *co-evolution*, that is, if the symbiosis induced not only phenotypic modifications, but also allelic modulations on some specific genes. The human interest granted *Cannabis* a worldwide dissemination, supported by the impressive adaptable capability of the plant. From a genetic standpoint, the plant surely had induced the allelism B_T and B_D before the human domestication; however, the conscious or unconscious human selection led to a higher frequency of expression of one allele rather than the other one (or vice versa), resulting in the generation of two different chemotypes (Clarke R. a., 2013).

Could be possible that C. sativa has affected our evolution in a similar way?

The sociological, cultural, economic, and pharmacological impact that *C. sativa* can hardly be underestimated. Without Δ^9-THC, the plant could have remained "another flax" (Clarke R. a., 2013): the intoxicating properties made its fortune. The use of *Cannabis* has long been associated to recreational purposes, but the characterization of bioactive constituents made it possible the exploration of its medicinal properties (Pertwee, 2006) (Zou & al., 2018).

From an evolutionary standpoint, co-evolution between CB_1 and endogenous cannabinoids seems logical (McPartland & al., 2007b), but there is no evidence that the CB receptor genes underwent modification because of an exogenous agonist like Δ^9-THC.

4.1 CHEMICAL STUDIES

C. sativa was probably one of the earliest plants to be cultivated by man (Russo, 2007), and its medicinal use might already have been reported in China more than 4000 years ago. Nevertheless, scientific investigations started only in the 19th century. The early history of phytocannabinoids is confused.

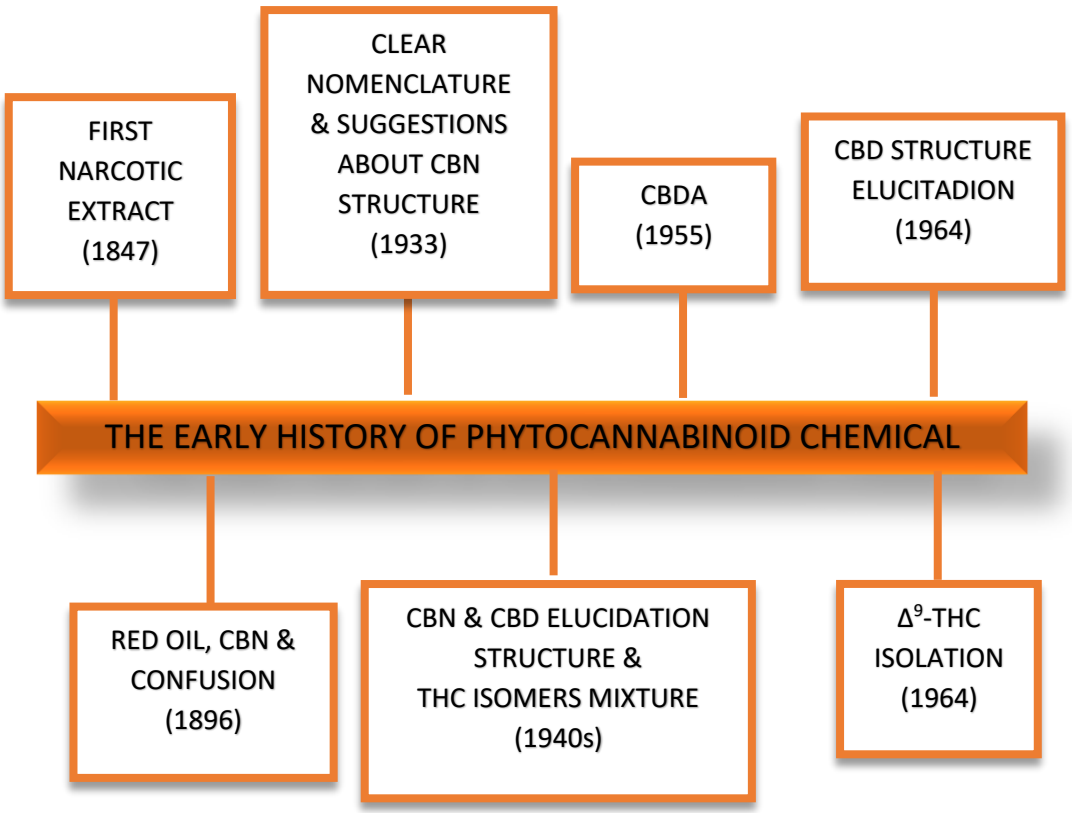

FIGURE 21 **TEMPORAL LINE OF CHEMICAL CANNABINOIDS RESEARCH.**

In 1847, the Smith pharmacists in Scotland obtained a narcotic resinous material from an alcoholic extraction of *Cannabis* purified by depigmentation with lime and by a sulfuric acid washings to eliminate basic compounds (Smith & and Smith, 1847). This work suggested the non-basic nature of phytocannabinoids but was found to be difficult to reproduce. 50 years later, a group of chemists from Cambridge (Wood,

Spivey and Easterfield) isolated from hashish a resinous "red oil" with all the narcotic properties of *Cannabis*, naming it *cannabinol* (Wood & al., 1896). The distillation conditions were harsh (Adams R. P., 1940a): an alcoholic or ether extract was distilled at high temperature (bath temperature 100-300 °C) and under reduced pressure (3 mmHg). The primary distillate — after water washings — was then subjected to a further fractionate distillation. The achievement of this "red oil" represents an important, but also confusing moment in the early cannabinoid research. This distilled resin was firstly believed a pure compound (Wood & al., 1896); however, after isolating a crystalline, not narcotic, and optically inactive product (**52**)— after acetylation of the distillate (Wood & al., 20-36) — the "red oil" was shown to be a mixture, but the Cambridge group decided to retain the name cannabinol also for the compound that had yielded the crystalline acetate. (Figure 22)

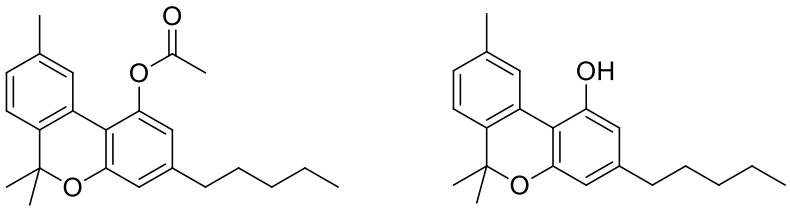

FIGURE 22 **STRUCTURES OF ACETYLATED COMPOUND FROM "RED OIL" AND CANNABINOL.**

Unfortunately, Sparvey's untimely and accidental death, as well as Easterfield's move to New Zealand, ended the research works in Cambridge (Mills, 2003) (Appendino, 2020). From this point on, cannabinoid research went through a further slowing-down period caused by messy nomenclature, difficulty in isolating compound **52**, and eventually confusion on its optical rotation. During the Thirties, Cahn's elucidated the gross structure of cannabinol, clarified the semantic ambiguities on the name, and demonstrated it had no intoxicating properties. The

benzopyran structure he proposed only missed the location of the substituents. This was eventually established by *Roger Adams* in USA and *Alexander R. Todd* in England (Adams & al, 1940b) (Gosh & al., 1941). Despite his early age and his economic and manpower limited resources, Todd brilliantly managed to compete with Adams, the spearhead of American chemistry of the first half of the 20th century. The two competitors belonged to different chemical generations. While Todd exploited chromatography and spectroscopy to elucidate the CBN structure, Adams synthesized both Cahn's proposed structural isomers, applying successively UV spectroscopy and the logic of reactivity to settle the issue. (Appendino, 2020)

During the CBN structure elucidation, both groups serendipitously discovered a novel and non-narcotic phytocannabinoid, CBD. The aim of Adam research was initially to characterize the psychoactive principle of *C. sativa*; however, since the difference between marijuana and hemp was not so clear at that time, he was assigned a THC-poor plant sample. The starting troubles in the CBN isolation as a crystalline product — arising from the chemotype of botanical material — were the driving force to CBD finding. Using *3,5-dinitrobenzoyl chloride* as an alternative acylating reagent, and hydrolysing (I) the consequent compound **53**, CBD was isolated (Appendino, 2020).

The CBD structure was clarified through these decomposition reactions (II and III). (Scheme 5)

Nevertheless, Adams was not able to locate the endocyclic double bond in the right position and to establish the absolute configuration of CBD (Adam & al., 1940c).

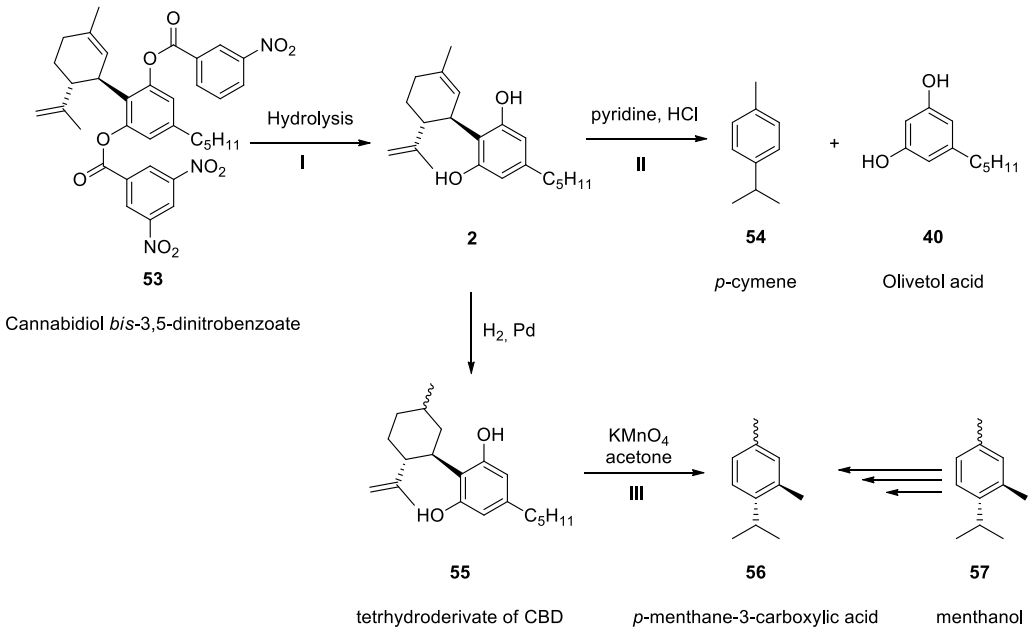

SCHEME 5 **REACTIONS APPLIED FOR ISOLATION OF CBD AND FOR ELUCIDATION OF ITS STRUCTURE. (I) HYDROLYSIS OF CBD BIS-3,5-DINITROBENZOATE. (II) PYROLYTIC Β-ELIMINATION TO P-CYMENE AND OA. (III) PERMANGANATE DEGRADATION OF TETRAHYDODERATIVE OF CBD TO P-MENTHANE3-CARBOXYLIC ACID, ALTERNATEVELY OBTAINED FROM MENTHOL.** *SOURCE: (APPENDINO, 2020)*

In parallel, in England Todd went ahead Cahn's research using initially an Indian hashish sample as starting material — so he did not face the same Adam's difficulties for the CBN isolation. He found that performing the acylation with *p*-nitrobenzoyl chloride facilitated the removal of all phytocannabinoids from the red distillate (Work, Bergel, & Todd, 1939). In 1940 Todd first submitted to *Nature* a paper about the CBD isolation (Jacob & Todd, 1940a), without any particular details, and successively a second paper to the *Journal of Chemical Society*, in which some suggestions about the CBD structure had been provided citing Adam's work (Jacob & Todd, 1940b).

Both Adams and Todd discovered that in *acidic* condition CBD undergoes a *cyclisation* reaction that affords a narcotic mixture of two non-crystalline compounds having a different optical rotation ("high-rotation" one and "low-rotation" one). Adams correctly assigns to these compounds (**16** e **58**) a tetrahydrocannabinol structure, with unknown location of the endocyclic double bond and the stereochemistry. (Scheme 6)

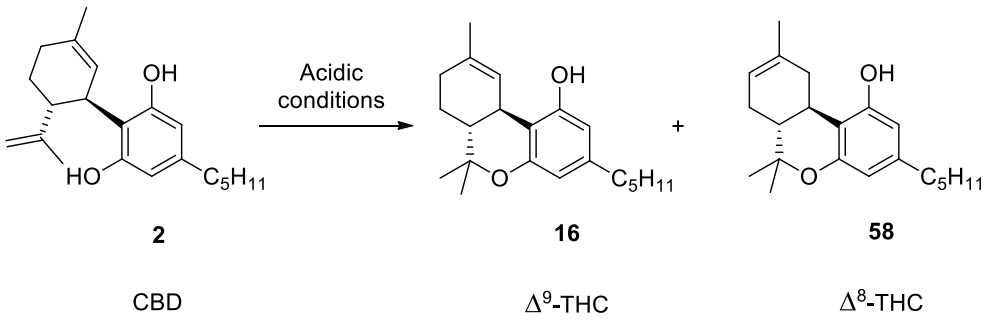

SCHEME 6 **ACIDIC CONDITIONS AFFORD A MIXTURE OF Δ^9- AND Δ^8-THC.**

Apart from his phytochemical and organic chemistry contributions, Adams also investigated the structure-activity relationship of the narcotic mixture, using a more easily available analogue. The phytocannabinoids history next moved East, in Czechoslovakia, where the brilliant work made by Šantavý and Krejčí led to the isolation of the first native *Cannabis* products.

In the course of studies on the discovery of plant-derived antibacterial agents, CBDA was obtained as the major native constituent of a sample of hemp, characterized as a crystalline diacetate (Appendino, 2020).

Additional work by Šantavý based exclusively on optical rotation and IR data, led to the elucidation of the constitution and configuration of CBD and Δ^9-THC, Šantavý published his results in a journal of very limited circulation, and still today fails to deserve the merits he deserves (Šantavý, 1964) (Appendino, 2020).

Only in 1964 Δ^9-THC was eventually identified as the natural intoxicating agent of marijuana, identical to the less optically negative isomer obtained by Adams (Gaoni, 1964). The year before, based on NMR studies, Mechoulam had also established the structure of CBD (Mechoulam & Shvo, 1963).

5. THE PHARMACOLOGICAL PROFILE OF CANNABINOIDS

5.1 THE EARLY STUDIES AND THE DISCOVERY OF CANNABINOID RECEPTORS

The earliest studies on the pharmacological profile of phytocannabinoids date back at the time of their discovery (Paton & Pertwee, 1973): both natural occurring meroterpenoids (Δ^9-THC, CBN and CBD as *Cannabis* extracts) and synthetic ones ($^{\Delta 6a,10a}$- THC **59** and its hexyl analogous, *synhexyl* **60**) had been investigated. (Figure 23)

A marked excitant central activity had been reported for Δ^9-THC and **60** whose administration caused catalepsy in mice and corneal areflexia in rabbits. While CBN showed a psychoactive activity similar to Δ^9-THC one, but with significantly lower potency, CBD did not show any remarkable central action, but interference with the metabolism of barbiturates was discovered (Loewe, 1946) (Pertwee, 2006). Modern studies have shown that this activity is due to the modulation (inhibition or induction) of some P450 (CYP) (Pertwee, 2004). The early studies showed that cannabinoids showed strict structure-activity relationships, but investigations were focused on their narcotic properties, eventually traced to Δ^9-THC (Gaoni, 1964) (Mechoulam & Gaoni, 1967), whose molecular target remained long unknown (Pertwee, 2006).

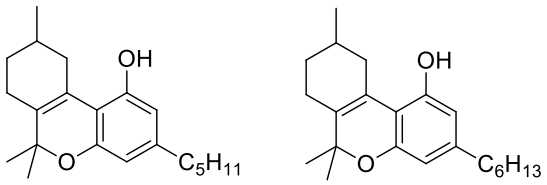

59 $\Delta^{6a,10a}$–THC

60 Synhexyl

FIGURE 23 **CHEMICAL STRUCTURES OF TESTED CANNABINOIDS IN THE EARLY PHARMACOLOGICAL STUDIES.**

Just like the world of fashion, also the one of science is affected by trends and the topics that are hot end up draining the attention. During the 1970s drug metabolism and the CYP enzymes were popular, and cannabinoids research focused on the pharmacokinetic and the metabolic pathway of Δ⁹-THC (Agurell & al., 1986). Δ⁹-THC was found to undergo liver phase I metabolization to *11-hydroxy-Δ⁹-tetrahydrocannabinol* (11-hydroxy-Δ⁹-THC, **61**), with a residual psychoactive action, and *11-nor-9-carboxy-Δ⁹-tetrahydrocannabinol* (Δ⁹-THC-COOH, **62**), inactive. Phase II glucuronidation then follows, with eventual urinary excretion. (Scheme 7)

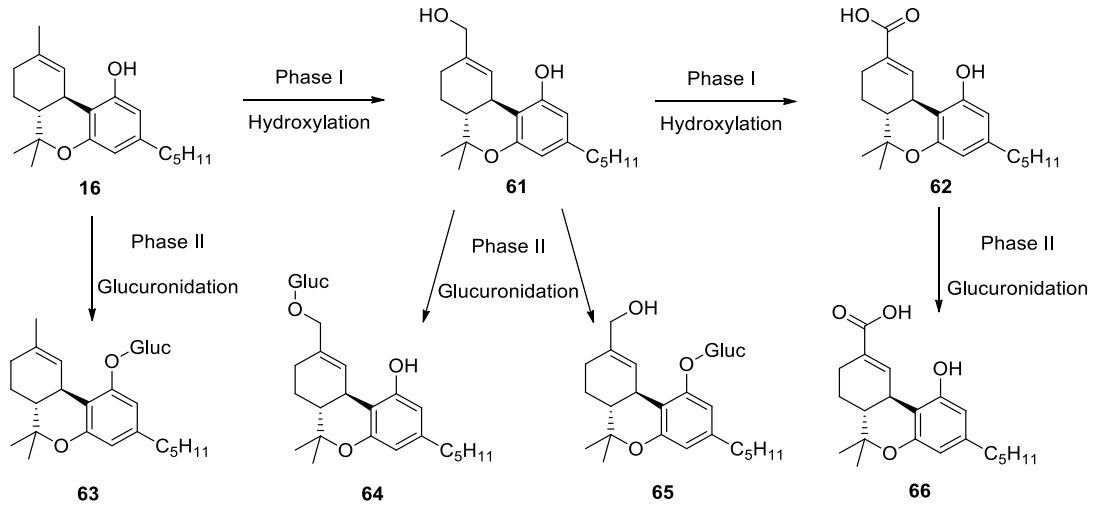

SCHEME 7 **PHASE I AND II METABOLISMS OF Δ⁹-THC AND MAIN METABOLITES INVOLVED.** WHILE THE METABOLISM OF Δ⁹-THC AND Δ⁹-THC-COOH HAVE BEEN MAINLY CHARACTERISED, MORE DIFFICULT HAS BEEN THE UNDERSTANDING OF 11-HYDROXY-Δ⁹-THC BIOTRANSFORMATION. ONLY THIS YEAR, HASSENBERG ET AL. (2020) HAVE DEMONSTRATED THAT 11-HYDROXY-Δ⁹-THC GLUCURONIDATION SURELY TAKES PLACE IN ALCOHOLIC POSITION, AND PROBABLY IN PHENOLIC ONE THROUGH, EXPLOITING BOTH *IN VIVO* AND *IN VITRO* ASSAYS**.** *SOURCE: ADAPTED FROM (HASSENBERG & AL, 2020)*

The initial investigations on the biological targets of cannabinoid led to confusing results. Based on *in vitro* experiments on artificial membranes constituted only by cholesterol and phospholipids, Δ⁹-THC was considered a simple modulator of membrane fluidity (Lawrence & Gill, 1975) (Pertwee, 1988), but interaction with a specific receptor was suggested by several observations, namely: a) strict *structure-*

activity relationships (SAR); b) *enantiodifferentiation*: (+) *trans*-Δ^9-THC was inactive when compared to natural (-) Δ^9-THC (Pertwee, 1988) (Howlett & al., 2002).

In the mid-1980s, it was discovered that cannabinoids inhibit adenylate cyclase (Howlett & Fleming, 1984), mimicking a signal transduction mechanism similar to neurotransmitters. This inhibition was mediated by a G_i-protein (Howlett, 1985), since it was *pertussis toxin-sensitive* (Howlett & al, 1986). The turning point in the study of cannabinoid receptors was the use of ultrapotent analogues of Δ^9-THC inspired by the early work of Adams on the replacement of the pentyl side-chain with a branched one (Adams & al., 1949). In 1974, CP-55-940 (**67**) was synthesized by Pfizer. (Figure 24)

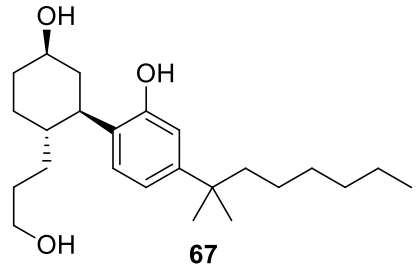

FIGURE 24 **CHEMICAL STRUCTURE OF SYNTHETIC ANALOG OF Δ^9-THC, CALLED AS *CP-55-940*.**

Although never been marketed, this compound in its tritium-labelled form [^{3}H-CP-55-940] has become a workhorse for research on cannabinoids (Pertwee, 2006), since its more polar features compared to [^{3}H-Δ^9-THC] make it less "stick" to biological membranes (Howlett, 2005).

Eventually, the existence of *cannabinoid* (CBs) *receptors* was experimentally proven by displacement studies between Δ^9-THC and CP-55-940 (Devane & al., 1988) (Howlett & al., 1988), and two specific proteins (CB_1 and CB_2) were characterized (Gerard & al, 1990) (Munro & al, 1993).

In the light of these advancements, the structure-activity relationships could be better defined, identifying as critical elements for CB_1 and CB_2 binding three structural elements, namely the C-9 methyl, the phenolic 1-OH and he C-3 pentyl group (Howlett & al, 1988). (Figure 25)

The validity of this model was established by a potent CB receptors agonist, a structurally-new synthetic analogous of *classic* cannabinoids, referred to as WIN-55,212-2 (**68**) (Martin & al, 1991).

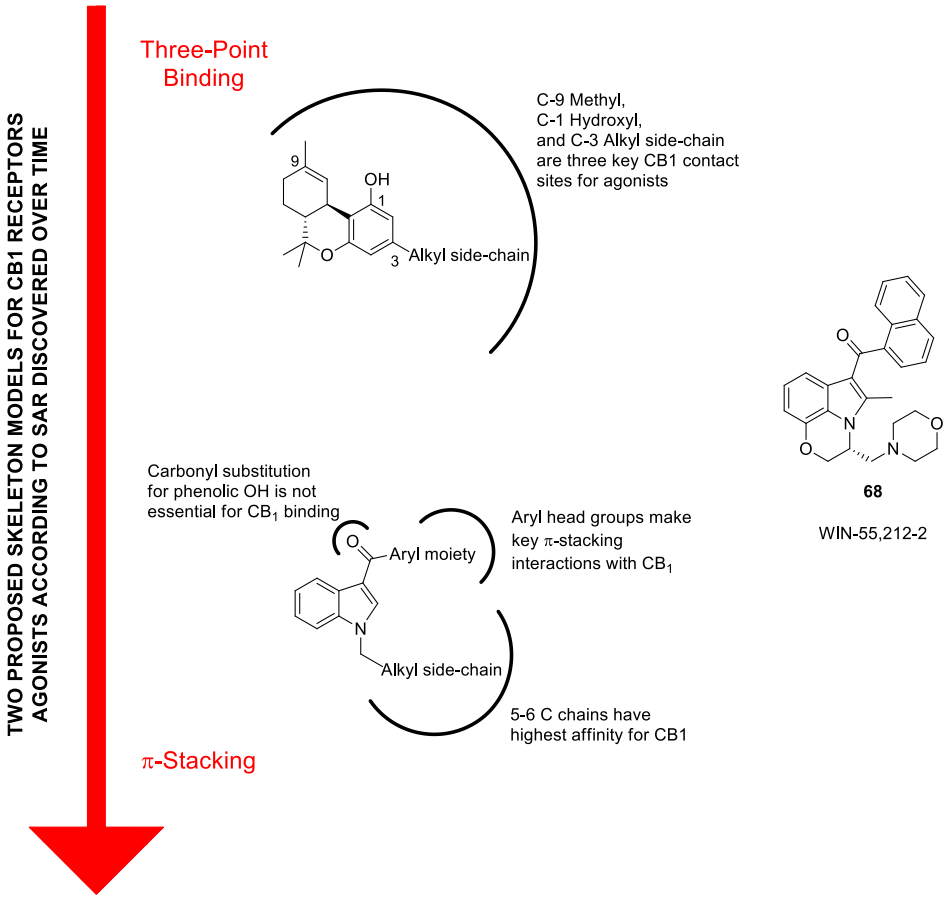

FIGURE 25 **EVOLUTION OF SKELETON MODEL OF CANNABINOID RECEPTORS AGONISTS OVER TIME BASED ON SAR STUDIES.** *SOURCE: ADAPTED FROM (WOROB & WENTHUR, 2020)*

Chemically different compounds from the indole series were next found to act as biological analogues of Δ^9-THC (Worob & Wenthur, 2020).

CB receptors studies have increased exponentially due to their involvements in a host of physiological and diseased states. CB_1 and CB_2 belong to the *rhodopsin-like* family of *seven-transmembrane-spanning* (7-TM) receptors, coupled to G-protein whose activity changes from cell to cell, according to its type and function (Howlett & al., 2005). (Figure 26)

Cannabinoid receptors generally *inhibit* the *adenylate cyclase* activity (through a $G_{i/o}$ proteins), and induce the *mitogen-activated protein kinase* (MAPK) (through a $G_{i/o}$ proteins), regulate the certain *ion channels* activity (through a $G_{i/o}$ proteins), and can even *induce* the *adenylate cyclase* activity (through a G_s protein) (Howlett & al., 2002) (Howlett, 2005) (Pertwee, 2005).

This promiscuity of the signalling transduction pathway is probably attributable to a "biased signalling" mechanism, which is ligand and tissue specific. After the binding, the "functionally selective" ligand causes a particular receptor conformation, and consequently a particular signalling transduction pathway (Ibsen & al., 2017).

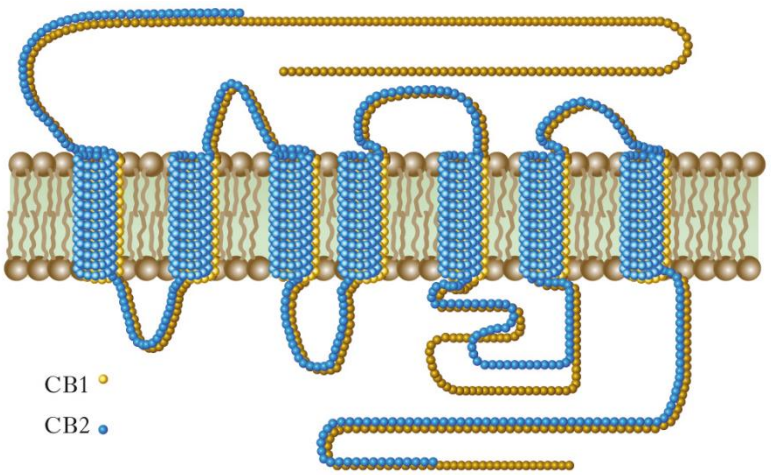

FIGURE 26 **STRUCTURE OF HUMAN CB RECEPTORS.** *SOURCE: (CAPRIOGLIO, 2016)*

CB_1 are principally located within the *nervous central system* (CNS) in cortex, cerebellum, hippocampus, and basal ganglia nuclei: for this reason, CB_1 receptors are involved in the regulation of analgesia, motor function, cognition, and memory (Howlett & al., 2002). They are disseminated in the central and peripheral neurons terminals – especially in GABAergic rather than glutamatergic neurons (Katona & al., 1999) — and modulate the neurotransmitters release (Szabo & Schlicker, 2005). The capability to regulate synaptic transmission and plasticity is due to their presence in astrocytes (Han & al., 2012). Eventually, outside of CNS, CB_1 receptors are located in different peripheral tissue, such as heart, lung, ovary, testis, prostate and in a circulating immune cells range (Bouaboula & al., 1999) (Galiegue & al., 1995). CB_2 receptors are found at significantly higher levels in peripheral organs having immune function, as tonsils, spleen, thymus, and macrophages (Brown & al., 2002). The presence of CB_2 receptors in the adult brain represents a controversial question because it is not yet clear if their occurrence in brain cells — including astrocytes, microglia and astrocytomas — could be related or not to some neurological diseases (as Alzheimer) (Brown & al., 2002) (Ellert-Miklaszewska & al., 2007) (Benito & al., 2003) (Van Sickle & al., 2005) (Soethoudt & al., 2017).

Following the discovery of CB receptors, the next crucial step was the search for endogenous compounds capable to mimic their activity. In collaboration with Raphael Mechoulam, Bill Devane found out a lipophilic substance with promising activity from pig brain: this compound was able to displace [^{3}H]-HU243 — a powerful receptor CB agonist — from the receptor binding site (Devane & al., 1992). After further assays (Howlett & al., 2002), this endogenous compound was validated as an CB receptor partial agonist, and, eventually was identified through its synthesis as *arachidonoyl ethanolamide* (**69**), commonly known as *anandamide* (AEA) - from *Ananda* which in Sanskrit means "bliss". (Figure 27) (Pertwee, 2006)

This discovery made it possible to detect other fatty acid derivatives with an action similar to anandamide one, like *2-arachidonoyl glycerol* (2-AG, **70**) (Mechoulam & al., 1995). (Figure 27)

All fatty acid derivatives with a marked modulation activity of CB receptors are considered as *endocannabinoids*.

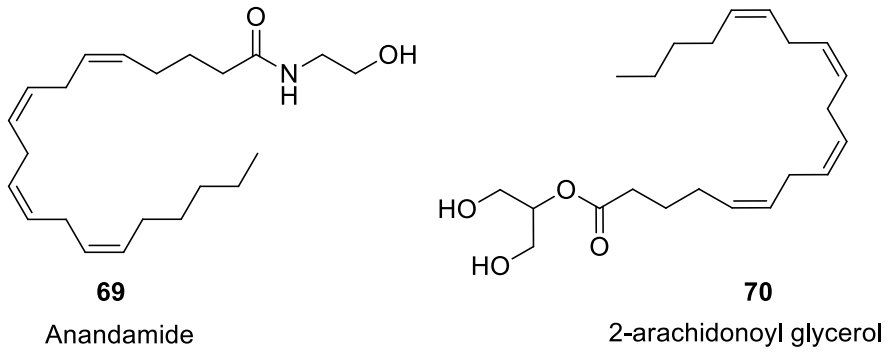

FIGURE 27 **CHEMICAL STRUCTURES OF THE TWO MAIN ENDOCANNABINOIDS.**

AEA and 2-AG are derived from two different biosynthetic pathways and two different precursors: *N-arachidonoyl phosphatidyl ethanolamine* (NAPE) is the AEA starter, while *diacylglycerols* (DAGs) are the 2-AG starters (Zou & al., 2018).

In contrast to neurotransmitters synthesis, the one of endocannabinoid is activated on demand, that is, only when is necessary. After binding their receptors (usually presynaptic or retrograde synaptic (Howlett & al., 2002), they are removed from the extracellular space by different transport mechanisms — anandamide, in particular, by *carrier-mediated* transport (Hillard & Jarrahian, 2003). After reuptake, endocannabinoid are not stored, but rather degraded by specific enzymes: *fatty acid amide hydrolase* (FAAH) for AEA and *monoacylglycerol lipase* (MAGL) for 2-AG (Di Marzo & al., 2005). Moreover, the degradation of both endocannabinoids is also handled by *cyclooxygenase-2* (COX-2) that acts on their arachidonoyl residues (Lu & al., 2016).

5.2 ADDITIONAL TARGETS OF CANNABINOIDS

In addition to cannabinoid receptors, AEA also activates the *transient receptor potential vanniloid type 1* (TRPV1) channels (Zygmunt & al., 1999) (Ross, 2003), and this observation triggered studied aimed at the identification of additional targets for phytocannabinoids (Pertwee, 2005). Two major ones are the *orphan G-protein coupled receptors* GPR55 and GPR18. They only show ca 10% homology with CB receptors, but can nevertheless bind cannabinoids, and are involved in cancer and metabolic disorders (Morales & Reggio, 2017). Also, the *glycine receptors* (GlyRs) are modulated by cannabinoids, that could exert at least part of their analgesic activity with this mechanism (Ahrens & al., 2009) (Xiong & al., 2011). Other targets have also been identified, and the ones more relevant for the project of my thesis will be briefly introduced.

5.2.1 TRP CHANNELS

TRP channels are figuratively our sensory window to the external world: they are able to recognise a variety of external stimuli, evoking specific responses. (Venkatachalam & Montell, 2007). There are 28 mammalian TRP channels, organised into six subfamilies and into two different groups:

- Group 1:
    1. **TRPC** (*canonical*)
    2. **TRPV** (*vanilloid*)
    3. **TRPA** (*ankyrin*)
    4. **TRPM** (*melastatin*)
- Group 2:
    5. **TRPP** (*polycystic*)
    6. **TRPML** (*mucolitin*)

All channels present a six segments transmembrane domain, share a little sequence homology, are permeable to cations, and their *C-* and *N-termini* are intracellular. Their pore loop is created through a homo- or hetero-tetramerization and is located between V and VI segments (Caterina, 2014). (Figure 28)

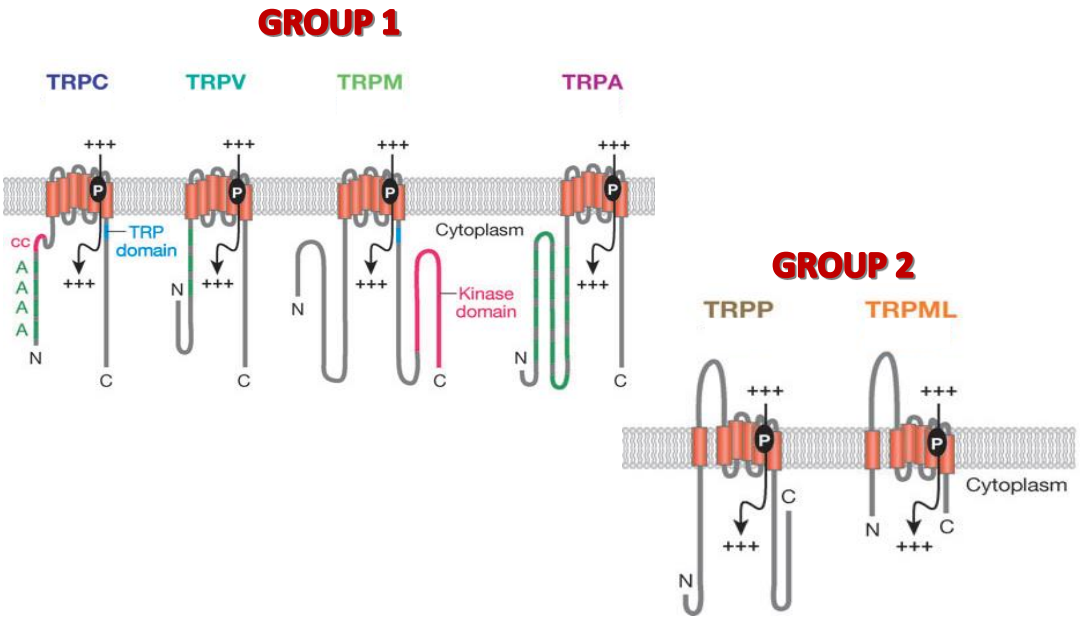

FIGURE 28 **THE MAMMALIAN TRP CHANNELS VARIETY. LEGEND: A, ANKYRIN REPEATS; CC, COILED-COOL DOMAIN; P, PORE LOOP; CATIONS, +++; TRP DOMAIN; KINASE DOMAIN, PROTEIN KINASE DOMAIN.** *SOURCE: ADAPTED FROM (VENKATACHALAM & MONTELL, 2007)*

Phytocannabinoids, endocannabinoids and synthetic cannabinoids can regulate the activity of three TRP channels subfamilies: TRPV, TRPA and TRPM (Muller & al., 2018).

5.2.1.1 TRPV CHANNELS

The term "vanilloid" used to describe this TRP channels subfamily is linked to the discovery of TRPV1: in 1997 it was defined as *capsaicin* (CPS, a vanilloid-like molecule) *receptor* or *VR1* (Caterina & al, 1997). *TRPV1* is the only one channel of this

subfamily activated by CPS. It is also activated by temperature > 42 °C and by protons (Tominaga & al., 1998) (Wang & Woolf, 2005), and is preferentially expressed in nociceptive neurons (Caterina, 2014).

	CBG **CBDV**	**CBD** **Δ⁹-THCV** **CBGV**	**CBDA** **CBGA**	**Δ⁹-THC** **Δ⁹-THCA**	**CBC** **CBN**	**CBGV**
Activity on TRPV1	High potency, but low efficacy	High potency and high efficacy	High efficacy, but low potency	No modulation activity found	Low efficacy	Efficient **desensitization**

TABLE 5 **SUMMARY OF PHYTOCANNABINOID MODULATION ON TRPV1 CHANNELS.** *SOURCE: (DE PETROCELLIS & AL., 2011) (IANNOTTI, 2014) (MULLER & AL., 2018)*

While CPS is not active on **TRPV2**, this channel, sensible to inflammation and heat (De Petrocellis & al., 2017), is activated by phytocannabinoids (Caterina, 2014) and represents a pharmacological target for chronic and inflammatory pain (Levine & al., 2007). The phytocannabinoid activity profile on these TRP channels is summarised in Table 6.

	CBD **CBGV**	**Δ⁹-THC**	**Δ⁹-THCA, Δ⁹-THCV** **CBN** **CBDV**	**CBC** **CBDA** **CBGA**	**Δ⁹-THCV**
Activity on TRPV2	High potency and high efficacy	High potency and high efficacy. The phase I metabolism (11-OH-Δ⁹-THC) reduces activity (interesting SARs)	High efficacy, but low potency	No activity	Efficient **desensitization**

TABLE 6 **SUMMARY OF PHYTOCANNABINOID MODULATION ON TRPV2 CHANNELS.** *SOURCE: (DE PETROCELLIS & AL., 2011) (MULLER & AL., 2018)*

TRPV3 is involved in perception of itch and pain and is disseminated not only in CNS, but also in peripheral organs and tissues (De Petrocellis & al., 2017).

In addition to stimulation due to warm temperature (33-39 °C) (Muller & al., 2018), *carvacrol* and *camphor*, two examples of oxygenated monoterpenes, are TRPV3 lead agonists (Caterina, 2014). Some phytocannabinoids rather than activators act as desensitizers of this receptor. (Table 7)

	CBD **Δ⁹-THCV**	**CBGV** **CBG** **CBGA**
Activity on TRPV3	Efficacy of **activation** (like the carvacrol one)	Efficient **desensitization** to the carvacrol action

TABLE 7 **SUMMARY OF PHYTOCANNABINOID MODULATION ON TRPV3 CHANNELS.** *SOURCE: (DE PETROCELLIS & AL, 2012) (MULLER & AL., 2018)*

TRPV4 has a broad distribution throughout the body, from brain to peripheral organs, as heart, kidney, and skin (Nilius & Owsianik, 2011). It is activated by mechanical and osmotic inputs as well as by phytocannabinoidsm(De Petrocellis & al, 2012). (Table 8)

	CBD **Δ⁹-THCV**	**CBGV, CBG** **CBGA, CBN**
Activity on TRPV4	Efficacy of **activation** (like the carvacrol one)	Efficient **desensitization** to the 4αPDD action

TABLE 8 **SUMMARY OF PHYTOCANNABINOID MODULATION ON TRPV4 CHANNELS.** *LEGEND*: **4αPDD, Α-PHORBOL 12,13-DIDECANOATE.** *SOURCE: (DE PETROCELLIS & AL, 2012) (MULLER & AL., 2018)*

CBD and Δ^9-THCV are able to interact with all TRP channels of this subfamily (promiscuous activity), while Δ^9-THC mainly causes a TRPV2 agonist stimulation, and CBC exhibits high potency and efficacy for TRPV1 (De Petrocelli & al., 2008) (De Petrocellis & al., 2011). Phytocannabinoids can also induce desensitization of TRPV through a functional agonism: this phenomenon is quite typical for the TRP channels superfamily and inhibits an additional stimulation by their classic ligands (De Petrocellis & al, 2012).

5.2.1.2 TRPA1 CHANNEL

Defined *ankyrin* due to 14-17 ankyrin repeats in the *N*-domain, TRPA1 is the only one channel belonging to this subfamily (Jaquemar & al., 1999), and is expressed in peripheral sensory neurons, as well as in non-neuronal cells (Samanta & al., 2018). Due to its capability to be activated by low temperatures (17 °C), TRPA1 was initially believed to be a noxious cold sensor, but now it is generally considered a chemo-nociceptor implicated in inflammatory and neuropathic pain (Story & al., 2003) (Yekkirala, 2013). Within phytocannabinoids, CBC was shown to be the most potent one, activating TRPA1 in a non-covalent fashion (De Petrocelli & al., 2008).

5.2.1.3 TRPM8 CHANNEL

The TRPM channels family has greater structural differences compared to the other group 1 TRP subfamilies, namely:

a) the presence of *N*-terminal "TRPM homology region" (Kraft & Harteneck, 2005);
b) the lack of *N*-terminal ankyrin repeats (Kraft & Harteneck, 2005);
c) the occurrence of *C*-terminal tetrameric coiled-coil domain (Fujiwara & Minor, 2008).

Only TRPM8 bind phytocannabinoids, that can behave as agonists or antagonists. This particular channel is usually modulated by "cooling" molecules, as *menthol*, *eucalyptol*, and *icilin* (Muller & al., 2018). In addition to its involvement in certain cancer types, TRPM8 is related to pain, bladder function and thermoregulation (Liu & al., 2016).

5.2.2 PEROXISOME PROLIFERATOR-ACTIVATED RECEPTORS (PPARS)

The PPARs are a superfamily of transcription factors nuclear receptors which control gene expression (Greene & al., 1995) (Sun & Bennett, 2007). They are located in numerous tissues and take part in diversified biological processes, such as *insulin sensitivity*, *glucose homeostasis*, *inflammation*, and *fatty acid storage* (O'Sullivan, 2016).

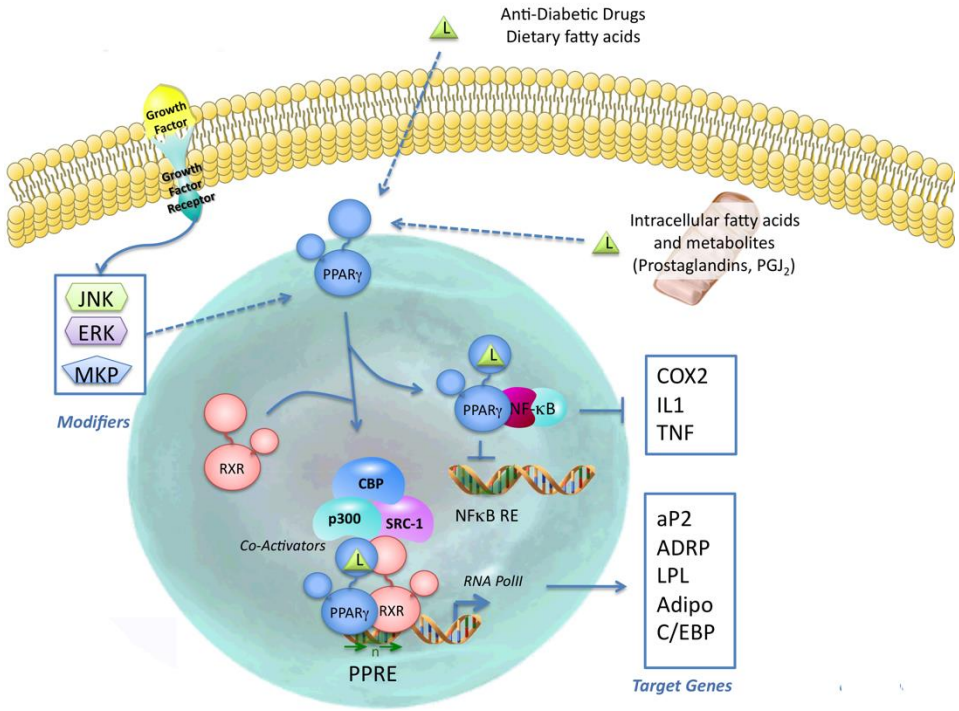

FIGURE 29 **PPARS ACTIVATION PATHWAY.** *SOURCE: (CAPRIOGLIO, 2016)*

There are three PPARs isotypes (Berger & Moller, 2002): α (alpha), β/δ (beta/delta) and γ (gamma).

PPARs are characterized by a DNA binding domain in the *N*-terminal region and a ligand binding domain in *C*-terminal one (Grygiel-Górniak, 2014): after ligand binding, these transcription factors migrate into the nucleus and heterodimerize with the *retinoid X receptor* (RXR). Eventually, this transcriptional machinery — after a previous modulation by specific factors as steroid receptor coactivator 1 — binds to the target gene DNA on PPREs (*peroxisome proliferator hormone response elements*), increasing or decreasing the transcription (Grygiel-Górniak, 2014). (Figure 29)

Although phytocannabinoids are able to interact with PPARα and PPARγ (O'Sullivan, 2016), the latter displays a more interesting pharmacological profile due to its involvement in the control of metabolism and inflammation — inhibition of inflammatory gene transcription is modulated by PPARγ activity (Jones & al., 2005) (Vandoros & al., 2006) (O'Sullivan, 2016).

5.2.3 THE TRANSCRIPTION FACTOR BTB AND CNC HOMOLOGY 1 (BACH1)

BTB and CNC homology (Bach1) is a transcription factor broadly expressed in mammalian tissues: it displays a *N*-terminus with a protein interaction domain and a *C*-terminus that, after interaction with a small Maf proteins, is able to bind DNA and so mediate its transcriptional suppressing activity (Oyake & al., 1996). Indeed, Bach1 — as heterodimer with Maf protein — attaches DNA in *Maf recognition elements* (MAREs) of the gene promoters and inhibits the transcription of certain genes involved in oxidative stress-response, like *heme oxygenase-1* (HO-1) and *NADPH quinone oxidoreductase* (NQO1) (Zhang & al., 2018). By inducing its removal from the nucleus through *heme* binding, *antioxidant* action or *cadmium*, this transcriptional

suppressor cannot carry out its activity (Ogawa & al., 2001) (Kaspar & Jaiswal, 2009) (Suzuki & al., 2003).

Bach1 action is closely related to the function of another transcriptional factor, referred to as *nuclear factor erythroid-derived 2-like 2* (Nrf2): the activity of Bach1 is perfectly balanced by the Nrf2 one, and vice versa (Jyrkkänen & al., 2011).

Under physiological oxygen conditions, Bach1 is bound in the nucleus to MAREs, while in the cytoplasm Nrf2 is repressed by *Kelch-like ECH-associated protein 1* (Keap1) binding (Kwak & al., 2003). In non-physiological situation, the oxidative stress induces the Nrf2-Keap1 binding cleavage, leading the nuclear factor to migrate into the nucleus, to heterodimerize with small Mafs and eventually to allow the transcription of HO-1 and NQO1, genes for the oxidative-stress response (Chapple & al., 2016). (Figure 30)

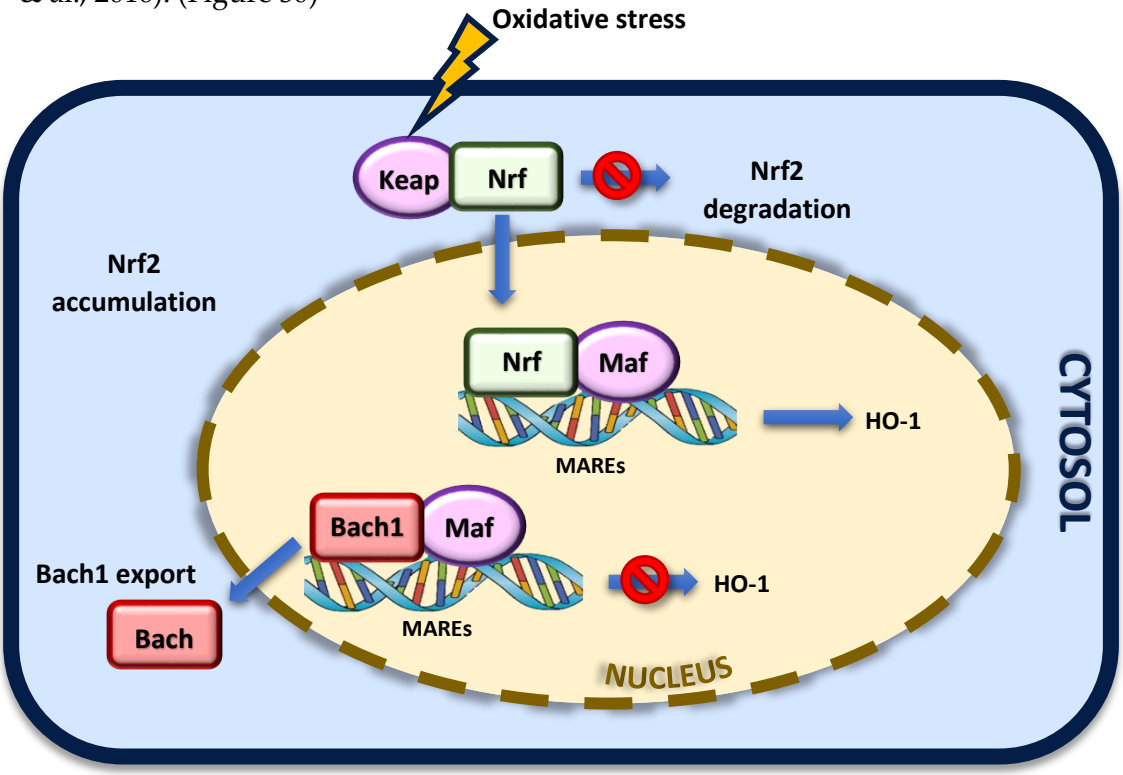

FIGURE 30 **GRAPHIC REPRESENTATION OF THE WORKING OF THE BACH1-NRF2 AXIS IN RESPONSE TO OXIDATIVE STIMULI**. *SOURCE: ADAPTED FROM (ZHANG, 2018)*

At the same time, Bach1 is released from the binding with MAREs and successively shipped outside the nucleus in the cytosol (Zhang & al., 2018). This response to an oxidative-stress is masterminded by *sirtuin* (Sirt). The Bach1-Nfr2 axis is involved in numerous physiological processes (cell cycle, homeostasis, ROS generation) and in different diseases (cancer, cardiovascular pathologies) (Zhang & al., 2018). Therefore, this pair of transcription factors could represent an important pharmacological target. Recently, Casares et al. (2019) have demonstrated that CBD could be used as a topical treatment for different skin diseases because this phytocannabinoid induces an inhibition of Bach1 though without any activity on Nfr2.

6. CONCLUSIONS

The ECS is present in all animals — except insects — and has a long evolutive history. The ECS might have been present already in the primitive animals Cambrian era, and its wide distribution in the animal kingdom is seemingly crucial to maintain homeostasis, performing all the essential physiological functions and adapting to environmental changes (McPartland & al., 2007). (Figure 31)

The ECS is also fundamental to perpetuate a species: it has been defined by Maccarrone as the "guardian angel of human reproduction", since it controls and regulates our entire reproductive process (from spermatogenesis to the early postnatal stages) (Maccarrone, 2005) (Fride E., 2004) (Fride & al., 2008). In addition to regulating and coordinating the organisms main activities [*sleeping*, *eating*, *relaxing*, and *protecting* (Di Marzo & al., 1998)], the ECS represents a "safety net" as it collaborates with the immune system and other physiological systems (Pope & al., 2009). However, in my opinion its most important role is to allow us to:

"Tolerate our human condition, bear and forget selectively the arrows that life is addressing us, and start again, day after day."
(Allyn Howlett)

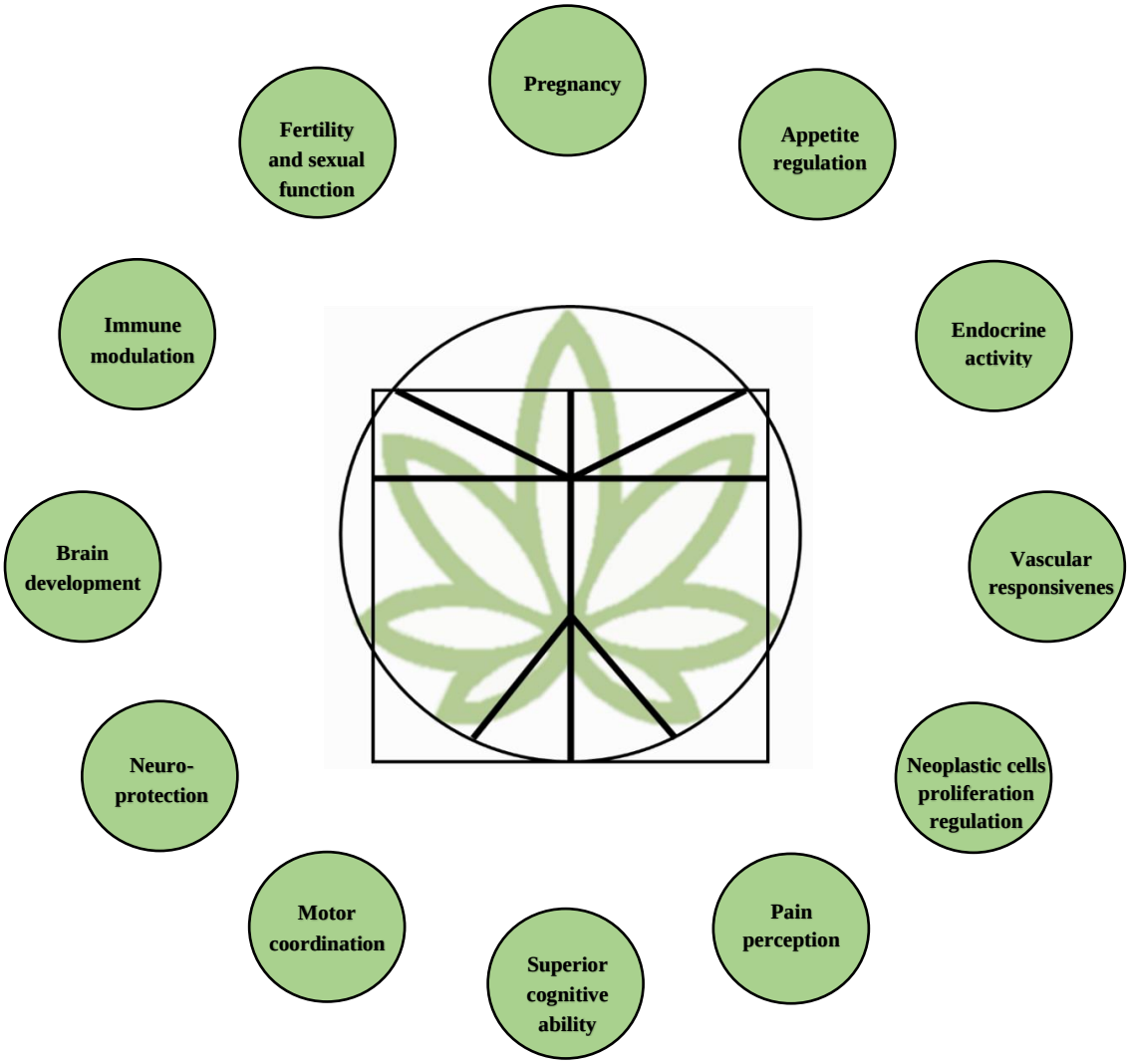

FIGURE 31 **SCHEMATIC REPRESENTATION OF THE PLETHORA OF ECS CARRIED OUT ACTIVITY IN HUMAN BODY.** *(AMERI, 1999) (DI MARZO & AL., 1998) (CORREA & AL., 2005) (VAN DER STELT M, 2005) (WANG & AL., 2006) (IDRIS & AL., 2005) (DE OLIVEIRA ALVARES & AL., 2006) (ARENOS & AL., 2006) (MIKICS & AL., 2006) (GUINDON & AL., 2006)*

The case of Acomplia® is exemplificative of Howlett's consideration. Acomplia® (*rimonabant*, **71**) was marketed in Europe in 2006 and in Italy in 2008 for the pharmacological treatment of obesity and overweight pathological, being able to contrast food craving (Howlett & al., 2004). Rimonabant is a synthetic cannabinoid

designed considering the CB_1 receptor-ligand SAR studies (Figure 32): it is a CB_1 receptor inverse agonist (Xie & al., 2007).

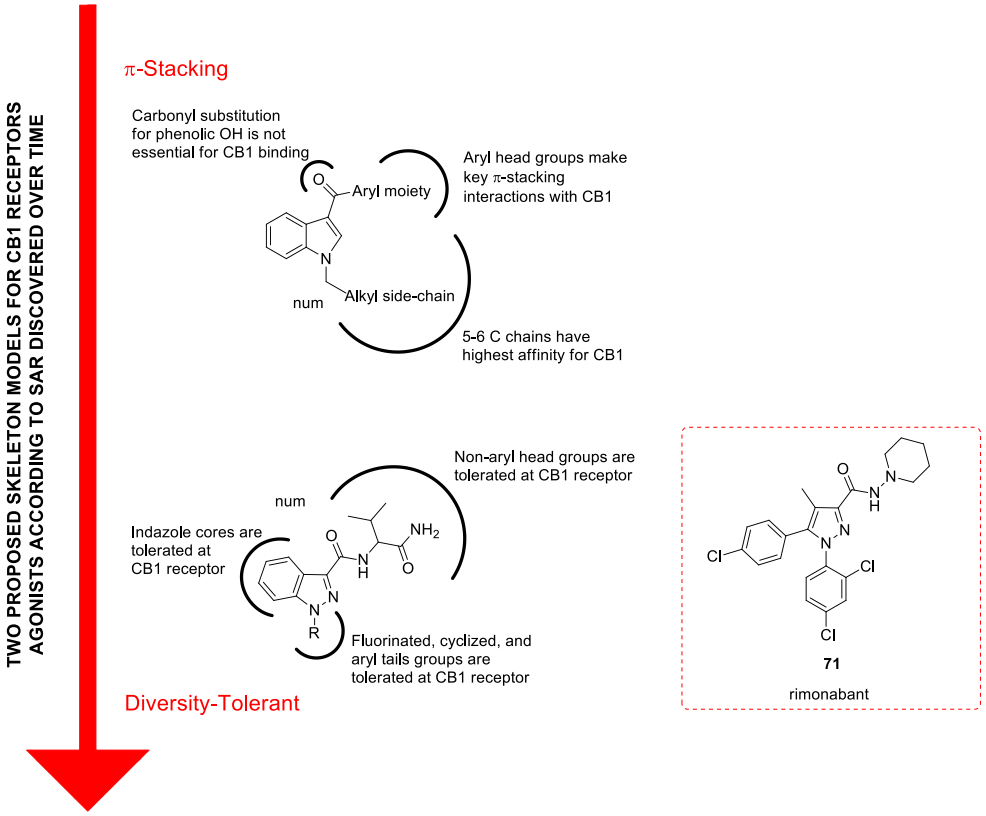

FIGURE 32 **STRUCTURE OF RIMONABANT AS THE PRODUCT OF SAR STUDIES OVER TIME.** *SOURCE: ADAPTED FROM (WOROB & WENTHUR, 2020)*

In Italy Acomplia® was withdrawn after only 5 months (AIFA, 2008) because *CHMP* (Committee for Medicinal Products for Human Use of EMA) revealed that patients taking rimonabant had a doubled risk of psychiatric disorders compared to *control*. The use of CB receptor reverse agonist can cause the appearance of anxious and depressive effects, which in some cases induce to a suicidal drift. This striking case demonstrates how ECS is a system very delicate and difficult to modulate, where sometimes an equilibrium alteration can provoke a reaction similar to the "butterfly effect".

7. REFERENCES

Adams, R. P. (1940a). Isolation of cannabinol, cannabidiol and quebrachitol from red oil of Minnesota wild hemp. J. Am. Chem. Soc., 62, 2194-2196.

Adams, R., & al, e. (1940b). J. Am. Chem. Soc., 62, 2204-2207.

Adam, R., & al. (1940c). Structure of cannabidiol V. Position of the alicyclic double bond. J. Am. Chem. Soc., 62, 2215-2219.

Adams, R., & al. (1949). New Analogs of Tetrahydrocannabinol. XIX. J. Am. Chem. Soc., 71 (5), 1624-1628.

Agurell, S., & al. (1986). Pharmacokinetics and metabolism of delta1-tetrahydrocannabinol and other cannabinoids with emphasis on man. Pharmaco. Rev., 38, 21-43.

Ahrens, J., & al. (2009). The nonpsychotropic cannabinoid cannabidiol modulates and directly activates alpha-1 and alpha-beta glycine receptor function. Pharmacology, 83 (4), 217-222.

AIFA. (2008, Ottobre 23). Comunicato n. 83. Vietata la vendita del farmaco Acomplia.

Ameri, A. (1999). The effects of cannabinoids on the brain. Prog Neurobiol., 58, 315-348.

Anderson, L. (1980). Leaf variation among *Cannabis* species from a controlled garden. Harvard University Botanical Museum Leaflets, 28, 61-69.

Andre C.M., H. J. (2016). *Cannabis* sativa: The Plant of the Thousand and One Molecules. Front Plant Sci, 7: p. 19.

Appendino, G. (2020). The early history of cannabinoid research. Rendiconti Lincei. Scienze Fisiche e Naturali, 31, 919-929.

Arenos, J., & al. (2006). Blockade of cannabinoid CB1 receptors alters contextual learning and memory. Eur J Pharmacol., 539, 177-183.

Benito, C., & al. (2003). Cannabinoid CB2 receptors and fatty acid amide hydrolase are selectively overexpressed in neuritic plaque-associated glia in Alzheimer's disease brains. The Journal of Neuroscience, 23 (35), 11136-11141.

Berger, J., & Moller, D. E. (2002). Annu. Rev. Med., 53, 409–435.

Booth, J. (2020). Terpene and isoprenoid biosynthesis in *Cannabis* sativa. Vancouver: The University of British Columbia.

Bouaboula, M., & al. (1999). Regulation of peripheral cannabinoid receptor CB2 phosphorylation by the inverse agonist SR 144528. Implications for receptor

biological responses. The Journal of Biological Chemistry, 274(29), 20397-20405.

Brown, S., & al. (2002). Cloning and molecular characterization of the rat CB2 cannabinoid receptor. Biochimica et Biophysica Acta, 1576(3), 255–264.

Burke, C. e. (1999). Geranyl diphosphare synthase: Cloning, expression, and characterization of this prenyltransferase as heterodimer. Proceedings of the National Academy of Sciences of the United States of America, 96, 13062-13067.

Cahn, R. (1933). Cannabis sativa resin. Part IV. The synthesis of some 2,2-dimethylbenzopyrans, and confirmation of the structure of cannabinol. J. Chem. Soc., 1400-1405.

Caprioglio, D. (2016). SPICE SPACE RACE: A "SPICY" JOURNEY TO THE CHEMICAL GALAXY OF BIOACTIVE COMPOUNDS. PhD Thesis. Università del Piemonte Orientale.

Casares, L., & al. (2019). Cannabidiol induces antioxidant pathways in keratinocytes by targeting BACH1. Redox Biology, 28.

Caterina, M. (2014). TRP channel cannabinoid receptors in skin sensation, homeostasis, and inflammation. ACS Chem. Neurosci., 5, 1107-1116.

Caterina, M., & al. (1997). The capsaicin receptor: a heat-activated ion channel in the pain pathway. Nature, 389 (6653), 816-824.

Chapple, S., & al. (2016). Bach1 differentially regulates distinct Nrf2-dependent genes in human venous and coronary artery endothelial cells adapted to physiological oxygen levels. Free Radical Biology & Medicine, 92, 152-162.

Chen, H. e. (2011). Malonyl-CoA synthetase, encoded by ACYL ACTIVATINF ENZYME13, is essential for growth and development of Arabidopsis. The Plant Cell, 23, 2247-2262.

Clarke, R. (1981). Marijuana Botany. Berkeley, CA: And/Or.

Clarke, R. a. (2013). Cannabis. Evolution and ethnobotany. Berkeley: University of California Press.

Citti, C. *et al.* A novel phytocannabinoid isolated from *Cannabis sativa* L. with an in vivo cannabimimetic activity higher than Δ9-tetrahydrocannabinol: Δ9-Tetrahydrocannabiphorol. *Sci. Rep.* **9**, 1–13 (2019).

Correa, F., & al. (2005). The role of cannabinoid system on immune modulation: therapeutic implications on CNS inflammation. . Mini Rev Med Chem., 5, 671-675.

Dayanandan, P. K. (1976). Trichomes of Cannabis sativa L. Am. J. Bot. 63 (5), 578-591.

de Meijer, E. (2014). The Chemical Phenotypes (Chemotypes) of Cannabis. In R. Pertwee, Handbook of Cannabis (p. 89-110). Oxford: Oxford University Press.

de Meijer, E., & al., e. (2003). The inheritance of chemical phenotype in *Cannabis sativa* L. Genetics, 163, 335-346.

de Meijer, E., & al., e. (2009a). The inheritance of chemical phenotype in *Cannabis sativa* L. (III): variation in cannabichromene proportion. Euphytica, 165, 293-311.

de Meijer, E., & al., e. (2009b). The inheritance of chemical phenotype in *Cannabis sativa* L. (IV): cannabinoid-free plants. Euphytica, 168, 95-112.

de Meijer, E., & Hammond, K. (2005). The inheritance of chemical phenotype in *Cannabis sativa* L. (II): cannabigerol predominant plants. Euphytica, 145, 189-198.

De Oliveira Alvares, L., & al. (2006). AM251, a selective antagonist of the CB1 receptor, inhibits the induction of long-term potentiation and induces retrograde amnesia in rats. Brain Res., 1075, 60-67.

De Petrocelli, L., & al. (2008). Plant-derived cannabinoids modulate the activity of transient receptor potential channels of ankyrin type-1 and melastatin type-8. J Pharmacol Exp Ther, 325, 1007–1015.

De Petrocellis, L., & al. (2012). Cannabinoid actions at TRPV channels: effects on TRPV3 and TRPV4 and their potential relevance to gastrointestinal inflammation. Acta Physiologica, 255-266.

De Petrocellis, L., & al. (2011). Effects of cannabinoids and cannabinoid-enriched Cannabis extracts on TRP channels and endocannabinoid metabolic enzymes. Br. J. Pharmacol., 163, 1479-1494.

De Petrocellis, L., & al. (2017). Actions and regulation of ionotropic cannabinoid receptors. Adv. Pharmacol., 80, 249–289.

Degenhardt, F., & al. (2017). Chapter 2: The biosynthesis of Cannabinoids. In Handbook of Cannabis and Related Pathologies (p. 13-23).

Devane WA, Dysarz FA, III, Johnson MR, Melvin LS, Howlett AC (1988) Determination and characterization of a cannabinoid receptor in rat brain. Mol Pharmacol, 34: 605–613

Devane, B., & al. (1992). Isolation and structure of a brain constituent that binds to the cannabinoid receptor. Science, 258, 1946-1949.

Di Marzo, V., & al. (1998). Endocannabinoids: Endogenous cannabinoid receptor ligands with neuromodulatory action. Trends Neurosci., 21 (12), 521-528.

Di Marzo, V., & al. (2005). The biosynthesis, fate and pharmacological properties of endocannabinoids. In R. Pertwee, Cannabinoids. Handbook of Experimental Pharmacology. (p. 147-185). Heidelburg: Springer-Verlag.

Ellert-Miklaszewska, A., & al. (2007). Distinctive pattern of cannabinoid receptor type II (CB2) expression in adult and paediatric brain tumours. Brain Research, 1137(1), 161–169.

ElSohly M. A., S. D. (2005). Chemical constituents of marijuana: The complex mixture of natural cannabinoids. Life Sciences, Volume 78, Issue 5, page 539-548.

Fairbairn, J. (1972). Trichomes and glands of Cannabis sativa L. Bulletin on Narcotics, 24 (4), 1972.

Farag S., K. O. (2017). The Cannabis Plant: Botanical Aspects. In Handbook of Cannabis and Related Pathologies: Biology, Pharmacology, Diagnosis, and Treatment (p. 3-12). Victor Preedy.

Fellermeier, M. e. (2001). Biosynthesis of cannabinoids. Incorporation experiments with 13C-labeled glucoses. European Journal of Biochemistry, 268, 1596-1604.

Fellermeier, M., & Zenk, M. (1998). Prenylation of olivetolate by a hemp transferase yields cannabigerolic acid, the precursor of tetrahydrocannabinol. FEBS Lett. 427, 283-285.

Forster, P. (2004). Ice Ages and the Mitochondrial DNA Chronology of Human Dispersals: a review. Philosphical Transactions of the Royal Society of London B., 359, 255-264.

Fournier, G., & al., e. (1987). Planta Medica, 277-280.

Fournier, G., & al., e. (1987). Plant. Med., 53, 277-280.

Fride, E. (2004). The endocannabinoid-CB1 receptor system in pre-and postnatal life.". European journal of pharmacology, 500, 289-297.

Fride, E., & al. (2008). Multiple Roles for the Endocannabinoid System During the Earliest Stages of Life: Pre- and Postnatal Development.". Journal of Neuroendocrinology, 20 (1), 75-81.

Friedland, S., & al. (2012). The cardiovascular effects of peroxisome proliferator activated receptor agonists. Am J Med, 125, 126–133.

Fuhr, L., & al., e. (2015). J. Nat. Prod., 78, 1160-1164.

Fujiwara, Y., & Minor, D. J. (2008). X-ray crystal structure of a TRPM assembly domain reveals an antiparallel four-stranded coiled-coil. J. Mol. Bioll., 383 (4), 854-870.

Gagne, S. e. (2012). Identification of olivetolic acid cyclase from Cannabis sativa reveals a unique catalytic route to plant polyketides. Proc. Natl. Acad. Sci. U.S.A., 109, 12811-12816.

Galiegue, S., & al. (1995). Expression of central and peripheral cannabinoid receptors in human immune tissues and leukocyte subpopulations. European Journal of Biochemistry, 232(1), 54-61.

Gaoni, Y. a. (1964). Proc. Chem. Soc., 82.

Gerard, C., & al. (1990). Nucleotide sequence of a human cannabinoid receptor cDNA. Nucleic Acids Res, 18, 7142.

Gorshkova, L., & al. (1988). Referativnyi Zhurnal, 12.65.322.

Gosh, R., & al. (1941). J. Chem. Soc., 137-140.

Greene, M., & al. (1995). Gene Expr, 4, 281-299.

Grygiel-Górniak, B. (2014). Nutr. J., 13, 17.

Guindon, J., & al. (2006). Local interactions between anandamide, an endocannabinoid, and ibuprofen, a nonsteroidal anti-inflammatory drug, in acute and inflammatory pain. Pain., 121, 85-93.

Gul, W., & al. (2015). Determination of 11 Cannabinoids in Biomass and Extracts of different varieties of cannabis Using High-Performance Liquid Chromatography. Journal of AOAC International, 98 (6), 1523-1528.

Gülck, T. a. (2020). Phytocannabinoids: Origins and Biosynthesis. Trends in Plant Science, 25(10):985-1004.

Han, J., & al. (2012). Acute cannabinoids impair working memory through astroglia CB1 receptor modulation of hippocampal LTD. Cell, 148 (5), 1039-1050.

Hanus, L., & al. (2016). Phytocannabinoids: a unified critical inventory. Natural Product Reports, 33, 1357-1392.

Happyana, N. A. (2013). Analysis of cannabinoids in laser-microdissected trichomes of medicinal Cannabis sativa using LCMS and cryogenic NMR. Phytochemistry, 87, 51-59.

Hartsel J.A., E. J. (2016). Cannabis sativa and Hemp. In Nutraceuticals: Efficacy, Safety and Toxicity. Ramesh Gupta.

Hassenberg, C., & al. (2020). International Journal of Legal Medicine, 2105-2119.

Hazekamp A, (2010). J. Chemistry of Cannabis. Elsevier.

Hendriks, H., & al. (1978). Pharm. Weekbl., 113, 413-424.

Herkenham M, Lynn AB, Little MD, Johnson MR, Melvin LS, De Costa BR, Rice KC (1990), Cannabinoid receptor localization in brain. Proc Natl Acad Sci USA 87:1932–1936

Herkenham M, Lynn AB, Johnson MR, Melvin LS, De Costa BR, Rice KC (1991), Characterization and localization of cannabinoid receptors in rat brain: a quantitative in vitro autoradiographic study. J Neurosci 11:563–583

Hillard, C., & Jarrahian, A. (2003). Cellular accumulation of anandamide: consensus and controversy. Br. J. Pharmacol., 140, 802-808.

Hilling, K., & Mahlberg, P. (2004). A chemotaxonomic analysis of cannabinoid variation in Cannabis. American Journal of Botany, 91, 966-975.

Howlett, A. (1985). Cannabinoid inhibition of adenylate cyclase. Biochemistry of the response in neuroblastoma cell membranes. Mol Pharmacol, 27, 429-436.

Howlett, A. (2005). Cannabinoid receptor signalling. In R. Pertwee, Handbook of Experimental Pharmacology (p. 53-79). Heidelburg: Springer-Verlag.

Howlett, A., & al. (1986). Involvement of Gi in the inhibition of adenylate cyclase by cannabimimetic drugs. Mol Pharmacol, 29, 307-313.

Howlett, A., & al. (1988). Nonclassical Cannabinoid Analgesics Inhibit Adenylate Cyclase: Development of a Cannabinoid Receptor Model. Mol. Pharmacol., 33 (3), 297-302.

Howlett AC, Champion TM, Wilken GH, Mechoulam R (1990) Stereochemical effects of 11-OH-delta 8-tetrahydrocannabinol-dimethylheptyl to inhibit adenylate cyclase and bind to the cannabinoid receptor. Neuropharmacology 29:161–165

Howlett, A., & al. (2002). International Union of Pharmacology. XXVII. Classification of cannabinoid receptors. Pharmacological Reviews, 54, 161-202.

Howlett, A., & al. (2004). Cannabinoid physiology and pharmacology: 30 years of progress. Neuro Pharmacology, 47, 345-358.

Howlett, A., & Fleming, R. (1984). Cannabinoid inhibition of adenylate cyclase. Pharmacology of the response in neuroblastoma cell membranes. Mol Pharmacol, 26, 53-70.

Hülskamp, M. (2004). Trichomes: A model for cell differentiation. Molecular Cell Biology, 5, 471-480.

Husni, A., & al., e. (2014). Med. Chem. Res., 23, 4295-4300.

Iannotti, F. (2014). Nonpsychotropic plant cannabinoids, cannabidivarin (CBDV) and cannabidiol (CBD), activate and desensitize transient receptor potential vanilloid 1 (TRPV1) channels in vitro: potential for the treatment of neuronal hyperexcitability. ACS Chem. Neurosci., 5, 1131-1141.

Ibsen, M., & al. (2017). Cannabinoid Cb1 and CB2 receptors signalling and bias. Cannabis Cannabinoid Res, 2 (1), 48-60.

Idris, A., & al. (2005). Regulation of bone mass, bone loss and osteoclast activity by cannabinoid receptors. Nat Med., 11, 774-779.

Il sistema endocannabinoide e le sue funzioni. (s.d.). Tratto da Cannabis e danni salute: http://cannabis.dronetplus.eu/danni.html

Jacob, A., & Todd, A. (1940a). Nature, 145, 350.

Jacob, R., & Todd, A. (1940b). J. Chem. Soc., 649-650.

Jaquemar, D., & al. (1999). An ankyrin-like protein with transmembrane domains is specifically lost after oncogenic transformation of human fibroblasts. J Biol Chem., 274(11), 7325-7333.

Jones, J., & al. (2005). Proc. Natl. Acad. Sci. U. S. A., 102, 6207–6212.

Jyrkkänen, H., & al. (2011). Novel insights into the regulation of antioxidant-response-element mediated gene expression by electrophiles: induction of the transcriptional repressor BACH1 by Nrf2. Biochemical Journal, 440 (2), 167-174.

Kajima, M. a. (1982). Phytochemistry, 21, 67-69.

Kaspar, J., & Jaiswal, A. (2009). Antioxidant-induced phosphorylation of tyrosine 486 leads to rapid nuclear export of Bach1 that allows Nrf2 to bind to the antioxidant response element and activate defensive gene expression". J. Biol. Chem., 285 (1), 153-162.

Katona, I., & al. (1999). Presynaptically located CB1 cannabinoid receptors regulate GABA release from axon terminals of specific hippocampal interneurons. The Journal of Neuroscience, 19 (11), 4544-4558.

Kimura, M. a. (1970). Distribution of tetrahydrocannabinolic acid in fresh wild Cannabis. Experientia 26, 819-20.

Kojoma, M. S. (2006). DNA polymorphisms in the tetrahydrocannabinolic acid (THCA) synthase gene in "drug type" and "fibre type" Cannabis sativa L. Forensic Science International, 159, 132-140.

Kojoma, M., & al., e. (2006). DNA polymorphisms in the tetrahydrocannabinolic acid (THCA) synthase gene on "drug type" and "fiber type" Cannabis sativa L. Forensic Science Internationa, 159, 132-140.

Kraft, R., & Harteneck, C. (2005). The mammalian melastatin-related transient receptor potential cation channels: an overview. Pflugers. Arch., 451 (1), 201-211.

Krejčí, R., & Šantavý, F. (1955). Acta Univ. Palacki. Olomuc., Fac. Med., 6, 59-66.

Krings M., T. T. (2002). Touch-sensitive glandular trichomes: a mode of defence against herbivorous arthropods in the Carboniferous. Evolutionary Ecology Research, 4, 779-786.

Kwak, M., & al. (2003). Modulation of gene expression by cancer chemopreventive dithiolethiones through the Keap1-Nrf2 pathway. Identification of novel gene clusters for cell survival. Journal of Biological Chemistry, 278 (10), 8135-8145.

Lawrence, D., & Gill, E. (1975). he effects of Δ1-tetrahydrocannabinol and other cannabinoids on spin-labelled liposomes and their relationship to mechanisms of general anaesthesia. Mol. Pharmacol., 11, 595-602.

Levine, J. D., & al. (2007). TRP channels: targets for the relief of pain. Biochim. Biophys. Acta, 1772, 989–1003.

Linciano, P., & al. (2020). Identification of a new cannabidiol n-hexyl homolog in a medicinal cannabis variety with an antinociceptive activity in mice: cannabidihexol. Scientific Reports 10 (1).

Liu, Z., & al. (2016). TRPM8: a potential target for cancer treatment. J. Cancer. Res. Clin. Oncol., 142 (9), 1871-1881.

Livingston, S. e. (2020). Cannabis glandular trichomes alter morphology and metabolite content. Plant J, 101, 37-56.

Loewe, S. (1946). Studies on the pharmacology and acute toxicity of compound with marijuana activity. J. Pharmacol. Exp. Ther., 88, 154-161.

Lu, H., & al. (2016). An introduction to the Endogenous Cannabinoid System. Biol. Psychiatry, 79 (7), 516-525.

Luo, X. e. (2019). Complete biosynthesis of cannabinoids antheir unnatural analogues in yeast. Nature 567, 123-126.

Lux, S., & al. (1990). Analysis of cDNA for human erythrocyte ankyrin indicates a repeated structure with homology to tissue-differentiation and cell-cycle control proteins. Nature, 344(6261), 36-42.

Lydon, J. a. (1987). Photochemical decomposition of cannabidiol in its resin base. Phytochemistry, 26, 1216-1217.

Lydon, J., & Teramura, A. (1987). Photochemical decomposition of cannabidiol in its resin base. Phytochemistry, 26, 1216-1217.

Maccarrone, M. (2005). Endocannabinoids and regulation of female and male fertility. Pharmacologyonline, 2, 30-37.

Mahlberg P.G., K. E. (2004). Accumulation of Cannabinoids. Journal of Industrial Hemp, 9:1, 15-36.

Martin, B., & al. (1991). Behavioral, Biochemical, and Molecular Modeling Evaluations of Cannabinoid Analogs. . Pharmacol. Biochem Behav., 40 (3), 471-478.

McPartland, J., & al., e. (2007). Coevolution betweer Cannabinoid Receptors and Endocannabinoid Ligands. Gene, 397 (1-2), 126-135.

Mechoulam, R., & Shvo, Y. (1963). Tetrahedron, 2073-2078.

Mechoulam, R. (2005). Plant cannabinoids: a neglected pharmacological treasure trove. British Journal of Pharmacology, 146, 913-915.

Mechoulam, R., & al. (1995). Identification of an endogenous 2-monoglyceride, present in canine gut, that binds to cannabinoid receptors. Biochem. Pharmacol., 50, 83-90.

Mechoulam, R., & al., e. (1968). Tetrahedron, 24, 5612-5624.

Mechoulam, R., & Gaoni, Y. (1967). The absolute configuration of Delta1-tetrahydrocannabinol, the major active constituent of hashish. Tetrahedron Lett., 8, 1109-1111.

Meijer, E., & Keizer, L. (1996). Patterns of diversity in Cannabis. Genetic Resources and Crop Evolution, 43, 41-52.

Melvin, L., & al. (1993). Structure-activity relationships for cannabinoid receptor-binding and analgesic activity: studies of bicyclic cannabinoid analogs. Mol Pharmacol, 44, 1008-1015.

Melvin, L., & al. (1995). Structure-activity relationships defining the ACD-tricyclic cannabinoids: cannabinoid receptor binding and analgesic activity. . Drug Des Discov, 13, 155-166.

Menendez-Gutierrez, M., & al. (2012). Biology and therapeutic applications of peroxisome proliferator-activated receptors. Curr Top Med Chem ,12, 548–584.

Mikics, E., & al. (2006). The effects of cannabinoids on contextual conditioned fear in CB1 knockout and CD1 mice. Behav Pharmacol., 17, 223-230.

Mills, J. (2003). Cannabis britannica: empire, trade and prohibition. Oxford: Oxford University Press.

Morales, P., & Reggio, P. (2017). An update on non-CB1, non-CB2 cannabinoid related G-protein-coupled receptors. Cannabis Cannabinoid Res., 2(1), 265-273.

Morimoto, S., & al., e. (1997). Enzymological evidence for cannabichromenic acid biosynthesis. Journal of Natural Products, 60, 854-857.

Morimoto, S., & al., e. (1998). Purification and characterization of cannabichromene acid synthase from Cannabis sativa. Phytochemistry, 1525-1529.

Muller, C., & al. (2018). Cannabinoid Ligands Targeting TRP Channels. Front. Mol. Neurosci., 11, 487.

Munro, S., & al. (1993). Molecular characterization of a peripheral receptor for cannabinoids. Nature, 365, 61-65.

Nilius, B., & Owsianik, G. (2011). The tansient receptor potential family of ion channels. Genome Biol., 12, 218.

Ogawa, K., & al. (2001). Heme mediates derepression of Maf recognition element through direct binding to transcription repressor Bach1. he EMBO Journal, 20 (11), 2835-2843.

O'Sullivan, S. (2016). An update on PPAR activation by cannabinoids. Br. Journ. Pharmacol., 173, 1899-1910.

Oyake, T., & al. (1996). Bach proteins belong to a novel family of BTB-basic leucine zipper transcription factors that interact with MafK and regulate

transcription through the NF-E2 site". Molecular and Cellular Biology, 16 (11), 6083-6095.

Pacifico, D., & al., e. (2006). Genetics and marker-assisted selection of the chemotype in Cannabis sativa L. Molecular Breeding, 17, 257-268.

Page, J. a. (2012). Aromatic prenyltransferase from Cannabis. U.S. Patent No. 2012/0144523 A1.

Paton, W., & Pertwee, R. (1973). The pharmacology of cannabis in animals. In Mechoulam, Marijuana (p. 191-285). New York: Academic Press.

Pertwee, R. (1988). The central neuropharmacology of psychotropic cannabinoids. Pharmacol. Ther., 36, 189-261.

Pertwee, R. (1997). Pharmacology of CB1 and CB2 receptors. Pharmacol. Ther., 129-180.

Pertwee, R. (2004). The pharmacology and therapeutic potential of cannabidiol. In V. Di Marzo, Cannabinoids (p. 32-83). New York: Kluwer Academic/Plenum Publishers.

Pertwee, R. (2005). Pharmacological actions of cannabinoids. In R. Pertwee, Cannabinoid. Handbook of Experimental Pharmacology (p. 1-51). Heidelburg: Springer-Verlag.

Pertwee, R. (2006). Cannabinoid pharmacology: the first 66 years. British Journal of Pharmacology, 147, S163-S171.

Pertwee, R., & al. (1993). Cross tollerance between delta-9-tetrahydrocannabinol and the cannabinomimetic agents, CP-55-940, WIN-55,212-2 and anandamide. Br. J. Pharmacol., 110, 1483-1490.

Pollastro, F., & al, e. (2011). J. Nat. Prod., 74, 2019-2022.

Pollastro, F., & al., e. (2017). Amorfrutin-tyoe phytocannabinoids from Helichrisum umbraculigerum. Fitoterapia, 123, 13-17.

Pope, C., & al. (2009). Endocannabinoid Signaling in Neurotoxicity and Neuroprotection.". Neurotoxicology.

Qin, N., & al. (2008). TRPV2 is activated by cannabidiol and mediates CGRP release in cultured rat dorsal root ganglion neurons. J. Neurosci., 28, 6231–6238.

Raboune, S., & al. (2014). Novel endogenous N-acyl amides activate TRPV1–4 receptors, BV-2 microglia, and are regulated in brain in an acute model of inflammation. Front. Cell. Neurosci., 8, 195.

Radwan, M., & al., e. (2008). Phytochemistry, 69, 2627-2633.

Rahajo, T. e. (2004). Olivetol as product of a polyketide synthase in Cannabis sativa L. Plant Science, 166, 381-385.

Rigdon, A. (2015, July 29th). Accurate Quantification of Cannabinoid Acids by GC — Is it Possible? Tratto da ChromaBLOGraphy — Topical and timely insights from top chromatographers: https://blog.restek.com/accurate-quantification-of-cannabinoid-acids-by-gc-is-it-possible/

Robertson, L., & al., e. (1975). Biomed. Mass Spectrom., 2, 266-271.

Ross, R. (2003). Anandamide and vanilloid TRPV1 receptors. Br. J. Pharmacol, 140, 790-801.

Russo, E. (2007). Historu of cannabis and its preparations in saga, science, and sobriquet. Che. Biodivers., 4, 1614-1648.

Samanta, A., & al. (2018). Transient Receptor Potential (TRP) Channels. Subcell Biochem, 87, 141-165.

Šantavý, F. (1964). Notes on the structure of cannabidiol compounds. Acta Univ. Olomuc. Fac. Med., 35, 5-9.

Schultes, R., & al., e. (1974). Cannabis: an example of taxonomic. Harvard University Botanical Museum Leaflets, 23, 337-367.

Schulz, O., & and Haffner, G. (1960). Arch. Pharm., 293, 1-6.

Shani, A., & and Mechoulam, R. (1974). Tetrahedron, 30, 2437-2444.

Shoyama, Y. e. (1972). Chem. Pharm. Bull., 20, 2072.

Shoyama, Y., & al. (2005). Acta Cristallogr., Sect. F: Struct. Biol. Cryst. Commun. 61, 799-801.

Sirikantaramas, S. e. (2004). J. Biology Chem, 279, 39767-39774.

Sirikantaramas, S. e. (2005). Tetrahydrocannabinolic Acid Synthase, the Enzyme Controlling Marijuana Psychoactivity, is Secreted into the Storage Cavity of the Glandular. Plant Cell Physiol, 46(9), 1578-1582.

Small, E., & Cronquist, A. (1976). A practical and natural taxonomy for Cannabis. Taxon, 25, 405-435.

Smith, T., & and Smith, H. (1847). Process for preparing cannabine or hemp resin. Phar. J. Trans., I, 2881-2886.

Soethoudt, M., & al. (2017). Cannabinoid CB2 receptor ligand profiling reveals biased signalling and offtarget activity. Nature Communications, 8, 13958.

Steinberg, S. O. (1975). Investigation of the influence of soil types, environmental conditions, age and morphological plant parts on the chemical composition of Cannabis sativa (Dagga) plants. South Africa Medical Journal 45, 279.

Story, G., & al. (2003). ANKTM1, a TRP-like channel expressed in nociceptive neurons, is activated by cold temperatures. Cell, 112 (6), 819-829.

Stout, J. e. (2012). The hexanoyl-CoA precursor for cannabinoid biosynthesis is formed by an acyl-activating enzyme in Cannabis sativa trichomes. Plant J. 71, 353-365.

Sun, Y., & Bennett, A. (2007). Cannabinoids: A new group of agonists of PPARs. PPAR Research, 7.

Suzuki, H., & al. (2003). "Cadmium induces nuclear export of Bach1, a transcriptional repressor of heme oxygenase-1 gene". J. Biol. Chem., 278 (49), 49246-49253.

Szabo, B., & Schlicker, E. (2005). Effects of cannabinoids on neurotransmission. In R. Pertwee, Handbook of Experimental Pharmacology, 168 (p. 327-365).

Tatsuo, Y., & al., e. (1968). Chem. Phar. Bull., 16, 1164-1165.

Taura, F. e. (2009). Characterization of olivetol synthase, a polyketide synthase putatively involved in cannabinoid biosynthetic pathway. FEBS Lett., 583, 2061-2066.

Taura, F. S. (2007). Phytocannabinoids in Cannabis sativa: recent studies on biosynthetic enzymes. Chem. Biodiver, 4 (8), 1649-1663.

Tominaga, M., & al. (1998). Neuron, 21, 531-543.

Valliere, M. e. (2019). A cell-free platform for the prenylation of natural product and application to cannabinoid production. Nat. Commun., 10, 565.

Van der Stelt M, D. M. (2005). Cannabinoid receptors and their role in neuroprotection. Neuromolecular Med., 7, 37-50.

Van Sickle, M. D., & al. (2005). Identification and functional characterization of brainstem cannabinoid CB2 receptors. Science, 310(5746), 329–332.

Vandoros, G., & al. (2006). J. Cancer Res. Clin. Oncol., 132, 76–84.

Venkatachalam, K., & Montell, C. (2007). TRP channels. Annu. Rev. Biochem., 76, 387-417.

Wagner, G. (1991). Secreting glandular trichomes: more than just hairs. Plant Physiol. 96 (3), 675-679.

Wang, H., & al. (2006). M. Jekyll and Hyde: two faces of cannabinoid signaling in male and female fertility. Endocr Rev., 27, 427-448.

Wang, H., & Woolf, C. (2005). Neuron, 46, 9-12.

Wang, M., & al., e. (2016). Cannabis cannabinoid Res., 1 (1), 262-271.

Wells, R., & al., e. (2002). The Journey of Man: A Genetic Odyssey. Prinston, NJ: Prinston Univeristy.

Wood, T., & al., e. (1896). Charas. The resin of Indian hemp. J. Chem. Soc., 69, 539-546.

Wood, T., & al., e. (20-36). Cannabino, part I. J. Chem. Soc., 75, 1899.

Work, Bergel, & Todd. (1939). Biochem. J., 33, 123.

Worob, A., & Wenthur, C. (2020). DARK Classics in Chemical Neuroscience: Synthetic Cannabinoids (Spice/K2). ACS Chem. Neurosci., 11, 3881-3892.

Xie, S., & al. (2007). The endocannabinoid system and rimonabant: a new drug with a novel mechanism of action involving cannabinoid CB1 receptor antagonism -- or inverse agonism -- as potential obesity treatment and other therapeutic use. J. Clin. Pharm. Ther.

Xiong, W., & al. (2011). Cannabinoid potentiation of glycine receptors contributes to cannabis-induced analgesia. Nat Chem Biol, 7(5), 296-303.

Yekkirala, A. S. (2013). Two to tango: GPCR oligomers and GPCR-TRP channel interactions in nociception. Life Sci., 92, 438–445.

Zhang, X., & al. (2018). Bach1: function, regulation, and involvement in disease. Oxidative Medicine and Cellular Longevity, 8.

Zou, S., & al. (2018). Cannabinoid receptors and the endocannabinoid system: signalling and function in the central Nervous System. Int J Mol Sci, 19 (3).

Zygmunt, P. M., & al. (1999). anilloid receptors on sensory nerves mediate the vasodilator action of anandamide. Nature, 400, 452–457.

CHAPTER 2

OBJECTIVES OF THE WORK

Despite extensive and multidisciplinary studies, many aspects of the biomedical profile of phytocannabinoids and their plant source are still incompletely known, justifying the statement of the neuropharmacologist Leo Hollister that

"*the more one studies cannabis chemically, the more complicated it becomes*".

This thesis builds on the expertise on the chemistry and pharmacology of cannabinoids acquired in almost two decades of studies by the research group where I have been working. The topics I was asked to investigate were *the reactivity of CBC*, *the oxidation of phytocannabinoids,* and the clarification of some aspects of *the structure-activity relationships of the phytocannabinoid pharmacophore.*

Based on *dihydrochromenone* (**1**) behavior, the possibility to interconvert CBC in THC by thermal degradation has been extensively explored.

The acidic and native form of phytocannabinoids is primed not only to decarboxylation, but also to oxidation of its resorcinyl core to quinoid forms, and the second target of my work was to investigate the mechanism of this reaction and shed light on its biological meaning, evaluating its potential to expand the biological space of the cannabinoid pharmacophore. In the course of these studies, a unique reactivity was evidenced in two classes:

- *the chromenic cannabinoids* — exemplified by CBC (**2**), a natural phytocannabinoid;
- *the dimethylheptyl cannabinoids* — a class of synthetic cannabinoids related to Adams' pyrahexyl (**3**).

Finally, my ultimate task was to investigate, by total synthesis of analogues, the biological space associated to these lead structures.

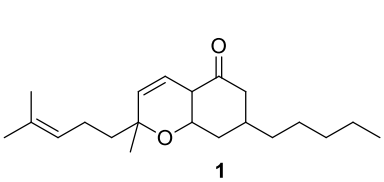

1

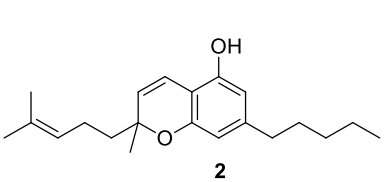

2

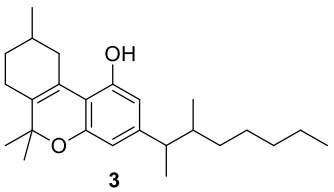

3

CHAPTER 3

THE CHEMISTRY OF PHYTOCANNABINOIDS

Despite the large and decades-long efforts aimed to the clarification of the chemical reactivity of phytocannabinoids – that have already led to the discovery of several new bioactive entities – the chemical structure of this class of compounds still reserves various aspects that require further elucidation.

In the first part of this PhD thesis, *two aspects* regarding the chemical reactivity of phytocannabinoids have been deepened:

1. *Iodine promoted phytocannabinoids rearrangement:* the research group I belong has already observed how some phytocannabinoids could undergo interconversion and rearrangement through treatment with molecular iodine. During my thesis I carried out this project by completing the reactivity framework of the main phytocannabinoids towards iodine, discovering an interesting deconstructive annulation which – after several optimizations – led to the first *one-pot synthesis of CBN*;
2. *Oxidation of the resorcinyl core*: cannabinoquinones are a particular class of compounds with a marked bioactivity. Despite this type of reactivity was already known, it was appropriate to investigate this aspect through the study of oxidants based on hypervalent iodine, and the results of this research have led us to *the optimization of regioselective reactions* for phytocannabinoids and their derivatives.

SUBCHAPTER 3.1

ONE-POT TOTAL SYNTHESIS OF CANNABINOL VIA IODINE-MEDIATED DECONSTRUCTIVE ANNULATION

OL | Organic Letters

Letter

Cite This: *Org. Lett.* XXXX, XXX, XXX−XXX

pubs.acs.org/OrgLett

One-Pot Total Synthesis of Cannabinol via Iodine-Mediated Deconstructive Annulation

Diego Caprioglio,[†] Daiana Mattoteia,[†] Alberto Minassi,[†] Federica Pollastro,[†] Annalisa Lopatriello,[‡] Eduardo Muñoz,[§] Orazio Taglialatela-Scafati,*[,‡] and Giovanni Appendino*[,†]

[†]Dipartimento di Scienze del Farmaco, Università del Piemonte Orientale, Largo Donegani 2, 28100 Novara, Italy

[‡]Dipartimento di Farmacia, Università di Napoli Federico II, Via Montesano 49, 80131 Napoli, Italy

[§]Maimonides Biomedical Research Institute of Córdoba, University of Córdoba, Avda Menéndez Pidal s/n, 14004 Córdoba, Spain

Supporting Information

ABSTRACT: The thermal degradation of cannabichromene (CBC, **3**) is dominated by cationic reactions and not by the pericyclic rearrangements observed in model compounds. The rationalization of these differences inspired the development of a process that coupled, in an aromatization-driven single operational step, the condensation of citral and alkylresorciniols to homoprenylchromenes and their *in situ* deconstructive annulation to benzo[*c*]chromenes. This process was applied to a total synthesis of cannabinol (CBN, **5**) and to its molecular editing.

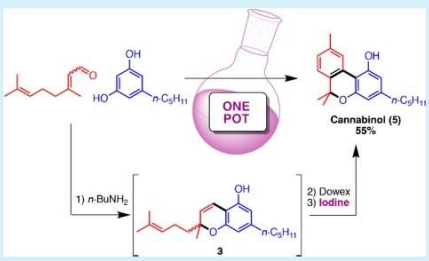

ABSTRACT

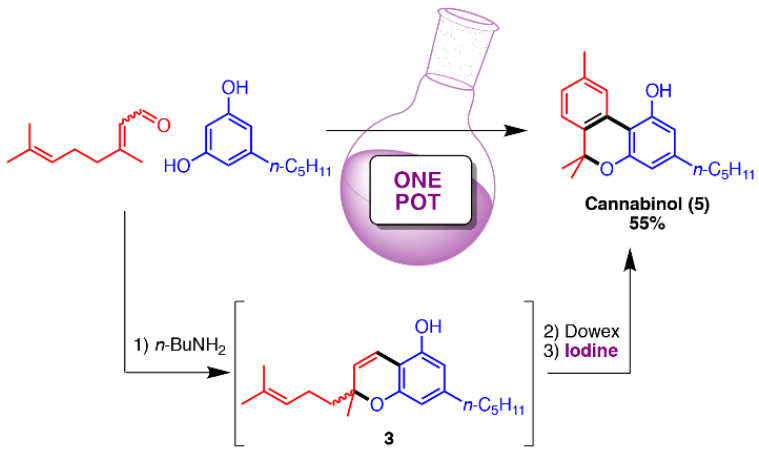

The thermal degradation of cannabichromene (CBC, **3**) is dominated by cationic reactions and not by the pericyclic rearrangements observed in model compounds. The rationalization of these differences inspired the development of a process that coupled, in an aromatization-driven single operational step, the condensation of citral and alkylresorcinols to homoprenylchromenes and their *in situ* deconstructive annulation to benzo[c]chromenes. This process was applied to a total synthesis of cannabinol (CBN, **5**) and to its molecular editing.

Despite the availability of phytocannabinoid-based mainstream drugs and significant advances in our knowledge on their targets and mode of action,[1] medicinal marijuana, that is the inhaling of vapors of crude *Cannabis* products (flowerheads, *cannabis* oil, hashish), is still receiving considerable attention by both the media and the biomedical community.[2] Within the various arguments raised to justify research in medicinal marijuana, a popular one is our limited knowledge on the complex phytocannabinoid mixtures that originate when crude *Cannabis*

products are vaporized.[3] By decarboxylating acidic cannabinoids to their neutral forms[4] heating dramatically changes the profile of *Cannabis* products, and more complex reactions that generate new phytocannabinoids and/or interconvert existing ones are also possible because of the tendency of phytocannabinoids to undergo complex rearrangements.[5] In this context, based on the reactivity of the dihydrochromenone model **1** (Figure 1) and on calculations, it was postulated that cannabichromene (CBC, **3**), a non-narcotic major constituent of hemp leaves, could generate a mixture of narcotic tetrahydrocannabinols (THCs, **4**) by electro-reversion to a quinone methide and intramolecular cycloaddition to the terminal isoprenyl double bond (Figure 1).[6] If confirmed, this claim would have the significant implication that also the leaves of fiber hemp could be considered potentially narcotic. The claim was, however, surprising, since the chemistry of cannabichromene has been investigated since the outset of modern studies on cannabinoids,[7] and such an important reaction could hardly have escaped detection, especially if the conversion yield were so high (77%) as claimed for compound **1**.[6] The model reaction, while mimicking with silica gel the acidic pyrolytic milieu of *Cannabis*, was, nevertheless, mechanistically questionable in terms of substrate selection. Thus, because of regulatory considerations associated to the generation of THC, a Schedule 1 compound in USA, a non-aromatic version of CBC (**1**) was used,[6] overlooking the relevance of aromaticity loss for the electrocyclic opening that triggers the deconstructive annulation. Surprisingly, this study had no follow-up, and the possibility that THC could be generated from CBC under pyrolytic conditions was not further investigated.

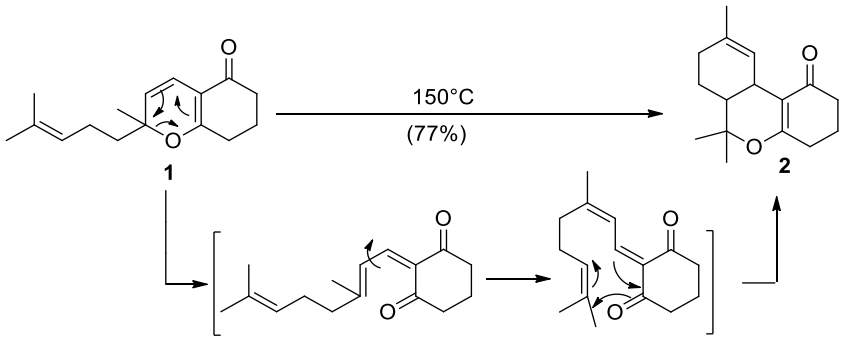

Figure 1. Thermal rearrangement of the cannabichromene (CBC) model compound **1** to afford a mixture of *cis*/*trans* Δ^9-THC analogues (**2**).

These considerations, and our interest in the rearrangements of cannabinoids,[8] provided a rationale to study the thermal degradation of CBC (**3**) under the conditions of the conversion of **1** to **2**. While disproving this conversion, our study led to the development of a practical one-pot synthesis of cannabinol (CBN, **5**), the first phytocannabinoid to be purified[9] and structurally elucidated.[10]

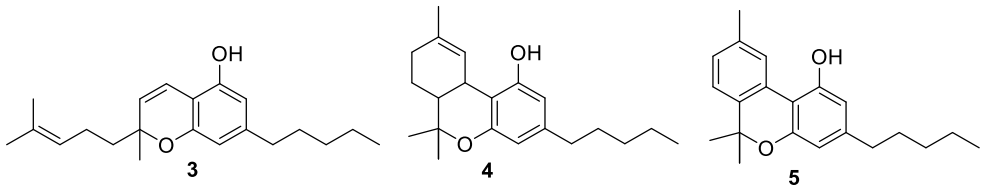

When CBC was treated with silica gel under the conditions used for the model compound **1** (Fig.1),[6] a mixture of three compounds (**6-8**) was obtained (Figure 2). Any THC isomer, if formed at all, was below the detection threshold of the ^{1}H NMR spectrum (700 MHz) of the reaction mixture.

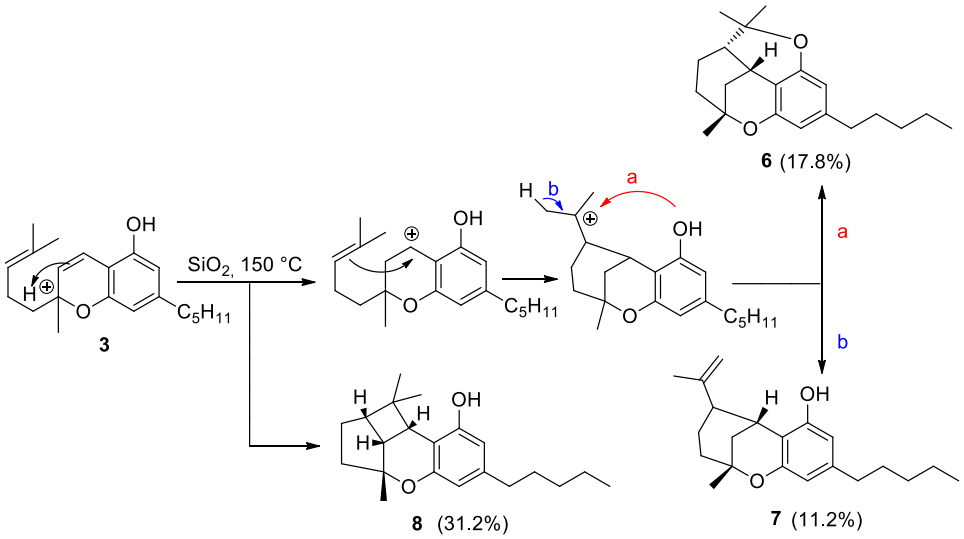

Figure 2. Pyrolysis of cannabichromene (150 °C, microwave 300 W, 210 min) in the presence of silica gel.

Cannabicitran (citrylidene-*cannabis*, bicyclo-CBC, **6**)[11] and Δ⁸-*iso*-*cis*-THC (cyclo-CBC, **7**)[12] derive from the protonation of the chromene olefin bond and formation of a benzyl cation, next trapped by the terminal isoprenyl double bond, with termination either by proton loss to Δ⁸-*iso*-*cis*-THC (**7**) or by intramolecular oxygen trapping to cannabicitran (**6**). The structure of the third compound, cannabicyclol (CBL, **8**), was confirmed by comparison with an authentic sample prepared by intramolecular [2+2] photocycloaddition of CBC (45% yield),[13] and CBC treatment with $FeCl_3$ (65% yield).[14] The three compounds formed in the pyrolytic study had already been described from the treatment of CBC and other cannabinoids with acids and/or by heating or irradiation.[5] The formal [2π + 2π] thermal cyclization of CBC (**3**) to CBL (**8**) was, nevertheless, mechanistically intriguing, and a similar transformation is documented also for other homoisoprenylchromenes.[15-17] The reaction has been considered a Gassman-type cationic [2π + 2π] cyclization,[18] but the anti-Markovnikow regiochemistry is at odd with the considerations of carbocation

stability that govern this type of cycloadditions.[18,19] An alternative, and more plausible mechanism is presented in Figure 3. The reaction might involve a cyclopropane intermediate (**9**), the result of a concerted process triggered by electrophilic (acidic) activation of the carbonyl tautomer of the resorcinyl moiety and terminated by electrophilic Markovnikov addition to the electron-rich homoisoprenyl terminal double bond (Figure 3). This process, somewhat reminiscent of the santonine-desmotroposantonine rearrangement,[20] generates a tertiary cation that is turned into an oxonium ion by opening of the cyclopropane ring. Regeneration of aromaticity by decomplexation and tautomerization eventually terminates the reaction.

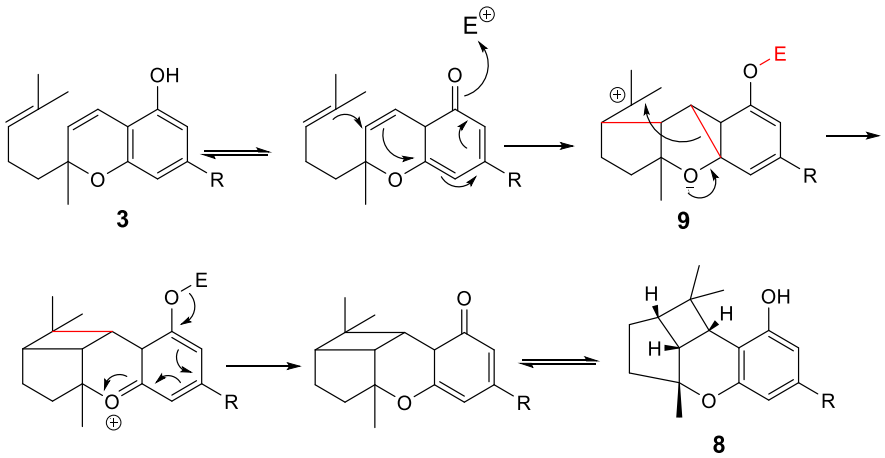

Figure 3. Possible rationalization for the formation of cannabicyclol (CBL, **8**) from the acidic thermolysis of cannabichromene (CBC, **3**) ($E^+ = H^+$ or a Lewis acid, R = n-C_5H_{11}). The reaction is a mechanistic pericyclic "false friend", just like the Staudinger β-lactam synthesis.

Compared to the thermal degradation of the model compound **1**, the one of CBC (**3**) is characterized by replacement of the electrocyclic opening of the chromene ring by a series of cationic processes, a predictable behavior since in the natural product electroreversion involves loss of aromaticity. Dihydroresorcinols are difficult to aromatize,[15] and the deconstructive annulation exemplified by the conversion of **1** to

2 has therefore remained relegated into the limbo of the generation of "model compounds" for natural chromenes. Spurred by the potential of the reaction to generate natural products diversity, we wondered if aromatization of the carbocyclic moiety could provide an alternative driving force to steer the reaction toward the electrocyclization, overcoming, or at least balancing, the unfavorable initial de-aromatization step. Since iodine can efficiently aromatize *p*-menthenes, including Δ^9-THC, via a tandem iodine addition-hydrogen iodide elimination mechanism,[21,22] we wondered if iodine, rather than acids, could materialize the chemistry postulated for the model compound, eventually turning CBC into cannabinol (CBN, **5**), the aromatized version of Δ^9-THC. CBN is a major constituent of traditionally produced hashish[10] but, mostly for its limited availability, it has largely remained *terra incognita* in terms of bioactivity studies. This is surprising, since the conversion of Δ^9-THC into CBN is relatively fast (5% per month at room temperature in hashish and even faster in extracts),[23] suggesting that the early clinical studies on *Cannabis* were carried out on a material containing significant amounts of CBN, possibly even higher than those of its precursor Δ^9-THC.[24]

In the event, we were pleasingly surprised to observe that the treatment of CBC (**3,** general formula **13** with R = *n*-C_5H_{11}) under the conditions we had developed for the aromatization of Δ^9-THC (refluxing in toluene with two equivalents of iodine)[22] led, in a spot-to-spot fashion, to its conversion to CBN in 82% yield (**5**, general formula **14** with R = *n*-C_5H_{11}, Figure 4).

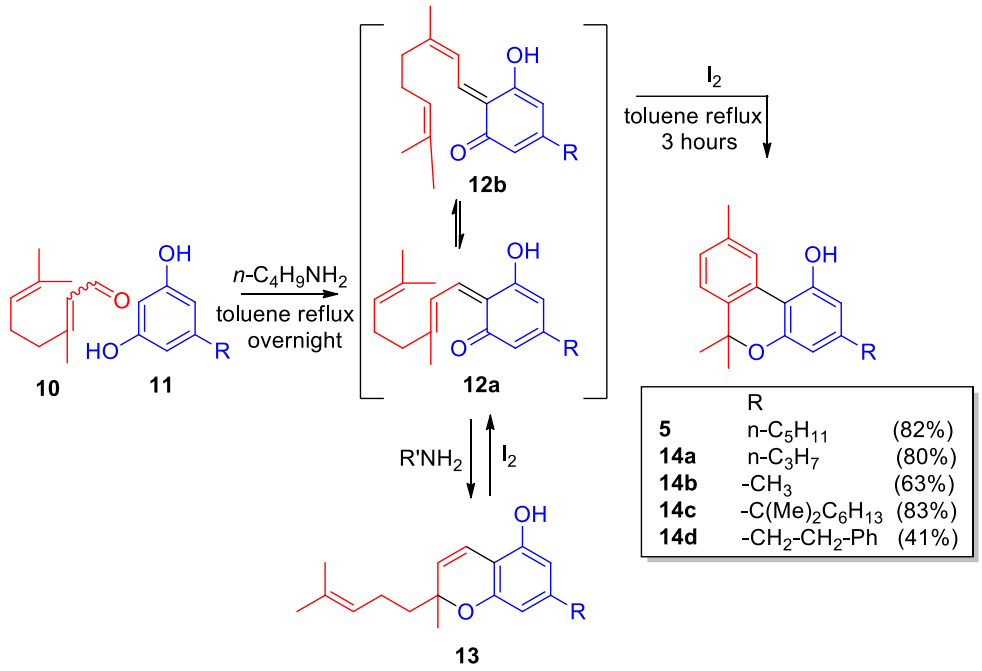

Figure 4. Total synthesis of cannabinol (**5**) and analogues. In the one-pot procedure for cannabinol (**5**), Dowex 50 WX8 was added after the first step and, after filtration over celite, iodine was added. CBN was obtained in 55% yield.

Other sources of electrophilic iodine species gave a decreased yield (ICl), or, in the case of *N*-iodosuccinimide (NIS), afforded a mixture of iodinated products derived from attack to the aromatic resorcinyl moiety (**15**, 20.6% and **16**, 5.6%) or from a iodine-induced citran-type cyclization (**17**, 21.0%) (Figure 2). Taken together, these observations highlight the delicate role of the iodine source to trigger the deconstructive annulation. The hidden Brönsted acidity of iodine, that is, its capacity to generate HI by interaction with hydroxyl groups from the substrate or from traces of protic solvents,[25] was ruled out as a possible mechanism, since treatment of CBC with Broensted acids affords compounds resulting from formation of a benzyl cation and not by cycloreversion.[7] A soft polarizability/polarization of the I-X bond seems, conversely, critical to avoid electrophilic attack to the electron-rich aromatic ring and

the dihydropyrane double bond. Electroreversion could then be promoted by halogen-bonding to the chromene oxygen and/or to its aromatic ring,[25] while the final aromatization eventually funnels the various equilibria toward the generation of dibenzochromenes. It is remarkable that, despite the plethora of reaction pathways available, only the deconstructive annulation was observed, at least within the limit of ^{1}H NMR sensitivity, by analysis of the crude reaction mixture.

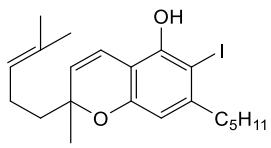

15

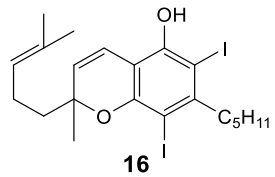

16

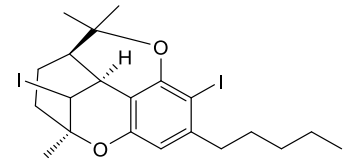

17

In a further development of the reaction, we wondered if iodine-promoted aromatization could redirect the condensation of citral (**10**) and resorcinols (**11**) from the generation of chromenes (**13**) to the one of benzochromenes (**14**), since it generates the same quinonmethide intermediate **12** postulated for the deconstructive annulation of chromenes to benzochromenes (Figure 4), and iodine has been reported to promote the condensation of cyclic β-dicarbonyls and unsaturated aldehydes to dihydrochromenes.[26] However, the direct treatment of citral (**10**) and olivetol (**11**, R = n-C_5H_{11}) with iodine only produced a complex mixture, confirming that cyclohexandiones are not good models of resorcinols, and that amine catalysis is required for the initial condensation step. Amines (pK_{BI2} ca. 3,8)[27] show a stronger affinity for iodine than an oxygen ether or an aromatic ring (pK_{BI2} ca 0 in both cases),[27] and complexation with an amine evidently completely neutralizes the σ-hole electrophilicty of iodine.[25] To overcome this impasse, we scavenged the amine required for the chromenylation (*n*-butylamine)[28] with an acidic ion resin, adding then iodine to the filtered solution, and continuing refluxing. In this way, after

aqueous work-up of the reaction, CBN could be obtained in a rewarding 55% yield directly from olivetol and citral (Figure 4).

The one-pot total synthesis of CBN from two commodities (citral and olivetol) solves a long-stainding problem in cannabinoid chemistry and natural product synthesis, since aryl coupling of a resorcinyl benzoates, the most obvious retrosynthetic strategy to cannabinol, gives the wrong regioisomer (unnatural CBN).[29] Thus, in his classic studies on cannabinoids, Adams managed to synthesize via aryl coupling of resorcinyl benzoates all possible regioisomers of CBN except the natural one.[10] This regiochemical issue was only recently solved by Hertweck using a different tether and a different aryl coupling strategy (photosplicing of a benzylsulfonamidic precursor).[30]

Our one-pot synthesis of dibenzochromenes is general for 5-alkylresorcinols, an important and densely populated class of plant and microbial secondary metabolites,[31] and citral (Figure 4). In this way, it was possible to edit the structure of cannabinol, expeditely generating natural (**14a, b**) and synthetic analogues from the α,α-dimethylheptyl- (**14c**)[5] and the phenethyl (**14d**) series[5] useful to explore the biological space associated to its chemotype (Figure 4).

However, the deconstructive annulation of homoprenylchromenes has also some limitations. The reaction was investigated with higher homologues of citral (C-10), namely farnesal (C-15) and geranylgeranial (C-20), but, in both cases, complex mixtures were formed. In addition, non-symmetric resorcinols like 4-hexylresorcinols afford isomeric chromenes in the condensation step and, even when the single isomers were reacted with iodine, parasite reactions plagued the deconstructive annulation, affording mixtures. Conjugating groups, like double

bonds or a carbonyl, on the resorcinyl moiety are not tolerated, and, regrettably, the reaction could not be applied to resorcinyl flavonoids and stilbenoids, two very common classes of natural products. Attempts to expand the application of the reaction to heteroaromatic analogues of alkylresorcinols met also with limited success. Thus, the pyranocoumarin ferprenin (**18**)[32] gave the corresponding dibenzochromene (**19**) in mixture with two "benzylic" cyclization products (**20a,b**), that became the exclusive reaction products with the pyranopyrone **21** (Figure 5).

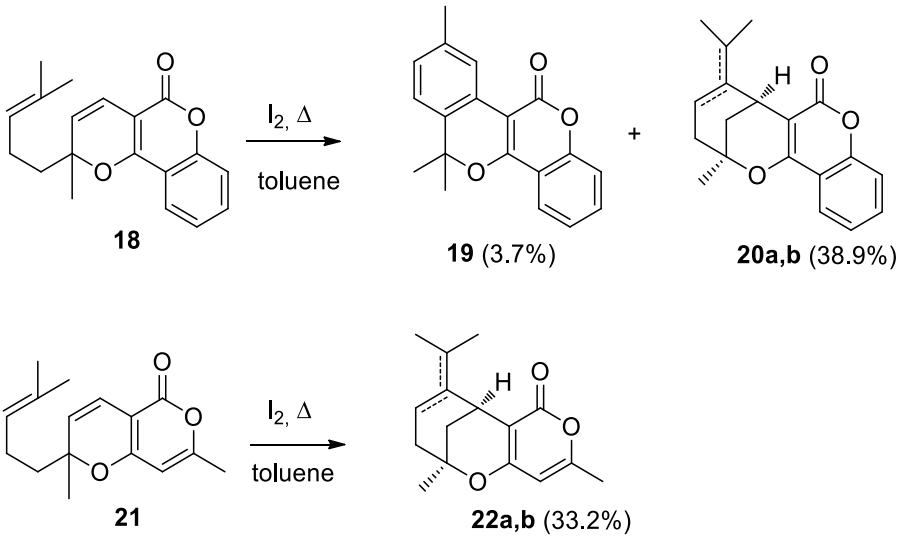

Figure 5. Attempts to extend the chromene deconstructive annulation to isosteric cannabichromene analogues.

Even with these limitations, the simplicity and the easy availability of its starting material make the iodine-mediated deconstructive annulation of homo-isoprenylchromenes to benzo[c]chromenes a remarkable example of expedite generation of biologically relevant chemical diversity from simple building blocks, encouraging the biological evaluation of compounds of limited availability by isolation.

AUTHOR INFORMATION

Corresponding Authors

* Prof. O. Taglialatela-Scafati, E-mail: scatagli@unina.it

* Prof. G. Appendino, E-mail: giovanni.appendino@uniupo.it

Author contributions

All authors have given approval to the final version of the manuscript.

ACKNOWLEDGMENT

We are grateful to Emerald Biotechnology Spain and MIUR, Italy (PRIN2017, Project 2017WN73PL, bioactivity-directed exploration of the phytocannabinoid chemical space) for financial support. We also thank Vittorio Farina (Janssen Pharmaceutica) for discussions and suggestions on the mechanistic aspects of the formation of cannabicyclol from cannabichromene.

REFERENCES

(1) Di Marzo V. Nat. Rev. Drug Discov. 2018, 17, 623.

(2) Mouhamed Y., Vishnyakov A., Qorri B., Sambi M., Frank S. S., Nowierski C., Lamba A., Bhatti U., Szewczuk M. R. Drug Health Patient Saf. 2018, 10, 45-66.

(3) Hazekamp A., Ruhaak R., Zuurman L., van Gerven J., Verpoorte R. J. Pharm. Sci. 2006, 95, 1308.

(4) Wang M., Wang Y.-H., Avula B., Radwan M. M., Wanas A. S., van Antwerp J., Parcher J. F., ElSohly M. A., Khan I. A. Cannabis Cannabinoid Res. 2016, 1, doi:10.1089/can.2016.0020 .

(5) L. O. Hanuš, S. M. Meyer, E. Muñoz, O. Taglialatela-Scafati, G. Appendino, Nat. Prod. Rep. 2016, 33, 1357.

(6) Garcia A., Borchardt D., Chang C.-D. A., Marsella M. J. *J. Am. Chem. Soc*. **2009**, *131*, 16640. For a study on the biological profile of *cis*-THC, see: Chicca A., Schafroth M. A., Reynoso-Moreno I., Erni R., Petrucci V., Carreira E. M. Gertsch, J. *Sci. Adv.* **2018**, *4*, 2166.

(7) Pollastro F., Caprioglio D., Del Prete D., Rogati F., Minassi A., Taglialatela-Scafati O., Muñoz E., Appendino G. *Nat. Prod. Commun*. **2018**, *13*, 1189.

(8) Lopatriello A., Caprioglio D., Minassi A., Schiano Moriello A., Formisano C., De Petrocellis L., Appendino G., Taglialatela-Scafati O. *Bioorg. Med. Chem.* **2018**, *26*, 4532.

(9) Wood T. B., Spivey W. T. S., Easterfield T. H. *J. Chem. Soc.***1896**, *69*, 539.

(10) Adams R., Hunt M., Clark J. H. *J. Am. Chem. Soc.* **1940**, *62*, 196.

(11) Crombie L., Redshaw S. D., Whiting D. A. *J. Chem. Soc. Chem. Commun.* **1979**, 630.

(12) Yagen B., Mechoulam R. *Tetrahedron Lett.* **1969**, 5353. Modern numbering would locate the double bond at C-11, and the name *iso*-THC is, nevertheless, confusing.

(13) Crombie L., Ponsford R., Shani A., Yagnitinsky B., Mechoulam R. *Tetrahedron Lett.* **1968**, 5771.

(14) Li X., Lee Y. R. *Biomol. Chem*. **2014**, *12*, 1250.

(15) Riveira M. J., La-Venia A., Mischne M. P. *J. Org. Chem.* **2016**, *81*, 7977-7983.

(16) Yeom H.-S., Li H., Tang Y., Hsung R. P. *Org. Lett.* **2013**, *15*, 3130.

(17) Kurdyumov A. V., Hsung R. P. *J. Am. Chem. Soc*., **2006**, *128*, 6272.

(18) Gassman P. G., Lattes A. C. *Tetrahedron Lett.* **1992**, *33*, 157.

(19) Roberts R. M., Landolt R. G., Greene R. N., Heyer E. W. *J. Am. Chem. Soc.*, **1967**, *58*, 1404.

(20) Andreocci A. *Gazz. Chim. Ital.* **1893**, *23*, 469.

(21) Domingo V., Prieto C., Silva L., Rodilla J. M. L., Quílez del Moral J. F., Barrero A. F. *J. Nat. Prod.* **2016**, *79*, 831.

(22) Pollastro F., Caprioglio D., Marotta P., Schiano Moriello A., De Petrocellis L., Taglialatela-Scafati O., Appendino G. *J. Nat. Prod.* **2018**, *81*, 630.

(23) Lerner P. *Bull. Narcotics* **1969**, *21*, 39.

(24) For an account of the early studies on hashish and cannabinol, see: Mills J. H. *Cannabis Britannica: Empire, Trade, and Prohibition 1800-1928*, Oxofrd University Press, Oxford, 2005.

(25) Breugst M., von der Heiden D. *Chem. Eur. J.* **2018**, *24*, 9187.

(26) Jung E. J., Lee Y. R. Lee H.-J. *Bull. Korean Chem. Soc.* **2009**, *30*, 2833.

(27) Laurence C., Graton J., Berthelot M., El Ghomari M J. *Chem. Eur. J.* **2011**, *17*, 10431.

(28) Elsohly E. A., Turner C. E., Clark A. M., Elsohly M. A. *J. Pharm. Sci.* **1982**, *71*, 1319.

(29) Adams R., Baker B. B., Wearn R. B. *J. Am. Chem. Soc.* **1940**, *62*, 2204.

(30) Kloss F. Neuwirth T., Haensch V. G., Hertweck C. *Angew. Chem. Int. Ed.* **2018**, *57*, 14476.
(31) Kozubek A., Tyman J. H. P. *Chem. Rev.* **1999**, *99*, 1.
(32) Appendino G., Tagliapietra S., Nano G. M., Picci V., *Phytochemistry* **1988**, *27*, 944.

ASSOCIATED CONTENT

Supporting Information

GENERAL EXPERIMENTAL PROCEDURES. IR spectra were registered on an Avatar 370 FT-IR Techno-Nicolet apparatus. ^{1}H (500 and 400 MHz) and ^{13}C (125 and 100 MHz) NMR spectra were measured on Varian INOVA NMR spectrometers. Chemical shifts were referenced to the residual solvent signal ($CDCl_3$: $\delta_H = 7.26$, $\delta_C = 77.0$; CD_3OD: $\delta_H = 3.34$, $\delta_C = 55.0$). Homonuclear ^{1}H connectivities were determined by the COSY experiment. One-bond heteronuclear ^{1}H-^{13}C connectivities were determined with the HSQC experiment. Two- and three-bond ^{1}H-^{13}C connectivities were determined by gradient 2D HMBC experiments optimized for a $^{2,3}J = 9$ Hz. Low- and high-resolution ESIMS were obtained on a LTQ OrbitrapXL (Thermo Scientific) mass spectrometer. Silica gel 60 (70- 230 mesh) used for gravity column chromatography (CC) was purchased from MachereyNagel. Flash chromatography was carried out on a Biotage apparatus, and a Knauer HPLC instrument equipped with Phenomenex LUNA silica gel and reverse phase columns (100 × 4.6 mm ID) was used for HPLC. Reactions were monitored by TLC on Merck 60 F254 (0.25 mm) plates, visualized by staining with 5% H_2SO_4 in ethanol and heating. Organic phases were dried with Na_2SO_4 before evaporation. Chemical reagents and solvents were from Aldrich and were used without any further purification unless stated otherwise.

PYROLYSIS OF CANNABICHROMENE (3) in presence of silica gel. CBC (100 mg, 0.32 mmol) was adsorbed onto silica (200 mg) and heated to 150 °C by microwave (CEM Discover SP Microwave, 300 W) at regular intervals of 30 minutes for a total of 210

minutes, until complete consumption of the starting material by TLC (PE-EtOAc 9:1, R*f* CBC= 0.27, Rf product mixture= 0.43). The crude product mixture was first purified by gravity column chromatography on silica gel using 9:1 PE-EtOAc solution as eluent to afford 68 mg of brown oil. Further HPLC purification (UV detector set at λ_{max} 227 nm; flow 0.8 mL/min) using as eluent a gradient from CH_3CN/H_2O (0.1% HCOOH) 7:3 to CH_3CN in 25 min afforded pure cannabicitran (**6**, 18.0 mg, 0.057 mmol, 17.8% yield), Δ^8-*iso*-*cis*-THC (**7**, 3 11.3 mg, 0.036 mmol, 11.2% yield), and cannabicyclol (**8,** 31.3 mg, 0.10 mmol, 31.2%). Cannabicitran,1 Δ^8 -*iso*-*cis*-THC,[2] and cannabicyclol[3] showed spectral properties identical to those reported in the literature.

IODINE-MEDIATED ANNULATION OF HOMO-ISOPRENYLCHROMENES TO BENZO[C]CHROMENES: SYNTHESIS OF CBN (5). To a stirred solution of CBC (300 mg, 0,954 mmol) in toluene (20 mL), iodine (472 mg, 1,860 mmol) was added. The mixture was refluxed and monitored by TLC (PE-EtOAc 9:1, R*f* CBC= 0,27, R*f* product= 0,29). After 3 hours, the reaction was quenched by addition of sat. Na_2SO_3 s.s. and extraction with EtOAc. After drying (Na_2SO_4) and evaporation, the residue was purified by gravity column chromatography on silica gel with PE-EtOAc 95:5 solution to afford CBN (**5**) as a brown oil (236 mg, 82%). One-pot total synthesis of CBN. To a stirred solution of olivetol (**11**, 100 mg, 0,554 mmol) toluene (5mL), citral (10, 91 μL, 0,533 mmol) and *n*-butylamine (53 μL, 0,533 mmol) were added. The mixture was refluxed overnight, then cooled to room temperature. Dowex 50 W X 8 (200 mg) was added, and the solution was stirred for 10 minutes at room temperature then filtered over celite pad in a new round bottomed flask. To the filtered solution, iodine (268 mg, 1,066 mmol) was added. The mixture was refluxed for 3 hours, then quenched by addition of sat. Na_2SO_3 and extraction with EtOAc. After drying (Na_2SO_4) and evaporation, the residue was purified by gravity column

chromatography on silica gel with PE-EtOAc 95:5 solution to afford CBN (**5**) as a brown oil (94 mg, 0.305 mmol, 55% yield). The spectra obtained for cannabinol (5) matched those reported in the literature.[4]

SYNTHESIS OF 14A. To a stirred solution of **13a** (260 mg, 0.914 mmol) in toluene (20 mL), iodine (463 mg, 1.828 mmol) was added. The mixture was refluxed and monitored by TLC (PE-EtOAc 9:1, R*f* **13a**= 0.55, R*f* product= 0.45). After 2 hours, the reaction was quenched by addition of sat. Na_2SO_3 s.s. and extraction with EtOAc. After drying (Na_2SO_4) and evaporation, the residue was purified by gravity column chromatography on silica gel with PE-EtOAc 98:2 solution to obtain compound 14a as a brown oil (207 mg, 80% yield). Compound **14a** was identified on the basis of a comparison of its spectral data with those reported in the literature.[5]

SYNTHESIS OF 14B: To a stirred solution of **13b** (300 mg, 1.161 mmol) in toluene (30 mL), iodine (590 mg, 2.323 mmol) was added. The mixture was refluxed and monitored by TLC (PE-CH_2Cl_2 6:4, R*f* 13b= 0.35, R*f* product= 0.42). After 2 hours, the reaction was quenched by addition of sat. Na_2SO_3 s.s. and extraction with EtOAc. After drying (Na_2SO_4) and evaporation, the residue was purified by gravity column chromatography on silica gel with PE-EtOAc 95:5 solution to afford compound cannabiorcol (**14b**) as a brown solid (188 mg, 63%). Compound **14b** was identified on the basis of a comparison of its spectral data with those reported in the literature.[6]

SYNTHESIS OF 14C: To a stirred solution of **13c** (200 mg, 0.540 mmol) in toluene (20 mL), iodine (273 mg, 1.080 mmol) was added. The mixture was refluxed and monitored by TLC (PE-EtOAc 9:1, R*f* **13c**= 0.38, R*f* product= 0.44). After 2 hours, the reaction was quenched by addition of sat. Na_2SO_3 s.s. and extraction with EtOAc. After drying (Na_2SO_4) and evaporation, the residue was purified by gravity column chromatography on silica gel with PE-EtOAc 95:5 solution to afford compound **14c**

as a brown solid (165 mg, 83%). Compound **14c** was identified on the basis of a comparison of its spectral data with those reported in the literature.[7]

SYNTHESIS OF 14D: To a stirred solution of **13d** (280 mg, 0.774 mmol) in toluene (20 mL), iodine (393 mg, 1.549 mmol) was added. The mixture was refluxed and monitored by TLC (PE-EtOAc 9:1, R*f* **13d** = 0.44, R*f* product = 0.46). After 2 hours, the reaction was quenched by addition of sat. Na2SO3 s.s. and extraction with EtOAc. After drying (Na_2SO_4) and evaporation, the residue was purified by gravity column chromatography on silica gel with PE-EtOAc 95:5 solution to afford compound **14d** as dark yellow oil (113 mg, 41%). ESIMS m/z 343 $[M - H]^-$; HRESIMS m/z $[M - H]^-$ 343.1700 (calcd for $C_{24}H_{23}O_2$, 343.1704). ^{1}H NMR (CD_3OD, 700 MHz): δ 8.34 (1H, s, H-8), 7.26-7.14 (overlapped, H-7, H-4' to H-8'), 7.03 (1H, d, *J* = 7.0 Hz, H-8), 6.36 (1H, s, H-2), 6.26 (1H, s, H-4), 2.88 (2H, t, *J* = 7.2 Hz, H-1'), 2.78 (2H, t, *J* = 7.2 Hz, H-2'), 2.34 (3H, s, H-11), 1.53 (6H, s, H-12, H-13). ^{13}C NMR (CD_3OD, 175 MHz): δ 156.5 (C-1), 155.7 (C-4a), 144.2 (C-10a), 143.1 (C-3), 141.8 (C-3'), 129.5 (C-8), 129.3 (C-6'), 128.3 (C-4', C-8'), 128.2 (C-5', C-7'), 126.9 (C-10), 123.3 (C-7), 110.7 (C-4), 110.5 (C-2), 109.8 (C-10b), 78.1 (C-6), 39.0 (C-1'), 38.6 (C-2'), 27.5 (C-12, C-13), 21.6 (C-11).

Reaction of CBC with N-iodosuccinimide. To a stirred solution of CBC (220 mg, 0.709 mmol) in toluene (15 mL), N-iodosuccinimide (318 mg, 1.418 mmol) was added. The mixture was refluxed and monitored by TLC (PE-EtOAc 95:5, R*f* CBC= 0.16, Rf product mix A= 0.54, R*f* product mix B= 0.32). After 3 hours, the reaction was quenched by addition of sat. Na_2SO_3 s.s. and extraction with EtOAc. After drying (Na_2SO_4) and evaporation, the residue was purified by gravity column chromatography on silica gel with PE-EtOAc 95:5 solution to afford two major product mixtures (A: yellow oil, 132 mg; B: brown oil, 134 mg). Further HPLC purification of fraction A (UV detector set at λmax 227 nm; flow 1.0 mL/min) using as eluent a gradient from MeOH/H_2O (0.1% HCOOH) 8:2 to MeOH in 15 min

afforded pure compound **17** (85 mg, 21%). Further HPLC purification of fraction B (UV detector set at λmax 227 nm; flow 1.0 mL/min) using as eluent a gradient from MeOH/H2O (0.1% HCOOH) 6:4 to MeOH in 25 min afforded pure compounds **15** (64.3 mg, 20.6%) and **16** (21.1 mg, 5.6%).

COMPOUND 15. ESIMS m/z 441 $[M + H]^+$; HRESIMS m/z $[M + H]^+$ 441.1290 (calcd for $C_{21}H_{30}IO_2$, 441.1285). ^{1}H NMR (CD_3OD, 700 MHz) δ 6.69 (1H, d, *J* = 10.0 Hz, H-1′), 6.32 (1H, s, H-4), 5.56 (1H, d, *J* = 10.0 Hz, H-2′), 5.10 (1H, t, *J* = 7.2 Hz, H-6′), 2.63 (2H, t, *J* = 7.5 Hz, H-1″), 2.09 (2H, m, H-5′), 1.66 (2H, overlapped, H-4′), 1.65 (3H, s, H-8′), 1.56 (3H, s, H-10′), 1.55 (2H, overlapped, H-2″), 1.37 (4H, m, H-3″-4″), 1.34 (3H, s, H-9′), 0.93 (3H, t, *J* = 6.4 Hz, H-5″). ^{13}C NMR (CD_3OD, 175 MHz): δ 157.8 (C-1), 153.0 (C-5), 143.0 (C-3), 131.6 (C-7'), 127.5 (C-2'), 123.9 (C-6'), 117.5 (C-1'), 109.9 (C-6), 109.4 (C-4), 87.0 (C-2), 77.9 (C-3'), 40.9 (C-4'), 40.7 (C-1''), 31.3 (C-3''), 29.6 (C-2''), 25.1 (C-5'), 22.3 (C-8', C-4''), 17.2 (C-9'), 13.0 (C-5'').

COMPOUND 16. ESIMS m/z 567 $[M + H]^+$; HRESIMS m/z $[M + H]^+$ 567.0241 (calcd. for $C_{21}H_{29}I_2O_2$, 567.0251).^{1}H NMR (CD_3OD, 700 MHz) δ 6.63 (1H, d, *J* = 10.0 Hz, H-1′), 5.57 (1H, d, *J* = 10.0 Hz, H-2′), 5.12 (1H, t, *J* = 7.1 Hz, H-6′), 3.10 (2H, t, *J* = 7.5 Hz, H-1″), 2.09 (1H, m, H-5′a), 2.03 (1H, m, H-5′b), 1.92 (1H, m, H-4′a),1.66 (1H, overlapped, H-4′b), 1.65 (3H, s, H-8′), 1.57 (3H, s, H-10′), 1.55 (2H, overlapped, H-2″), 1.40 (3H, s, H-9′), 1.37 (4H, m, H-3″-4″), 0.96 (3H, s, H-5″). ^{13}C NMR (CD_3OD, 175 MHz): δ 157.1 (C-1), 151.2 (C-5), 146.5 (C-3), 131.6 (C-7'), 128.6 (C-2'), 123.9 (C-6'), 117.5 (C-1'), 110.7 (C-6), 81.7 (C-2), 80.4 (C-3'), 79.0 (C-4), 41.4 (C-4'), 40.7 (C-1''), 31.3 (C-4''), 29.6 (C-2''), 25.1 (C-5'), 25.2 (C-8'), 22.3 (C-4''), 17.2 (C-9'), 13.0 (C-5'').

COMPOUND 17. ESIMS m/z 567 $[M + H]^+$; HRESIMS m/z $[M + H]^+$ 567.0239 (calcd for $C_{21}H_{29}I_2O_2$, 567.0251).^{1}H NMR (CD_3OD, 700 MHz) δ 6.42 (1H, s, H-4), 4.98 (1H, bs, H-2'), 3.00 (1H, bs, H-1′), 2.76 (1H, m, H-1″a), 2.68 (1H, m, H-6′), 2.61 (1H, m, H-1″b),

2.16 (1H, td, *J* = 13.9, 6.8 Hz, H-4'a), 1.68 (1H, dd, *J* = 15.5, 5.6 Hz H-5'a), 1.55 (6H, s, H-8'-10'), 1.38-1.29 (6H, m, H-3''-4''-4'b-5'b), 1.07 (3H, s, H-9'), 0.92 (3H, t, *J* = 6.9 Hz, H-5''), 0.53 (1H, qd, *J* = 12.7, 6.1 Hz, H-5); ^{13}C NMR (CD_3OD, 125 MHz): δ 157.7 (C-1), 153.2 (C-5), 143.0 (C-3), 109.7 (C-6), 109.4 (C-4), 87.3 (C-2), 86.2 (C-7'), 76.7 (C-3'), 45.1 (C-6'), 40.7 (C-1''), 35.1 (C-2'), 32.0 (C-4'), 31.3 (C-3''), 29.6 (C-2''), 28.1 (C-8'), 25.5 (C-1'), 23.5 (C-9'), 23.2 (C-10'), 22.4 (C-4''), 21.5 (C-5'), 13.0 (C-5'').

REACTION OF PYRANOPYRONES WITH IODINE. To a stirred solution of ferprenine (300 mg, 1.035 mmol) in toluene (20 mL), iodine (515 mg, 2.03 mmol) was added. The mixture was refluxed and monitored by TLC (PE-EtOAc 9:1, R*f* ferprenine= 0.40, R*f* product mix= 0.54). After 3 hours, the reaction was quenched by addition of sat. Na_2SO_3 and extraction with EtOAc. After drying (Na_2SO_4) and evaporation, the residue was purified by gravity column chromatography on silica gel to afford 180 of brown oil. Further HPLC purification (UV detector set at λ_{max} 227 nm; flow 1.0 mL/min) using as eluent a gradient from CH_3CN/H_2O (0.1% HCOOH) 7:3 to CH_3CN in 20 min afforded pure compounds **19** (11.3 mg, 3.7%), **20a** (57.4 mg, 18.7%) and **20b** (61.9 mg, 20.2%). When the same reaction and purification conditions were applied to compound **21** (200 mg, 0.77 mmol), compounds **22a** and **22b** (mixture 66.3 mg, 33.2%) were obtained.

COMPOUND 19. ESIMS m/z 293 $[M + H]^+$; HRESIMS m/z $[M + H]^+$ 293.1181 (calcd. for C19H17O3, 293.1172).^{1}H NMR (CD_3OD, 500 MHz) δ 8.41 (1H, s, H-13), 7.95 (1H, d, *J* = 8.0 Hz, H-1), 7.66 (1H, t, *J* = 8.0 Hz, H-2), 7.39 (2H, overlapped, H-3, H-4), 7.23 (1H, d, *J* = 7.8 Hz, H-16), 7.19 (1H, d, *J* = 7.8 Hz, H-15), 2.38 (3H, s, H-17), 1.77 (6H, s, H-18-19). ^{13}C NMR (CD_3OD, 125 MHz) δ 164.5 (C-9), 159.8 (C-7), 152.3 (C-5), 144.2 (C-11), 137.9 (C14), 132.2 (C-2), 131.2 (C-6), 129.4 (C-15), 124.8 (C-13), 124.7 (C-3), 123.7 (C-1), 123.5 (C-12), 122.5 (C-16), 116.1 (C-4), 101.9 (C-8), 81.1 (C-10), 25.2 (C-18, C-19), 20.0 (C-17).

COMPOUND 20A. ESIMS m/z 297 $[M + H]^+$; HRESIMS m/z $[M + H]^+$ 297.1501 (calcd for $C_{19}H_{21}O_3$, 297.1485).^{1}H NMR (CD_3OD, 500 MHz) δ 7.86 (1H, d, *J* = 7.8 Hz, H-1), 7.58 (1H, t, *J* = 7.8 Hz, H-3), 7.31 (1H, t, *J* = 7.8 Hz, H-2), 7.29 (1H, d, J = 7.8 Hz, H-4), 4.18 (1H, bs, H-12), 2.57 (1H, dd, *J* = 14.9, 5.4 Hz, H-14a), 2.12 (1H, dt, *J* = 13.8, 2.4 Hz, H15a), 1.96 (1H, dd, *J* = 13.3, 2.2 Hz, H-11a), 1.93 (3H, s, H-19), 1.89 (1H, overlapped, H11b), 1.81 (1H, overlapped, H-14b), 1.69 (3H, s, H-18), 1.67 (1H, overlapped, H-15b), 1.53 (3H, s, H-17). ^{13}C NMR (CD_3OD, 125 MHz) δ 164.5 (C-9), 162.1 (C-7), 153.2 (C-5), 130.1 (C-3), 127.4 (C-13), 123.0 (C-16), 122.3 (C-2), 120.6 (C-1), 114.6 (C-4), 79.4 (C-10), 38.2 (C-15), 34.7 (C-11), 28.7 (C-12), 25.3 (C-17), 20.5 (C-14), 18.2 (C-18), 17.8 (C-19).

COMPOUND 20B. ESIMS m/z 297 $[M + H]^+$; HRESIMS m/z $[M + H]^+$ 297.1481 (calcd for $C_{19}H_{21}O_3$, 297.1485).^{1}H NMR (CD_3OD, 500 MHz) δ 7.81 (1H, d, *J* = 7.8 Hz, H-1), 7.57 (1H, t, *J* = 7.9 Hz, H-3), 7.32 (1H, overlapped, H-2), 7.30 (1H, overlapped, H-4), 5.32 (1H, t, *J* = 3.1 Hz, H-14), 3.69 (1H, t, *J* = 3.3 Hz, H-12), 2.54-2.51 (3H, overlapped, H-11-16), 2.11 (1H, dd, *J* = 13.02, 3.3 Hz, H-15a) 1.88 (1H, d, *J* = 13.0 Hz, H-15b), 1.65 (3H, s, H17), 1.12 (3H, d, *J* = 6.8 Hz, H-19), 1.00 (3H, d, *J* = 6.8 Hz, H-18). ^{13}C NMR (CD_3OD, 125 MHz) δ 164.9 (C-9), 162.1 (C-7), 153.6 (C-5), 150.7 (C-13), 132.9 (C-3), 125.3 (C-2), 123.6 (C-1), 117.4 (C-4), 116.3 (C-14), 105.3 (C-8), 80.4 (C-10), 41.6 (C-11), 35.6 (C-15), 33.7 (C-16), 30.1 (C-12), 28.3 (C-17), 22.7 (C-18), 21.1 (C-19).

REFERENCES (FOR SUPPORTING INFORMATION)

(1) Crombie L., Redshaw S. D., Whiting D. A. J. Chem. Soc. Chem. Commun. 1979, 630.

(2) Yagen B., Mechoulam R. Tetrahedron Lett. 1969, 5353.

(3) Crombie L., Ponsford R., Shani A., Yagnitinsky B., Mechoulam R. Tetrahedron Lett. 1968, 5771.

(4) Choi YH., Hazekamp A., Peltenburg-Looman A.M., Frédérich M., Erkelens C., Lefeber AW., Verpoorte R. Phytochem Anal. 2004,15, 345.

(5) Pollastro F., Caprioglio D., Marotta P., Schiano Moriello A., De Petrocellis L., Taglialatela-Scafati O., Appendino G. J. Nat. Prod. 2018, 81, 630.

(6) Meltzer, P. C., Dalzell, H. C., Razdan, R. K. Synthesis 1981, 985.

(7) Khanolkar A. D., Lu D., Ibrahim M., Duclos, Jr. R. I., Thakur G. A., Malan Jr. T. P., Porreca F., Veerappan V., Tian X., George C., Parrish D. A., Papahatjis D. P., Makriyannis A. J. Med. Chem. 2007, 50, 6493.

SUBCHAPTER 3.2

THE OXIDATION OF PHYTOCANNABINOIDS TO CANNABINOQUINOIDS

JOURNAL OF NATURAL PRODUCTS

pubs.acs.org/jnp Note

The Oxidation of Phytocannabinoids to Cannabinoquinoids

Diego Caprioglio, Daiana Mattoteia, Federica Pollastro, Roberto Negri, Annalisa Lopatriello, Giuseppina Chianese, Alberto Minassi, Juan A. Collado, Eduardo Munoz, Orazio Taglialatela-Scafati,* and Giovanni Appendino*

Cite This: https://dx.doi.org/10.1021/acs.jnatprod.9b01284 Read Online

ACCESS | Metrics & More | Article Recommendations | Supporting Information

ABSTRACT: Spurred by a growing interest in cannabidiolquinone (CBDQ, HU-313, **2**) as a degradation marker and alledged hepatotoxic metabolite of cannabidiol (CBD, **1**), we performed a systematic study on the oxidation of CBD (**1**) to CBDQ (**2**) under a variety of experimental conditions (base-catalyzed aerobic oxidation, oxidation with metals, oxidation with hypervalent iodine reagents). The best results in terms of reproducibility and scalability were obtained with λ^5-periodinanes (Dess-Martin periodinane, 1-hydroxy-1λ^5,2-benziodoxole-1,3-dione (IBX), and SIBX, a stabilized, nonexplosive version of IBX). With these reagents, the oxidative dimerization that plagues the reaction under basic aerobic conditions was completely suppressed. A different reaction course was observed with the copper(II) chloride-hydroxylamine complex (Takehira reagent), which afforded a mixture of the hydroxyiminodienone **11** and the halogenated resorcinol **12**. The λ^5-periodinane oxidation was general for phytocannabinoids, turning cannabigerol (CBG, **18**), cannabichromene (CBC, **10**), and cannabinol (CBN, **19**) into their corresponding hydroxyquinones (**20**, **21**, and **22**, respectively). All cannabinoquinoids modulated to a various extent peroxisome proliferator-activated receptor gamma (PPAR-γ) activity, outperforming their parent resorcinols in terms of potency, but the iminoquinone **11**, the quinone dimers **3** and **23**, and the haloresorcinol **12** were inactive, suggesting a specific role for the monomeric hydroxyquinone moiety in the interaction with PPAR-γ.

ABSTRACT

Spurred by a growing interest in cannabidiolquinone (CBDQ, HU-313, **2**) as a degradation marker and alleged hepatotoxic metabolite of cannabidiol (CBD, **1**), we have carried out a systematic study on the oxidation of CBD (**1**) to CBDQ (**2**) under a variety of experimental conditions (base-catalyzed aerobic oxidation, oxidation with metals, oxidation with hypervalent iodine reagents). The best results in terms of reproducibility and scalability were obtained with λ^5-periodinanes (DMP, IBX, SIBX). With these reagents, the oxidative dimerization that plagues the reaction under basic aerobic conditions was completely suppressed. A different reaction course was observed with the copper (II) chloride-hydroxylamine complex (Takehira reagent), that afforded a mixture of the hydroxyiminoquinone **11** and the halogenated resorcinol **12**. The λ^5-periodinane oxidation was general for phytocannabinoids, turning cannabigerol (CBG, **18**), cannabichromene (CBC, **10**), and cannabinol (CBN, **19**) into their corresponding hydroxyquinones (**20**, **21**, and **22**, respectively). All cannabinoquinoids modulated to a various extent PPARγ activity, outperforming their parent resorcinols in terms of potency, but the iminoquinone **11,** the quinone dimers **3** and **23**, and the haloresorcinol **12** were inactive, suggesting a specific role for the monomeric hydroxyquinone moiety in the interaction with PPAR-γ.

Color development has played a significant role in the early studies on *Cannabis* (*Cannabis sativa* L.) and cannabinoids. Thus, the first phytocannabinoids were purified from *Cannabis* red oil, a deep-red high-vacuum distillation fraction of *Cannabis extracts*.[1,2] A red-purple color was also observed when fiber hemp or hashish were treated with methanolic KOH.[3] Under these conditions, the development of a color is specific for *Cannabis* and *Cannabis*-derived products (marijuana, hashish),[4]

and the reaction has long been proved as an expeditious method for their identification in a forensic context (Beam test)[4].

The nature of the pigment from *Cannabis* red oil is still unclear, but color formation in the Beam test is the result of the aerobic oxidation of cannabidiol (CBD, **1**) to the hydroxyquinone **2** (cannabidiolquinone, CBDQ, HU-331),[5] a compound that has attracted considerable interest because of its selective anticancer activity[6,7] and catalytic inhibitory properties on topoisomerase IIα.[8] While development of **2** as a drug was abandoned, possibly because of unfavorable stability properties (*vide infra*) and cellular toxicity,[9] distinct lines of research rekindled interest in this compound**.** Thus, microsomal formation of **2** from CBD (**1**) has been associated to P450 covalent inhibition and perturbation of hepatic xenobiotics metabolism,[10] and a similar process could also underlie the liver toxicity reported for high dosages of CBD.[11] Furthermore, **2** is formed during long-term storage of CBD under aerobic conditions,[12] and its availability is therefore important for quality control of this API (Active Pharmaceutical Ingredient).

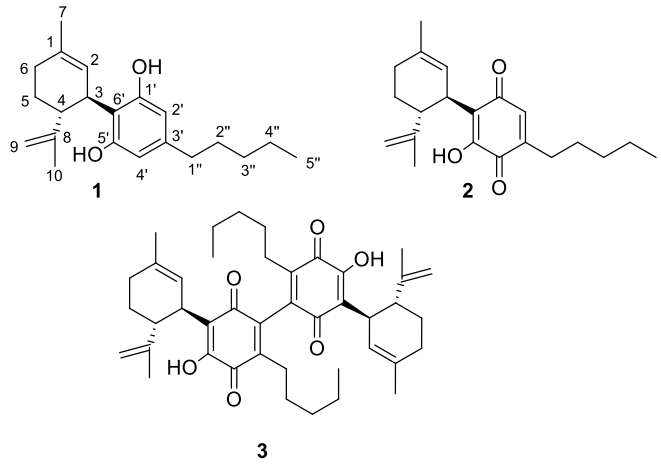

Despite the convergence of interest for CBDQ (**2**) from various areas of cannabinoid research, its only reported synthesis is the one inspired by the Beam test, that is, the aerobic oxidation of CBD in a cooled biphasic petroleum ether / 5% ethanolic KOH

system.[5,6] Under these conditions, yields are erratic, scale-dependent, and modest (ca 20% at best),[5,6] while significant amounts of the dimeric quinone **3** are also formed by oxidative dimerization of CBDQ.[5] Both reaction products, especially **3**, are unstable and rapidly turn into a complex mixture of polar compounds.[5] In our hands, the oxidation reaction was poorly reproducible, and could not be scaled up over a few hundred milligrams of starting material, even when air or 80% oxygen were bubbled into the biphasic reaction system. A more reproducible behavior was observed with KH or LiH in THF or toluene under heterogeneous conditions but scale up was still problematic. While Beam-type oxidation strategies were eventually abandoned, their mechanism is worth mentioning. Thus, the reaction is presumably triggered by formation of a phenolate anion, next oxidized to an electrophilic radical (**4**) that adds to dioxygen to form a hydroperoxy radical. The latter is reduced to the corresponding anion (**5)** by a second phenolate ion, and, after tautomerization to **6**, the hydroperoxy anion is trapped by the *para*-carbonyl group. This generates the bridged keto-peroxyhemiacetal **7**, whose α-deprotonation triggers cleavage of the peroxidic bond, eventually affording the hydroxylated quinone **2** via the hydrate **8** (Figure 1).

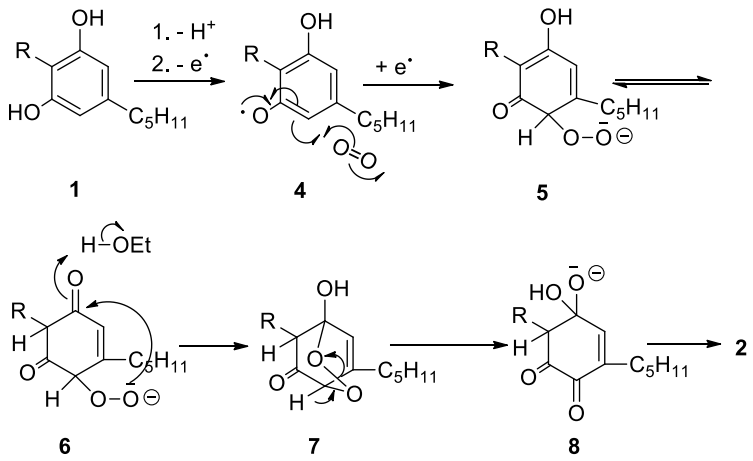

Figure 1. Possible mechanism of the base-mediated aerobic formation of cannabidiolquinone (CBDQ, **2**) from cannabidiol (CBD (**1**) in ethanolic KOH. (R= 3-*p*-mentha-1,8-dienyl).

This process is reminiscent of the transformation of vitamin K hydroquinone into its epoxyquinone form,[13] and the mechanism outlined in Figure 1 could explain the sensitivity of the reaction to radical traps like BHT as well as the unreactivity of mono-alkylated phytocannabinoids, like Δ^9-tetrahydrocannabinol (Δ^9-THC, **9**) and cannabichromene (CBC, **10**), where the prototropic equilibrium required for the formation of the peroxyhemiacetal is not possible (cf. the formation of **6** from **5** in Scheme 1).

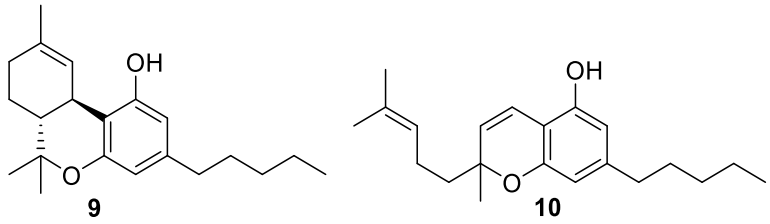

9 **10**

The reaction profile of the Beam test was basically replicated, without any substantial improvement of yield, by metal oxidants [$FeCl_3$, $K_3[Fe(CN)_6]$, MnO_2, Cr^{+6}-based reagents, CuCl, $CuCl_2$, Ag_2O, $NH_4Ce(NO_3)_5$] under both catalytic and stoichiometric conditions, as well as by peroxides (TBHP, basic H_2O_2), with significant amounts of the dimer **3** being always formed under basic conditions or during the long reaction times required to achieve a significant conversion. A surprising and notable exception was the behaviour of the Takehira complex ($CuCl_2$-hydroxylamine),[14] that afforded a mixture of the hydroxyiminodienone **11** and the chlororesorcinol **12**. The regioselectivity of the formation of **11** was deduced from the diagnostic ^3J HMBC cross-peaks of H-1″ with the hydroxyiminocarbonyl carbon.

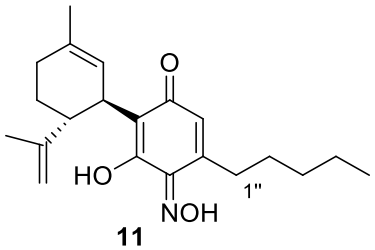

11

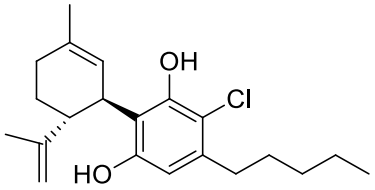

12

The Takehira complex was originally developed for the oxidation of methylpolyphenols to their corresponding hydroxyquinones,[14] a reaction of relevance for the industrial synthesis of vitamin E,[14] and was later modified by replacement of hydroxylamine with other nitrogen bases.[15] In control experiments, copper (II) chloride alone gave CBDQ (**2**) and the dimer **3** as the only reaction product, while the quinone **2** did not react with hydroxylamine, suggesting a role for hydroxylamine in the chemoselective halogenation reaction, possibly via the generation of an *N*-chlorinated species, and of copper (II) in the activation of the quinonecarbonyl carbon toward nucleophilic attack by hydroxylamine.

Hypervalent iodine derivatives have become increasingly popular for a wide range of oxidative reactions,[16] and bis(trifluoroacetoxy)iodobenzene (BTIB) was reported to oxidize the mono-*O*-alkylated cannabinoid Δ^9-THC (**9**), otherwise unreactive in Beam-type oxidations,[6] to its corresponding hydroxyquinone.[6] This λ^3-iodane was also able to oxidize CBD to CBDQ , but λ^5 iodanes like 2-iodoxybenzoic acid (1-hydroxy-1-λ^5,2-benziodoxole-1,3-dione, IBX, **13**)[17] and the Dess-Martin periodinane (DMP)[18] gave much better and more reproducible yields, with a stabilized and not explosive version of IBX (SIBX)[19] emerging as the reagent of choice. The superior behaviour of SIBX compared to IBX might be related to the acidity of the stabilizing matrix (isophtalic- and benzoic acids), that could help the hydrolytic cleavage of iodic esters formed in the reaction.[19]

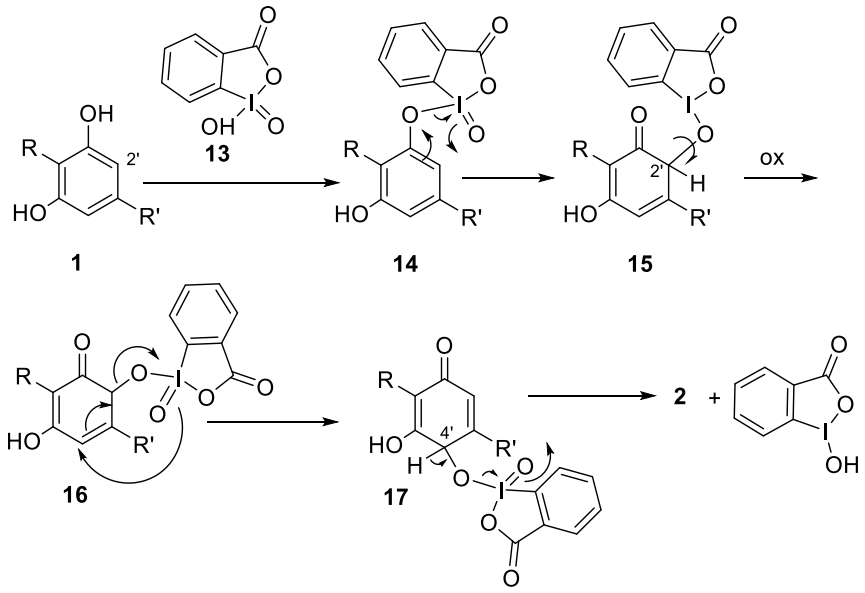

Figure 2. Possible mechanism for thr SIBX-mediated formation of cannabidiolquinone (CBDQ, **2**) from cannabidiol (CBD (**1**) (R= 3-*p*-mentha-1,8-dienyl, R′ = *n*-pentyl).

The oxidation is presumably initiated by the sigmatropic rearrangement of the iodine-oxygen bond in the mixed λ^5 iodane ester **14** formed by interaction of IBX and the C-1′ phenolic hydroxy group (Figure 2). The resulting C-2′ λ^3-quinol **15,** after oxidation to the corresponding λ^5-iodane **16**, is transformed by [3.3]-sigmatropic rearrangement of the carbon-oxygen bond into the C-4′ λ^5-iodinane **17**, with β-elimination eventually generating the hydroxyquinone **2** and a reduced λ^3-iodinane. Remarkably, dimerization was completely suppressed under iodinane oxidation, and yields in the range of 50-60% could be obtained at multigram reaction scale. CBDQ, an orange powder,[20] is unstable in solution, rapidly degrading in both protic (methanol) and aprotic (acetone, $CHCl_3$) solvents, with generation of the more polar dimer **3** next to a host of uncharacterized more polar products. On the other hand, it could be stored for at least 10 months as a powder at – 18 °C in a sealed flask, or for additional time as a frozen benzene or DMSO solution at 4 °C.[21]

The oxidation with SIBX is general for phytocannabinoids, and, apart from cannabigerol (**18**), it could also be applied to mono-etherified compounds [cannabichromene (CBC, **10**), cannabinol (**19**)] that are unreactive under Beam-test conditions, to afford their corresponding hydroxyquinones **20**-**22.**

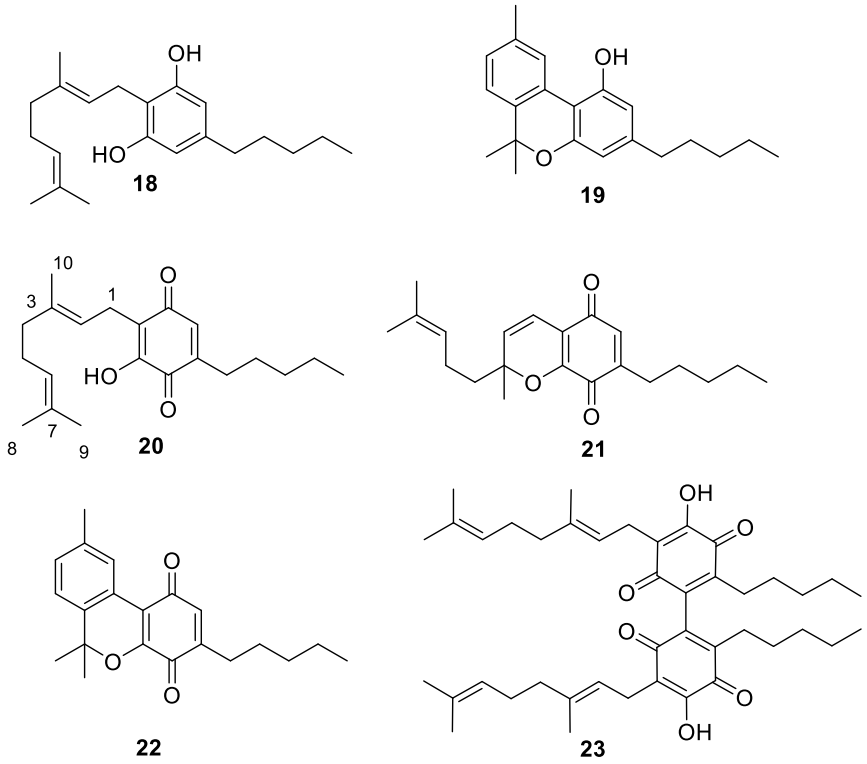

CBDQ (**2**) has been reported to be non-narcotic,[6] and lacks significant affinity for CB_1 and CB_2 receptors.[9] Nevertheless, it showed powerful modulating activity on PPAR-γ[9,22] and various degrees of PPAR-γ activating activity were also shown by the other cannabinoquinoids (Table 1). However, dimerization was detrimental for activity, and dimeric quinones were devoid of significant activity in PPARγ-activity assays.[23] Dimeric quinones are axially chiral, and, since enantiomeric cannabinoids can show markedly different profiles of bioactivity,[2] the one from CBG (CBGQ, **23**), was resolved by chromatography on a chiral-phase column packed with amylose-tris(5-chloro-2-methylphenylcarbamate). However, both the *(aR)* and the *(aS)* enantiomers

turned out to be inactive.[23] Similarly, the hydroxyiminodienone **11** and the chlorinated resorcinol **12** were also devoid of activity.[23]

Compound	EC_{50}
1	> 25 μM
10	> 25 μM
18	15.7 μM
19	> 25 μM
2	10.5 μM
21	14.7 M
20	4.9 μM
22	23.1 μM

Table 1. PPAR-γ Modulation Activity of the Phytocannabinoids **1, 10, 18, 19** and Their Corresponding Cannabinoquinones (**2, 21,20, 22**). 1 μM Rosiglitazone was used as Positive Control for PPAR-γ Activation (50-Fold Induction over Basal Activity).

In conclusion, we have developed a reproducible and scalable synthesis of cannabinoquinoids, including CBDQ (**2**), significantly enhancing access to this compound of relevance not only for its bioactivity profile, but also for the analytics of CBD, the study of its binding to P450 apoproteins, and its effects on liver function.

EXPERIMENTAL SECTION

GENERAL EXPERIMENTAL PROCEDURES. IR spectra were recorded on an Avatar 370 FT-IR Techno-Nicolet apparatus. ^{1}H (400 and 500 MHz) and ^{13}C (100 and 125 MHz) NMR spectra were measured on Varian INOVA NMR spectrometers. Chemical shifts were referenced to the residual solvent signal (methanol-d_4: δ_H = 3.34, δ_C = 49.0 or $CDCl_3$: δ_H = 7.21, δ_C = 77.0). Homonuclear ^{1}H connectivities were determined by the COSY experiment. One-bond heteronuclear ^{1}H-^{13}C connectivities were determined with the HSQC experiment. Two- and three-bond ^{1}H-^{13}C connectivities were determined by gradient 2D HMBC experiments optimized for a $^{2,3}J$ = 9 Hz. Low- and high-resolution ESIMS data were determined on an LTQ OrbitrapXL (Thermo Scientific) mass spectrometer.

Reactions were monitored by TLC on Merck 60 F254 (0.25 mm) plates, visualized by staining with 5% H_2SO_4 in EtOH and heating. Organic phases were dried with Na_2SO_4 before evaporation. Chemical reagents and solvents were purchased form Sigma-Aldrich (Germany) and were used without further purification unless stated otherwise. Petroleum ether with boiling point of 40-60 °C was used. Silica gel 60 (70-230 mesh) used for gravity column chromatography (GCC).

SIBX OXIDATION OF PHYTOCANNABINOIDS. REACTION WITH CBD (1) AS EXAMPLE. To a cooled (ice bath) solution of CBD (5 g, 15,6 mmol) in EtOAc (75 mL), SIBX (21.1 g, 31,5 mmol, 2 molar equiv.) was added in six portions of ca 5 g each. The cooling bath was removed, the suspension was stirred at room temp. for 18 h, and then filtered over a pad of Celite. The filtration cake was washed with EtOAc (50 mL), and the pooled filtrates were washed with sat. $Na_2S_2O_3$ (4 x 75 mL), and next with brine. After drying and evaporation, the residue was purified by GCC on silica gel (150 g, petroleum ether-EtOAc 9:1 as eluant) to obtain a brown oil that solidified upon

storing in the refrigerator. Washing with cold petroleum ether removed some of the coloured impurities, and afforded an orange powder (3.17 g, 61%). The same protocol was used for the oxidation and the purification of the other phytocannabinoids investigated (CBC, **10**; CBG, **18**; CBN, **19**). The scale was 100-200 mg, and the yield were 59, (CBCQ, **21**), 37 (CBGQ, **20**), and 58%, (CBNQ, **22**).

CANNABIGEROQUINONE (CBGQ, 20): red powder, IR ν_{max} (KBr disc): 3272, 2955, 2923, 2856, 1644, 1637, 1350,1316, 1191, 1175, 580 cm^{-1}; ^{1}H NMR ($CDCl_3$, 400 MHz) δ 6.94 (1H, s, OH), 6.45 (1H, bs, H-2′), 5.13 (1H, t, *J* = 7.4 Hz, H-2), 5.04 (1H, t, *J* = 6.7 Hz, H-7), 3.13 (2H, d, *J* = 7.4 Hz, H-1), 2.41 (2H, t, *J* = 7.6, H-1″), 1.99-1.90 (4H, m, H-4, H-5), 1.73 (3H, s, H-8), 1.64 (3H, s, H-9), 1.57 (3H, s, H-10), 1.50 (2H, m, H-2″), 1.33 (4H, m, H-3″, H-4″), 0.89 (3H, t, *J* = 6.8 Hz, H-5″); ^{13}C NMR ($CDCl_3$, 100 MHz) δ 187.7, 184.2, 150.9, 145.1, 137.3, 134.4, 131.5, 124.3, 120.2, 119.7, 39.8, 31.5, 28.3, 27.4, 26.7, 25.8, 22.5, 22.0, 17.8, 16.3, 14.0; ESIMS: *m*/*z* 331 $[M + H]^+$; HRESIMS *m*/*z* 331.2262 $[M + H]^+$, calcd. for $C_{21}H_{31}O_3$, 331.2268.

CANNABICHROMENQUINONE (CBCQ, 21): red oil, IR ν_{max} (KBr disc): 2957, 2926, 2852, 1648, 1580, 1324, 1078, 969, 891cm^{-1}; ^{1}H NMR ($CDCl_3$, 400 MHz) 6.47 (1H, d, *J* = 9.9 Hz, H-1), 6.40 (1H, bs, H-2′), 5.56 (1H, d, *J* = 9.9 Hz, H-2), 5.07 (1H, t, *J* = 6.9 Hz, H-6), 2.39 (2H, t, *J* = 7.6 Hz, H-1″), 2.08 (1H, m, H-5a), 1.88 (1H, m, H-5b), 1.66 (2H, overlapped, H-4), 1.64 (3H, s, H-8), 1.55 (3H, s, H-9), 1.49 (2H, m, H-2″), 1.46 (3H, s, H-10), 1.32 (4H, m, H-3″, H-4″), 0.89 (3H, t, *J* = 6.7 Hz, H-5″); ^{13}C NMR ($CDCl_3$, 100 MHz) δ 184.6, 181.9, 150.8, 147.7, 132.2, 131.4, 128.8, 123.4, 115.4, 115.0, 83.0, 41.5, 31.4, 28.7, 27.4, 27.3, 25.6, 22.6, 22.4, 17.7, 13.9; ESIMS *m*/*z* 329 $[M + H]^+$; HRESIMS *m*/*z* 329.2107 $[M + H]^+$, calcd for $C_{21}H_{29}O_3$, 329.2111.

CANNABINOLQUINONE (CBNQ, 22): red oil, IR ν_{max} (KBr disc): 2955, 2924, 2855, 1649, 1382, 1145, 1110, 811 cm^{-1}; ^{1}H NMR ($CDCl_3$, 400 MHz) δ 8.30 (1H, s, H-2), 7.09 (1H, d, *J* = 7.9 Hz, H-6), 7.02 (1H, d, *J* = 7.9 Hz, H-5), 6.63 (1H, t, *J* = 1.4 Hz, H-2′), 2.40 (2H, t,

J = 7.7 Hz, H-1''), 2.36 (3H, s, H-7), 1.69 (6H, s, H-9, H-10), 1.56 (2H, m, H-2''), 1.32 (4H, m, H-3'', H-4''), 0.90 (3H, t, *J* = 6.8 Hz, H-5''); ^{13}C NMR ($CDCl_3$, 100 MHz) δ 180.2, 175.3, 163.3, 144.7, 138.1, 133.8, 131.8, 128.9, 125.7, 122.3, 111.0, 82.7, 53.6, 31.6, 29.8, 29.0, 28.3, 27.4, 22.4, 21.4, 13.9; ESIMS *m*/*z* 325 $[M + H]^+$; HRESIMS *m*/*z* 325.1791 $[M + H]^+$, calcd. for $C_{21}H_{25}O_3$, 325.1798.

DIMERIC CANNABIGEROQUINONE (23) AND CHIRAL-PHASE CHROMATOGRAPHY: red powder, IR ν_{max} (KBr disc): 3280, 2955, 1350, 1188, cm^{-1}; ^{1}H NMR ($CDCl_3$, 400 MHz) δ 6.98 (1H, s, OH), 5.17 (1H, t, *J* = 7.4 Hz, H-2), 5.06 (1H, t, *J* = 6.7 Hz, H-7), 3.16 (2H, d, *J* = 7.4 Hz, H-1), 2.32 (2H, t, *J* = 7.6, H-1''), 2.05-1.90 (4H, m, H-4, H-5), 1.73 (3H, s, H-8), 1.64 (3H, s, H-9), 1.57 (3H, s, H-10), 1.49 (2H, m, H-2''), 1.32 (4H, m, H-3'', H-4''), 0.89 (3H, t, *J* = 6.8 Hz, H-5''). ESIMS: *m*/*z* 645 $[M + H]^+$; HRESIMS *m*/*z* 645.4159 $[M + H]^+$, calcd. for $C_{41}H_{57}O_6$, 645.4155.

A sample of compound **23** (2.0 mg) was separated on a chiral-phase Lux 5 μ Amylose-2 250 x 4.60 mm column, Phenomenex, eluent *n*-hexane/isopropanol 9:1 (0.2% TFA) with a flow of 0.7 mL/min and two peaks were obtained with Rt = 8 min (0.9 mg) and Rt = 13 min (0.7 mg).

OXIDATION OF CANNABIDIOL (CBD, 1) WITH THE TAKEHIRA REAGENT: To a stirred solution of CBD (**1**, 200 mg, 0,64 mmol) in toluene – *tert*-butanol (3:1, 20 mL), copper (II) chloride (43 mg, 0,32 mmol, 0,5 molar equiv.) and hydroxylamine hydrochloride (22 mg, 0,32 mmol, 0,5 molar equiv.) were added. The solution turned from yellow to brown, and was stirred for 2 hours at room temp., worked up by dilution with 2N H_2SO_4, and extraction with EtOAc. The organic phase was washed with brine, dried with Na_2SO_4, filtered, and evaporated. The residue was purified by GCC (5 g silica gel, petroleum ether-EtOAc gradient, from to petroleum ether to 95:5 petroleum ether –EtOAc as eluent) to give **12** (135 mg, 34%) and **11** (20%).

HYDROXYIMINOCANNABIQUINONE (11): Brownish oil, IR ν_{max} (KBr disc): 2960, 2924, 2856, 1617, 1420, 1420, 1260, 1092, 1016, 797 cm^{-1}; ^{1}H NMR (methanol-d_4, 400 MHz) δ 6.25 (1H, s, H-2′), 5.12 (1H, s, H-2), 4.50 (1H, s, H-9a), 4.49 (1H, s, H-9b), 3.82 (1H, m, H-3), 2.92 (1H, td, *J* = 11.7, 3.2 Hz, H-4), 2.70 (2H, t, *J* = 7.5 Hz, H-1″), 2.18 (1H, m, H-6a), 1.99 (1H, m, H-6b), 1.73 (2H, overlapped, H-5), 1.65 (3H, s, H-7), 1.63 (3H, s, H-10), 1.60 (2H, overlapped, H-2″), 1.34 (2H, overlapped, H-3″), 1.33 (2H, overlapped, H-4″), 0.91 (3H, t, *J* = 6.9 Hz, H-5″); ^{13}C NMR (methanol-d_4, 100 MHz) δ 176.3 (C-1′), 168.1 (C-5′), 150.2 (C-8), 148.7 (C-3′), 148.1 (C-4′), 133.6 (C-1), 125.6 (C-2), 120.6 (C-2′), 119.1 (C-6′), 110.8 (C-9), 45.6 (C-4), 36.2 (C-3), 32.8 (C-3″), 31.6 (C-6), 31.5 (C-1″), 30.8 (C-5), 30.5 (C-2″), 23.6 (C-7), 23.5 (C-4″), 19.1 (C-10), 14.3 (C-5″) ; ESIMS *m*/*z* 344 $[M + H]^+$; HRESIMS *m*/*z* 344.2210 $[M + H]^+$ calcd for $C_{21}H_{30}NO_3$, 344.2220.

2-CHLOROCANNABIDIOL (12): Yellow oil, IR ν_{max} (KBr disc): 3500, 3421, 2962, 2924, 2859, 1623, 1421, 1258, 1193, 1054, 888, 817, 698 cm^{-1}; ^{1}H NMR (methanol-d_4, 400 MHz): δ 6.21 (1H, s, H-2′), 5.25 (1H, s, H-2), 4.46 (1H, s, H-9a), 4.44 (1H, s, H-9b), 3.99 (1H, m, H-3), 2.95 (1H, m, H-4), 2.56 (2H, t, *J* = 7.4 Hz, H-1″), 2.20 (1H, m, H-5a), 2.01 (1H, d, *J* = 17.1 Hz, H-5b), 1.76 (2H, m, H-6), 1.68 (3H, s, H-7), 1.65 (3H, s, H-10), 1.56 (2H, m, H-2″), 1.35 (4H, m, H-3″-4″). 0.91 (3H, t, *J* = 6.8 Hz, H-5″); ^{13}C NMR (methanol-d_4, 100 MHz): δ 156.1, 152.7, 150.2, 139.3, 134.2, 126.6, 118.2, 112.8, 110.7, 109.6, 46.2, 38.3, 34.7, 32.7, 31.7, 30.7, 30.5, 23.7, 23.5, 19.3, 14.4. ESIMS *m*/*z* 349, 351 $[M + H]^+$ ratio 3:1; HRESIMS *m*/*z* $[M + H]^+$ 349.1919 (calcd for $C_{21}H_{30}{}^{35}ClO_2$, 349.1929).

PPARγ ACTIVITY EVALUATION: Human embryonic kidney epithelial cells 293T cells were obtained from the American Type Culture Collection (CRL-3216) and cultured in DMEM supplemented with 10% FCS and antibiotics. To analyze PPAR-γ transcriptional activity HEK-293T cells were cultured in 24-well plates (2×104 cells/well) and transiently co-transfected with GAL4-PPAR-γ (50 ng) GAL4-luc (firefly luciferase, 50 ng) vectors using Roti-Fect (Carl Roth, Karlsruhe, Germany).

Twenty hours after transfection the cells were stimulated with increasing concentrations of the compounds for 6 h and luciferase activities were quantified using Dual-Luciferase Assay (Promega, Madison, WI, USA). Rosiglitazone (1 μM, Cayman Chemical, MI, USA), was used as a positive control for PPAR-γ activation (50-fold induction over basal activity). Test compounds and controls stocks were prepared in DMSO and the final concentration of the solvent was always less than 0.5% v/v. The plasmid GAL4-PPAR-γ was obtained from Prof. Christopher Sinal (Dalhousie University, Canada). Half-maximal effective concentration (EC_{50}) was estimated using Prism software (GraphPad). All transfection experiments were performed at least three times.

ASSOCIATED CONTENT

Supporting Information

Full experimental details and the characterization of compounds are provided in the Supporting Information.

The Supporting Information is available free of charge on the ACS Publications website.

AUTHOR INFORMATION

Corresponding Authors

* Tel: +39-081-678509. Fax: +39-081678552. E-mail: scatagli@unina.it (O. Taglialatela-Scafati).

* Tel: +39-0321-375744. Fax: +39-0321375744. Email address: giovanni.appendino@uniupo.it (G. Appendino).

Notes

The authors declare no competing financial interest.

ACKNOWLEDGMENTS

We are grateful to Dr. Gianpaolo Grassi (CREA, Rovigo) for generously supplying the Carmagnola strain of *Cannabis* used for the isolation of cannabidiol. We thank MIUR for financial support to the groups in Novara and Naples (PRIN2017, Project 2017WN73PL, Bioactivity-directed exploration of the phytocannabinoid chemical space).

REFERENCES

1) Wood, T. B.; Spivey, W. T. N.; Easterfield, T. H. J. Chem. Soc. 1896, 69, 539-546.

2) Isolation and Structure Elucidation of Cannabidiol: Adams, R.; Pease, D. C.; Clark, J. H.; Baker, B. R. *J. Am. Chem. Soc*. **1940**, *62*, 2197-2200. Structure Elucidation of Cannabinol: Adams, R.; Hunt, M.; Clark, J. H. *J. Am. Chem. Soc.* **1940**, *62*, 196-200.

3) Beam, W. *4th Report, Wellcome Trop. Research Lab., Rep. Sudan Gov.*, **1911**, 25.

4) Grlic, L. A Comparative Study on Some Chemical and Biological Characteristics of Various Samples of Cannabis Resin. United Nations Office of Drugs and Crime, 1962 (https://www.unodc.org/unodc/en/data-and-analysis/bulletin/bulletin_1962-01-01_3_page005.html)

5) Mechoulam, R.; Ben-Zvi, Z.; Gaoni, Y. *Tetrahedron* **1968**, *24*, 5615-5624.

6) Kogan, N. M.; Rabinowitz, R.; Levi, P.; Gibzon, D.; Sandor, P.; Schlesinger, M.; Mechoulam, R. *J. Med. Chem.* **2004**, *47*, 3800-3806.

7) Peters, M.; Kogan, N. M. *Expert Opin. Investig. Drugs* **2007**, *16*, 1405-1413.

8) Regal, K. M.; Mercer, S. L.; Dewessee, J. E. *Chem. Res. Toxicol.* **2014**, *27*, 2044-2051.

9) del Río, C.; Navarrete, C.; Collado, J. A.; Bellido, M. L.; Gómez-Cañas, M.; Pazos, M. R.; Fernández-Ruiz, J.; Pollastro, F.; Appendino, G.; Calzado, M. A.; Cantarero, I.; Muñoz, E. *Sci. Rep.* **2016**, *6*, 21703. doi: 10.1038/srep21703.

10) Bornheim, L. M.; Grillo, M. P. *Chem. Res. Toxicol.* **1998**, *10*, 1209-1216.

11) Ewing, L. A.; Skinner, C. M.; Quick, C. M.; Kennon-McGill, S.; McGill, M. R.; Walker, L. A.; ElSohly, M. A.; Gurley, B. J.; Koturbash, I. *Molecules* **2019**, *24*, doi:10.3390/moleulces24091694.

12) Appendino, G.; Allegrini, P. Manuscript in preparation

13) Dowd, P.; Hershline, R.; Wook, S.; Naganathan, S. *Science* **1995**, *269*, 1684-1691.

14) Takehira, K.; Shimizu, M.; Watanabe, Y.; Orita, H.; Hayakawa, T. *J. Chem. Soc., Chem. Commun.*, **1989**, 1705-1706.

15) Takehira, K.; Shimizu, M.; Watanabe, Y.; Orita, H.; Hayakawa, T. *Tetrahedron Lett.* **1989**, *30*, 6691-6692.

16) Nicolaou, K. C.; Montagnon, T.; Baran, P. S.; Zhong, Y.-L. *J. Am. Chem. Soc.* **2002**, *124,* 2245–2258.

17) Frigerio, M.; Santagostino, M.; Sputore, S. (1999). *J. Org. Chem.* **1999**, *64*, 4537–4538.

18) Dess, D. B.; Martin, J. C. *J. Org. Chem.* **1983**, *48*, 4155-4156.

19) Ozanne, A.; Pouységu, L.; Depernet, D.; Bruno, F.; Quideau, S. *Org Lett.* **2003**, *5*, 2903-2906. We previously disclosed the use of SIBX for the telescoped synthesis of aminoderivatives of cannabinoquinoids in the proprietary literature: Appendino, G.; Cabello de Alba, M. L. B.; Munoz, E. WO2015/158381.

10) The product resulting from the Beam-type oxidation was reported as a brown powder.[6] We confirmed this observation, presumably related to the formation of highly colored impurities under the basic conditions of the Beam oxidation that could not be removed by hexane washing or recrystallization.

21) Appendino, G.; Pollastro, F.; Verotta, L.; Ballero, M.; Romano, A.; Wyembek, P.; Szcuzuraszeck, K.; Mozrzymas, J. W.; Taglialatela-Scafati, O. *J. Nat. Prod.* **2009**, *73*, 962-965.

22) Granja, A. G.; Carrillo-Salinas, F.; Pagani, A.; Gómez-Cañas, M.; Negri, R.; Navarrete, C.; Mecha, M.; Mestre, L.; Fiebich, B. L.; Cantarero, I.; Calzado, M. A.; Bellido, M. L.; Fernandez-Ruiz, J.; Appendino, G.; Guaza, C.; Muñoz, E. *J Neuroimmune Pharmacol.* **2012**, 7, 1002-1016.

23) Compounds were considered inactive if unable to induce 5-fold PPARγ-induction at 50 μM concentration.

24) Hanuš, L. O.; Tchilibon, S.; Ponde, D. E.; Breuer, A.; Fride, E.; Mechoulam, R. *Org. Biomol. Chem.* **2005**, *3*, 1116-1123.

SUBCHAPTER 3.3

REGIODIVERGENT SYNTHESIS OF *ORTHO*- AND *PARA*-CANNABIQUINONES

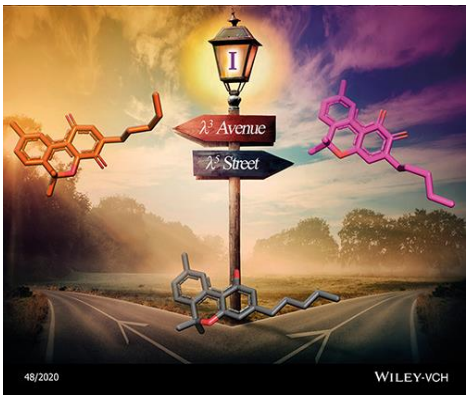

WILEY-VCH

FULL PAPER

Regiodivergent Synthesis of *ortho*- and *para*-Cannabinoquinones

Daiana Mattoteia,[a] Orazio Taglialatela-Scafati,[b] Eduardo Muñoz,[c] Laureano de la Vega,[d] Diego Caprioglio[a]* and Giovanni Appendino,[a]*

We would like to dedicate this article to Prof. Marco D'Ischia for his remarkable work on the oxidation of phenolic natural products

[a] Dr. Daiana Mattoteia, Prof. Diego Caprioglio, Prof. Giovanni Appendino,
Dipartimento di Scienze del Farmaco, Università del Piemonte Orientale,
Largo Doengani 2, 28100 Novara, Italy
E-mail: diego.caprioglio@uniupo.it; giovanni.appendino@uniupo.it.
URL: https://upobook.uniupo.it/diego.caprioglio (DC) https://upobook.uniupo.it/giovanni.appendino (GA)
[b] Prof. Orazio Taglialatela-Scafati,
Dipartimento di Farmacia, Università di Napoli Federico II,
Via Montesano 49, 80131 Napoli, Italy
[c] Prof. Eduardo Muñoz,
Departamento de Biología Celular, Fisiología e Inmunología, Universidad de Córdoba,
Hospital Universitario Reina Sofía, v. Menendez Pidal, s/n, 14004 Córdoba, Spain
[d] Prof. Laureano de la Vega
Jacqui Wood Cancer Centre, School of Medicine, University of Dundee,
James Arnott Drive, Dundee DD2 1U, UK

ABSTRACT

Spurred by the remarkable biological profile of cannabinoquinoids, we have systematically investigated the periodinane oxidation of their resorcinolic precursors, discovering that the regiochemistry of oxidation, a critical maneuver for bioactivity, depends not only on the nature of the oxidant (λ^3- vs λ^5-iodanes), but also on post-oxidative prototropic- and valence tautomeric equilibria that isomerize *ortho*-quinones to *para*-quinones. By complementary selection of the periodinane oxidant and by freezing prototropic equilibration with *O*-methylation, isomeric *ortho*- and *para*-quinones could be obtained from mono- and diphenolic cannabinoids, setting the stage for the exploration of novel areas of the biological space, and establishing a blueprint for the extension of this strategy to other classes of bioactive alkylresorcinols.

INTRODUCTION

The development of a deep-violet color upon treatment of hashish with bases under aerobic conditions was first re-ported in 1911, at the outset of studies on cannabinoids.[1] This chromatic oxidative reaction (Beam test) was then extensively used as a forensic assay for narcotic *cannabis* (hashish, marijuana), even though, as studies progressed, it became clear that only non-narcotic diphenolic cannabinoids like cannabidiol (CBD, **1a,** Figure 1) and cannabigerol (CBG, **2a**) develop a color under the conditions of the assay.[2] The hydroxylated *para*-quinone structures **3a** and Δ **4a** were assigned to the colored pigments formed by oxidation of, respectively, CBD and CBG (**3a** and **4a**, respectively),[2] but the nature of the quinones obtained from monophenolic cannabinoids like Δ^9-tetrahydrocannabinol (^{9}-THC, **5a**) and cannabinol (CBN, **6a**) was long debated.[3] In these compounds, the tautomeric interconversion of *o*- and *p*-hydroxyquinoid forms is locked (Scheme 1), and both

structures can, in principle, exist (*see infra*). These uncertainties were eventually clarified by an X-ray study of the quinones formed by Δ^{3}-iodane [phenyliodine (III)bis(trifluoroacetate), PIFA] oxidation of Δ^{8}-THC (**5b**) and CBN (**6a**), unambiguously assigning a *p*-quinone structure to both oxidation products (**7b** and **8a**, respectively).[3] A *p*-quinone structure was then assigned by default to all cannabinoquinoids next reported by isolation [4,5] or by semi-synthesis. [6,7]

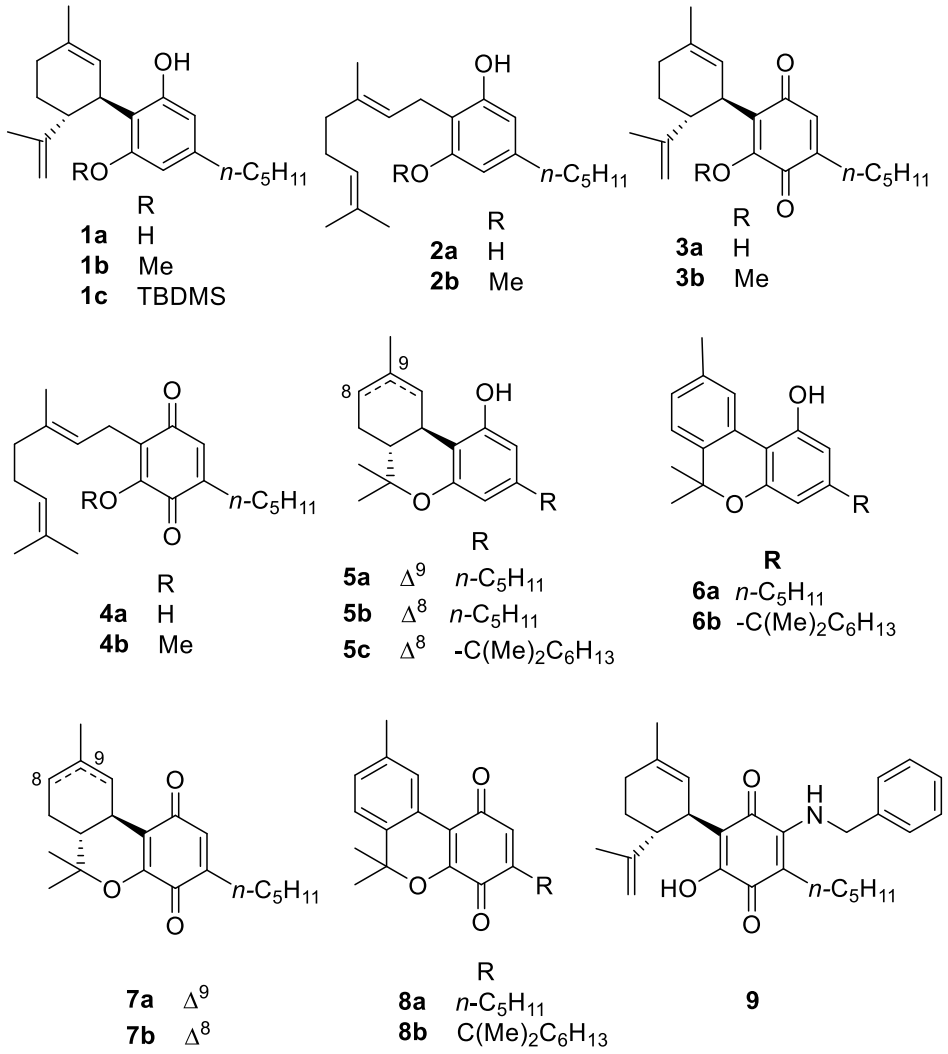

Figure 1. Examples of cannabinoids and cannabinoquinoids.

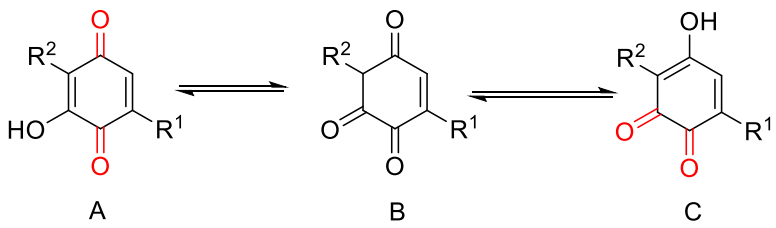

Scheme 1. Tautomeric interconversion of hydroxy o- and p-cannabinoquinoids (R^1 = alkyl, R^2 = terpenyl).

After an initial and then faded excitement for the selective anti-cancer activity of cannabinoquinoids,[3] interest was re-kindled by the discovery of the immunomodulating properties of VCE.004.8 (**9**),[7] a 2-aminoalkylderivative of cannabidiolquinone (CBDQ, **3a**) currently undergoing Phase II clinical development under orphan drug designation in EU and USA and fast track status in USA for systemic sclerosis, an autoimmune disease.[8] An improved and scalable synthesis of CBDQ (**3a**) was developed using SIBX,[9] a non-explosive formulation of the λ^5-iodane iodoxybenzoic acid (IBX) as the oxidant,[10] while the electrochemical version of the oxidation of cannabinoids to cannabinoquinoids was investigated in the context of the development of a marijuana breathalyzer based on the formation of the quinone **7a** from Δ^9-THC (**5a**).[11] These developments provided a rationale to systematically explore the chemical and biological space of cannabinoquinoids.

RESULTS AND DISCUSSION

Cannabinoquinones are chemically unstable, and *O*-methylation was investigated as a stabilizing maneuver alternative to the *aza*-Michael addition/dehydrogenation strategy that led to the discovery of VCE004.8.[7] Two alkylation strategies were investigated, namely, the direct methylation of CBDQ (**3a**), the SIBX oxidation product of CBD,[9] or, alternatively, the SIBX oxidation of *O*-methyl CBD (**1b**), a natural constituent of *cannabis*.[12] Despite the use of the same iodane oxidant, the two

strategies afforded a different quinone as the only reaction product (**3b** and **10**, respectively) (Scheme 2). *O*-Methylation of cannabinoquinoids is associated to modulation properties on the NRF2-BACH1 axis, a phenotype not expressed by their corresponding natural phytocannabinoids and quinones.[13]

The relevance of this profile for the management of neurodegenerative diseases [13] made the clarification of the structure of the methylation products and of the regiochemical aspects of their synthesis a critical issue.

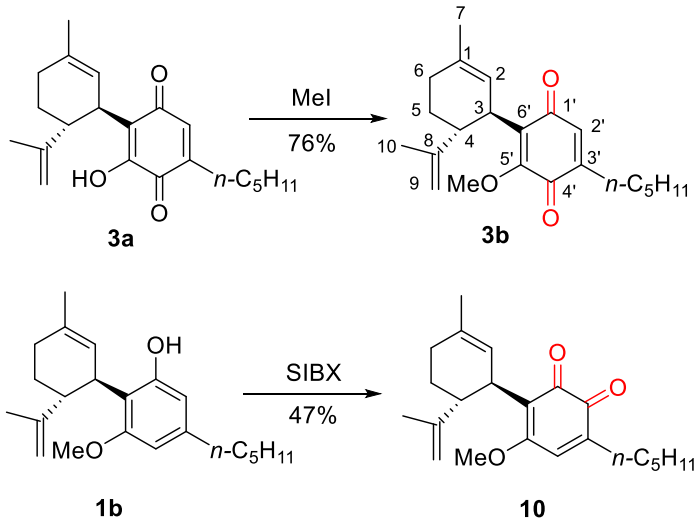

Scheme 2. Chemoselective formation of isomeric *O*-methylcannabinoquinones

The ^{1}H NMR spectra of the isomeric quinoids **3b/10** were very similar, but two distinctive differences were present in the low-field region of their ^{13}C NMR spectra. Thus, the methoxy-substituted olefin carbon (C-5′) resonated at δ 164.4 in **10**, and δ 156.8 in **3b**, and also the carbonyl signals were shifted downfield in **10** compared to **3b** (δ 187.8 and 184.1 vs δ 180,6 and 178.6). Due to its more electrophilic nature, an *ortho*-quinone carbonyl is a better electron sink than a *para*-quinone carbonyl for the

mesomeric delocalization of the oxygen lone pair of the 5′-methoxy group. The contribution of the dipolar resonance form where C-5′ is part of an oxonium ion, is therefore larger in *ortho*-cannabinoquinones compared to *para*-cannabinoquinones (Scheme 3), rationalizing the marked downfield shift of C5′ in **10** when compared to **3b**.

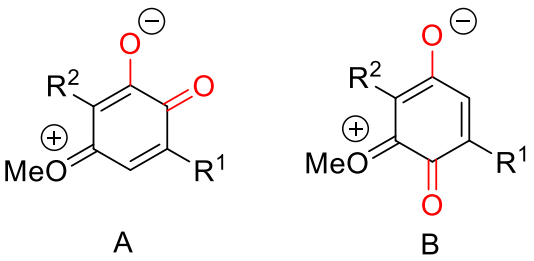

Scheme 3. Dipolar resonance formulas of methoxy-substituted *ortho*- and *para*-cannabinoquinones (R^1 = *n*-C_5H_{11}, R^2 = terpenyl).

Additionally, a NOESY correlation between the methoxy group and the single quinone proton (H-4′ in **10**, H-2′ in **3b**) was observed only in **10**. Overall, these observations identified **3b** as a *para*-quinone, and **10** as an *ortho*-quinone, establishing a simple and clear-cut differentiation between compounds of the two classes, additionally supported by a set of 2D NMR experiments. Similar observations were done for the preparation of *O*-methylcannabigeroquinone (*O*-methyl CBGQ) by methylation of the corresponding quinone (CBGQ, **4a**), or, alternatively, by oxidation of *O*-methylcannabigerol (**2b**), providing a second pair of isomeric quinones (**4b** and **11**, respectively) whose spectroscopic features fully matched those of the **3b**/**10** pair.

SIBX has been reported to selectively oxidize 2-alkylphenols to 2-hydroxycyclohexadienones (*o*-quinols), and some simple phenols lacking *o*-substituents to *o*-quinones,[15] with the tendency for functionalization of the *ortho*-position being also backed up by DFT calculations.[16] The opposite site-selectivity observed with CBD (**1a**) and CBG (**2a**)[10] is presumably the result of tautomeric isomerization of originally formed *o*-quinones (Scheme 1, C) to their more stable and intramolecularly hydrogen-bonded *para*-tautomers (Scheme 1, A). On this basis, the impossibility of tautomeric equilibration could provide a simple explanation as to why the oxidation of the *O*-methyl analogues of CBD and CBG (**1b** and **2b**, respectively) gave exclusively *o*-quinones and not the *p*-quinones obtained from their corresponding resorcinols.

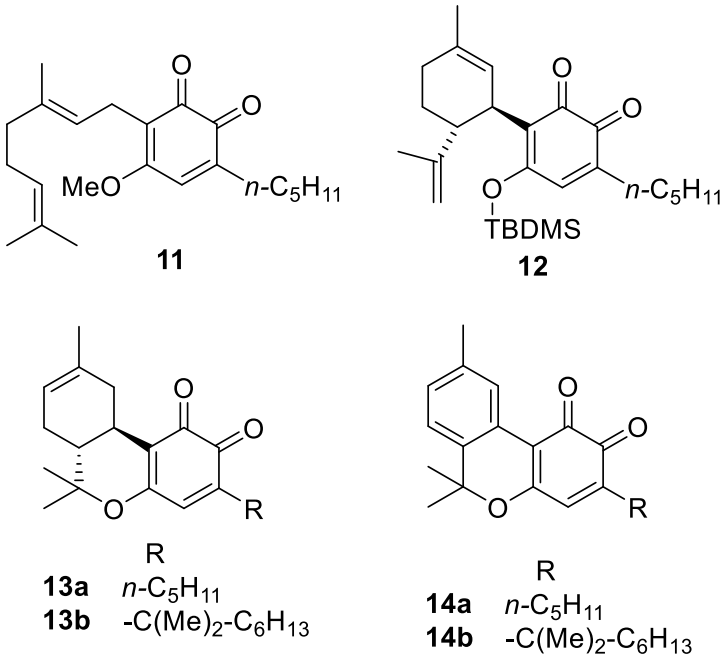

Figure 2. Additional cannabinoquinoids synthesized. TBS = *tert*-butyldimethylsilyl.

A similar chemoselectivity was also observed with monophenolic cannabinoids where one resorcinolic oxygen is linked by an ether bond to the isoprenoid moiety

[Δ^8-THC (**5b**), CBN (**6a**), and their dimethylheptyl analogues (**5c**, **6b**)]. All these compounds afforded *o*-quinones as the only reaction products (**13a**, **14a**, **13b**, and **14b**, respectively).[16] Conversely, the oxidation of Δ^8-THC (**5b**) and CBN (**6a**) with the λ^3-periodinane PIFA exclusively afforded the *p*-quinones **7b** and **8a**, in accordance to the literature report.[3] To demonstrate the post-oxidative tautomerization of hydroxy *o*-quinones to hydroxy *p*-quinones, an attempt was undertaken to oxidize the monosilyl ether of CBD (**1c**) to the *o*-quinone **12**, expected to next generate the *p*-quinone **3a** by desilylation. However, the acidity of SIBX led to silyl loss in the course of the reaction, and **3a** was, instead, directly obtained.

A tautomeric equilibrium of different type could underlie the exclusive formation of the *p*-quinones **16a** and **16b** from the SIBX oxidation of cannabichromene (CBC, **15a**) and its dimethylheptyl analogue (**15b**) (Figure 3).

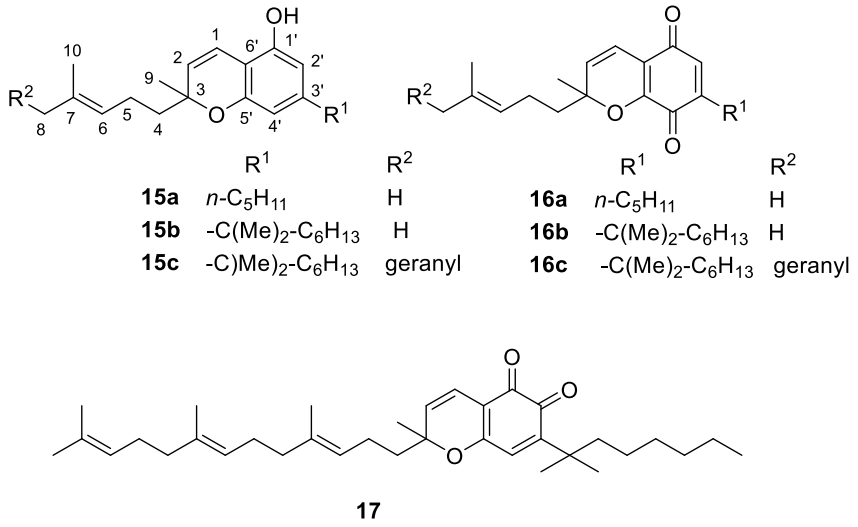

Figure 3. Quinones formed from the oxidation of cannabichromene-type cannabinoids. (geranyl = (*E*)-Me_2C=CH-CH_2-(Me)CH=CH-CH_2-).

Cannabichromene (CBC, **15a**) shows a remarkable reactivity associated to valence tautomerism.[17] Thus, the regiochemistry of the oxidation could be the result of this tautomeric manifold, declined in terms of a) electrocyclic opening of the *o*-quinone chromene ring to an alkylidientrione, b) re-aromatizative isomerization of the proximal olefin double bond, and, c) eventual electrocyclization on the α-dicarbonyl system to a *p*-quinone (Scheme 4). This mechanistic rationale was backed up by the formation of a mixture of the *o*-quinone **17** and *p*-quinone **16c** from the oxidation of **15c**, the bis-prenylogue analogue of **15b**. The mixture could be resolved by gravity column chromatography, but the *o*-quinone **17** could not be stored and isomerized spontaneously to **16c**.

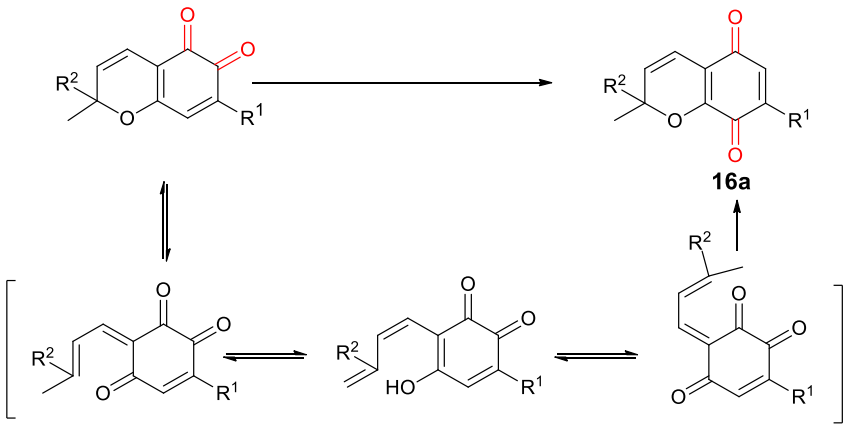

Scheme 4. Possible mechanism for the isomerization of *o*--CBCQ to *p*-CBCQ (**16a**) by chromene-alkylidiencyclohexadienone valence tautomerism (R_1 = nC_5H_{11}, R_2 = isoprenyl).

Some mechanistic hypotheses on the observed regioselectivity of periodinane oxidation are worth discussing.[18] The reaction is started by ligand exchange on iodine and formation of an aryloxyiodonium species (Scheme 5). Next, assuming a two-electron process,[18] an iodonium (III) intermediate could undergo nucleophilic attack by an external water molecule (or by trifluoroaetic acid), preferentially at the

less encumbered *para*-position. Elimination of *o*-iodobenzoic acid and formation of a hydroquinone could next follow, with ligand exchange on iodine and elimination, this time triggered by phenol deprotonation, eventually affording a *p*-quinone (Scheme 5, A). [19,20] With an iodonium (V) intermediate, the oxidation can occur intramolecularly by [2,3]-sigmatropic rearrangement of the iodine-oxygen bond. This process is isosterically equivalent to the orthologue *N*-*S* sigmatropic shift in the Gassman indole synthesis (Scheme 5, B).[21] β-Elimination of iodobenzoic acid will next afford an *o*-quinone, either directly as in Scheme 5, or after isomerization of the *o*-quinol ester to a catechol ester.[22] Longer [2,n] sigmatropic shifts of heteroatomic bonds, as in the semidine rearrangement,[23] are apparently disfavored in aryloxydiodonium (V) species, since, with the exception of **17**, mixture of regioisomeric quinones were never observed as primary oxidation products. λ^3-Periodinanes can only react with the intermolecular mechanism, and therefore normally generate *p*-quinones because steric effects shield the *o*-position from nucleophilic attack.

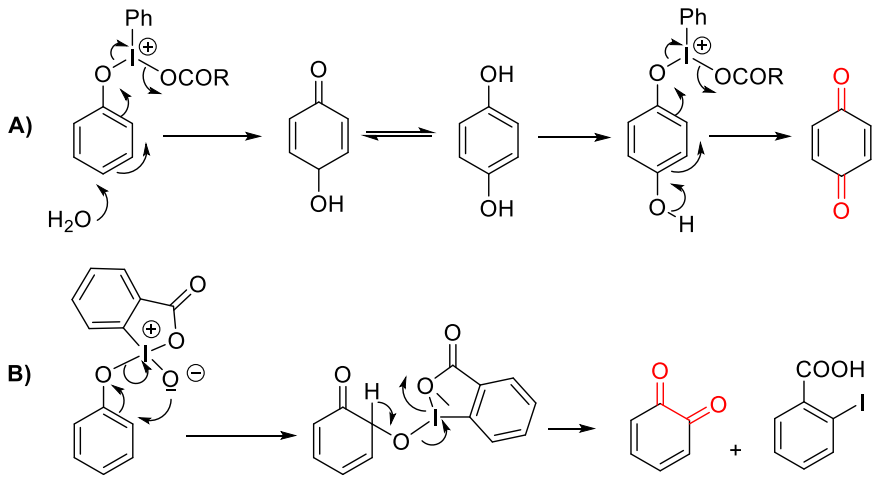

Scheme 5. Possible mechanism for the formation of *p*-quinones and *o*-quinones from aryloxyiodonium (III) and aryloxyiodonium (V) intermediates (A and B) from, respectively, PIFA and SIBX.

Ortho- and *para*-cannabinoquinoids showed differences not only in their color, particularly marked in the quinones from CBN because of aryl conjugation (See the Graphycal Abstract) but , as expected, also in their stability, The *o*-quinone of CBG (**11**) was unstable at room temperature, possibly due to polymerization induced by the presence of the nucleophilic isoprenyl terminal bond, but could be fully characterized, as could **17**, despite its quick valence isomerization to **16c**. All the other *o*-cannabinoquinoids (**10**, **12**, **13a**, **13b, 14a**, **14b**) showed acceptable shelf life, although lower than the one of their corresponding *p*-isomers.

CONCLUSION

The complementary use of λ^3-and λ^5-iodanes, as such or associated to *O*-methylation to block post-oxidative tautomeric equilibria, represents an interesting diversification strategy for phenolic lead structures. This opportunity, as well as the possibility to use SIBX for the synthesis of *p*-quinones, has so far overlooked, despite its mechanistic rationale and its potential to provide a blueprint to explore novel areas of the biological space associated to phenolic lead structures.

EXPERIMENTAL SECTION

GENERAL: IR spectra were recorded on an Avatar 370 FT-IR Techno-Nicolet apparatus. ^{1}H (400 MHz) and ^{13}C (100 MHz) NMR spectra were measured on Bruker Avance 400 MHz spectrometer or on a Bruker Avance 500 MHz. Chemical shifts were referenced to the residual solvent signal ($CDCl_3$: δ_H = 7.21, δ_C = 77.0). Homonuclear ^{1}H connectivities were determined by the Correlation spectroscopy (COSY) experiment. One-bond heteronuclear ^{1}H–^{13}C connectivities were determined with the heteronuclear single quantum coherence (HSQC) spectroscopy experiment. Two- and three-bond ^{1}H–^{13}C connectivities were determined by gradient two-dimensional (2D) heteronuclear multiple bond correlation (HMBC) experiments optimized for a

$^{2,3}J$ = 9 Hz. Low- and high-resolution electrospray ionization mass spectrometry (ESI-MS) data were determined on an LTQ OrbitrapXL (Thermo Scientific) mass spectrometer. Reactions were monitored by thin-layer chromatography (TLC) on Merck 60 F254 (0.25 mm) plates, visualized by staining with 5% H_2SO_4 in EtOH and heating. Organic phases were dried with Na_2SO_4 before evaporation. Chemical reagents and solvents were purchased form Sigma-Aldrich and were used without further purification unless stated otherwise. Petroleum ether with boiling point of 40–60 °C was used. Silica gel 60 (70–230 mesh) was used for gravity column chromatography (GCC).All starting cannabinoids were available from previous studies in the area.[9,13,17]

SIBX OXIDATION OF CANNABINOIDS.

OXIDATION OF *O*-METHYL CBD (1B) AS REPRESENTATIVE: To a cooled (ice bath) solution of *O*-methyl CBD (**1b**, 200 mg, 0.61 mmol, Rf= 0.47, petroleum ether-EtOAc 95:5 as eluant) in ethyl acetate (10 mL), SIBX (39 wt. %, 1.44 g, 2.01 mmol, 3.3 molar equiv.) was added in small portions. At the end of the addition, the cooling bath was removed, and the suspension was stirred at room temperature, following the course of the reaction by TLC (R*f* **10** = 0.19, petroleum ether-EtOAc 95:5). After 18 h, the reaction mixture was filtered over a pad of Celite. The filtration cake was washed with EtOAc (10 mL), and the pooled filtrates were washed with saturated $Na_2S_2O_3$ (4 × 15 mL) and next with brine. After drying and evaporation, the residue was purified by GCC on silica gel (10 g, petroleum ether–EtOAc 95:5 as eluant) to obtain 98 mg (47%) **10**. In all other iodane (SIBX, PIFA) oxidations, a similar difference in Rf values between reactants and reaction products was observed. The reaction yield is provided along with the description of their physical state for each product.

***ORTHO*-*O*-METHYLCANNABIDIOLQUINONE (*O*-ME-CBDQ, 10**): Dark red oil (47%), FT-IR (cm^{-1}): ν= 2955, 2924, 2857, 1643, 1431, 1107, 886. ^{1}H NMR ($CDCl_3$, 400 MHz) δ = 6.83 (bs, H-4′), 5.06 (bd, *J* = 2.5 Hz, H-2), 4.56 (bs, H-9a), 4.52 (bs, H-9b), 3.87 (s, 5′-OMe), 3.65 (m, H-3), 2.67 (dt, *J* = 9.2, 3.0 Hz, H-4), 2.41 (t, *J* = 7.5 Hz, H-1′′), 2.17 (m, H-6a), 2.04 (m, H-6b), 1.95 (m, H-5), 1.64 (bs, H-7), 1.61 (bs, H-10), 1.50 (m, H-2′′), 1.32 (overlapped, H-3′′), 1.30 (overlapped, H-4′′), 0.89 (t, J = 6.9 Hz, H-5′′). ^{13}C NMR (CDCl3, 100 MHz): δ = 180.6 (C-1′), 178.6 (C-2′), 164.4 (C-5′), 148.7 (C-8), 142.6 (C-4′), 133.0 (C-1), 128.0 (C-3′), 124.2 (C-6′), 123.6 (C-2), 110.4 (C-9), 45.1 (C-4), 31.8 (C-1′′), 31.5 (C-3′′), 30.6 (C-5), 30.4 (C-6), 30.2 (C-2′′), 29.3 (C-3), 24.0 (C-7), 22.5 (C-4′′), 18.5 (C-10), 14.5 (C-5′′). ESI-MS *m*/*z* 343 $[M+H]^+$; HRESI-MS: *m*/*z* calcd. for $C_{22}H_{31}O_3$ $[M+H]^+$ 343.2273, found 343.2279.

***ORTHO*-*O*-METHYLCANNABIGEROQUINONE (*O*-ME-CBGQ, 11):** Dark red oi (37%). FT- IR (cm^{-1}): ν 2956, 2925, 2855, 1655, 1638, 1345, 1107. ^{1}H NMR ($CDCl_3$, 400 MHz): δ = 6.89 (bs, 1H), 5.08 (m, 2H), 3.97 (s, 3H), 3.05 (d, *J* = 7.4 Hz, 2H), 2.37 (t, *J* = 7.4 Hz, 2H), 2.04 (m, 2H), 1.98 (m, 2H), 1.72 (bs, 3H), 1.67 (bs, 3H), 1.50 (bs, 3H), 1.49-1.32 (m, 6H), 0.90 (t, *J* = 6.9 Hz, 3H). ^{13}C NMR ($CDCl_3$, 100 MHz): δ =180.6, 178.9, 163.3, 142.4, 136.1, 134.3, 131.3, 127.7, 124.3, 120.7, 56.6, 39.7, 31.4, 29.7, 27.9, 26.7, 25.7, 22.4, 21.6, 17.7, 16.1, 13.9. HRESI-MS: *m*/*z* calcd. for $C_{22}H_{33}O_3$ $[M+H]^+$ 345.2430, found 345.2430.

***ORTHO*-Δ^8-TETRAHYDROCANNABINOLQUINONE (*O*-THCQ, 13A)**: Dark red oil (51%). FT-IR (cm^{-1}): ν = 2956, 2925, 2852, 1639, 1584, 1388, 1184, 1112. ^{1}H NMR ($CDCl_3$, 400 MHz): δ = 6.49 (bs, 1H), 5.30 (bs, 1H), 3.10 (m, 1H), 2.49 (dt, J^1 = 11.0 Hz, J^2 = 4.9 Hz, 1H), 2.35 (t, *J* = 7.7 Hz, 2H), 2.12 (m, 1H), 1.83 (m, 1H), 1.75-1.20 (overlapped m, 6H), 1.45 (s, 1H), 1.21 (s, 6H), 0.91 (t, *J* = 6.9 Hz, 3H). ^{13}C NMR ($CDCl_3$, 100 MHz): δ =181.2, 177.7, 162.9, 143.3, 134.4, 118.6, 114.9, 82.1, 43.6, 35.2, 31.4, 29.8, 28.7, 27.4, 27.1, 26.9, 23.3, 22.4, 19.4, 13.9. HRESI-MS: *m*/*z* calcd. for $C_{21}H_{29}O_3$, $[M+H]^+$ 329.2122, found 329.2122.

3′-DEPENTYL-3′-(α,α-DIMETHYLHEPTYL)-*ORTHO*-Δ⁸-TETRAHYDROCANNABINOL QUINONE (*O*-DMH-THCQ, 13B): Dark red oil (54%). FT-IR (cm^{-1}): ν = 2956, 2925, 2856, 1589, 1379, 1112, 919. ^{1}H NMR ($CDCl_3$, 400 MHz): δ = 6.38 (bs, 1H), 5.31 (bs, 1H), 2.98 (m, 1H), 2.39 (dt, J^1 = 11.1 Hz, J^2 = 5.0 Hz, 1H), 2.02 (m, 1H), 1.74 (m, 1H), 1.67-1.49 (overlapped m, 8H), 1.37 (s, 1H), 1.27-0.89(overlapped m, 16H), 0.78 (t, *J* = 6.8 Hz, 3H). ^{13}C NMR ($CDCl_3$, 100 MHz): δ =180.7, 177.8, 162.9, 149.8, 134.7, 134.5, 118.6, 114.9, 82.2, 43.5, 40.6, 38.5, 35.1, 31.8, 29.8, 29.7, 27.3, 27.2, 27.1, 27.0, 25.1, 23.3, 22.7, 19.5, 14.1. HRESI-MS: *m*/*z* calcd. for $C_{25}H_{37}O_3$, $[M+H]^+$ 385.2672, found 385.2677.

***ORTHO*-CANNABINOLQUINONE (*O*-CBNQ, 14A):** Purple oil (58%). FT-IR (cm^{-1}): ν = 2955, 2924, 2855, 1649, 1382, 1145, 1110, 811. ^{1}H NMR ($CDCl_3$, 400 MHz): δ = 8.30 (s, 1H,), 7.09 (d, *J* = 8.9 Hz, 1H), 7.02 (d, *J* = 7.9 Hz, 1H), 6.63 (bs, 1H), 2.40 (t, *J* = 7.7 Hz, 1H), 2.36 (s, 3H), 1.69 (s, 6H), 1.56 (m, 2H), 1.32 (m, 2H), 0.90 (t, J = 6.8 Hz, 3H). ^{13}C NMR ($CDCl_3$, 100 MHz): δ =180.2, 175.3, 163.3, 144.7, 138.1, 133.8, 131.8, 128.9, 125.7, 122.3, 111.0, 82.7, 53.6, 31.6, 29.8, 29.0, 28.3, 27.4, 22.4, 21.4, 13.9. HRESI-MS: *m*/*z* calcd. for $C_{21}H_{25}O_3$, $[M+H]^+$ 325.1798, found 325.1791.

3′-DEPENTYL-3′-(α,α-DIMETHYLHEPTY)-*ORTHO*-CANNABINOLQUINONE (*O*-DMH-CBNQ, 14B): FT-IR (cm^{-1}): ν = 2955, 2924, 2856, 1649, 1376, 1145, 1110, 813. ^{1}H NMR ($CDCl_3$, 400 MHz): δ = 8.33 (s, 1H,), 7.12 (d, *J* = 8.9 Hz, 1H), 7.04 (d, *J* = 7.9 Hz, 1H), 6.63 (bs, 1H), 2.39 (s, 3H), 1.73 (s, 6H), 1.70 (overlapped m, 2H) 1.33-0.99 (m, 14H), 0.87 (t, *J* = 6.9 Hz, 3H); ^{13}C NMR ($CDCl_3$, 100 MHz): δ =179.9, 176.4, 163.1, 151.2, 137.9, 134.1, 131.8, 128.9, 125.7, 124.6, 122.3, 110.8, 82.7, 40.6, 38.8, 31.7, 29.7, 29.7, 28.4, 27.3, 25.1, 22.6, 21.3, 14.0. HRESI-MS: *m*/*z* calcd. for $C_{25}H_{33}O_3$, $[M+H]^+$ 381.2430, found 381.2437.

***PARA*-CANNABICHROMENQUINONE (CBCQ, 16A):** Red oil (59%). FT-IR (cm^{-1}): ν = 2957, 2926, 2852, 1648, 1580, 1324, 1078, 969, 891. ^{1}H NMR ($CDCl_3$, 400 MHz): δ = 6.48 (d, *J* = 10.2 Hz, H-1), 6.42 (s, H-2'), 5.57 (d, *J* = 10.2 Hz, H-2), 5.09 (bt, *J* = 8.5 Hz, H-6), 2.42 (t, *J* = 8.5 Hz, H-1''), 2.07 (m, H-5), 1.95 (m, H-4a), 1.66 (bs, H-8), 1.63 (overlapped, H-4b), 1.58 (bs, H-9), 1.50 (m, H-2''), 1.48 (s, H-10), 1.32 (overlapped, H-3''), 1.30 (overlapped, H-4''), 0.89 (t, *J* = 6.9 Hz, H-5'').^{13}C NMR ($CDCl_3$, 100 MHz): δ = 184.6 (C-1'), 181.8 (C-4'), 150.9 (C-5'), 147.8 (C-3'), 132.5 (C-7), 131.1 (C-2'), 128.5 (C-2), 123.3 (C-6), 115.1 (C-1), 114.9 (C-6'), 82.6 (C-3), 41.5 (C-4), 31.5 (C-3''), 30.2 (C-2''), 28.4 (C-1''), 27.2 (C-10), 25.5 (C-8), 22.7 (C-4''), 22.3 (H-5), 17.6 (C-9), 14.2 (C-5''). HRESI-MS: *m*/*z* calcd. for $C_{21}H_{29}O_3$ $[M+H]^+$ 329.2117, found 329.2122.

3'-DEPENTYL-3'(α,α-DIMETHYLHEPTYL)CANNABICHROMENQUINONE (DMH-CBCQ, 16B): Red oil (57%). FT-IR (cm^{-1}): ν = 2957,2924, 2856, 1648, 1080. ^{1}H NMR ($CDCl_3$, 400 MHz): δ = 6.47 (d, J = 10.0 Hz, 1H), 6.42 (bs, 1H), 5.56 (d, *J* = 10.0 Hz, 1H), 5.09 (bt, *J* = 7.8 Hz, 1H), 2.11 (m, 2H), 1.89 (m, 1H), 1.77-1.52 (m, 4H), 1.67 (bs, 3H), 1.49 (s, 3H), 1.32-0.97 (m, 16H), 0.86 (t, *J* = 6.9 Hz, 3H). ^{13}C NMR ($CDCl_3$, 100 MHz): δ = 184.7, 181.4, 153.2, 151.3, 132.2, 132.1, 128.6, 123.3, 115.2, 114.2, 83.2, 41.5, 40.7, 38.7, 31.7, 29.7, 27.6, 27.3, 25.6, 25.1, 22.6, 22.5, 17.6, 14.0. HRESI-MS: *m*/*z* calcd. for $C_{25}H_{37}O_3$ $[M+H]^+$ 385.2743, found 385.2739.

3'-DEPENTYL-3'(α,α-DIMETHYLHEPTYL)GERANYL-PARA-CANNABICHROMENQUINONE (16C): Red oil (51%). FT-IR (cm^{-1}): ν = 2956,2923, 2855, 1649, 1449, 1181, 1080. ^{1}H ^{1}H NMR (400 MHz, $CDCl_3$,) δ= 6.47 (d, *J* = 10.0 Hz, 10H), 6,42 (s, 1H), 5.57 (d, *J* = 10.0 Hz, 1H), 5.11 (m, 3H), 2.13-1.96 (m, 10H), 1.74-1.59 (m, 16H), 1.49 (s, 3H), 1.29-1.18 (m, 12 H), 1.05 (m, 2H), 0.87 (t, *J* = 6.9 Hz, 1H). ^{13}C NMR (100 MHz, $CDCl_3$) δ= 184.71, 181.45, 153.22, 151.35, 135.97, 135.05, 132.18, 131.27, 128.67, 124.38, 124.08, 123.14, 115.22, 114.25, 83.21, 41.55, 40.76, 39.72, 39.65, 38.71,

31.71, 29.77, 27.65, 27.63, 27.30, 26.76, 26.54, 25.71, 25.14, 22.62, 22.45, 17.70, 16.01, 14.06.

3′-DEPENTYL-3′(α,α-DIMETHYLHEPTYL)GERANYL-ORTHO-CANNABICHROMENQUINONE (17): Purple oil (5%). ^{1}H NMR (400 MHz, $CDCl_3$) δ = 6.53 (s, 1H), 6.49 (d, *J* = 10.1 Hz, 1H), 5.34 (d, *J* = 10.1 Hz, 2H), 5.11 (m, 3H), 2.15-1.96 (m, 10H), 1.74-1.54 (m, 16H), 1.49 (s, 3H), 1.3-1.14 (m, 12H), 1.05 (m, 2H), 0.87 (d, *J* = 6.8 Hz, 3H). ^{13}C NMR (100 MHz, $CDCl_3$) δ = 180.38, 174.72, 163.44, 151.24, 136.06, 135.13, 132.74, 131.31, 124.38, 124.36, 124.01, 123.18, 123.09, 115.71, 109.98, 84.60, 41.88, 40.64, 39.72, 39.68, 39.00, 31.75, 29.78, 27.77, 27.43, 27.40, 26.76, 26.53, 25.71, 25.13, 23.83, 22.65, 22.50, 17.70, 16.03, 14.07. We were not able to collect IR and mass spectra due to the fast interconversion of 17 in 16c.

PIFA OXIDATION OF CANNABINOIDS

OXIDATION OF CANNABICHROMENE (CBC) AS REPRESENTATIVE: To a stirred solution of CBC (**15a**, 150 mg, 0.48 mmol), a solution of bis(trifluoroacetoxy)iodobenzene (PIFA, 641 mg, 1.49 mmol, 3.1 molar equiv.) in MeCN-H_2O 6:1 (2 mL) was added dropwise. The progress of the reaction was monitored by TLC. After completion of the reaction (20 minutes), the mixture was diluted with EtOAc (10 mL) and washed with saturated Na_2CO_3 (4 × 15 mL) and next with brine. After drying and evaporation, the residue was purified by GCC on silica gel (10 g, petroleum ether–EtOAc 95:5 as eluant) to give 86 mg (55%) CBCQ (**16a**), identical to the product obtained from the SIBX oxidation.

METHYLATION OF CANNABINOQUINOIDS

METHYLATION OF CBDQ (3A) AS EXEMPLIFICATIVE: To a stirred solution of CBDQ (**3a**, 200 mg, 0.61 mmol, in dry DMF (5 mL), $NaHCO_3$ (102 mg, 1.22 mmol, 2 molar equiv) was added. The resulting solution was stirred at room temperature for 5

minutes, and then methyl iodide (282 μL, 3,04 mmol, 5 mkol. eq) was added dropwise. The solution was stirred at room temperature overnight, and then worked up by dilution with EtOAc (15 mL). The organic phase was washed with 2M NaOH (3x 15 mL) and next with brine. After drying and evaporation, the residue was purified by GCC on silica gel (10 g, petroleum ether as eluant) to obtain 160 mg (76%) **3b**.

***PARA*-*O*-METHYLCANNABIDIOLQUINONE (*P*-ME-CBDQ, 3B):** Dark orange oil, (76%). FT-IR (cm^{-1}): ν = 2956,2926, 2857, 1649, 1260, 890. ^1H NMR ($CDCl_3$, 400 MHz): δ = 6.37 (bs, H-2′), 5.09 (bd, *J* = 2.5 Hz, H-2), 4.54 (bs, H-9a), 4.50 (bs, H-9b), 3.87 (s, 5′-OMe), 3.72 (m, H-3), 2.67 (dt, *J* = 9.2, 2.5 Hz, H-4), 2.36 (t, *J* = 7.5 Hz, H-1′′), 2.17 (m, H-6a), 1.97 (overlapped, H-6b), 1.94 (overlapped, H-5), 1.67 (bs, H-7), 1.61 (bs, H-10), 1.50 (m, H-2′′), 1.32 (overlapped, H-3′′), 1.30 (overlapped, H-4′′), 0.89 (t, J = 6.9 Hz, H-5′′). ^{13}C NMR ($CDCl_3$, 100 MHz): δ = 187.9 (C-1′), 184.1 (C-4′), 156.8 (C-5′), 148.2 (C-8), 147.3 (C-3′), 135.5 (C-6′), 133.2 (C-1), 132.5 (C-2′), 122.8 (C-2), 110.9 (C-9), 45.3 (C-4), 31.3 (C-1′′), 31.5 (C-3′′), 30.6 (C-5), 30.4 (C-6), 30.2 (C-2′′), 29.1 (C-3), 24.2 (C-7), 22.5 (C-4′′), 18.1 (C-10), 14.5 (C-5′′). HRESI-MS: *m*/*z* calcd. for $C_{22}H_{31}O_3$ $[M+H]^+$ 343.2273, found 343.2279.

PARA-*O*-METHYLCANNABIGEROLQUINONE (*P*-ME-CBGQ, 4B): Orange oil (35%). FT-IR (cm^{-1}): ν = 2926, 2857, 1650, 1445, 1265, 1199, 1107, 894. ^1H NMR ($CDCl_3$, 400 MHz): δ = 6.89 (bs, 1H), 4.98 (m, 2H), 3.90 (s, 3H), 3.06 (d, J = 7.3 Hz, 2H), 2.31 (td, J^1 = 7.9 Hz, J2 = 1.4, 2H), 1.97 (m, 2H), 1.89 (m, 2H), 1.66 (bs, 3H), 1.58 (bs, 3H), 1.50 (bs, 3H), 1.42 (m, 2H), 1.26 (m, 4H), 0.83 (t, J = 6.9 Hz, 3H). ^{13}C NMR ($CDCl_3$, 100 MHz): δ = 188.2, 184.1, 155.6, 147.6, 137.1, 132.2, 131.9, 131.4, 124.2, 120.0, 60.9, 39.7, 31.5, 29.7, 28.6, 27.5, 26.6, 25.7, 22.4, 17.7, 16.1, 13.9. HRESI-MS: *m*/*z* calcd. for $C_{22}H_{33}O_3$ $[M+H]^+$ 345.2430, found 345.2422.

ACKNOWLEDGEMENTS

We are grateful to MIUR Italy (PRIN2017, Project 2017WN73PL, bioactivity-directed exploration of the phyto-cannabinoid chemical space) for financial support.

Keywords: quinones • oxidation • phytocannabinoids • iodanes • tautomerism

REFERENCES

[1] W. Beam, *Fourth Report Wellcome Tropical Research Lab. Chem Sect. Khartoum* **1911**, B25.

[2] R. Mechoula, Z. Ben-Zvi, Y. Gaoni. *Tetrahedron* **1968**, 24, 5615-5624.

[3] N. M. Kogan, R. Rabinowitz, P. Levi, D. Gibson, P. Sandor, M. Schlesinger, R. Mechoulam. *J. Med. Chem*. **2004**, *47*, 3800-3806.

[4] M. M. Radwan, M. A. ElSohly, D. Slade, S. A. Ahmed, L. Wilson, A. T. El-Afly, I. Khan, S. A. Ross. *Phytochemistry* **2008**, *69*, 2627-2633.

[5] A. S. Husni, C. R. McCurdy, M. M. Radwan, A. S. Ahmed, D. Slade, S. A. Ross, M. A. ElSohly, J. S. Cutler. *Med. Chem. Res.* **2014**, *23*, 4295-4300.

[6] A. G. Granja, F. Carrillo-Salinas, A. Pagani, M. Gómez-Cañas, R. Negri, C. Navarrete, M. Mecha, L. Mestre, B. L. Fiebich, I. Cantarero, M. A. Calzado, M. L. Bellido, J. Fernan-dez-Ruiz, G. Appendino, C. Guaza, E. Muñoz. *J. Neuroimmune Pharmacol.* **2012**, *7*, 1002-1016.

[7] C. del Río, C. Navarrete, J. A. Collado, M. L. Bellido, M. Gómez-Cañas, M. R. Pazos, J. Fernández-Ruiz, F. Pollastro, G. Appendino, M. A. Calzado, I. Cantarero, E. Muñoz, *Sci. Rep*. **2016**, *6*:21703. doi: 10.1038/srep21703.

[8] https://sclerodermanews.com/2018/02/20/emerald-health-scleroderma-treatment-orphan-drug-designation/ (accessed on September 4, 2020).

[9] D. Caprioglio, D. Mattoteia, F. Pollastro, R. Negri, A. Lopa-triello, G. Chianese, A. Minassi, J. A. Collado, E. Munoz, O. Taglialatela-Scafati, G. Appendino. *J. Nat. Prod.* **2020**, *83*, 1711-1715.

[10] L. Ozanne, L. Pouységu, D. Depernet, B. François, S. Quideau. *Org. Lett.* **2003**, *5*, 2903-2906. For an acidity study on IBX, see: M. J. Gallen, R. Goumont , T. Clark, F. Terrier, Craig M. Williams. *Angew. Chem. Int. Ed. Engl.* **2006**, *45*, 2929-2934. For a study on the sensitiveness and potential hazards of oxidants, see: M. A. Dallaston, C. J. Bettencourt, S. Chow J. Gebhardt, J. Spangler, M. R. Johnston, C. Wall, J. S. Brusnahan, C. M. Williams. *Chem. Eur. J.* **2019**, *25*, 9614-9618.

[11] E. R. Darzi, N. K. Garg. *Org. Lett.* **2020**, *22*, 3951-3955. For a recent study on the dearomatization of phenols with hypervalent iodine reagents, see: X. Xiao, N. S. Greenwood, S. E. Wengryniuk. *Angew.Chem. Int. Ed.* **2019**, *58*,16181-16187.

[12] D. Caprioglio, G. Allegrone, F. Pollastro, S. Valera, A. Lopatriello, A. Collado, E. Muñoz, G. Appendino, O. Taglialatela-Scafati. *Planta Med.*, **2019**, *85*, 981-986.

[13] L. Casares, J. D. Unciti, M. E. Prados, D. Caprioglio, M. Higgins, G. Appendino, A. T. Dinkova-Kostova, E. Muñoz, L. de la Vaga. *Redox Biol.* **2020** (in press).

[14] D. Magdziak, A. A. Rodriguez, R. W. Van de Water, T. R. R. Pettus. *Org. Lett.* **2002**, *4*, 285-288.

[15] A. Kaur, A. Ariafard. *Org. Biomol. Chem.* **2020**, *18*, 1117-1129.

[16] The oxidation of CBN with SIBX was reported to provide a *p*-quinone (ref. 9), whose structure, in the light of this study, should be reversed to the one of an *o*-quinone.

[17] D. Caprioglio, D. Mattoteia, A. Minassi, F. Pollastro, A. Lopatriello, E. Muñoz, O. Taglialatela-Scafati, G. Appendino. *Org. Lett.* **2019**, *21*, 6122-6125.

[18] R. M. Moriarty, O. Prakash. *Org. Reactions*, **2001**, *57*, 327-415.

[19] Y. Tamura, T. Yakura, H. Tohma, K. Kikuchi, Y. Kita. *Synthesis* **1989**, 126-127.

[20] R. Barret, M. Daudon. *Tetrahedron Lett.* **1990**, *34*, 4871-4872.

[21] P. T. Gassman, T. van Bergern, D. P. Gilbert, B. W. A. Cue Jr. *J. Am. Chem. Soc.* **1974**, *96*, 5495-5508.

[22] Calculations have shown that the isomerization of a quinol ester to a catechol ester is exergonic (see ref. 16).

[23] D. V. Banthorpe, C. Ingold, J. Roy. *J. Chem. Soc. B*, **1968**, 64-66.

SUBCHAPTER 3.4

OXIDATIVE QUINONE HETEROFUNCTIONALIZATION METHOD APPLIED TO CANNABINOIDS

(UNPUBLISHED DATA)

3.4.1 INTRODUCTION

As described in previous works (subsection 3.2), phytocannabinoid quinones have a significant pharmacological potential: the quinone derivative of CBD (*HU-331)* is a catalytic inhibitor of topoisomerase IIα and show selective anticancer activity, that is activity only on cancerous cells and not on normal cells (Mechoulam & Ben-Zvi, 1968) (Kogan, et al., 2004) (Kogan & al., 2007).

Development was, however, stopped most probably for the inherent chemical instability of these compounds, and their potential mutagenicity *in vivo*: the unsubstituted position of the quinone is highly electrophilic, so these compounds are reactive towards thiol residues via thia-Michael reactivity as well as reactive at the quinone carbonyl via Schiff-type reactivity (Wu & Jan, 2010).

Furthermore, they easily undergo to dimerization, with total loss of bioactivity.

In previous studies, it was found that primary amines add easily in *aza*-Michael fashion to cannabinoquinoids, next undergoing spontaneous dehydrogenation, and generating aminoquinones devoid of affinity for thiol group. Two of these aminoquinones (*VCE-004.8* ***1*** and *VCE-003.2* **2**, derived from CBD and CBG respectively), have completed preclinical and toxicological evaluation, and are now in clinical development for autoimmune (VCE-004.8, phase II) and neurodegenerative (VCE-003.2, phase I) disease. These compounds show affinity for CB_2, negligible activity on CB_1, and powerful activity at PPAR-γ (Del Río & al., 2016) (Díaz-Alonso & al., 2016).

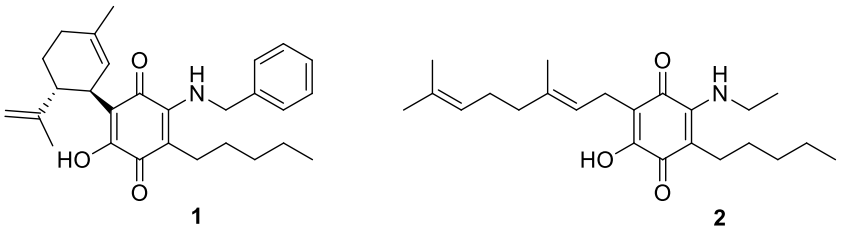

FIGURE 1 **CHEMICAL STRUCTURES OF VCE-004.8 AND VCE-003.2.**

3.4.2 DEVELOPMENT OF A TELESCOPED SYNTHESIS OF AMINOCANNABINOQUINOIDS

The synthesis of aminoquinoids from phytocannabinoids is a two-step procedure, that involves oxidation to cannabinoquinoids and then *aza*-Michael addition and dehydrogenation. Inspired by a 2018 report by *Poulsen* that certain metals ($Fe(OAc)_2$, $Mn(OAc)_3*2H_2O$ and $Co(OAc)_2$) promote the addition of oxygen nucleophiles to quinones (Yu & al., 2018), we wondered if resorcinolic cannabinoids, that are easily oxidized by metal ions in the presence of atmospheric oxygen, could be directly converted into aminoquinoids. Apart from a shortening of the synthetic sequence, the method could avoid the purification of unstable cannabinoquinones, and potentially increasing the reaction yield by avoiding the degradative loss of the unstable intermediates. Additionally, the overall atom economy of the process could be significantly improved, since atmospheric oxygen was the only oxidant employed.

The project was started by screening the metal catalysts described by Poulsen, in a probe reaction consisting in the trapping of HU-331 with *n*-butylamine. Only manganese (III) acetate was able to accelerate the reaction, while the other metal catalysts based on Co(II) and Fe(II) caused extensive degradation of the starting

material. We next investigated if Mn(III) under aerobic conditions could also promote the oxidation of resorcinolic phytocannabinoids to their corresponding quinones, that would then be trapped as amine adducts. (Scheme 1)

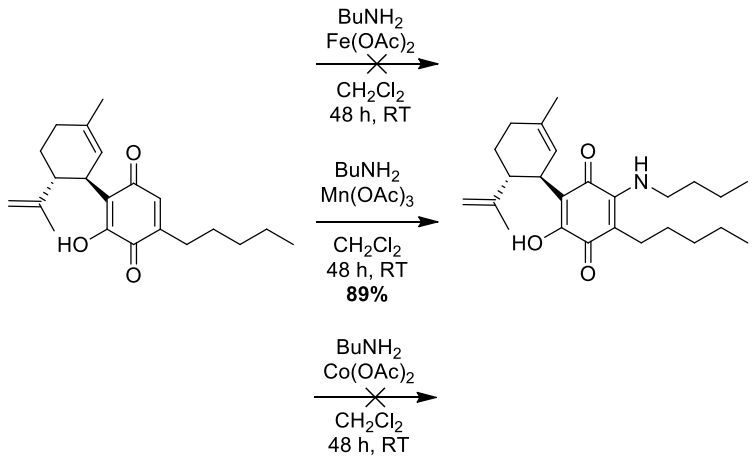

SCHEME 1 **METAL CATALYZED FORMATION OF AMINOQUINONES.**

A systematic work was carried out to assess the possibility of the reaction and its optimization in terms of metal load, time and work-up protocol. (Table 1)

The one-pot process was indeed successful, but stoichiometric and not catalytic amounts of the metal were necessary (entry 4), undermining the relevance of the finding. Since the second step required "catalytic" amounts of metal, the catalyst was consumed in the first step of the reaction, that is, the oxidation of cannabinoids to cannabinoquinoids.

	SM	**$Mn(OAc)_3$ eq**	**AMINE**	**t (h)**	**N_2**	**AIR**	**WORK-UP**	**YIELD**
1	CBDQ	0,1	$BuNH_2$	48	-	✔	H_2SO_4 2M	89%
2	CBD	0,1	$BuNH_2$	24	-	✔	H_2SO_4 2M	*a*

3	CBD	0,1	$BuNH_2$	72	-	✔	H_2SO_4 2M	*A*
4	CBD	0.5	$BuNH_2$	24	-	✔	H_2SO_4 2M	*B*
5	CBD	1	$BuNH_2$	48	-	✔	H_2SO_4 2M	78%
6	CBD	1	$BuNH_2$	72	-	✔	NTA	54%
7	CBD	1	$BzNH_2$	96	✔	-	Citric acid	30%*
8	CBD	1	$PhEtNH_2$	24	-	✔	H_2SO_4 2M	48%*
9	CBGQ	0,1	$BuNH_2$	24	-	✔	Citric acid	96%
10	CBGQ	0,1	$BzNH_2$	24	-	✔	Citric acid	73%
11	CBGQ	0,1	$PhEtNH_2$	24	-	✔	Citric acid	85%
12	CBG	1	$BuNH_2$	60	-	✔	H_2SO_4 2M	47%
13	CBG	1	$BzNH_2$	24	-	✔	H_2SO_4 2M	*C*
14	CBG	1	$PhEtNH_2$	36	-	✔	H_2SO_4 2M	45%
15	CBG	1	$BuNH_2$	48	-	✔	Citric acid	65%
16	CBG	1	$BzNH_2$	72	-	✔	Citric acid	69%
17	CBG	1	$BzNH_2$	72	-	$+O_2$	-	40%
18	CBC	1	$BzNH_2$	48	-	✔	-	*D*

***TABLE 1* TEST REACTIONS. LEGEND: *A*= CALCULATED BY ^{1}H NMR INTEGRATION, 1.2:1 RATIO WITH STARTING MATERIAL. *B*= *A*= CALCULATED BY ^{1}H NMR INTEGRATION, 5:1 RATIO WITH STARTING MATERIAL. *C*= CALCULATED BY ^{1}H NMR INTEGRATION, 1.3:1 RATIO WITH STARTING MATERIAL. *= CALCULATED BY ^{1}H NMR INTEGRATION. *D*= ONLY QUINOID FORM WAS ACHIEVED**

With sub-stoichiometric amounts of metal, the oxidation did not go to completion, raising therefore the issue of the removal of metal salts from the reaction product, that, due to the presence of the hydroxyquinone moiety, shows predictable metal-chelating properties. The reaction was clean, and removal of manganese salts by washing with chelating acids (nitrilotriacetic (NTA), citric acid), that, however, was not sufficient to avoid the chromatographic purification of the reaction product. The

results obtained with CBD could be replicated with CBG, a compound that gives lower yields in the conventional iodane oxidation to its corresponding quinone. The use of pure oxygen rather than air did not significantly improve the reaction yield (entry 9), rather triggering degradation and eroding the final yield. The oxidative amination protocol fails with *O*-methyl phytocannabinoids, and the same results was observed with our protocol (entry 18).

Surprisingly, Mn(III) failed to promote the addition of oxygen nucleophiles to our substrates, despite being reported as selective for this reaction.

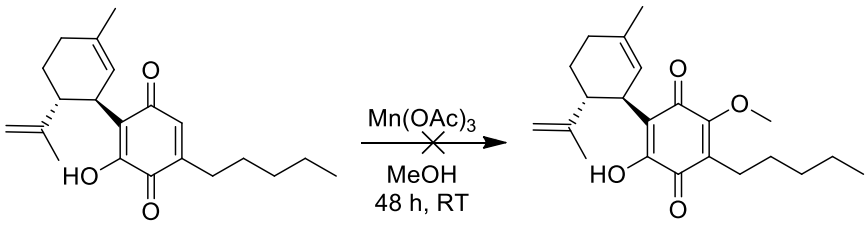

FIGURE 2 **FAILED ATTEMPT OF ALCOHOL ADDITION.**

3.4.3 CONCLUSIONS

Using metal catalysis by Mn(III), it is possible to telescope the synthesis of aminocannabinoquinoids to a single step reaction, where a resorcinolic phytocannabinoid is first oxidized by air to its corresponding quinoid form, then trapped by an amine and eventually dehydrogenated. However, the increased yield and the simplicity of the protocol, is marred by the need to use stoichiometric amounts of metal. The reaction therefore needs further optimization. Possible avenues of investigation will be the use of two catalytic metals, one for the oxidation to quinone and the other one for the dehydrogenative amination. In alternative, more reactive oxygen species like oxone or peroxides could be used. The mechanism by which certain metals promote the Michael addition to quinones is unclear. Binding

the quinone carbonyl, that is, Lewis acid catalysis, could be one mechanism, and therefore also oxyphilic ions will be worth investigating, like lanthanides.

3.4.4 EXPERIMENTAL SECTION

GENERAL EXPERIMENTAL PROCEDURES: IR spectra were recorded on an Avatar 370 FT-IR Techno-Nicolet apparatus. ^{1}H (400 MHz) and ^{13}C (100 MHz) NMR spectra were measured on Bruker Avance 400 MHz spectrometer. Chemical shifts were referenced to the residual solvent signal ($CDCl_3$: δ_H = 7.21, δ_C = 77.0). Homonuclear ^{1}H connectivities were determined by the Correlation spectroscopy (COSY) experiment. One-bond heteronuclear ^{1}H–^{13}C connectivities were determined with the heteronuclear single quantum coherence (HSQC) spectroscopy experiment. Two- and three-bond ^{1}H–^{13}C connectivities were determined by gradient two-dimensional (2D) heteronuclear multiple bond correlation (HMBC) experiments optimized for a $^{2,3}J$ = 9 Hz. Low- and high-resolution electrospray ionization mass spectrometry (ESI-MS) data were determined on an LTQ OrbitrapXL (Thermo Scientific) mass spectrometer. Reactions were monitored by thin-layer chromatography (TLC) on Merck 60 F254 (0.25 mm) plates, visualized by staining with 5% H_2SO_4 in EtOH and heating. Organic phases were dried with Na_2SO4 before evaporation. Chemical reagents and solvents were purchased from Sigma-Aldrich, TCI Europe or Fluorchem and were used without further purification unless stated otherwise. Petroleum ether with boiling point of 40–60 °C was used. Silica gel 60 (70–230 mesh) was used for gravity column chromatography (GCC).

GENERAL PROCEDURE FOR MANGANESE CATALYZED OXIDATION-AMINATION-OXIDATION: to a stirred solution of cannabinoid (1 eq) in CH_2Cl_2 (20mL/ 1 mmol substrate) under air or nitrogen atmosphere (see Table 1), manganese (III) acetate (0,1-1 eq, see Table 1) was added. Amine (5 eq) was then added dropwise. The stirred

solution was left in the dark at room temperature for 12-96 hours, then diluted with acidic solution (see Table 1) and extracted with CH_2Cl_2. The mixed organic phases were dried with Na_2SO_4, filtered and the solvent evaporated. The residue was filtered on silica gel using CH_2Cl_2 as eluent and was identified as aminoquinone, slightly impure (OPTIONAL, see Table 1). The latter was purified by chromatography over silica gel to afford the final aminocannabinoquinoid. All reactions were performed on 50 mg scale.

Isolated aminocannabinoquinoid showed identical properties to those reported in literature (Patent n. WO2015/158381 A1, 2015) (Patent n. WO 2015/128200 A1, 2015).

3.4.5 REFERENCES

Appendino, G., Bellido Cabello De Alba, M., & Munoz Blanco, E. (2015). Brevetto n. WO 2015/128200 A1.

Appendino, G., Bellido Cabello De Alba, M., & Munoz Blanco, E. (2015). Brevetto n. WO2015/158381 A1.

Del Río, C., & al. (2016). The cannabinoid quinol VCE-004.8 alleviates bleomycin-induced scleroderma and exerts potent antifibrotic effects through peroxisome proliferator. Scientific Reports, 6(1), 1-14.

Díaz-Alonso, J., & al. (2016). VCE-003.2, a novel cannabigerol derivative, enhances neuronal progenitor cell survival and alleviates symptomatology in murine models of Huntington's disease. Scientific reports, 6, 1-15.

Kogan, N. M., & al. (2007). Mol Cancer Ther, 6, 173-183.

Kogan, N. M., Rabinowitz, R., Levi, P., Gibson, D., Sandor, P., Schlesinger, M., & Mechoulam, R. (2004). J. Med. Chem., 47, 3800-3806.

Mechoulam, R., & Ben-Zvi, Z. (1968). Tetrahedron, 24, 5615-5624.

Wu, H. Y., & Jan, T. R. (2010). Cannabidiol hydroxyquinone-induced apoptosis of splenocytes is mediated predominantly by thiol depletion. Toxicol Lett, 195, 68–74.

Yu, W., & al. (2018). A Catalytic Oxidative Quinone Heterofunctionalization Method – Synthesis of Strongylophorine-26. Angewandte.

CHAPTER 4

STRUCTURE-ACTIVITY RELATIONSHIPS OF PHYTOCANNABINOIDS

The second topic of this PhD thesis was to investigate the structure-activity relationship of two cannabinoid chemotypes that had shown an interesting chemical behaviour in their oxidation to quinoid structures.

These compounds were all obtained by total synthesis, and the modification investigated where mainly focused on the terpenyl tail and the alkyl chain — since it is proven that changes on these moieties can dramatically modify the biological profile (Table 1) — and partially on the resorcinyl core. The alkyl chain was varied in terms of length and branching, the terpenyl moiety in terms of deprenylation or prenylogation, and the resorcinyl core oxidized to quinoid forms, using the protocol developed for the first part of the work.

ORIGINAL PRECURSOR	MODIFIED ANALOG	EFFECT
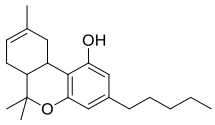 Δ⁸-THC	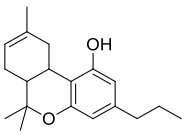 Δ⁸-THC orcinoid analog	**Reduced potency** by 75% and change of activity (from agonism to **antagonism** with Ki values of 75.4 and 62.8 nm)
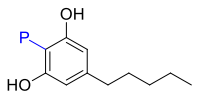 C-5 analog	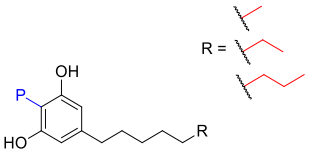 C-6/C-7/C-8 analogues	Systematic **increase** in **affinity** (with Ki values ranging from 41 to 8.5 nm) and **potency**
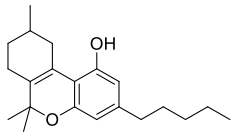 Δ⁶ᵃ⁻¹⁰ᵃ-THC	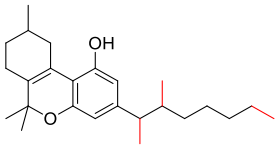 1',2'-DMH analog of Δ⁶ᵃ⁻¹⁰ᵃ-THC	**Increased potency** (by ca. 500-fold)
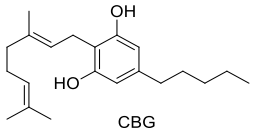 CBG	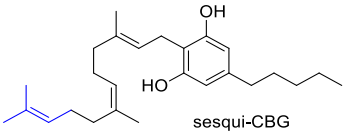 sesqui-CBG	**Increased potency** toward CB_2 (by ca. 5-fold) and **decreased affinity** for TRPM8

TABLE 2 **EXAMPLES REPORTED IN LITERATURE OF MODULATIONS ON ISOPRENYL AND ALKYL MOIETIES.** *SOURCE: (RAZDAN, 1986) (MARTIN & AL., 1999) (THOMAS & AL., 2005) (ADAMS & AL. 1948A, 1948B) (POLLASTRO & AL., 2011)*

REFERENCES

Adams, R., & al. (1948a). Tetrahydrocannabinol homologs. XVII, 70. *J am Chem Soc, 70*, 662-664.

Adams, R., & al. (1948). Tetrahydrocannabinol homologs with doubly branched alkyl groups in the 3-position. XVIII, . *J Am Chem Soc, 70*, 664-668.

Martin, R., & al. (1999). *J. Pharmacol. Exp. Ther., 290*, 1065.

Pollastro, F., & al. (2011). Bioactive Prenylogous Cannabinoid from Fiber Hemp (cannabis sativa). *Journal of Natural Products, 74*, 2019-2022.

Razdan, R., & al. (1986). *Pharmacol. Rev., 38*, 75.

Thomas, A., & al. (2005). *Br. J. Pharmacol., 146*, 917.

SUBCHAPTER 4.1

CANNABICHROMENOIDS

(UNPUBLISHED DATA)

4.1.1 INTRODUCTION

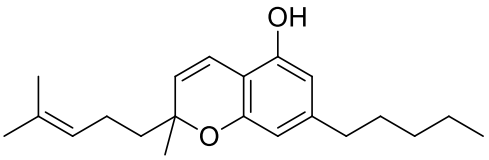

1

CBC

FIGURE 1 **STRUCTURE OF CBC.**

CBC (**1)** is the most hidden and enigmatic phytocannabinoid among the so called "big four". (Figure 1)

Isolated for the first time in 1966 and 2 years before its acidic precursor (Gaoni & Mechoulam, 1966), its concentration in *Cannabis* is much lower compared to the other major cannabinoids, rarely exceeding 0.2-0.3% on dry weight basis, and has never been found to accumulate in modern medicinal and recreational strains of *Cannabis* at the levels typical of the other phytocannabinoids (Hanuš & al., 2016).

The literature around this product is odd and bizarre, as exemplified by some curious feature like its physical properties: his aspect range between crystalline and initially optically active compound (Claussen & al., 1966) to a gummy and oily aspect (Mazzoccanti & al., 2017), and unlike the other *Cannabis* major compounds it has been demonstrated to be scalemic in natural sources, as shown by chromatography on chiral stationary phases (Mazzoccanti & al., 2017). Another curious feature is its high stability throughout decades: samples of non-degraded CBC have been found in 140 years old ethanolic extract (Harvey, 1985).

CBC was wrongly considered the most abundant natural cannabinoid after Δ^9-THC — due to low level chromatographic technologies available in 1960s-1970s (Turner & al., 1975) — its activity on CB receptors was immediately tested: no intoxicating

effects were detected *in vivo* and a weak activity on CB_1 and CB_2 was registered, suggesting that the development of a partial *tetrad response* (analgesia, catalepsy, hypothermia, hypomotility) at high concentrations was ascribed to other targets interaction (Davis & Hatoum, 1983) (DeLong & al., 2010) (Cascio & Pertwee, 2014) (De Petrocellis & al., 2011).

Nevertheless, spurred by the CBC ability to induce a weak anti-inflammatory, and antinociceptive action — which can be partly credited to CBC activity on endocannabinoid tone (De Petrocellis & al., 2011) – and to strengthen Δ^9-THC activity *in vivo* assays, an Australian research group has recently demonstrated the agonism of CBC towards CB_2 receptors (Udoh & al., 2019).

Within phytocannabinoids, CBC is the most potent TRPA1 non-covalent agonist (De Petrocelli & al., 2008). Most activators of TRPA1 are *electrophilic compounds* like allylisothiocyanate and cinnamaldehyde. These compounds covalently interact with nucleophilic residues (cysteine and lysine) in the cytoplasmatic *N*-terminal region. It is still unclear how *non-electrophilic modulators* like *propofol* and *lidocaine* modulate the activity of this channel (Nilius & al., 2012).

Apart from CBD whose behaviour deviates from this evidence, the other phytocannabinoids tested seem to follow this rule.

From a pharmacological point of view, CBC has shown activity in animal models of several diseases:

- murine colitis induced by *dinitrobenzensulfonic acid* (DNBS) (Romano & al., 2012);
- inflammation-induced intestinal hypermotility (Izzo & al., 2012);
- carrageenan-induced rat paw edema (Turner & Elsohly, 1981);
- acne (Olàh & al., 2016).

Remarkably, compounds related to CBC have also been isolated from non-*cannabis* sources, like plants from the Rhododendron genus, various liverworts, the fungus *Cylindrocarpon olidum* Wollenw., that produces the chromenoids **2a** and **2b**, (Quaghebeur & al., 1994), and the mushroom *Albatreluss* spp. with *confluetin* (**3**) (Hellwig & al., 2003). (Figure 2)

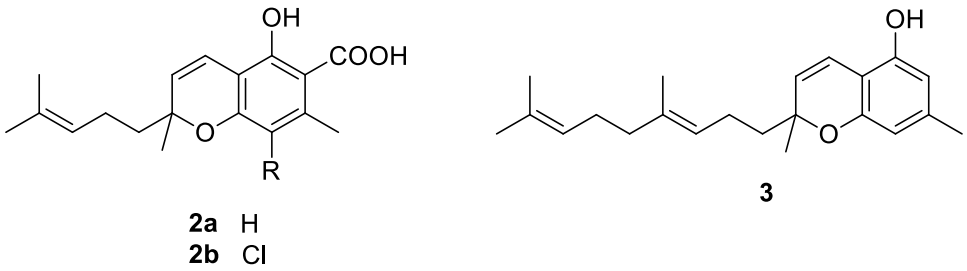

FIGURE 2 **STRUCTURES OF FUNGI-DERIVED CBC-LIKE PHYTOCANNABINOIDS.**

The structure of naturally occurring cannabinochromenoids is strictly related to the modular scheme of their biosynthesis, expressed by the prenylation or deprenylation of different isoprenyl residues and/or shortening of the pentyl residue. The differentiation grade in natural cannabichromenoids is the outcome of the combination of a different iteration of the isoprenoid pathway elongation step — that generates the electrophilic isoprenylating agent— and of the nature of the polyketide starter that generates the alkyl-substituent of the resorcinyl core. Replacement by a phenethyl-type group as well as isomerization to the abnormal series have also been reported, with alkyl residues typical of *Cannabis* and higher plants (Type A) and phenethyl analogues mostly found in liverworts (Type B) (Hanuš & al., 2016). Alterations of the benzochromene portion are rare, involving hydration of the pyrane double bond as well as functionalization of the "peri-position" by chlorination or acetoxylation, and oxidative modification of the isoprenoid group at the terminal and electron-rich double bond.

All cannabinochromenoids are — like the other phytocannabinoids — generated as their acidic form and next decarboxylated by the action of enzymes or during storage of the plant crude material (Hanuš & al., 2016). (Figure 3)

CBC is the only phytocannabinoid from *Cannabis* easily achievable by total synthesis, and this partially offsets its very low isolation yield form plant material; moreover, unlike other phytocannabinoids, it is racemic or highly scalemic: so, an enantioselective synthesis is not required. Its classic preparation involves a *tandem Knoevenagel reaction* between citral **4** and olivetol **5** using an amine catalyst, generating the *quinone methide intermediate* **6** that undergoes an electrocyclization to CBC (Crombie & Ponsford, 1968) (Crombie & Ponsford, 1971).

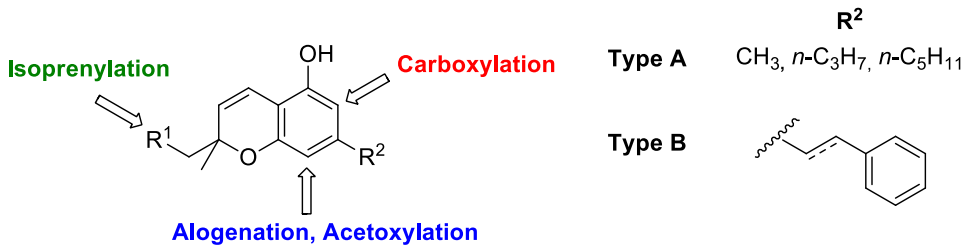

FIGURE 3 **DIVERSITY OF NATURALLY OCCURRING CANNABICHROMENOIDS.**

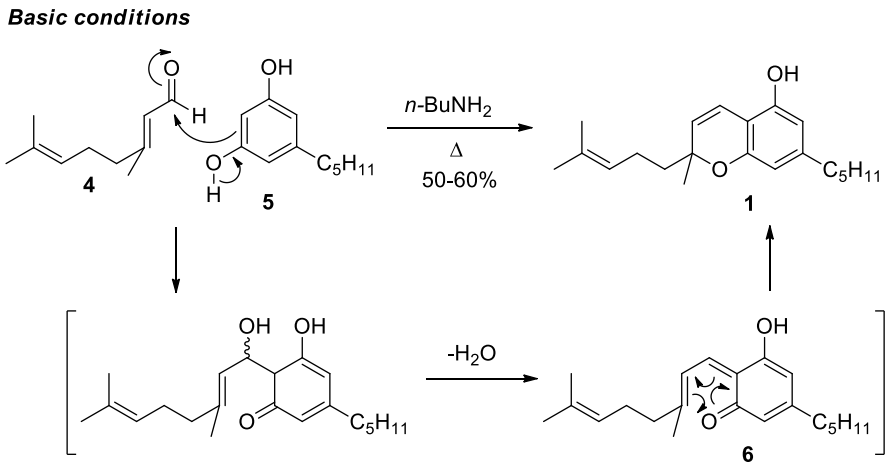

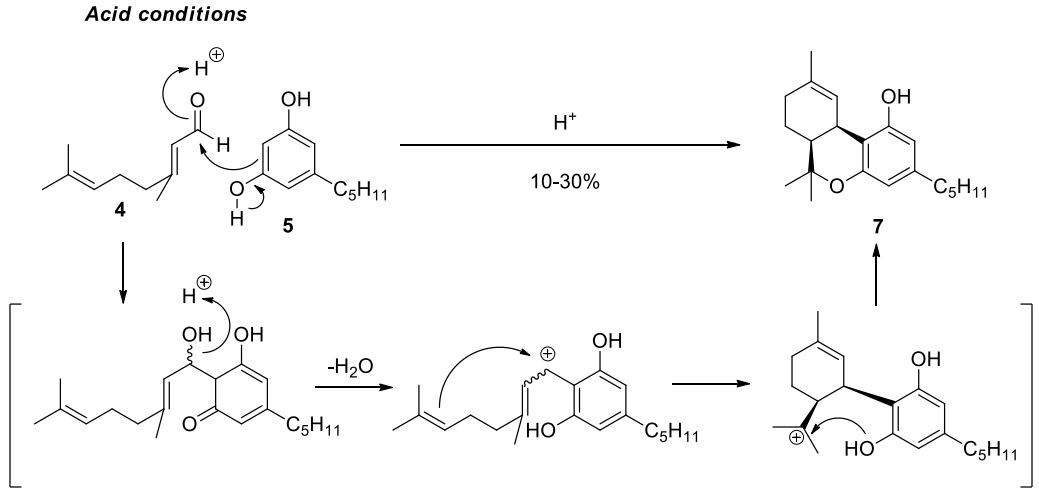

FIGURE 4 **REACTION OF CITRAL (4) AND OLIVETOL (5) AFFORDS DIFFERENT COMPOUNDS DEPENDING ON THE ACIDITY OF THE ENVIRONMENT.**

Curiously, the same starting materials treated in acidic media give completely different results, with the major product *cis*-Δ^9-THC **7** as the result of a terpenic-type intramolecular cationic cyclization (Kane & al., 1968). (Figure 4)

4.1.2 RESULTS AND DISCUSSION

A small library of cannabichromene analogues was synthesized, focusing on the functionalization of three different main moieties (Figure 5):

1. Isoprenylation-Deprenylation of the terpenyl tail (*red*)
2. Shortening, elongation or ramification of the ketide chain (*green*)
3. Modification of the aromatic core (*blue*) by:
    - Substitution of the benzene with a heterocycle
    - Oxidation to cannabinoquinoid
    - Methylation in position 2

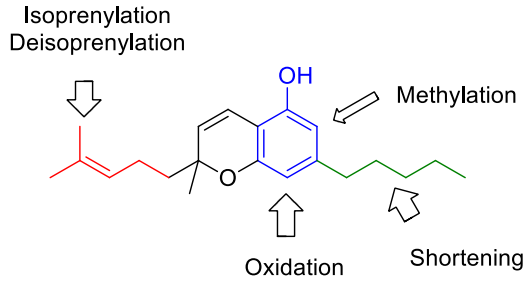

FIGURE 5 **SITES OF MODIFICATION OF CBC STRUCTURE.**

Most of the derivatives were obtained by condensation of different 1,3-aryldiols (1.04 mol) with several aliphatic aldehydes (1 mol) in the presence of butylamine (1 mol); the reaction was carried out in refluxing toluene for 10 hours. (Figure 6)

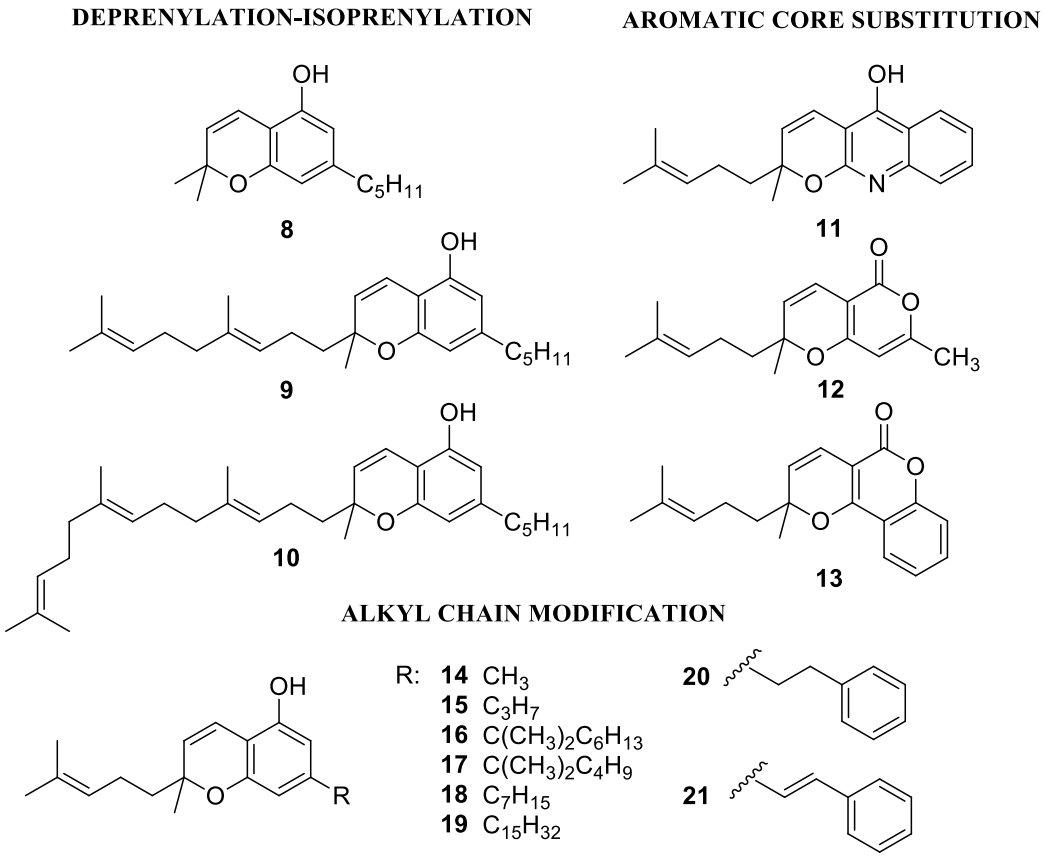

FIGURE 6 **FIRST PART OF CBC ANALOGUES.**

Sometimes, in order to facilitate the purification process (see experimental), the raw reaction mixture, after acidic work-up, drying and dissolving in ethanol, was further treated with sodium boron hydride (100mg/g substrate) to reduce aldehydes residues to the corresponding alcohol. Several chromenes have *Rf* extremely like the starting aldehydes, a factor that prevents their correct purification at chromatographic level; their reduction to alcohol considerably increases their polarity allowing a simple purification by chromatography. The coumarin derivative **13** (*deprenylferprenin*) was synthesized according to literature using Ytterbium (III) triflate.

While senecialdehyde, citral and farnesal — the aldehydes used for the synthesis of compounds **8**, **1**, and **9,** respectively — are commercially available, *geranylgeranial* **23**, used for the synthesis of compound **10** was obtained by oxidation of *geranylgeraniol* **22** obtained by extraction from *Bixa Orellana* L. dry seeds (see experimental).

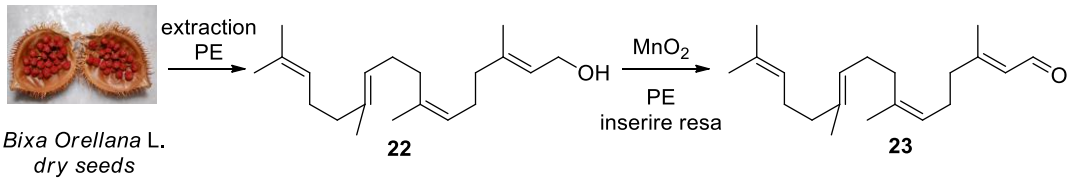

FIGURE 7 **EXTRACTION AND SYNTHESIS OF ALDEHYDE 23**.

The introduction of methyl groups is one of the most powerful maneuver to increase the biological activities of a molecule by altering its solubility, binding affinity and metabolism (Belshaw & al., 1995) (Barreiro & al., 2011) (Schönherr & Cernak, 2013) (Cernak & al., 2016).

In the cannabinoid chemical space, the introduction of a methyl in position 2 could have major effects on the PK of the molecule, providing a benzylic proton for metabolization alternative to the allylic methyl. The synthesis of *2-methyl CBC* **26** was performed as a late-stage functionalization by reaction of CBC itself with the

Mannich reagent obtained by formaldehyde **24** and morpholine **25**, in refluxing ethanol and then reduction by sodium cyanoborohydride in *n*-butanol. Since CBC is non-symmetrical, methylation could occur in two different positions (2 and 6), and the regiochemistry of alkylation was confirmed by derivatization: methylation of **26** with *trimethylsylildiazomethane* in methanol gave compound **27**, that shows a NOE correlation between the -OCH_3 group and the 2-methyl portion. The *2-formyl* derivative of CBC **28** was obtained by Vilsmeier-Haack reaction: this compound reminds the structure of the acidic form CBCA, but the different level of oxidation prevents its decarboxylation. (Figure 8)

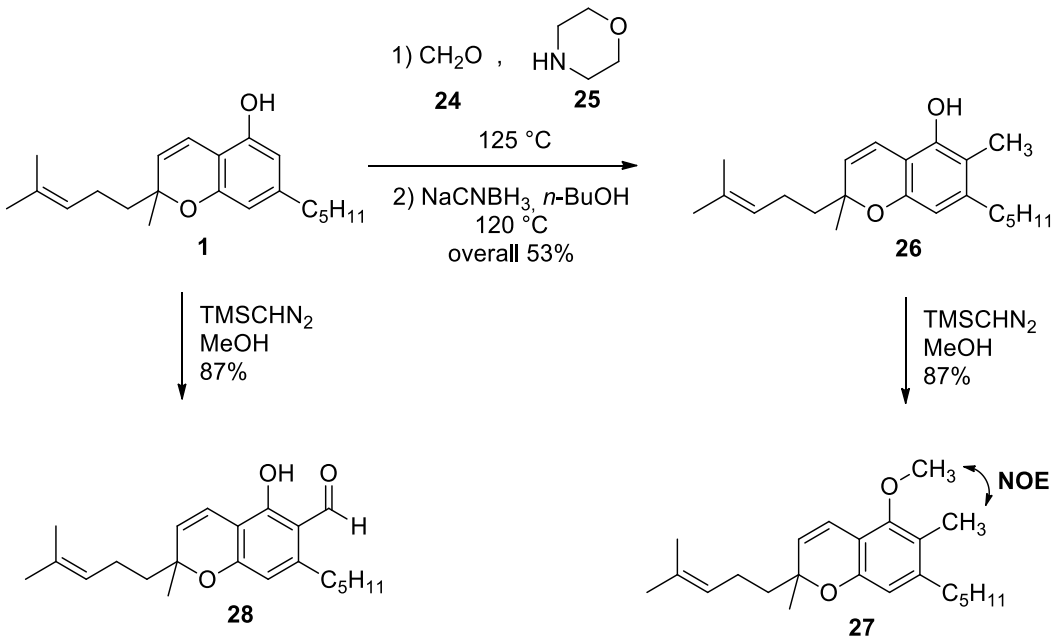

FIGURE 8 **SYNTHESIS OF 2-ALKYL DERIVATIVES OF CBC.**

As last modification, a selection of CBC derivatives were oxidated to their corresponding *cannabinoquinoids* (**29**-**35**, Figure 9) by oxidation with SIBX in EtOAc;

as already saw in Chapter 3, quinoid forms of cannabinoids shows a distinct profile of activity from their resorcinyl precursors.

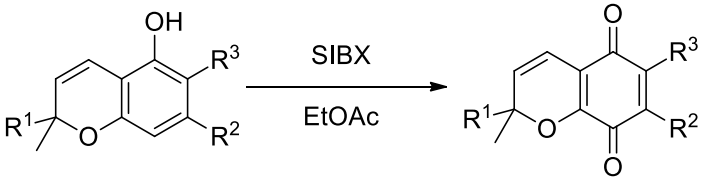

	R^1	R^2	R^3
29	CH_3	C_5H_{11}	H
30	Prenyl	C_5H_{11}	H
31	Geranyl	C_5H_{11}	H
32	Farnesyl	C_5H_{11}	H
33	Prenyl	C_3H_{11}	H
34	Prenyl	$C(CH_3)_2C_6H_{13}$	H
35	Prenyl	C_5H_{11}	CH_3

FIGURE 9 **OXIDATION WITH SIBX OF A CHROMENES SELECTION, LEADING TO THE CORRESPONDING CANNABINOQUINOIDS.**

The biological activity of all compounds is currently ongoing on cannabinoid receptors and on a selection of thermo-TRPs (TRPV1, V3, V4, A1, M8), and has been completed on PPAR-γ, where some docking experiments have also been carried out. Due to the unfinished status of their activities, their discussion seems premature.

4.1.3 EXPERIMENTAL SECTION

GENERAL EXPERIMENTAL PROCEDURES: IR spectra were recorded on an Avatar 370 FT-IR Techno-Nicolet apparatus. ^1H (400 MHz) and ^{13}C (100 MHz) NMR spectra were measured on Bruker Avance 400 MHz spectrometer. Chemical shifts were referenced to the residual solvent signal ($CDCl_3$: δH = 7.21, δC = 77.0). Homonuclear ^1H connectivities were determined by the Correlation spectroscopy (COSY) experiment. One-bond heteronuclear ^1H–^{13}C connectivities were determined with the heteronuclear single quantum coherence (HSQC) spectroscopy experiment. Two-

and three-bond $^{1}H–^{13}C$ connectivities were determined by gradient two-dimensional (2D) heteronuclear multiple bond correlation (HMBC) experiments optimized for a $^{2,3}J$ = 9 Hz. Low- and high-resolution electrospray ionization mass spectrometry (ESI-MS) data were determined on an LTQ OrbitrapXL (Thermo Scientific) mass spectrometer. Reactions were monitored by thin-layer chromatography (TLC) on Merck 60 F254 (0.25 mm) plates, visualized by staining with 5% H_2SO_4 in EtOH and heating. Organic phases were dried with Na_2SO4 before evaporation. Chemical reagents and solvents were purchased from Sigma-Aldrich, TCI Europe or Fluorchem and were used without further purification unless stated otherwise. Petroleum ether with boiling point of 40–60 °C was used. Silica gel 60 (70–230 mesh) was used for gravity column chromatography (GCC). *Bixa Orellana* L. dry seeds were purchased by A. Minardi & figli (Bagnacavallo – RA).

GENERAL PROCEDURE FOR CHROMENES SYNTHESIS. CBC AS EXAMPLE: to a stirred solution of olivetol (1 g, 5.55 mmol, 1.04 eq) in dry toluene (30 mL), citral (0.914 mL, 5.33 mmol, 1 eq) and *n*-butylamine (0.527 mL, 5.335 mmol, 1 eq) were sequentially added. The reaction was heated to reflux for 10 hours, then quenched with H_2SO_4 2M and extracted with EtOAc. The combined organic phases were washed with BRINE and dried. The crude was dissolved in ethanol (10 mL) then sodium borohydride (100 mg, 100 mg/g substrate) was added; the solution was stirred for 15 minutes, then quenched with H_2SO_4 2M and extracted with EtOAc. The combined organic phases were washed with BRINE and dried. The crude was purified by chromatography on silica gel (PE/EtOAc 95:5, *Rf*: 0.85) to afford 896 mg of brown oil (50%), identified as CBC (**1**).

CBC (1): ^{1}H NMR (400 MHz, $CDCl_3$): δ 6.62 (d, *J* = 10.0 Hz, 1H), 6.25 (s, 1H), 6.12 (s, 1H), 5.49 (d, *J* = 10.0 Hz, 1H), 5.10 (t, *J* = 7.4 Hz, 1H), 2.43 (t, *J* = 7.8 Hz, 2H), 2.22 – 1.96

(m, 2H), 1.66 (s, 3H), 1.58 (s, 3H), 1.38 (s, 3H), 1.36 – 1.22 (m, 8H), 0.88 (t, *J* = 6.3 Hz, 3H).

DEPRENYL-CBC (8): Yellow oil (*Rf*: 0.65 in PE/EtOAc 9:1), 46%. ^{1}H NMR (400 MHz, $CDCl_3$): δ 6.58 (d, *J* = 9.9 Hz, 1H), 6.26 (s, 1H), 6.13 (s, 1H), 5.53 (d, *J* = 9.9 Hz, 1H), 2.44 (t, *J* = 7.7 Hz, 2H), 1.71 – 1.51 (m, 2H), 1.42 (s, 6H), 1.35 – 1.20 (m, 4H), 0.88 (t, *J* = 6.6 Hz, 3H).

PRENYL-CBC (9): Brown oil (*Rf*: 0.60 in PE/EtOAc 9:1), 57%.^{1}H NMR (400 MHz, $CDCl_3$): δ 6.67 (d, *J* = 10.0 Hz, 1H), 6.29 (s, 1H), 6.14 (s, 1H), 5.53 (d, *J* = 10.0 Hz, 1H), 5.14 (m, 2H), 2.46 (t, *J* = 7.6 Hz, 2H), 2.20-2.03 (m, 4H), 2.02-1.95 (m, 2H), 1.81 – 1.66 (m, 5H), 1.64-1.54 (m, 8H), 1.42 (s, 3H), 1.37 – 1.27 (m, 4H), 0.91 (t, *J* = 6.8 Hz, 3H).

BISPRENYL-CBC (10): Brown oil (*Rf*: 0.58 in PE/EtOAc 8:2), 44%. ^{1}H NMR (400 MHz, $CDCl_3$): δ 6.67 (d, *J* = 10.0 Hz, 1H), 6.30 (s, 1H), 6.15 (s, 1H), 5.54 (d, *J* = 10.0 Hz, 1H), 5.15 (m, 3H), 2.47 (t, *J* = 7.9 Hz, 2H), 2.20-1.99 (m, 10H), 1.82–1.55 (m, 15H), 1.42 (s, 3H), 1.39–1.28 (m, 4H), 0,92 (t, *J* = 6.9 Hz, 3H).

2-METHYL-2-(4-METHYLPENT-3-EN-1-YL)-2H-PYRANO[2,3B]QUINOLIN-5-OL (11): Brown oil (*Rf*: 0.25 in PE/EtOAc 9:1), 43%. ^{1}H NMR (400 MHz, $CDCl_3$): δ 7.88 (d, *J* = 8.1 Hz, 1H), 7.55 – 7.43 (m, 1H), 7.42 – 7.13 (m, 2H), 6.78 (d, *J* = 9.9 Hz, 1H), 5.50 (d, *J* = 9.9 Hz, 1H), 5.10 (t, *J* = 9.1 Hz, 1H), 2.14 (m, 2H), 2.04 (s, 1H), 1.91 – 1.68 (m, 2H), 1.62 (s, 3H), 1.55 (s, 3H), 1.50 (s, 3H).

2,7-DIMETHYL-2-(4-METHYLPENT-3-EN-1-YL)-2H-5H-PYRANO[4,3-B]PYRAN-5(2H)-ONE (12): Orange Oil (*Rf*: 0.2 in PE/EtOAc 95:5), 38%. ^{1}H NMR (400 MHz, $CDCl_3$): δ 6.42 (d, *J* = 10.1 Hz, 1H), 5.76 (s, 1H), 5.30 (d, *J* = 10.1 Hz, 1H), 5.06 (t, *J* = 8.6 Hz, 1H), 2.20 (s, 3H), 2.13 – 1.90 (m, 2H), 1.93 – 1.68 (m, 2H), 1.66 (s, 3H), 1.57 (s, 3H), 1.40 (s, 3H).

CANNABIORCICHROMENE (CBCO, 14): Brown oil (*Rf*: 0.35 in PE/CH_2Cl_2 6:4). 22%. ^{1}H NMR (400 MHz, $CDCl_3$): δ 6.61 (d, *J* = 10.0 Hz, 1H), 6.23 (s, 1H), 6.11 (s, 1H), 5.49 (d, *J* = 10.0 Hz, 1H), 5.09 (t, *J* = 7.1 Hz, 1H), 2.13 – 1.97 (m, 2H), 2.05 (s, 3H), 1.75 – 1.63 (m, 2H), 1.66 (s, 3H), 1.57 (s, 3H), 1.37 (s, 3H).

CANNABIVARINOCHROMENE (CBCV, 15): Brown Oil (*Rf*: 0.9 in Pe/EtOAc 9:1), 33%. ^{1}H NMR (400 MHz, $CDCl_3$): δ 6.61 (d, *J* = 10.0 Hz, 1H), 6.24 (s, 1H), 6.12 (s, 1H), 5.49 (d, *J* = 10.0 Hz, 1H), 5.09 (t, *J* = 5.6, 1H), 2.42 (t, *J* = 7.9 Hz, 2H), 2.18 – 2.05 (m, 2H), 1.65 (s, 3H), 1.57 (s, 3H), 1.72 – 1.48 (m, 4H), 1.37 (s, 3H), 0.91 (t, *J* = 7.3 Hz, 3H).

DIMETHYLHEPTYLCANNABICHROMENE (DMH-CBC, 16): Brown oil (*Rf*: 0.40 in PE/EtOAc 9:1), 40%. ^{1}H NMR (400 MHz, $CDCl_3$): δ 6.61 (d, *J* = 10.0 Hz, 1H), 6.39 (s, 1H), 6.25 (s, 1H), 5.51 (d, *J* = 10.0 Hz, 1H), 5.09 (t, *J* = 7.4 Hz, 1H), 2.32 – 2.02 (m, 2H), 1.76 – 1.62 (m, 2H), 1.65 (s, 3H), 1.57 (s, 3H), 1.55 – 1.44 (m, 2H), 1.39 (s, 3H), 1.31 – 1.12 (m, 6H), 1.19 (s, 6H), 1.11 – 0.99 (m, 2H), 0.94 – 0.60 (m, 3H).

DIMETHYLPENTYLCANNABICHROMENE (DMP-CBC, 17): Brown oil (*Rf*: 0.9 in PE/EtOAc 7:3, 57%). ^{1}H NMR (400 MHz, $CDCl_3$): δ 6.67 (d, *J* = 10.0 Hz, 1H), 6.42 (s, 1H), 6.31 (s, 1H), 5.52 (d, *J* = 10.0 Hz, 1H), 5.13 (t, *J* = 7.2 Hz, 1H), 2.18 – 2.12 (m, 2H), 1.80 – 1.55 (m, 2H), 1.69 (s, 3H), 1.60 (s, 3H), 1.54 – 1.50 (m, 2H), 1.25 – 1.17 (m, 2H), 1.22 (s, 6H), 1.11 – 1.03 (m, 2H), 0.87 – 0.83 (t, J = 7.4 Hz, 3H).

7-HEPTYL-2-METHYL-2-(4-METHYLPENT-3-EN-1-YL)-2H-CHROMEN-5-OL (18): Brown oil (*Rf*: 0.4 in PE/EtOAc 7:3, 52%). ^{1}H NMR (400 MHz, $CDCl_3$): δ 6.65 (d, *J* = 10.0 Hz, 1H), 6.27 (s, 1H), 6.16 (s, 1H), 5.51 (d, *J* = 10.0 Hz, 1H), 5.12 (t, *J* =5.7 Hz, 1H), 2.46 (t, *J* = 7.8 Hz, 2H), 2.18 – 2.06 (m, 2H), 1.82-1.54 (m, 13H), 1.41 (s, 3H), 1.38 – 1.23 (m, 13H), 0.90 (t, *J* = 6.4 Hz, 3H).

2-METHYL-2-(4-METHYLPENT-3-EN-1-YL)-7-PENTADECYL-2H-CHROMEN-5-OL (19): Brown oil (*Rf*: 0.67 in PE/EtOAc 95:5, 50%). ^{1}H NMR (400 MHz, $CDCl_3$): δ 6.61 (d, *J* =

10.0 Hz, 1H), 6.25 (s, 1H), 6.11 (s, 1H), 5.49 (d, *J* = 10.0 Hz, 1H), 5.09 (t, *J* = 7.6 Hz, 1H), 2.43 (t, *J* = 7.7 Hz, 2H), 2.09-2.02 (m, 2H), 1.66 (s, 3H), 1.58 (s, 3H), 1.38 (s, 3H), 1.34-1.20 (m, 28H), 0.88 (t, *J* = 6.8 Hz, 3H).

2-METHYL-2-(4-METHYLPENT-3-EN-1-YL)-7-PHENETHYL-2H-CHROMEN-5-OL (20): Brown Oil (*Rf*: 0.9 in PE/EtOAc 9:1), 40%. ^{1}H NMR (400 MHz, $CDCl_3$): δ 7.51 – 7.03 (m, 5H), 6.61 (d, *J* = 10.0 Hz, 1H), 6.29 (s, 1H), 6.11 (s, 1H), 5.51 (d, *J* = 10.2 Hz, 1H), 5.10 (t, *J* = 9.0 Hz, 1H), 3.13 – 2.63 (m, 4H), 2.10 (m, 2H), 1.78 – 1.70 (m, 2H) 1.66 (s, 3H), 1.57 (s, 3H), 1.38 (s, 3H).

(E)-2-METHYL-2-(4-METHYLPENT-3-EN-1-YL)-7-STYRYL-2H-CHROMEN-5-OL (21): Yellow oil (*Rf*: 0.25 in PE/EtOAc 9:1), 33%. ^{1}H NMR (400 MHz, $CDCl_3$): δ 7.47 (d, *J* = 7.5 Hz, 2H), 7.34 (t, *J* = 7.5 Hz, 3H), 7.03 (d, *J* = 16.2 Hz, 1H), 6.91 (d, *J* = 16.2 Hz, 1H), 6.65 (d, *J* = 10.0 Hz, 1H), 6.62 (s, 1H), 6.45 (s, 1H), 5.56 (d, *J* = 10.0 Hz, 1H), 5.11 (t, *J* = 9.2 Hz, 1H), 2.12 (m, 2H), 1.80 – 1.63 (m, 2H), 1.66 (s, 3H), 1.59 (s, 3H), 1.40 (s, 3H).

YTTERBIUM (III) TRIFLATE CATALYZED CHROMENILATION. SYNTHESIS OF FERPRENINE (13): to a stirred solution of 4-hydroxycoumarin (1g, 6.17 mmol, 2 eq) in methanol (30 mL), citral (530 mL, 3.09 mmol, 1eq) and a catalytic amount of Ytterbium (III) Triflate were added. The reaction was stirred overnight at room temeprature, then quenched with Na_2CO_3 s.s. and extracted with EtOAc. The combined organic phases were washed with BRINE and dryed. The crude was dissolved in ethanol (10 mL) then sodium borohydride (100 mg, 100 mg/g substrate) was added; the solution was stirred for 15 minutes, then quenched with H_2SO_4 2M and extracted with EtOAc. The combined organic phases were washed with BRINE and dryed. The crude was purified by chromatography on silica gel (PE/EtOAc 95:5, *Rf*: 0.45) to afford 668 mg of brown oil (73%), identified as ferprenine (**13**).

FERPRENINE (13): ^{1}H NMR (400 MHz, $CDCl_3$): δ 7.78 (d, *J* = 7.9, I H), 7.51 (t, *J* = 7.6, 1 H), 7.30-7.24 (m, 2 H), 6.57 (d, *J* = 10.1, 1 H), 5.46 (d, *J* = 10.1, 1 H), 5.08 (t, *J* = 6.5, 1H), 2.14-1.67 (m, 4 H), 1.60 (s, 3H), 1.54 (s, 3H), 1.51 (s, 3H).

EXTRACTION OF GERANYL GERANIOL (22) FROM BIXA SEEDS: 100g of *Bixa Orellana* L. dry seeds were suspended in 500 mL of petroleum ether 40-60 °C. The suspension was let in extraction for 3 days, then filtered over filter paper (particle retention: 40 μM). After solvent evaporation, an oily red residue was obtained: the latter was purified by chromatography on silica gel (PE/EtOAc 95:5, *Rf*: 0.42) to afford 588 mg of yellow oil identified as geranyl geraniol (**22**, 0.30 %). ^{1}H NMR (400 MHz, $CDCl_3$): δ 1.60 (m, 9 H), 1.69 (m, 6 H), 1.91-2.15 (m, 13 H), 4.15 (d, *J* = 6.6 Hz, 2 H), 5.08-5.14 (m, 3 H), 5.41 (t, *J* = 6.6 Hz, 1 H)

SYNTHESIS OF GERANYL GERANIAL (23). OXIDATION OF 22: to a stirred solution of **22** (560 mg, 1.76 mmol, 1 eq) in petroleum ether (30 mL), potassium carbonate (122 mg, 0.880 mmol, 0.5 eq), manganese (II) oxide (5 g, 1 g/100 mg substrate) was added. The suspension was stirred for 1 hour until complete consumption of the starting material (controlled by TLC), then filtered over a celite pad. After solvent evaporation, the crude was purified by chromatography on silica gel (PE/EtOAc 9:1, *Rf*: 0.82) to afford 220 mg of yellow oil identified as geranyl geranial **23** (40 %). ^{1}H NMR (400 MHz $CDCl_3$): δ 1.62 (s, 12 H), 1.70 (s, 3 H), 1.91-2.12 (m, 13 H), 2.19 (s, 3H), 2.24 (m, 3H), 5.10-5.12 (m, 3 H), 5.92 (d, *J* = 9.2 Hz, 1H), 10.1 (d, *J* = 8.2 Hz, 1H).

SYNTHESIS OF 2-METHYL-CBC (26): morpholine (142 μL, 1.636 mmol, 1 equiv.) and paraformaldehyde (50 mg, 1.636 mmol., 1 equiv.) were heated for 2 hours at 120 °C, then CBC (200 mg; 1.64 mmol; 1 equiv.) was added. The resulting solution was stirred at 125 °C for 1 h monitoring the course by TLC. The reaction was worked up by dilution with BRINE and extraction with EtOAc. The organic phase was dryed and

the solvent evaporated. The residue was purified by column chromatography (PE/EtOAc 9:1 as eluant and 10 mL of silica gel as stationary phase) to give 180 mg of an amber oil. The latter was dissolved in *n*-butanol (4 mL), and sodium cyanoborohydride (26 mg, 0.411 mmol., 1 equiv.) was added under continuous stirring at room temperature. The mixture was heated to 120 °C for 1 h monitoring the course by TLC. The reaction was worked up by cooling to room temperature, dilution with brine and extraction with Et_2O. The organic phase was dryed and the solvent evaporated. The residue was purified by column chromatography (PE/EtOAc 98:2) to give an amber oil (120 mg, yield 53% over two steps) identified as **26** (*Rf*: 0.54 in PE/EtOAc 9:1).

^{1}H NMR (400 MHz, $CDCl_3$): δ 6.66 (d, *J* = 10.0 Hz, 1H), 6.31 (s, 1H), 5.54 (d, *J* = 10.0 Hz, 1H), 5.14 (t, *J* = 8.5 Hz, 1H), 2.53 (t, *J* = 7.4 Hz, 2H), 2.21 – 2.07 (m, 2H), 2.11 (s, 3H), 1.69 (s, 3H), 1.61 (s, 3H), 1.38 (s, 3H), 1.44 – 1.29 (m, 8H), 0.93 (t, *J* = 6.3 Hz, 3H).

METHYLATION OF 26 (27): to a solution of **26** (80 mg; 0.243 mmol.; 1 equiv.) dissolved in MeOH (2 mL), TMS-CHN_2 2.0 M in *n*-hexane (1.2 mL, 2.43 mmol, 10 equiv.) was added under continuous stirring at room temperature. The mixture was left for 24 h monitoring the course by TLC. The reaction was worked up by decomposition of the TMS-CHN_2 excess with AcOH, quenched with BRINE and extracted with EtOAc. The combined organic phases were dryed and the solvent evaporated. The residue was purified by column chromatography (PE/EtOAc 98:2) to give an amber oil (70 mg, yield 87%) identified as **27**.

^{1}H NMR (400 MHz, $CDCl_3$): δ 6.52 (d, *J* = 10.0 Hz, 1H), 6.36 (s, 1H), 5.45 (d, *J* = 10.0 Hz, 1H), 5.02 (t, *J* = 7.4 Hz, 1H), 3.63 (s, 3H), 2.45-2.37 (m, 2H), 2.05 (s, 3H), 1.59 (s, 3H), 1.50 (s, 3H), 1.30 (s, 3H), 1.29-1.21 (m, 8H), 0.83 t, *J* = 7.2 Hz, 3H). ^{13}C NMR (100

MHz, $CDCl_3$): δ 154.2, 151.5, 143.1, 131.6, 128.4, 124.2, 120.4, 117.9, 112.5, 112.2, 77.8, 61.3, 41.0, 33.7, 31.8, 29.8, 26.2, 25.6, 22.7, 22.5, 17.6, 14.0, 11.0.

FORMYLATION OF 1 (28): to a solution of DMF (246 μL, 3.18 mmol, 10 equiv.) in dry CH_2Cl_2 (6 mL), $POCl_3$ (267 μL, 2.86 mmol, 9 equiv.) was added under nitrogen and stirred at 0 °C for 30 min. A solution of **1** (100 mg, 0.318 mmol, 1 equiv.) in dry CH_2Cl_2 (4 mL) was then added dropwise at 0 °C. The reaction was then left 12 h at room temperature and the course monitored by TLC, then quenched with BRINE and extracted with EtOAc. The combined organic phases were dryed and the solvent evaporated. The residue was purified by column chromatography (PE/EtOAc 95:5) to give an amber oil (30 mg, yield 30%) identified as **28**.

^{1}H NMR ($CDCl_3$, 400 MHz): δ 10.02 (s, 1H), 6.69 (d, *J* = 10.1 Hz, 1H), 6.17 (s, 1H), 5.47 (d, *J* = 10.1 Hz, 1H), 5.08 (t, , *J* = 6.7 Hz, 1H), 2.77 (t, *J* = 7.9 Hz, 2H), 2.16-1.93 (m, 2H), 1.65 (s, 3H), 1.52 (s, 3H), 1.41 (s, 3H), 1.40 – 1.17 (m, 8H), 0.88 (t, *J* = 4.0 Hz, 3H).

SIBX OXIDATION OF CANNABINOCHROMENOIDS. REACTION WITH CBC (1) AS EXAMPLE: to a cooled (ice bath) solution of **1** (1 g, 3.18 mmol) in ethyl acetate (EtOAc, 15 mL), SIBX (4.46 g, 6.36 mmol, 2 equiv.) was added in small portions. The cooling bath was removed, and the suspension was stirred at room temperature for 18 h and then filtered over a celite pad. The filtration cake was washed with EtOAc (10 mL), and the pooled filtrates were washed with saturated $Na_2S_2O_3$ and next with BRINE. After the drying and evaporation, the residue was purified by GCC on silica gel (PE/EtOAc 9:1 as eluant) to afford 638 mg of CBCQ **30** as a red oil (59%).

^{1}H NMR ($CDCl_3$, 400 MHz): δ 6.47 (d, *J* = 9.9 Hz, 1H), 6.40 (bs, 1H), 5.56 (d, *J* = 9.9 Hz, 1H), 5.07 (t, *J* = 6.9 Hz, 1H), 2.39 (t, *J* = 7.6 Hz, 2H), 2.08 (m, 1H), 1.88 (m, 1H), 1.66 (overlapped, 2H), 1.64 (s, 3H), 1.55 (s, 3H), 1.49 (m, 2H), 1.46 (s, 3H), 1.32 (m, 4H), 0.89 (t, *J* = 6.7 Hz, 3H).

DEPRENYL-CBC QUINONE (29): Red oil (*Rf*: 0.55 in PE/CH_2Cl_2 8:2), 63%. ^{1}H NMR (400 MHz, $CDCl_3$): δ 6.44 (d, *J* = 10.0 Hz, 1H), 6.43 (s, 1H), 5.62 (d, *J* = 10.0 Hz, 1H), 2.42 (t, *J* = 8.3 Hz, 2H), 1.58 – 1.47 (m, 2H), 1.52 (s, 6H), 1.38 – 1.31 (m, 4H), 0.90 (t, *J* = 6.3 Hz, 3H).

PRENYL-CBC QUINONE (31): Red oil (*Rf*: 0.85 in PE/EtOAc 9:1), 43%. ^{1}H NMR (400 MHz, $CDCl_3$): δ 6.48 (d, *J* = 10.1 Hz, 1H), 6.42 (s, 1H), 5.57 (d, *J* = 10.1 Hz, 1H), 5.12-5.07 (m, 2H), 2.42 (t, *J* = 7.5 Hz, 2H), 2.15-1.88 (m, 6H), 1.74 – 1.22 (m, 20H), 0.91 (t, *J* = 6.7 Hz, 3H).

BISPRENYL-CBC QUINONE (32): Red oil (*Rf*: 0.48 in PE/EtOAc 95:5), 53%. ^{1}H NMR (400 MHz, $CDCl_3$): δ 6.48 (d, *J* = 10.0 Hz, 1H), 6.42 (s, 1H), 5.57 (d, *J* = 10.0 Hz, 1H), 5.15-5.06 (m, 3H), 2.42 (t, *J* = 7.96 Hz, 2H), 2.16-1.88 (m, 10H), 1.75–1.45 (m, 15H), 1.41–1.31 (m, 4H), 1.27 (s, 3H), 0,91 (t, *J* = 6.5 Hz, 3H)

CANNABIVIRIDOCHROMENE QUINONE (CBCVQ, 33): Red oil (*Rf*: 0.3 in PE/EtOAc 98:2), 42%. ^{1}H NMR (400 MHz, $CDCl_3$): δ 6.46 (d, *J* = 10.1 Hz, 1H), 6.40 (s, 1H), 5.55 (d, *J* = 10.1 Hz, 1H), 5.06 (t, *J* = 7.8 Hz, 1H), 2.37 (t, *J* = 8.2 Hz, 2H), 2.17 – 2.02 (m, 2H), 1.69 – 1.46 (m, 4H), 1.64 (s, 3H), 1.55 (s, 3H), 1.45 (s, 3H), 0.96 (t, *J* = 7.3 Hz, 3H).

DIMETHYLHEPTYLCANNABICHROMENE QUINONE (DMH-CBCQ, 34): Red oil (*Rf*: 0.45 in PE/EtOAc 9:1), 60%.^{1}H NMR (400 MHz, $CDCl_3$): δ 6.38 (d, *J* = 10.0 Hz, 1H), 6.33 (s, 1H), 5.47 (d, *J* = 10.0 Hz, 1H), 4.99 (t, *J* = 7.1 Hz, 1H), 2.05 – 1.99 (m, 2H), 1.66-1.44 (m, 10H), 1.40 (s, 3H), 1.22 – 1.07 (m, 6H), 1.15 (s, 6H), 1.02 – 0.92 (m, 2H), 0.78 (t, *J* = 6.9 Hz, 3H).

2-METHYL CBC QUINONE (35): Red oil (*Rf*: 0.45 in PE/CH_2Cl_2 8:2), 51%. ^{1}H NMR (400 MHz, $CDCl_3$): δ 6.52 (d, *J* = 10.1 Hz, 1H), 5.54 (d, *J* = 10.1 Hz, 1H), 5.09 (t, *J* = 8.4 Hz, 1H), 2.49 (t, *J* = 9.0 Hz, 2H), 2.13 – 2.02 (m, 2H), 2.04 (s, 3H), 1.67 (s, 3H), 1.58 (s, 3H), 1.47 (s, 3H), 1.43 – 1.26 (m, 8H), 0.89 (m, 3H).

4.1.4 REFERENCES

Barreiro, E., & al. (2011). The methylation effect in medicinal chemistry. Chem. Rev., 111, 5215–5246.

Belshaw, & al. (1995). Rational design of orthogonal receptor-ligand combinations. Angew. Chem. Int. Ed. Engl., 34, 2129–2132.

Cascio, M., & Pertwee, R. (2014). Known pharmacological actions of nine nonpsychotropic phytocannabinoids. In R. Pertwee, *Handbook of Cannabis* (p. 137-151). Oxford: Oxford Scholarship.

Cernak, & al. (2016). The medicinal chemist's toolbox for late stage functionalization of drug-like molecules. *Chem. Soc. Rev., 45, 546–576; correction, 46, 1760 (2017).*

Claussen, U., & al. (1966). Chemical classification of plants. XXXI. Hashish. 10. Cannabichromene, a new hashish component. *Tetrahedron, 22*, 1477-1479.

Crombie, L., & Ponsford, R. (1968). Synthesis oif cannabinoids by terpenic cyclization. *Chemical Communications*, 894-895.

Crombie, L., & Ponsford, R. (1971). Synthesis of cannabinoids by pyridine catalyzed citral-olivetol condensation: synthesis and structure of cannabicyclol, cannabichromene (hashish extractives), citrilidene-cannabis, and related compounds. *Journal of the Chemical Society (Section C)*, 796-804.

Davis, W., & Hatoum, N. (1983). Neurobehavioral actions of cannabichromene and interactions with delta 9-tetrahydrocannabinol. *General Pharmacology*, 247-252.

De Petrocelli, L., & al. (2008). Plant-Derived Cannabinoids Modulate the Activity of Transient Receptor potential channels of ankyrin type-1 and melastatin type 8. *Journal of Pharmacology and experimental therapeutics* , 1007-1015.

De Petrocellis, L., & al. (2011). Effects of cannabinoids and cannabinoid-enriched Cannabis extracts on TRP channels and endocannabinoid metabolic enzymes. *British Journal of Pharmacology, 163*, 1479-1494.

DeLong, G., & al. (2010). Pharmacological evaluation of the natural constituent of Cannabis sativa, cannabichromene and its modulation by Δ(9)-tetrahydrocannabinol . *Drug Alcohol Dependence, 112*, 126-133.

Gaoni, Y., & Mechoulam, R. (1966). Cannabichromene, a new active principle in hashish. . *Chemical Communications*, 20-21.

Hanuš, L., & al. (2016). Phytocannabinoids: a unified critical inventory. *Natural Product Reports, 33*, 1357-1392.

Harvey, D. (1985). Examination of a 140 year old ethanolic extract of Cannabis: Identification of new cannabitriol homologues and ethyl homologue of cannabinol . *Proceeding of the Oxford Symposium on Cannabis*, 23-30.

Hellwig, V., & al. (2003). Activities of prenylphenol derivatives from fruitbodies of Albatrellus spp. on the human and rat vanilloid receptor 1 (VR1) and characterisation of the novel natural product, confluentin . *Archiv der Pharmazie (Weinheim), 336* , 119-126.

Izzo, A., & al. (2012). Inhibitory effect of cannabichromene, a major non-psychotropic cannabinoid extracted from Cannabis sativa, on inflammation-induced hypermotility in mice. *British Journal of Pharmacology, 166*, 1444-1460.

Kane, V., & al. (1968). Constituents of hashish. A novel reaction of olivetol with citral in the presence of pyridine. Total synthesis of dl-cannabicyclol and dl-cannabichromene. *Journal of the American Chemical Society, 90*, 6551-6553.

Mazzoccanti, G., & al. (2017). Cannabis through the looking glass: chemo- and enantio-selective separation of phytocannabinoids by enantioselective ultra high performance supercritical fluid chromatography. *Chemical Communications, 53*, 12262-12265.

Nilius, B., & al. (2012). The transient receptor potential channel TRPA1: from gene to pathophysiology. *Eur J Physiol, 464*, 425-458.

Olàh, A., & al. (2016). Differential effectiveness of selected non-psychotropic phytocannabinoids on human sebocyte functions implicates their introduction in dry/seborrhoeic skin and acne treatment . *Experimental Dermatology, 25* , 701-707.

Quaghebeur, K., & al. (1994). Cannabiorci- and 8-chlorocannabiorcichromenic acid as fungal antagonists from . *Cylindrocarpon olidum. Phytochemistry, 37* , 159-161.

Romano, B., & al. (2012). The cannabinoid TRPA1 agonist cannabichromene inhibits nitric oxide production in macrophages and ameliorates murine colitis. *British Journal of Pharmacology, 169*, 213-229.

Schönherr, H., & Cernak, T. (2013). Profound methyl effects in drug discovery and a call for new C–H methylation reactions. *Angew. Chem. Int. Ed., 52*, 12256–12267.

Turner, C., & al. (1975). Constituents of Cannabis sativa L. VIII: Possible biological application of a new method to separate cannabidiol and cannabichromene. *Journal of Pharmaceutical Sciences, 64*, 810-814.

Turner, C., & Elsohly, M. (1981). Biological activity of cannabichromene, its homologs and isomers. *Journal of Clinical Pharmacology, 21*, 283S-291S.

Udoh, M., & al. (2019). Cannabichromene is a cannabinoid CB2 receptor agonist. *British Pharmacological Society, 176*, 4537-4547.

SUBCHAPTER 4.2

DIMETHYLHEPTYLCANNABINOIDS

(UNPUBLISHED DATA)

4.2.1 INTRODUCTION

As said in Chapter 1, phytocannabinoids from *Cannabis* have a linear alkyl substituent spanning from one to seven carbons bound to their resorcinol core (Citti & al., 2019) (Hanuš & al., 2016). The existence of branched chain cannabinoids of the *iso-* and *ante-iso* series is, in principle, plausible from a biogenetic standpoint — since the alkyl resorcinol moiety of phytocannabinoids derives from ketide pathway: *branching* would therefore simply require the replacement of the acetate starter with a *starter* derived from a *branched amino acid*. However, branched phytocannabinoids of this type have only been tentatively detected as trace constituents of *Cannabis*, substantially remaining unconfirmed curiosities in its inventory of constituents (Hanuš & al., 2016). Conversely, non-biogenetic branching at the benzyl carbon of the alkyl residue has played a critical role in research on *Cannabis* and cannabinoids even since the early synthesis of these compounds by Adams in the early forties of the past century (Appendino, 2020).

After discovering that CBD in acidic conditions generated an intoxicating mixture of tetrahydrocannabinol isomers Adams decided to start a structure-activity systematic work using an isomer (**1**) of tetrahydrocannabinols as a starting point. This compound was not present in the mixture of tetrahydrocannabinols he had obtained from CBD, but was, nevertheless, relatively easy to synthesize.

Taking advantage of previous study on CBN and of Pechmann coumarin synthesis, Adams prepared — by condensation of a β-ketoester with olivetol **4** to afford ester **2** and then treatment with excess of methyl magnesium bromide (Scheme 1, pathway I) — a racemic mixture of $\Delta^{6a\text{-}10a}$-THC (Adams & al., 1941). Although this compound — which also obtained by Todd through a more direct synthesis (Scheme 1, pathway II) (Gosh & al., 1941) — showed only 10% of the activity of the intoxicating mixture

derived from CBD, the position of its endocyclic double bond was certain and this evidence allowed to start the SAR studies about the alkyl-side chain (Adams & al., 1942).

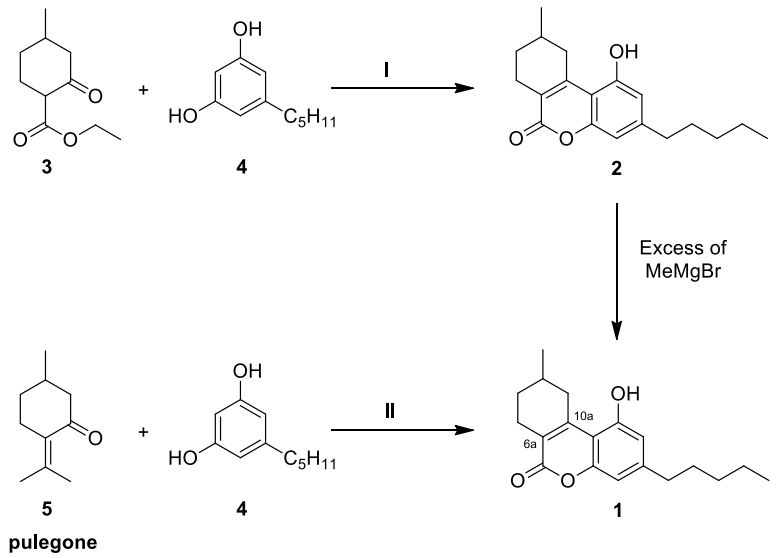

SCHEME 1 **SYNTHESIS OF Δ$^{6A\text{-}10A}$-THC PROPOSED BY ADAMS (I) AND TODD (II).** *SOURCE: ADAPTED FROM (APPENDINO, 2020)*

This work led Adams to make some interesting considerations:

- if the substituent in position 3 was a *n*-alkyl side-chain, the major potency was reached when this moiety corresponded to a six-carbons linear chain; (Table 1, point 1)
- a notable increment of activity was caused by branching in benzylic position: if the branching occurred in a different position of the straight side-chain, the potency linearly decreased; (Table 1, point 2)
- the concomitantly modulation of the lengthen and the branching of the alkyl side-chain increased the effect potency; (Table 1, point 3)
- the larger the steric bulk was, the higher the potency was. The maximum of peak effect was related to the presence of two methyl groups (1',1'-dimethyl

and 1′,2′-dimethyl analogs): an ethyl substituent did not extremely increment the potency. (Table 1, point 4)

c	3-Substituent	No. of expts.	Potency
	Natural tetrahydrocannabinol from cannabidiol	20	7.3 ± 0.89
1	-C_5H_{11}-*n*	20	1.00 Standard
	-C_6H_{13}-*n*	7	1.82 ± 0.18
	-C_7H_{15}-*n*	10	1.05 ± 0.15
	-C_8H_{17}-*n*	7	0.66 ± 0.12
2	-$CH(CH_3)C_4H_9$	8	3.17 ± 0.33
	-$CH(C_2H_6)C_3H_7$	11	1.67 ± 0.33
	-$CH_2CH(CH_3)C_3H_7$	7	1.58 ± 0.41
	-$CH_2CH_2CH(CH_3)C_2H_5$	10	1.26 ± 0.18
	-$CH_2CH_2CH_2CH(CH_3)_2$	4	1.14 ± 0.10
3	-$CH(CH_3)C_6H_{13}$	10	16.4 ± 3.67
	-$CH(CH_3)C_7H_{15}$	19	32.6 ± 3.02
	-$CH(CH_3)C_8H_{17}$	7	2.08 ± 1.49
4	-$C(CH_3)_2C_3H_7$	5	4.18 ± 0.34
	-$C(CH_3)_2C_6H_{13}$	5	21.8 ± 1.91
	-$CH(CH_3)CH(CH_3)C_4H_9$	6	39 ± 8
	-$CH(CH_3)CH(CH_3)C_5H_{11}$	**18**	**512 ± 72.6**
	-$CH(CH_3)CH(CH_3)C_6H_{13}$	5	19 ± 3.5

TABLE 3* ADAMS' SAR STUDIES ON THE ALKYL SIDE-CHAIN. THE BIOLOGICAL END-POINT USED TO CALCULATE THE POTENCY WAS "THE DOG ATAXIA ASSAY". *SOURCE*: ADAPTED FROM *(ADAMS & AL., 1948A) (ADAMS & AL., 1948B) (ADAMS & AL., 1949)

This systematic research led to the discovery of *pyrahexyl* **6** — the mixture of the eight different diastereomers of 1′,2′-dimethylheptyl analog of $\Delta^{6a\text{-}10a}$-THC — which generated a biological response several hundred time more potent than the one of its precursor. (Figure 1) (Table 1)

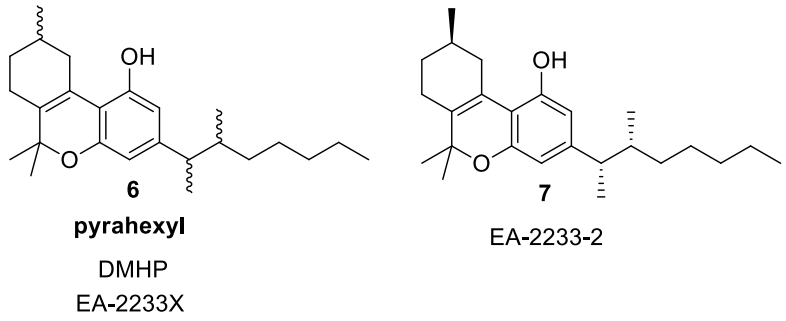

FIGURE 3 **CHEMICAL STRUCTURES OF PYRAHEXYL AND ITS MOST POTENT ANALOG EA-2233-2.**

Unfortunately, Adams' work on cannabinoids came to a stop when WWII broke, and his activity had to be redirected to areas of military interest like the discovery of antimalarial compounds and synthetic rubber (Appendino, 2020).

The Cold War era witnessed a race to incapacitating chemical weapons: in particular, the aim of U.S. Army Chemical Corps was to find non-lethal compounds able to make woozy the adversary soldiers (William & Himmelsbach, 1946). The activity profile of pyrahexyl made it a perfect lead compound for this army program: so, from 1948 to 1975 an intense chemical work was carried out to synthesize all the eight possible isomers of pyrahexyl — renamed *dimethyl heptylpyran* (DMHP) or *EA-2233* since the experiments took place at Edgewood Arsenal in Maryland — and to test their biological activity. (Figure 1)

EA-2233-2 (**7)** resulted the most promising isomer due to its great incapacitating action at low concentration and its relatively safe toxicological profile (Ketchum, 2006a, b).

In 1973, *Loev & al.* continued the Adam's SAR studies, using, however, a different animal models, replacing dogs with rabbits. Some changes in the order of potency were evidenced, but ultrapotency was confirmed (Loev & al., 1973). Starting from 1984, Pfizer joined this research field with the development of new antinociceptive

analogs of phytocannabinoids: the archetypal structure was represented by 9-nor-9β-hydroxyhexahydrocannabinol (**8**), a synthetic cannabinoid which retains the analgesic features of Δ^9-THC (Wilson & al, 1976). Capitalizing the Adams' and Loev's research studies, the a α,α-dimethylheptyl side-chain was introduced, and the dihydropyran ring fremoved, eventually obtaining two compounds that turned out to be of critical relevance for the study of the biological profile of cannabinoids:

- *CP-55-940* (**9**) was used in the studies that led to the discovery of cannabinoid receptors and of endocannabinoids (Johnson & al., 1981) (Matsuda & al., 1990) (Di Marzo, 2018); (Figure 2)
- *CP-47-497* (**10**), (Stern & Lambert, 2007), also known as *cannabicyclohexanol* was the first synthetic cannabinoid discovered in the illegal market, soon followed by analogues with longer chains (Weissman & al., 1982) (Appendino & al., 2014). (Figure 2)

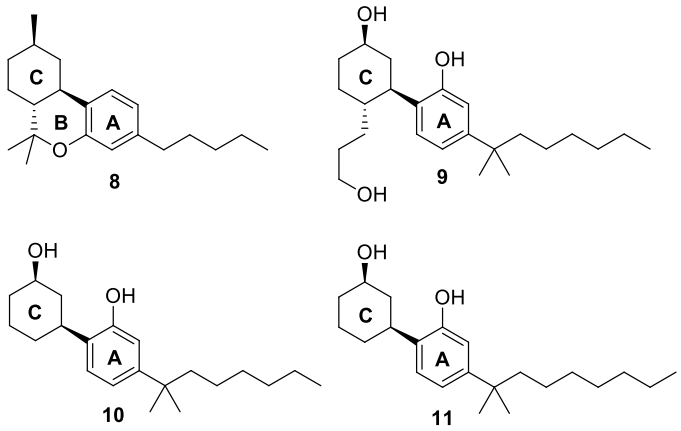

FIGURE 4 **CHEMICAL STRUCTURES OF Δ⁹-THC DERIVATES DEVELOPED BY PFIZER.**

In the late 1980s, attempting to obtain stereospecific cannabinoid ligands, the Mechoulam's research group developed a potent synthetic analog of metabolic

derivative of Δ^8-THC, which was preferred to its Δ^9 isomer due to its greater stability (Mechoulam & al., 1988)(Mechoulam & al., 1990).

As discussed in Chapter 1, during Phase I metabolism THC is oxidised at the allylic methyl group in position 9, leading to *11-hydroxy-THC* **12** which retains the lipophilicity and consequentially the intoxicating activity of its precursor.

Both α,α-dimethylheptyl enantiomeric analogs of 11-hydroxy-Δ^8-THC were synthesized. *(-)-(3R,4R)-11-hydroxy-Δ^8-THC* — renamed *HU-210* (**13**) — revealed high potency and affinity, as well as agonist marked activity for CB receptors (Mechoulam & al., 1988) (Stern & Lambert, 2007). (Figure 3)

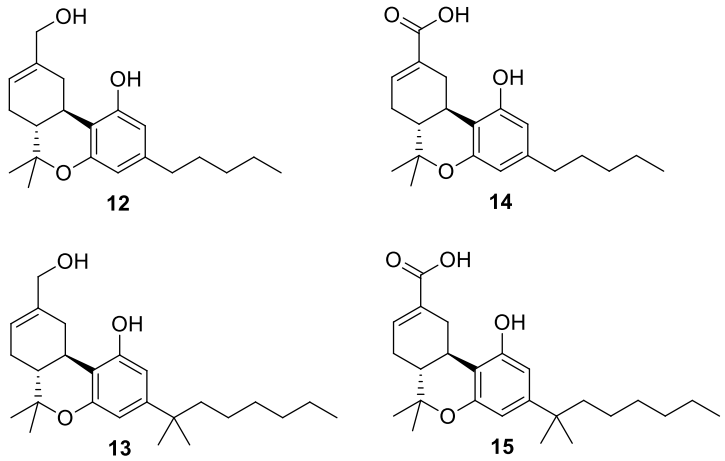

FIGURE 5 **CHEMICAL STRUCTURES OF 11-HYDROXY-Δ^8-THC (12), HU-210 (13), Δ^8-THC-11-OIC ACID (14), AND AJULEMIC ACID (15).**

According to this discovery, the following aim was obtaining a compound with a biological and pharmacological profile different from the Δ^9-THC one: in particular, it had to give a huge therapeutic action without inducing intoxicating and adverse side effects (Hanuš & Mechoulam, 2005).

Taking inspiration from the previous work, *Δ^8-THC-11-oic acid* **14** was selected as *hit* compound (since it was not able to cross the *blood-brain barrier* (BBB) due to its higher

hydrophilicity, and for this reason did not develop typical Δ^9-THC response), while its *n*-pentyl side-chain had been elongated and branched to improve the potency and affinity (Burstein & al., 1992). This easy and simple modulation provided the preparation of a new analgesic and anti-inflammatory analog, referred to as *ajulemic acid* (HU-239, **15**) (Burstein, 2000). (Figure 3)

Eventually, also the CBD scaffold was evaluated for the introduction of the "magic" dimethylheptyl residue (Leite & al, 1982) (Hanuš & Mechoulam, 2005).

Following this modification, no particular changes on affinity, and potency towards CB receptors were detected in *laevorotatory series* (3R,4R) (**16** & **17**), but surprisingly, in *dextrorotatory series*, (+)-DMH-CBD (**18**) showed a marked improved affinity towards CB_1 receptor compared to its *n*-pentyl analog **19** (Bisogno & al., 2001) (Morales & al., 2017). (Figure 6)

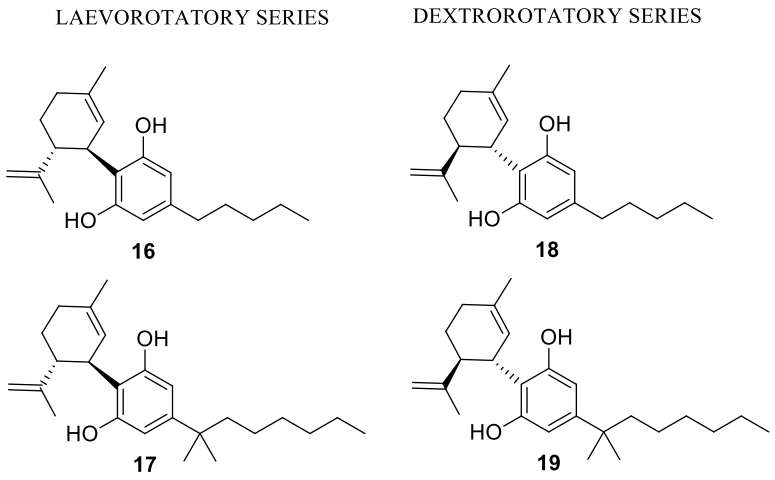

FIGURE 6 **CHEMICAL STRUCTURES OF LAEVO- AND DEXTROROTATORY SERIES OF CBD ANALOGS.**

The effect on the biological activity of the *gem*-dimethyl substitution at the *n*-benzylic position of phytocannabinoids has never been investigated systematically: only modulation on THC-type and CBD-type frameworks had been explored.

If the interaction with CB_1 and partially with CB_2 receptors has been intensively examined, very little is known on the effect of this small, but important pharmacological manoeuvre (Talele, 2017) on other cannabinoid targets (*ionotropic* like the TRP channels, and *genomic* like PPARγ).

Spurred by the limited literature available, the lack of a complete and clearly defined biological profile, and the relatively simple chemistry synthesis, we have implanted the α,α-dimethylheptyl motif in the major phytocannabinoids (Δ^8-THC, CBD, CBG, CBC, and CBN), as well as in their corresponding quinones. The biological investigation focused on the cannabinoid receptors (CB_1 and CB_2) and the thermos-TRPs ion channels.

4.2.2 Results and Discussion

These DMH analogs were obtained from the *1',1'-dimethylheptyl resorcinyl core* **27**, prepared as shown in ***Scheme 2***. The ketone **25** was obtained using chemistry developed by Weinreb. Commercially available 3,5-dimethoxycarboxilic acid **20** was reacted with oxalyl chloride **21**, providing the corresponding acyl chloride which underwent hydroxyamidation with N,O-dimethylhydroxylamine hydrochloride **22**. The resulting hydroxamide **23** was treated with hexylmagnesium bromide **24**, affording the ketone **25**. Treatment of **25** with $Al(Me)_3$ — in presence of $Ti(Cl)_4$ — afforded **26**, which was finally demethylated using BBr_3 to get dimethylheptyl resorcinyl core **27**. (Scheme 2)

Isoprenylation was then carried out by using the same chemistry applied to the synthesis of the corresponding *n*-pentyl cannabinoids, namely, Lewis-acid catalyzed geranylation with *geraniol* **28** for the α,α-dimethylheptyl analog of CBG (DMH-CBG, **31**), terpenylation with *2,9-p-menthadien-1-ol* **29** under different conditions for DMH-CBD (**32**) and DMH-Δ^8-THC (**33**), chromenyation with *citral* for DMH-CBC (**34**), and iodine-treatment of **34** for CBN-DMH (**35**). (Scheme 3)

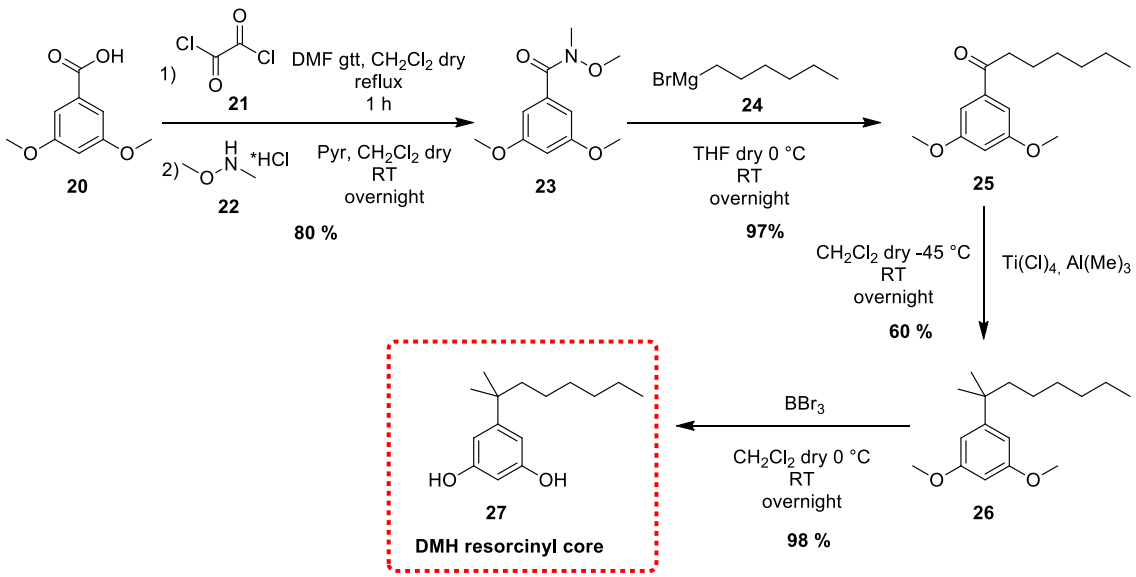

Scheme 2 **Synthesis of 1',1'-DMH resorcinyl core.**

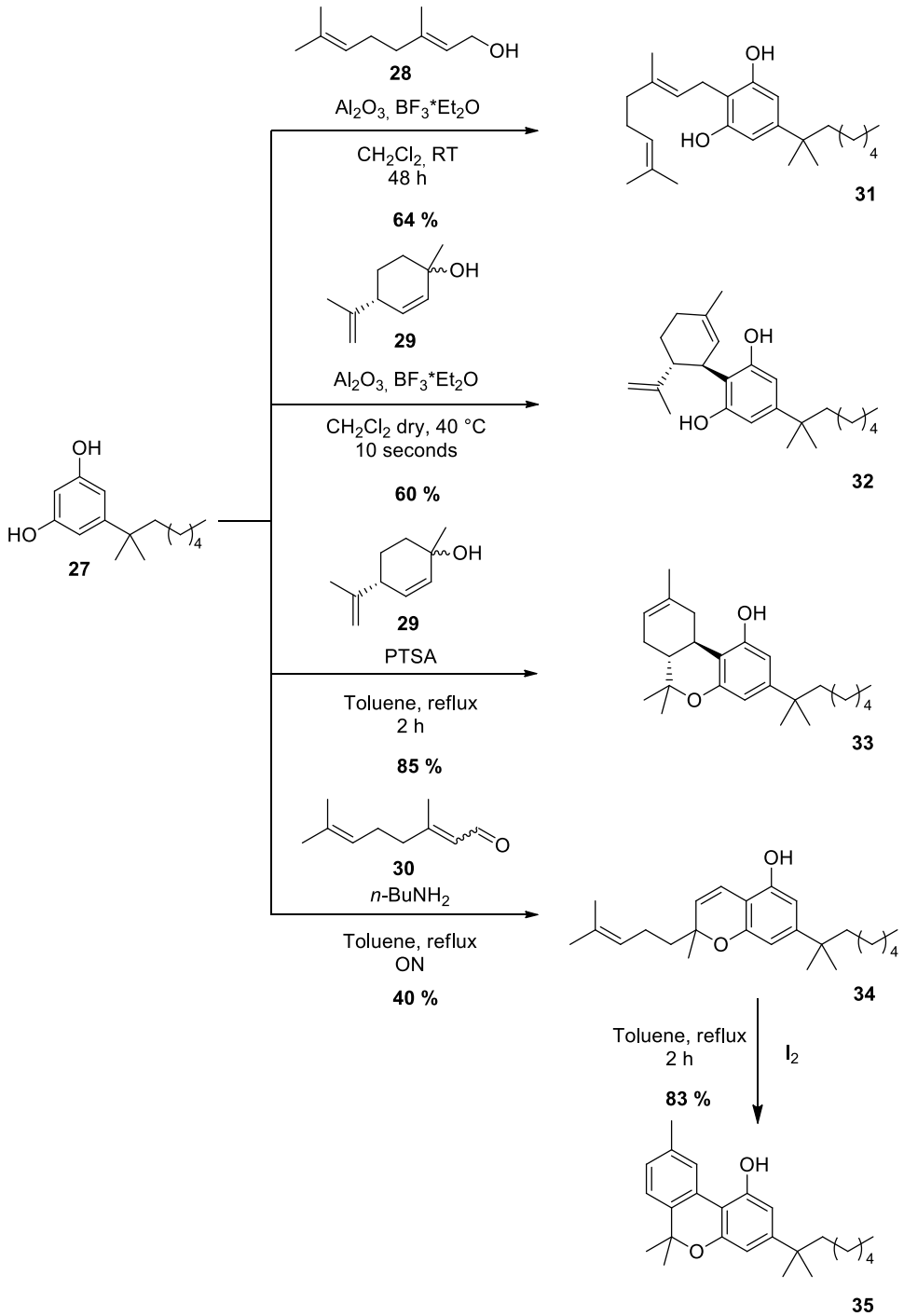

SCHEME 3 **CONVERSION OF THE DMH RESORCINYL CORE INTO THE CORRESPONDING *MAJOR* PHYTOCANNABINOIDS.** *SYNTHETIC PROTOCOLS APPLIED*: 31 **(BAEK & AL., 1985),** 32 **(BAEK & AL., 1995),** 33 **(CROMBIE & AL., 1988),** 34 **(ELSOHLY & AL., 1982) &** 35 **(CAPRIOGLIO & AL., 2019).**

A few experimental details are worth discussing. Thus, in order to get the CBG analog **31**, in dry ambient and under N_2 atmosphere BF_3-etherate was added dropwise to a stirred suspension of Al_2O_3 in CH_2Cl_2 dry. After stirring 15 minutes at room temperature, the suspension was heated to 40 °C for 1 minute, and geraniol and **27** were quickly added. The mixture was stirred at room temperature over two days. Following the procedure just described — by replacing geraniol with 2,9-*p*-menthandienol — compound **32** was obtained: after stirring at RT for only 10 seconds, the reaction was quenched with a $NaHCO_3$ solution to prevent the cyclisation. The Δ^8-THC analog **33** was obtained by reacting DMH resorcinol **27** with *p*-menthandienol in presence of *p*-toluenesulfonic acid (PTSA).

For the preparation of the CBC analogue, a solution of **27** and $BuNH_2$ heated at to 60 °C for 10 minutes. Citral was then added, and the mixture was refluxed overnight, affording compound **34**. Finally, treatment of **34** with I_2 in toluene reflux provided the CBN analog **35**.

The resorcinolic cannabinoids obtained in this way were then converted to their corresponding quinones, using the chemistry described in Chapter 3. (Scheme 4)

Surprisingly, all finale quinones resulted stable compounds and were refractory to *aza*-Michael addition.

The loss of Michael-acceptor properties was associated to an increase of stability. In a comparative experiment, CBDQ and DMH-CBDQ (**39**) were stored in a fume hood at room temperature under visible light: with the *n*-pentyl product degradation was already detectable after two days, and in two weeks was complete (confirmed by NMR spectra), while **39** was stable for at least three months under these conditions.

The biological activity of the dimethylheptyl cannabinoids is ongoing. As with the CBC analogues, the end-point investigated are the cannabinoid receptors and the thermo-TRPs.

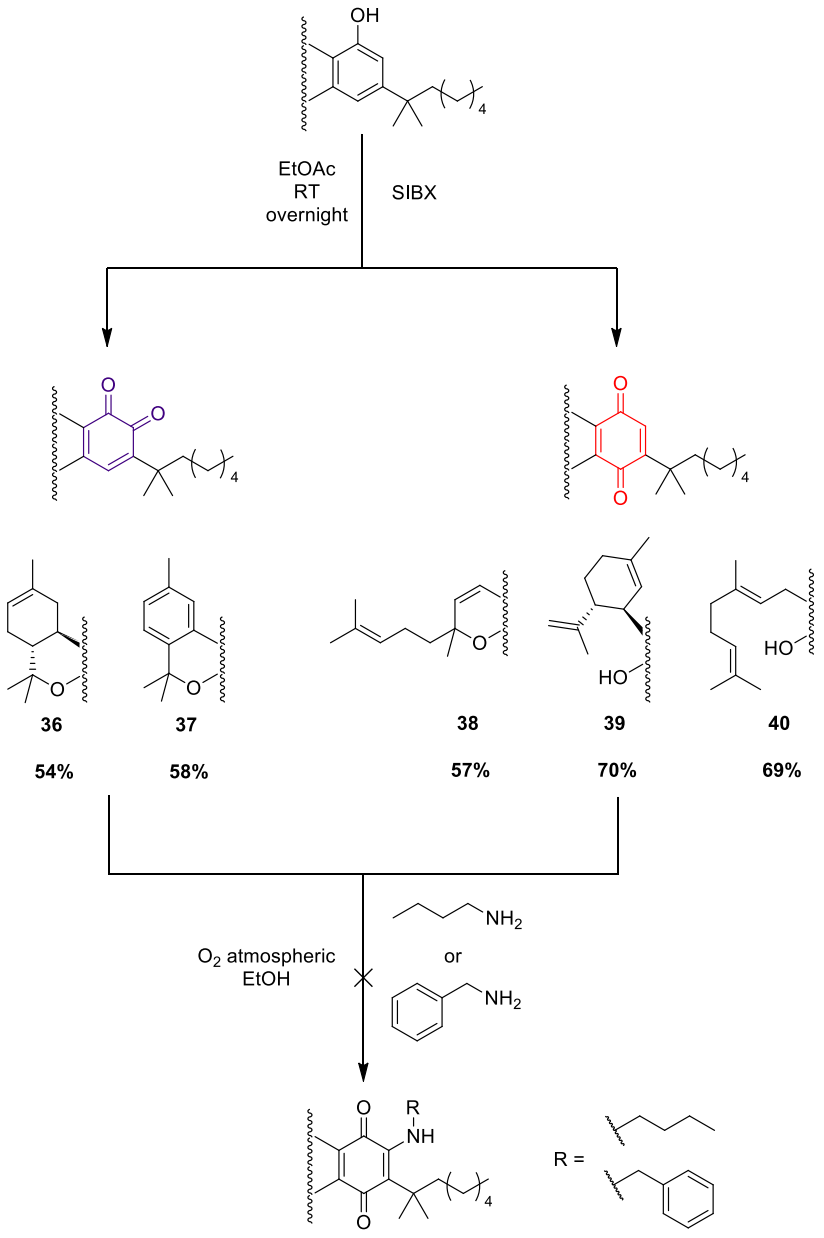

SCHEME 4 **OXIDATION OF DMH ANALOGS TO CORRESPONDING *ORTHO*- AND *PARA*-QUINONES, AND FAILED *AZA*-MICHAEL ADDITION/DEHYDROGENATION.**

4.2.3 EXPERIMENTAL SECTION

GENERAL EXPERIMENTAL PROCEDURES: IR spectra were recorded on an Avatar 370 FT-IR Techno-Nicolet apparatus. ^{1}H (400 MHz) and ^{13}C (100 MHz) NMR spectra were measured on Bruker Avance 400 MHz spectrometer. Chemical shifts were referenced to the residual solvent signal ($CDCl_3$: δH = 7.21, δC = 77.0). Homonuclear ^{1}H connectivities were determined by the Correlation spectroscopy (COSY) experiment. One-bond heteronuclear ^{1}H–^{13}C connectivities were determined with the heteronuclear single quantum coherence (HSQC) spectroscopy experiment. Two- and three-bond ^{1}H–^{13}C connectivities were determined by gradient two-dimensional (2D) heteronuclear multiple bond correlation (HMBC) experiments optimized for a $^{2,3}J$ = 9 Hz. Low- and high-resolution electrospray ionization mass spectrometry (ESI-MS) data were determined on an LTQ OrbitrapXL (Thermo Scientific) mass spectrometer. Reactions were monitored by thin-layer chromatography (TLC) on Merck 60 F254 (0.25 mm) plates, visualized by staining with 5% H_2SO_4 in EtOH and heating. Organic phases were dried with Na_2SO4 before evaporation. Chemical reagents and solvents were purchased from Sigma-Aldrich, TCI Europe or Fluorchem and were used without further purification unless stated otherwise. Petroleum ether with boiling point of 40–60 °C was used. Silica gel 60 (70–230 mesh) was used for gravity column chromatography (GCC).

SYNTHESIS OF (3,5-DIMETHOXYPHENYL)-N-METHOXY-N-METHYLCARBOXAMIDE (23): to a suspension of 3,5-dimethoxybenzoic acid (**20**) (2 g, MW 182.17 g/mol, 10.98 mmol) in 7 mL of CH_2Cl_2 at room temperature was added DMF (5 drops) followed by oxalyl chloride (**21**) (3.2 mL, MW 126.93 g/mol, d= 1.48 g/mL, 37.31 mmol, 3.33 eq). The reaction mixture was heated to reflux for 1 h, and the excess oxalyl chloride and solvent were removed by distillation under reduced pressure. The crude acid chloride was dissolved in 5 mL of dry CH_2Cl_2 and added via syringe to a solution of

N,O-dimethylhydroxylamine hydrochloride (**22**) (1.29 g, MW 97.54 g/mol, 24.8 mmol, 1.21 eq) and pyridine (2 mL, Molecular weight 79.10 g/mol, d= 0.982 g/mL, 24.8 mmol, 2.26 eq) in 4 mL of CH_2Cl_2 at 0 °C. The reaction mixture was warmed to room temperature, stirred for 12 h, and quenched with saturated KH_2PO_4. The organic phase was washed with water (2×) and brine (2×) and dried (Na_2SO_4). Concentration under reduced pressure gave amide **23** (2.37 g, 80% yield, *Rf*= 0.3 in PE/EtOAc 5:5) as a pale-yellow oil without further purification.

(3,5-DIMETHOXYPHENYL)-N-METHOXY-N-METHYLCARBOXAMIDE (23): ^{1}H NMR (400 MHz, $CDCl_3$) δ 6.75 (d, *J* = 2.4 Hz, 2H), 6.49 (t, *J* = 2.4 Hz, 1H), 3.76 (s, 6H), 3.55 (s, 3H), 3.29 (s, 3H) ppm; ^{13}C NMR (100 MHz, $CDCl_3$): δ 169.6, 160.4, 136.0, 105.9, 102.8, 61.2, 55.5, 34.1 ppm.

SYNTHESIS OF 1-(3,5-DIMETHOXYPHENYL)HEPTAN-1-ONE (25): to a stirred solution of amide **23** (1.29 g, MW 225.24 g/mol, 5.73 mmol) in dry THF (5 mL) at 0 °C under nitrogen atmosphere, hexylmagnesium bromide (**24**) (2M solution in THF, 7.16 mL, 14.3 mmol, 2.5 eq) was added dropwise. After 30 min, the reaction mixture was quenched with 1 M HCl and diluted with petroleum ether and water. The aqueous phase was extracted with petroleum ether (3×) and the combined organic extracts were washed with brine (1×) and dried (Na_2SO_4). Concentration under reduced pressure gave phenone **25** (1.29 g, 97% yield, *Rf*= 0.25 in PE/EtOAc 95:5) as a white solid without further purification.

1-(3,5-DIMETHOXYPHENYL)HEPTAN-1-ONE (25): ^{1}H NMR (400 MHz, $CDCl_3$) δ 7.09 (d, *J* = 2.5 Hz, 2H), 6.64 (t, *J* = 2.2 Hz, 1H), 3.83 (s, 6H), 2.91 (t, *J* = 7.4 Hz, 2H), 1.71 (quint, *J* = 7.3 Hz, 2H), 1.43-1.23 (m, 6H), 0.89 (t, *J* = 6.6 Hz, 3H); ^{13}C NMR (100 MHz, $CDCl_3$) δ 200.1, 160.8, 139.0, 105.9, 105.0, 55.6, 38.8, 31.7, 29.1, 24.5, 22.6, 14.1.

SYNTHESIS OF 5-(1,1-DIMETHYLHEPTYL)-1,3-DIMETHOXYBENZENE (26): to a solution of $TiCl_4$ (565 μL, 978 mg, MW 189.68 g/mol, d= 1.73 g/mL, 5.16 mmol, 1 eq) in 25 mL

of dry CH_2Cl_2 at -45 °C under nitrogen atmosphere, trimethylaluminum (5.16 mL, 2 M solution in CH_2Cl_2, 10.3 mmol, 2 eq) was added. The reaction mixture was stirred for 20 min, then a solution of ketone **25** (1.29 g, MW 250.33 g/mol, 5.16 mmol) in 5 mL of dry CH_2Cl_2 at -45 °C was added dropwise. The reaction mixture was warmed to room temperature, stirred for 18 h, quenched with water, and diluted with ether and 1 M HCl. The aqueous layer was extracted with ether (3×) and the combined organic layers were washed with 1 M HCl (1×) and brine (2×), dried (Na_2SO_4) and concentrated under reduced pressure. Purification by flash column chromatography on silica gel (PE/EtOAc 98:2 as eluent) gave **26** (1.02 g, 60% yield, *Rf*= 0.6 in PE/EtOAc 95:5) as a colorless oil.

5-(1,1-Dimethylheptyl)-1,3-dimethoxybenzene (26): ^{1}H NMR (400 MHz, $CDCl_3$): δ 6.40 (d, *J* = 2.2 Hz, 2H), 6.22 (t, *J* = 2.2 Hz, 1H), 3.71 (s, 6H), 1.48 (m, 2H), 1.18 (s, 6H), 1.20-1.07 (m, 6H), 0.98 (m, 2H), 0.77 (t, *J* = 7.1 Hz, 3H); ^{13}C NMR (100 MHz, $CDCl_3$): δ 160.3, 152.4, 104.6, 96.5, 55.1, 44.5, 38.0, 31.8, 30.0, 28.9, 24.6, 22.7, 14.1.

SYNTHESIS OF DIMETHYLHEPTYL RESORCINOL (27): to a stirred solution of **26** (1.14g, MW 264.41 g/mol, 4.32 mmol, 1eq) in dry CH_2Cl_2 (10 mL) at 0 °C under nitrogen atmosphere, BBr_3 (1 M solution in CH_2Cl_2, 12.9 mL, 12.94 mmol, 3 eq) was added dropwise. The reaction mixture was warmed to room temperature, stirred for 18 h, quenched with water, and diluted with EtOAc and 1 M $NaHCO_3$. The aqueous layer was extracted with EtOAc (3×) and the combined organic layers were washed with 1 M HCl (1×) and brine (2×), dried (Na_2SO_4) and concentrated under reduced pressure. Purification by flash column chromatography on silica gel (PE/EtOAc 9:1 as eluent) gave **27** (1.05 g, 98% yield, *Rf*= 0.4 in PE/EtOAc 7:3) as a brown oil.

DIMETHYLHEPTYL RESORCINOL (27): ^{1}H NMR (400 MHz, $CDCl_3$): δ = 6.35-6.45 (m, 2H), 6.16 (m, 1 H), 4.65 (bs, 2H), 1.45-1.50 (m, 2H), 1.22 (s, 6H), 1.21-1.10 (m, 6H), 1.03

(bs, 2H), 0.84 (t, *J* =6.5 Hz, 3H); ^{13}C NMR (100 MHz, $CDCl_3$): δ 163.2, 154.0, 111.2, 101.3, 45.0, 35.3, 31.1, 29.8, 23.9, 25.1, 14.8 ppm.

SYNTHESIS OF DIMETHYLHEPTYLCANNABIGEROL (DMH-CBG, 31): to a stirred suspension of aluminium oxide (10 g/g of substrate, 1 g) in dry CH_2Cl_2 (10 mL) under nitrogen atmosphere, BF_3*Et_2O (1.5 mL/g substrate, 150 μL) was added. The suspension was stirred for 15 minutes at room temperature and heated at 40 °C for 1 minute, then **27** (100 mg, MW 236.36 g/mol, 0.423 mmol, 1 eq) and geraniol (150 μL, 130 mg, MW 154.25 g/mol, 0.846 mmol, 2 eq) were sequentially added. The reaction was stirred at 40 °C for 2 days, then quenched with 20mL of H_2SO_4 2M. The crude was extracted with EtOAc, washed with BRINE, dried over Na_2SO_4 and concentrated under reduced pressure. Purification by flash column chromatography on silica gel (PE 100% to PE/EtOAc 95:5 as eluent) gave **31** (101 mg, 64%) as a colorless oil.

DIMETHYLHEPTYLCANNABIGEROL (DMH-CBG, 31): Colorless oil (*Rf:* 0.75 in PE/EtOAc 9:), 64%. ^{1}H NMR (400 MHz, $CDCl_3$): δ 6.40 (s, 2H), 5.32 (t, *J* = 6.6 Hz, 1H), 5.11 (bs, 2H), 5.08 (t, *J* = 6.7 Hz, 1H), 3.42 (d, *J* = 7.1 Hz, 2H), 2.21-2.07 (m, 4H), 1.84 (s, 3H), 1.70 (s, 3H), 1.62 (s, 3H), 1.55-1.51 (m, 2H), 1.29-1.16 (m, 12H) 1.12 – 1.05 (m, 2H), 0.87 (t, *J* = 6.9 Hz, 3H). ^{13}C NMR (100 MHz, $CDCl_3$) δ 154.5, 150.0, 139.0, 132.0, 123.7, 121.7, 110.2, 106.1, 44.4, 39.7, 37.4, 31.8, 30.0, 28.8, 26.4, 25.6, 24.6, 22.7, 22.3, 17.7, 16.2, 14.0.

SYNTHESIS OF DIMETHYLHEPTYLCANNABIDIOL (DMH-CBD, 32): to a stirred suspension of aluminium oxide (10g/g of substrate, 1 g) in dry CH_2Cl_2 (10 mL) under nitrogen atmosphere, BF_3*Et_2O (1.5 mL/g substrate, 150 μL) was added. The suspension was stirred for 15 minutes at room temperature and heated at 40 °C for 1 minute, then **27** (100 mg, MW 236.36 g/mol, 0.423 mmol, 1 eq) and (1S,4R)-*p*-mentha-2,8-dien-1-ol (52 mg, MW 152.50 g/mol, 0.339 mmol, 0.8 eq) were sequentially added. The reaction was stirred at 40 °C for 10 seconds, then quenched with 5 mL of sodium

carbonate saturated solution. The crude was extracted with EtOAc, washed with BRINE, dried over Na_2SO_4 and concentrated under reduced pressure. Purification by flash column chromatography on silica gel (PE 100% to PE/EtOAc 95:5 as eluent) gave **32** (94 mg, 60%) as a colorless oil.

DIMETHYLHEPTYLCANNABIDIOL (DMH-CBD, 32): Colorless oil (*Rf:* 0.75 in PE/EtOAc 9:1), 60%. ^{1}H NMR (400 MHz, $CDCl_3$): δ 6.25-6.23 (bs, 2H), 5.90-6.05 (bs, 1H), 5.56 (s, 1H), 4.65 (s, 1H), 4.54 (s, 1H), 4.55 (s, 1H), 3.85 (bs, 1H), 2.30-2.05 (m, 2H), 1.79 (s, 3H), 1.63 (s, 3H), 1.45-1.50 (m, 2H), 1.21 (bs, 12 H), 0.95-1.05 (bs, 2H), 0.83 (t, J = 7.5 Hz, 3H).; ^{13}C NMR (100 MHz, $CDCl_3$): δ 150.22, 149.5, 140.0, 124.1, 113.4, 110.7, 46.0, 44.6, 37.5, 37.3, 31.8, 30.4, 29.9, 28.7, 28.6, 28.4, 24.6, 23.6, 22.6, 20.7, 14.0.

SYNTHESIS OF DIMETHYLHEPTYL-Δ^8-TETRAHYDROCANNABINOL (DMH-Δ^8-THC, 33): to a stirred suspension of **27** (450 mg, MW 236.36 g/mol, 1.69 mmol, 1,0 eq) in toluene (2.5 mL), PTSA (60 mg, MW 172.2 g/mol, 0.338 mmol, 0.2 eq) and (1S,4R)-*p*-mentha-2,8-dien-1-ol (290 mg, MW 152.50 g/mol, 1.86 mmol, 1.1 eq) were sequentially added. The solution was heated at 120 °C for 2 hours, then cooled to room temperature and quenched with BRINE. The organic phase was extracted with EtOAc, dried over Na_2SO_4 and concentrated under reduced pressure. Purification by flash column chromatography on silica gel (PE 100% to PE/ CH_2Cl_2 8:2 as eluent) gave **33** (532 mg, 85%) as a brown oil.

DIMETHYLHEPTYL-Δ^8-TETRAHYDROCANNABINOL (DMH-Δ^8-THC, 33): Brown oil (*Rf:* 0.90 in PE/EtOAc 9:1), 85%. ^{1}H NMR (400 MHz, $CDCl_3$) δ 6.42 (d, *J* = 1.8 Hz, 1H), 6.25 (d, *J* = 1.8 Hz, 1H), 5.49-5.41 (m, 1H), 4.79-4.71 (m, 1H), 3.22 (dd, *J* = 16.4, 4.4 Hz, 1H), 2.72 (td, *J* = 10.9, 4.7 Hz, 1H), 2.19-2.13 (m, 1H), 1.96-1.78 (m, 4H), 1.73 (s, 3H), 1.54-1.50 (m, 2H), 1.41 (s, 3H), 1.33-1.16 (m, 10H), 1.14 (s, 3H), 1.11-1.06 (m, 2H), 0.87 (t, *J* = 6.9 Hz, 3H). ^{13}C NMR (100 MHz, $CDCl_3$) δ 154.5, 154.45, 150.0, 134.7, 119.3, 110.1,

108.0, 105.4, 44.8, 44.4, 37.3, 36.0, 31.8, 31.5, 30.0, 28.7, 28.6, 27.9, 27.6, 24.6, 23.5, 22.6, 18.5, 14.1.

SYNTHESIS OF DIMETHYLHEPTYLCANNABICHROMENE (DMH-CBC, 34): to a stirred suspension of **27** (350 mg, MW 236.36 g/mol, 1.48 mmol, 1.04 eq) in toluene (10 mL), butylamine (141 μL, 104 mg, MW 73.14 g/mol, 1.42 mmol, 1 eq) was added. The solution was heated at 60 °C for 10 minutes, then citral (241 μL, 217 mg, MW 152.23 g/mol, 1.42 mmol, 1 eq) was added, and the solution was heated at reflux overnight. The reaction was cooled to room temperature then quenched with 20mL of H_2SO_4 2M. The crude was extracted with EtOAc, washed with BRINE, dried over Na_2SO_4 and concentrated under reduced pressure. Purification by flash column chromatography on silica gel (PE 100% to PE/EtOAc 95:5 as eluent) gave **34** (210 mg, 40%) as a brown oil.

DIMETHYLHEPTYLCANNABICHROMENE (DMH-CBC, 34): Brownoil (*Rf:* 0.85 in PE/EtOAc 9:1), 54%. ^{1}H NMR (400 MHz, $CDCl_3$) δ 6.61 (d, J = 10.0 Hz, 1H), 6.39 (s, 1H), 6.25 (s, 1H), 5.51 (d, J = 10.0 Hz, 1H), 5.09 (t, J = 7.4 Hz, 1H), 2.32 – 2.02 (m, 2H), 1.76 – 1.62 (m, 2H), 1.65 (s, 3H), 1.57 (s, 3H), 1.55 – 1.44 (m, 2H), 1.39 (s, 3H), 1.31 – 1.12 (m, 6H), 1.19 (s, 6H), 1.11 – 0.99 (m, 2H), 0.94 – 0.60 (m, 3H). ^{13}C NMR (100 MHz, $CDCl_3$) δ 153.7, 152.0, 150.7, 131.6, 127.4, 124.1, 116.7, 107.0, 106.7, 105.5, 44.4, 41.0, 37.7, 31.7, 30.0, 28.7, 26.2, 25.6, 24.6, 22.7, 22.6, 17.6, 14.0.

SYNTHESIS OF DIMETHYLHEPTYLCANNABINOL (DMH-CBN, 35): to a stirred suspension of DMH-CBC (210 mg, MW 370.58 g/mol, 0.573 mmol, 1.0 eq) in toluene (40 mL), iodine (291 mg, MW 253.81 g/mol, 1.15 mmol, 2 eq) was added. The solution was refluxed for 3 hours, then cooled to room temperature and quenched with Na_2SO_3 s.s. The organic phase was extracted with EtOAc, dried over Na_2SO_4 and concentrated under reduced pressure. Purification by flash column chromatography

on silica gel (PE 100% to PE/CH2Cl2 9:1 as eluent) gave **35** (173 mg, 83%) as a brown oil.

DIMETHYLHEPTYLCANNABINOL (DMH-CBN, 35): Brown oil (*Rf:* 0.85 in PE/EtOAc 9:1), 83%. ^{1}H NMR (400 MHz, $CDCl_3$): δ 8.20 (s, 1H), 7.18 (d, *J* = 7.9 Hz, 1H), 7.10 (d, *J* = 8.9 Hz, 1H), 6.59 (d, *J* = 1.8 Hz, 1H), 6.44 (d, *J* = 1.8 Hz, 1H), 2.41 (s, 3H), 1.63 (s, 6H), 1.58-1.54 (m, 2H), 1.27 (s, 6H), 1.26-1.13 (m, 6H), 0.86 (t, *J* = 6.9 Hz, 3H). ^{13}C NMR (100 MHz, $CDCl_3$): δ 154.3, 152.7, 151.8, 136.9, 136.9, 127.6, 127.5, 126.3, 122.6, 108.6, 108.3, 107.6, 44.4, 37.6, 31.7, 29.9, 28.6, 27.1, 24.6, 22.6, 21.5, 14.0.

GENERAL PROCEDURE FOR SIBX OXIDATION OF DMH ANALOGS.

SYNTHESIS OF DMH-Δ^{8}-THC QUINONE (36) AS EXAMPLE: to a cooled (ice bath) solution of **35** (100 mg, MW 370.57 g/mol, 0.270 mmol) in ethyl acetate (EtOAc, 5 mL), SIBX (39%, 252 mg, MW 280.02, 0.807 mmol, 3.3 equiv.) was added in small portions. The cooling bath was removed, and the suspension was stirred at room temperature for 18 h and then filtered over a celite pad. The filtration cake was washed with EtOAc (10 mL), and the pooled filtrates were washed with saturated $Na_2S_2O_3$ and next with BRINE. After the drying and evaporation, the residue was purified by GCC on silica gel (PE/EtOAc 8:2 as eluant) to afford 88 mg of **36** as a dark red oil (54%).

DMH-Δ^{8}-THC QUINONE (36): Dark red oil (*Rf:* 0.45 in PE/EtOAc 95:5), 54%. ^{1}H NMR (400 MHz, $CDCl_3$): δ 6.38 (bs, 1H), 5.31 (bs, 1H), 2.98 (m, 1H), 2.39 (dt, *J* = 11.1, 5.0 Hz, 1H), 2.02 (m, 1H), 1.74 (m, 1H), 1.67-1.49 (overlapped m, 8H), 1.37 (s, 1H), 1.27-0.89 (overlapped m, 16H), 0.78 (t, *J* = 6.8 Hz, 3H). ^{13}C NMR (100 MHz, $CDCl_3$): δ 180.7, 177.8, 162.9, 149.8, 134.7, 134.5, 118.6, 114.9, 82.2, 43.5, 40.6, 38.5, 35.1, 31.8, 29.8, 29.7, 27.3, 27.2, 27.1, 27.0, 25.1, 23.3, 22.7, 19.5, 14.1.

DMH-CBN QUINONE (37): Purple oil (*Rf:* 0.55 in PE/EtOAc 9:1), 58%. ^{1}H NMR (400 MHz, $CDCl_3$): δ 8.33 (s, 1H,), 7.12 (d, *J* = 8.9 Hz, 1H), 7.04 (d, *J* = 7.9 Hz, 1H), 6.63 (bs,

1H), 2.39 (s, 3H), 1.73 (s, 6H), 1.70 (overlapped m, 2H) 1.33-0.99 (m, 14H), 0.87 (t, *J* = 6.9 Hz, 3H); ^{13}C NMR (100 MHz, CDCl3): δ 179.9, 176.4, 163.1, 151.2, 137.9, 134.1, 131.8, 128.9, 125.7, 124.6, 122.3, 110.8, 82.7, 40.6, 38.8, 31.7, 29.7, 29.7, 28.4, 27.3, 25.1, 22.6, 21.3, 14.0.

DMH-CBC QUINONE (38): Red oil (*Rf:* 0.53 in PE/EtOAc 9:1), 57%. ^{1}H NMR (400 MHz, $CDCl_3$): δ 6.47 (d, *J* = 10.0 Hz, 1H), 6.42 (bs, 1H), 5.56 (d, *J* = 10.0 Hz, 1H), 5.09 (bt, *J* = 7.8 Hz, 1H), 2.11 (m, 2H), 1.89 (m, 1H), 1.77-1.52 (m, 4H), 1.67 (bs, 3H), 1.49 (s, 3H), 1.32-0.97 (m, 16H), 0.86 (t, *J* = 6.9 Hz, 3H). ^{13}C NMR (100 MHz, $CDCl_3$): δ 184.7, 181.4, 153.2, 151.3, 132.2, 132.1, 128.6, 123.3, 115.2, 114.2, 83.2, 41.5, 40.7, 38.7, 31.7, 29.7, 27.6, 27.3, 25.6, 25.1, 22.6, 22.5, 17.6, 14.0.

DMH-CBD QUINONE (39): Red oil (*Rf:* 0.75 in PE/EtOAc 95:5 (2x)), 70%. ^{1}H NMR (400 MHz, $CDCl_3$): δ 7.13 (s, 1H), 6.31 (s, 1H), 5.08 (s, 1H), 4.48 (bs, 1H), 4.46 (bs, 1H), 3.68-3.60 (m, 1H), 2.68 (td, *J* = 12.2, 2.8 Hz, 1H), 2.21-2.07 (m, 2H), 1.92 (dd, *J* = 17.4, 4.6 Hz, 2H), 1.75-1.64 (m, 2H), 1.61 (bs, 3H), 1.56 (s, 3H), 1.20-1.05 (m, 12H), 1.00-0.89 (m, 2H), 0.78 (t, *J* = 6.9 Hz, 3H). ^{13}C NMR (100 MHz, $CDCl_3$): δ 187.2, 183.4, 151.7, 150.0, 148.4, 135.3, 133.8, 122.4, 121.7, 110.6, 44.6, 40.6, 38.1, 35.7, 31.6, 30.4, 29.7, 28.7, 27.2, 27.2, 24.9, 23.4, 22.5, 18.6, 14.0.

DMH-CBG QUINONE (40): Red oil (*Rf:* 0.78 in PE/EtOAc 9:1), 65%. ^{1}H NMR (400 MHz, $CDCl_3$): δ 7.13 (s, 1H), 6.44 (s, 1H), 5.20-5.11 (m, 1H), 5.00-5.08 (m, 1H), 3.12 (d, *J* = 7.3 Hz, 2H), 2.07-2.00 (m, 2H), 1.99-1.92 (m, 2H), 1.73 (s, 3H), 1.70-1.66 (m, 2H), 1.64 (s, 3H), 1.56 (s, 3H), 1.29-1.15 (m, 12H), 1.08-0.97 (m, 2H) 0.85 (t, *J* = 6.8 Hz, 3H). ^{13}C NMR (100 MHz, $CDCl_3$): δ 154.5, 150.0, 139.0, 132.0, 123.7, 121.7, 110.2, 106.1, 44.4, 39.7, 37.4, 31.8, 30.0, 28.8, 26.4, 25.6, 24.6, 22.7, 22.3, 17.7, 16.2, 14.0.

4.2.4 REFERENCES

Adams, R., & al. (1941). Tetrahydrocannabinol homologs and analogs with marijuana activity. X. *J Am. Chem. Soc, 63*, 1973-1976.

Adams, R., & al. (1942). Tetrahydrocannabinol homologs and analogs marihuana activity. XIII. *J. Am. Soc., 64*, 694-698.

Adams, R., & al. (1948a). Tetrahydrocannabinol homologs. XVII, 70. *J am Chem Soc, 70*, 662-664.

Adams, R., & al. (1948b). Tetrahydrocannabinol homologs with doubly branched alkyl groups in the 3-position. XVIII, 70. *J Am Chem Soc*, 664-668.

Adams, R., & al. (1949). New Analogs of Tetrahydrocannabinol. XIX. *J Am Chem Soc, 71*, 1624-1628.

Appendino, G. (2020). The early history of cannabinoid research. *Rend. Lincei, Sci. Fis. Nat., 31*, 919-929.

Appendino, G., & al. (2014). Recreational drug discovery: natural products as lead structures for the synthetisis of smart drugs. *Nat Prod Rep, 31*, 880-904.

Baek, S., & al. (1985). *Tetrahedron Lett., 26*, 1083-1086.

Baek, S., & al. (1995). *Chem. Soc., 16*, 293-296.

Bisogno, T., & al. (2001). Molecular targets for cannabidiol and its synthetic analogues: effect on vanilloid VR1 receptors and on the cellular uptake and enzymatic hydrolysis of anandamide . *Br. J. Pharmacol., 134* , 845–852.

Burstein, S. (2000). Ajulemic Acid (CT3): A potent analog of the acid metabolites of THC . *Curr. Pharmaceut Design, 6* , 1339–1345.

Burstein, S., & al. (1992). Synthetic nonpsychotropic cannabinoids with potent antiinflammatory, analgesic, and leukocyte antiadhesion activities. . *J Med Chem, 35* , 3135–3141.

Citti, C., & al. (2019). A novel phytocannabinoid isolated from Cannabis sativa L. with an in vivo cannabimimetic activity higher than Δ9-tetrahydrocannabinol: Δ9-Tetrahydrocannabiphorol. *Scientific Reports, 9*, 20335.

Crombie, L., & al. (1988). Acid catalyzed terpenylation of olivetol in the synthesis of cannabinoids. *Journal of the Chemical Society, Perkin Transactions 1: Organic and Bio-organic Chemistry (1972-1999), 5*, 1243-1250.

Di Marzo, E. (2018). New approaches and challenges to targeting the endocannabinoid system. *Nat Rev Drug Discov, 17*, 1711-1715.

ElSohly, H., & al. (1982). *J. Pharm. Sci., 71*, 1319-1323.

Gosh, R., & al. (1941). *J. Chem. Soc.*, 137-140.

Hanuš, L. O., & al. (2016). Phytocannabinoids: a unified critical inventory. *Nat. Prod. Rep., 33*, 1357-1392.

Hanuš, L., & Mechoulam, R. (2005). Cannabinoids chemistry: an overview. In R. Mechoulam, *Cannabinoids as Therapeutics* (p. 23-46). Birkhauser.

Johnson, M., & al. (1981). U.S. Patent 4,371,720.

Ketchum, J. (2006a). *Chemical warfare secrets almost forgotten. A personal story of medical testing of army volunteers.* Santa Rosa: ChemBooks Inc.

Ketchum, J. (2006b). *Chemical warfare secrets almost forgotten.* ChemBooks Inc. ISBN 978-1-4243-0080-8.

Leite, J., & al. (1982). Anticonvulsant effects of the (-) and (+)isomers of cannabidiol and their dimethylheptyl homologs. *Pharmacology, 24*, 141-146.

Loev, B., & al. (1973). Cannabinoids. Structure-Activity Studies Related to 1,2-Dimethylheptyl Derivatives. *Journal of Medicinal Chemistry, 16 (11)*, 1200-1206.

Matsuda, L., & al. (1990). *Nature, 346*, 561-564.

Mechoulam, R., & al. (1988). Enantiomeric cannabinoids: stereospecificity of psychotropic activity. *Experientia, 44*, 762–764.

Mechoulam, R., & al. (1990). Synthesis of the individual, pharmacologically distinct enantiomers of a tetrahydrocannabinol derivative. *Tetrahedron Asymmetry, 1*, 315-318.

Morales, P., & al. (2017). An Overview on Medicinal Chemistry of Synthetic and Natural Derivatives of Cannabidiol. *Frontiers in Pharmacology, 8 (422)*, 1-18.

Stern, E., & Lambert, D. (2007). Medicinal Chemistry endeavors around the phytocannabinoids. *Chemistry & Biodiversity, 4*, 1707-1728.

Talele, T. (2017). Natural-Products-Inspired Use of the gem-Dimethyl Group in Medicinal Chemistry. *Journal of Medicinal Chemistry*.

Weissman, A., & al. (1982). Cannabimimetic activity from CP-47,497, a derivative of 3-phenylcyclohexanol. *J. Pharm. Experim. Therap., 223 (2)*, 516-523.

William, E., & Himmelsbach, C. (1946). Studies on marihuana and pyrahexyl compound. *Public Health Rep, 61*, 1059-1083.

Wilson, R., & al. (1976). *J. Med. Chem., 19*, 1165.

CHAPTER 5

CONCLUSIONS AND FUTURE PERSPECTIVES

The easy oxidation of phytocannabinoids to quinones was reported already at the beginning of studies on this class of compounds, and their relevance has moved in the past decades from the analytics of *Cannabis* (the Beam test) to the medicinal chemistry of phytocannabinoids. The biological profile of cannabinoquinoids is different from the one of their corresponding resorcinols, with a negligible affinity for CB_1, a significant activity at CB_2, and an increased potency on PPR-γ. However, the exploitation of their bioactivity potential faces two challenges, namely, the development of a reliable protocol for their synthesis from resorcinolic precursors, and their stabilization. My thesis has addressed both issues, developing an iodane-based protocol that, afford *ortho*-quinones that then undergo prototropic rearrangement to *para*-quinones. The post-oxidative rearrangement can be avoided by *O*-methylation, and, by differently combining the sequence of methylation and oxidation, it was possible to obtain both *ortho*- and *para*-quinone derivatives, that provide an interesting profile of bioactivity, with potent modulation of the endogenous anti-oxidant response mediated by Bach1 and Nrf2.

Previous work had shown that the tandem *aza*-Michael addition-dehydrogenation sequence led to aminoquinones with retained, or even improved, the biological profile of the starting quinone, but that were much more stable. Using metal catalysis, it was possible to combine oxidation and the Michael-addition-dehydrogenation sequences into a single step, that offered in some cases advantages not only in terms of number of operations, but also of yields.

Some observations done during the investigation of the synthesis of cannabinoquinoids, and in particular the sluggish reactivity toward nucleophilic trapping, provided the opportunity to investigate the chemistry of CBC, with the eventual development of a one-step totally synthesis of cannabinol, the first cannabinoid to be isolated from *Cannabis*. Some puzzling reactions, like the formal

thermal 2π +2π cyclization of CBC, actually the result of a complex cationic process, were also clarified. CBC is a potent non-covalent activator of TRPA1, and the experience gained in the chemical studies was applied to the preparation of a series of analogues of the natural products to investigate the SARs for its interaction with TRPA1. For steric reasons, the quinones derivatives of dimethylheptylcannabinoids proved totally refractory to the *aza*-Michael addition, and the structure-activity relationships of this interesting class of compounds were investigated towards cannabinoid receptors and thermo-TRPs channels. Since the evaluation of these compounds is ongoing, only preliminary information has been provided.

The novel, and in some cases, surprising chemistry described in this work will, hopefully, pave the way to the exploration of the biological space of the cannabinoid chemotype. This has for too long been limited to the narcotic activity of Δ^9-THC but is actually much more diverse in terms of molecular targets and differentiated in terms of chemotypes.

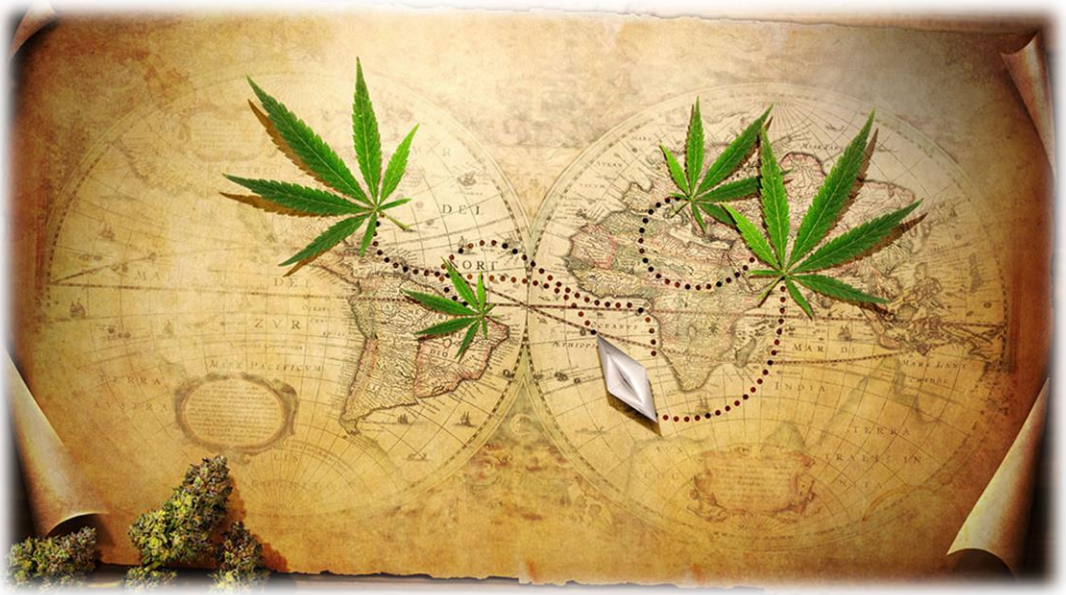

CHAPTER 6

PUBLICATIONS LIST

1. **Mattoteia, D.,** Taglialatela-Scafati, O., Muñoz, E., de la Vega, L., Caprioglio, D., Appendino, G. **Regiodivergent Synthesis of ortho- and para-Cannabinoquinones.** (2020) *European Journal of Organic Chemistry*, (48), pp. 7429-7434. DOI: 10.1002/ejoc.202001258

2. Casares, L., Unciti-Broceta, J.D., Prados, M.E., Caprioglio, D., **Mattoteia, D**., Higgins, M., Appendino, G., Dinkova-Kostova, A.T., Muñoz, E., de la Vega, L. **Isomeric O-methyl cannabidiolquinones with dual BACH1/NRF2 activity**. (2020) *Redox Biology*, 37. DOI: 10.1016/j.redox.2020.101689

3. Chianese, G., Lopatriello, A., Schiano-Moriello, A., Caprioglio, D., **Mattoteia, D.**, Benetti, E., Ciceri, D., Arnoldi, L., de Combarieu, E., Vitale, R.M., Amodeo, P., Appendino, G., de Petrocellis, L., Taglialatela-Scafati, O. **Cannabitwinol, a dimeric phytocannabinoid from hemp, cannabis sativa L., is a selective thermo-TRP modulator**. (2020) *J. Nat. Prod.*, 83 (9), pp. 2727-2736. DOI: 10.1021/acs.jnatprod.0c00668

4. Caprioglio, D., **Mattoteia, D**., Pollastro, F., Negri, R., Lopatriello, A., Chianese, G., Minassi, A., Collado, J.A., Munoz, E., Taglialatela-Scafati, O., Appendino, G. **The Oxidation of Phytocannabinoids to Cannabinoquinoids**. (2020)) *J. Nat. Prod.*, 83 (5), pp. 1711-1715. DOI: 10.1021/acs.jnatprod.9b01284

5. Caprioglio, D., **Mattoteia, D**., Minassi, A., Pollastro, F., Lopatriello, A., Muñoz, E., Taglialatela-Scafati, O., Appendino, G. **One-Pot Total Synthesis**

of Cannabinol via Iodine-Mediated Deconstructive Annulation. (2019) *Org. Lett.,* 21 (15), pp. 6122-6125. DOI: 10.1021/acs.orglett.9b02258

6. Travelli, C., Aprile, S., **Mattoteia, D.,** Colombo, G., Clemente, N., Scanziani, E., Terrazzino, S., Alisi, M.A., Polenzani, L., Grosa, G., Genazzani, A.A., Tron, G.C., Galli, U. **Identification of potent triazolylpyridine nicotinamide phosphoribosyltransferase (NAMPT) inhibitors bearing a 1,2,3-triazole tail group.** (2019) *Eur. J. Med. Chem*., 181, art. no. 111576. DOI: 10.1016/j.ejmech.2019.111576

CHAPTER 7

ACKNOWLEDGEMENTS

Grazie al **Prof. Giovanni Appendino** per avermi accolto nel suo gruppo e avermi permesso di raggiungere questo traguardo!

Grazie ad **Alberto**, che - nonostante non mi volesse e non fossi "voluta" - mi ha reso parte della sua "famiglia scientifica". Come in tutte le migliori relazioni ci son stati momenti up (moltissimi) e alcuni down (pochissimi, tipo le discussioni pseudopolitiche), ma per me Alba e il Minacci's Lab rimarranno sempre una seconda famiglia!

Grazie a **Fede P.** per aver rappresentato un esempio di competenza, passione, intelligenza, serietà, tenacia, perseveranza e educazione. Grazie per la vicinanza e la comprensione!
Grazie anche a tutt* coloro che sono gravitat* attorno a te e al tuo gruppo in questi anni: Patty, Lorenza, Adil, Ste e tutt* tesist*!

Grazie a **Diego** che è stato Post-doc e Doc-post, Papà Castoro, "Permaloso, ma non Rancoroso", Despota, Maestro, Piccolo Cuore. Grazie per aver creduto in me (oltre ogni ragionevole dubbio), per esserti confrontato con me (e che confronti!), per aver "pazientemente" ascoltato i miei sproloqui (EEEEMACARENA) e fugato ogni mia incertezza, per essere stato il mio Mentore (come il Maestro Splinter per le Tartarughe Ninja), il mio compagno di cappa preferito, il mio confessionale, il mio pungiball, il mio DJ! Grazie per essere stato l'altra metà del mio cielo cannabinoide! Io e te, due cuori e una canna... OPS capanna!

Grazie alla **Roghi**, prima collega e poi amica! La prima a chiarirmi come funzionasse il lab, sciorinandomi la gerarchia a mo' di "prima regola del Fight Club, mai parlare del Fight Club". Grazie per il tuo sopporto, per le chiacchierate, per i consigli, per il divertimento, per gli sfoghi, gli insegnamenti e le grandi risate. Sei mancata in questo ultimo anno e mezzo!
Dietro il tuo invalicabile muro (the waaaaallllll!) da Orso Roghi, c'è un cuore grande! (E sotto dei piedi curatissimi!)

Grazie a **Simone**, alla Diva, al Hola, al Adorooooo, all'uomo dai mille interessi, a quello che mi spiega il Giapponese quando a stento so l'Inglese, a quello acido come un limone acerbo, alla zabetta di turno che fa cacciare gli studenti dall'aula mensa, al massimo esperto conoscitore di pratiche bizzarre (tipo metodi per pulire efficacemente le orecchie o per defecare anche l'anima). Sicuramente questo viaggio non sarebbe stato lo stesso senza di te. PHARMACEUTICAL!

Grazie ad **Amin**, un collega umile, disponibile, empatico, sensibile, gentile e educato! E anche stramaledettamente simpatico (ma per lo più comunichiamo a gesti! Potrei essermi sbagliata). Auguro a te e alla tua famiglia tanta, tanta fortuna!

Grazie a **tutti i ragazzi** che hanno scandito con il loro passaggio la mia lunga maratona: vi ricordo tutti con grande affetto e con un sorriso! Ho trascorso con ognuno di voi dei momenti veramente irripetibili e ho cercato di rendere il vostro periodo di tesi il più divertente, spensierato e leggero possibile! E tentando di rendere il lab un posto accogliente per voi, l'ho fatto diventare il posto più accogliente per me!
Grazie davvero a **Marianna, Beatrice, Carina, Ivan, Chiara, Vittorio, Giusi, Anna, Davide, Rosa e Sefora**!

Un super saluto a **Carinsssss**, con cui ho inciso uno dei miei primi grandi successi (sulle note di Up&down di Billy Moore!). Grazie per avermi aperto le porte delle "Alternative Indie"! Spero di rivederti presto cosmopolita del mio cuor.
Un pensiero speciale a **Giusy** che, oltre ad essere stata collega per un periodo, è principalmente amica! Nonostante siano stati mesi frenetici, ci siamo ammazzate dal ridere (che dolore! C'è dolore dentro meeeee! Eeee scusa, ma non me importa... e sono qua un'altra volta).
Un abbraccio sorello (non voglio usare fraterno - sai quanto sia femminista) a **Chiara** e un "in culo alla balena" per il tuo futuro: non farti spegnere, da nessuno.
Una dedica speciale ad **Annina**: una ragazza amorevole, intelligente e capace, preparata, propositiva, gentile e buona! Credo in te, ragazza!

Grazie alla mia **mamma Adele** per aver sempre creduto ciecamente in me e nelle mie capacità! Per avermi insegnato quanto sia importante realizzarsi, essere indipendenti e lottare per ciò che ci sta a cuore! Questo traguardo è un po' anche tuo!

Grazie al mio **papà Roberto** per aver avuto sempre fiducia in me e nelle mie scelte (pur non condividendone alcune) e per avermi sempre appoggiato, dimostrandosi d'aiuto e vicino nella realizzazione dei miei sogni e progetti!

Grazie a **Bubu** per essere prima di tutto mio amico e poi mio fratello. Grazie per esserci quando ho bisogno!

Grazie ai **miei nonni**, a quelli che ci sono e a quelli che non ci sono più. Siete il mio passato, le mie radici, una parte di me. Sarete sempre il polo Nord verso cui punta la mia bussola, la mia Orsa Maggiore in un mare in tempesta.

Grazie alla **Zia Tella** per essere sempre orgogliosa di me, per sostenermi e appoggiarmi!

Grazie a **Zio Frency**, **Zia Simona** e **Anita** e a **Zio Mimmo**, **Zia Gigia**, **Alessandro**, **Angelo** e **Ilaria** perché senza l'appoggio incondizionato della propria famiglia si è semplicemente soli.

Infine, GRAZIE alle amiche e amici che – anche se inconsapevolmente – mi sono stat* d'aiuto nel raggiungere questo traguardo!

Vostra The Yenah,
Daianka
Dajana Mazzozeia
Diana Mattotica
Taiana
Faiana
Damiana
Danaia
Daia

CHAPTER 8

CURRICULUM VITAE

Daiana Mattoteia was born in 1992 in Torino (TO, Italy). After graduating from High School at *Liceo Classico L. Lagrangia* of Vercelli, in 2011 she began her university studies in Pharmacy at the Department of Pharmaceutical Sciences, Eastern Piedmont University, Novara. She graduated in March 2017 with a thesis in Medicinal Chemistry on "Synthesis of *bis*-triazolic and hydrophilic inhibitors of eNAMPT" in the laboratory of Prof. Ubaldina Galli. Then, since September 2017 she has been working in the laboratory of Prof. Giovanni Appendino as fellow – from September to November – and later as PhD student in "Chemistry & Biology".